

INFORMATION TO USERS

This manuscript has been reproduced from the microfilm master. UMI films the text directly from the original or copy submitted. Thus, some thesis and dissertation copies are in typewriter face, while others may be from any type of computer printer.

The quality of this reproduction is dependent upon the quality of the copy submitted. Broken or indistinct print, colored or poor quality illustrations and photographs, print bleedthrough, substandard margins, and improper alignment can adversely affect reproduction.

In the unlikely event that the author did not send UMI a complete manuscript and there are missing pages, these will be noted. Also, if unauthorized copyright material had to be removed, a note will indicate the deletion.

Oversize materials (e.g., maps, drawings, charts) are reproduced by sectioning the original, beginning at the upper left-hand corner and continuing from left to right in equal sections with small overlaps.

Photographs included in the original manuscript have been reproduced xerographically in this copy. Higher quality 6" x 9" black and white photographic prints are available for any photographs or illustrations appearing in this copy for an additional charge. Contact UMI directly to order.

**Bell & Howell Information and Learning
300 North Zeeb Road, Ann Arbor, MI 48106-1346 USA**

UMI[®]
800-521-0600

**Systematic Geochemical and Eruptive Relations in the Late Stage Evolution
of Volcanoes from the Hawaiian Plume - with Case Studies of
Waianae and East Molokai Volcanoes**

by

Nuni-Lyn E. Sawyer

**A dissertation submitted in partial fulfillment of the
requirements for the degree of**

Doctor of Philosophy

University of Washington

1999

Geological Sciences

UMI Number: 9952896

UMI[®]

UMI Microform 9952896

Copyright 2000 by Bell & Howell Information and Learning Company.

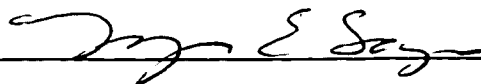
**All rights reserved. This microform edition is protected against
unauthorized copying under Title 17, United States Code.**

**Bell & Howell Information and Learning Company
300 North Zeeb Road
P.O. Box 1346
Ann Arbor, MI 48106-1346**

Doctoral Dissertation

In presenting this dissertation in partial fulfillment of the requirements for the Doctoral degree at the University of Washington, I agree that the Library shall make its copies freely available for inspection. I further agree that extensive copying of the dissertation is allowable only for scholarly purposes, consistent with "fair use" as prescribed in the U.S. Copyright Law. Requests for copying or reproduction of this dissertation may be referred to Bell and Howell Information and Learning, 300 North Zeeb Road, P.O. Box 1346, Ann Arbor, MI 48106-1346, to whom the author has granted "the right to reproduce and sell (a) copies of the manuscript in microform and/or (b) printed copies of the manuscript made from microform."

Signature



Date

12-11-1999


University of Washington
Graduate School

This is to certify that I have examined this copy of a doctoral dissertation by

Nuni-Lyn E. Sawyer

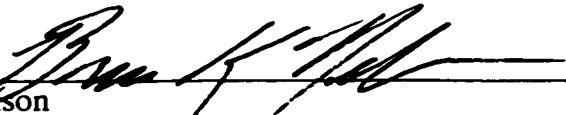
and have found that it is complete and satisfactory in all respects,
and that any and all revisions required by the final
examining committee have been made.

Chair of Supervisory Committee:




Bruce K. Nelson

Reading Committee:



Bruce K. Nelson



I. Stewart McCallum



George W. Bergantz

Date: 12/15/99

University of Washington

Abstract

**Systematic Geochemical and Eruptive Relations in the Late Stage Evolution
of Volcanoes from the Hawaiian Plume - with Case Studies of
Waianae and East Molokai Volcanoes**

by Nuni-Lyn E. Sawyer

Chairperson of the Supervisory Committee

Professor Bruce K. Nelson
Department of Geological Sciences

A significant geochemical event in the evolution of Hawaiian volcanoes is the decline in magmatic flux from shield to post-shield volcanism as each edifice is carried away from the mantle-plume source. This eruptive decline is accompanied by a shift from tholeiitic to alkalic basalt volcanism, although a full spectrum exists in the extent to which any particular volcano undergoes the transition. Evidence shows that systematic geochemical relations exist among volcanoes for this late-shield stage. Compositional correlations in subaerial tholeiitic basalt among Pb, Sr, and Nd isotope ratios and SiO₂, TiO₂, FeO, CaO, and Na₂O content indicate that, for any particular volcano, the proportion of the two identified endmember isotopic components of the Hawaiian shield-building stage, KOO and KEA, are related to what extent eruptions subsequently shift from tholeiitic to alkalic basalt. The spectrum is described by a model in which KOO-dominated lavas result from melting of a mantle plume with a steep marginal temperature gradient, which accounts for large degree melt production followed by abrupt termination as the volcano moves off the plume. KEA-dominated lavas result from melting of a plume that has developed a long

lateral temperature gradient, where large degree melts are followed by continued melt production of increasingly smaller degree. Detailed geochemical data for lavas of Waianae and East Molokai Volcanoes show evolutionary characteristics consistent with the overall model and provide further insight into mantle component characteristics and mixing. The Waianae tholeiite source is an intermediate mix of KEA and KOO. Otherwise apparently well-mixed in the source, the components are systematically sampled by late-shield lavas, where compositions vary stratigraphically from increased KEA to increased KOO. The appearance at Waianae of endmember KOO, previously identified only at Koolau, Lanai, and Kahoolawe, expands the identified isotopic range of Hawaiian lavas and defines KOO isotopic heterogeneity. The East Molokai tholeiite source is KEA-dominated. Late-shield compositions shift toward the isotopically-depleted Post-Erosional (PE) component, which is shown to be characteristic of KEA-dominated volcanoes. Mixing models, accounting for both Sr and Pb isotopic variations, describe PE involvement as metasomatism of the plume margin by small degree melts of a MORB source.

TABLE OF CONTENTS

List of Figures	vi
List of Tables	ix
Introduction	1
Objectives	2
Chapter 1: Characteristics of the Hawaiian Plume: Systematic Relations Between Major Element Variability, Isotopic Variability, and Eruptive Evolution of Hawaiian Volcanoes	4
Abstract	4
Introduction	5
Objectives	6
Previous Observations	7
Intershield Contrasts And Correlations	9
Style Of Late-Shield Volcanic Evolution	9
Intershield Geochemical Variations In Subaerial Tholeiites	12
Interpretation	15
Isotopic Correlation With Melt Segregation Conditions	15
Source Of Intershield Major Element Differences	18
The Role of Fractional Crystallization Processes	18
The Role of Melt Generation Processes	19
Source Of Intershield Correlations	23
Linking Tholeiite Chemistry to Late-Shield Eruptive Style	24
Sources of the KOO and KEA Isotopic Components	27
The Question of Mantle Major Element Heterogeneity	28
Character Of The Hawaiian Plume	30

Entrained Mantle Source Of Alkalic Cap Basalts	33
Conclusions	34
Chapter 2: Magnetostratigraphic Subdivision and Stratigraphic Relations at Waianae Volcano, Oahu, Hawaii	54
Abstract	54
Introduction	55
Objectives	56
Previous Work	57
Stratigraphy	57
Magnetostratigraphy	59
Field Observations	60
Faults and Talus Breccia	60
Soil And Ash Unconformity	61
Magnetic Polarity Units	61
Precaldera Magnetic Polarity units	62
Heleakala (R) flow unit	63
Nanakuli (N) flow unit	63
Intracaldera Magnetic Polarity Units	64
Paheehee (N) flow unit	65
Transition unit at Kamaileunu Ridge	65
Kepauula (R) flow unit	66
Kaala (N) flow unit	66
Stratigraphic Relations	67
Precaldera	67
Intracaldera	69
Unfinished Mapping	70

Constraints and Implications	71
Conclusions	72
CHAPTER 3: The Geochemistry of Waianae Volcano, Hawaii: Isotopic and Major Element Correlations in Late-Shield Lavas and the Identification of an Extreme Koolau Component in the Source	76
Abstract	76
Introduction	77
Objectives	78
Previous Observations	79
Sampling and Results	81
Nomenclature And General Rock Description	81
Alteration	82
Major Element Compositions	83
Trace Element Abundances	84
Radiogenic Isotope Ratios.....	85
Discussion	87
Geochemical Variations And Correlations.....	88
Isotopic and Major Element Relations	89
Isotopic and Trace Element Relations	91
Nature Of The Mantle Sources	92
Characteristics of KEA and KOO Component Mixing	92
Characteristics of KOO Component Heterogeneity	95
Conclusions	97
CHAPTER 4: Field Investigation and Composite Stratigraphy of East Molokai Volcano, Hawaii	119
Abstract	119
Introduction	119

Objectives	120
Previous Work	120
Stratigraphic Sections	122
Haupu Section	122
Hakaaano Section	123
Kamalo Gulch Section	123
Caldera Samples	124
Rejuvenated Sage Samples	124
Composite Stratigraphy	124
Conclusions	126
CHAPTER 5: The Geochemistry of East Molokai Volcano, Hawaii: Evidence for Common Mantle Processes in the Tholeiite to Alkali Basalt Transition of Haleakala-Type Volcanoes	129
Abstract	129
Introduction	130
Objectives	132
Previous Investigations	133
Results	133
Alteration	134
Major Element Compositions	135
Trace Element Compositions	137
Radiogenic Isotope Compositions	138
Discussion	140
Late-Shield Geochemical Characteristics	141
The Nature Of The Mantle Sources	143
PE Component Involvement in Hawaiian Volcanism	143
Model for the PE Component in East Molokai Basalts	145

Conclusions	150
Reference List	174
Appendix A: Analytical Methods	182
Appendix B: Section Descriptions Waianae Volcano	185
B.1 Puu Heleakala North Ridge Section Description	185
B.2 Nanakuli Ridge Section Description - lower section	191
B.3 Ulehawa Ridge Section Description	195
B.4 Puu Paheehee North Ridge Section Description	198
B.5 Kamaileunu Ridge Section Description	200
B.6 Nanakuli Ridge Section Description - upper section	205
Appendix C: Sample Descriptions East Molokai Volcano	207
C.1 Haupu Section Sample Description	207
C.2 Hakaano Section Sample Description	208
C.3 Kamalo Gulch Section Sample Description	209
C.4 Caldera Section Sample Description	210
C.5 Kalaupapa Peninsula Sample Description	210
Vita	211

LIST OF FIGURES

<i>Number</i>	
1.1	36
Hawaiian Islands with Case Study Areas Identified - Waianae and East Molokai Volcanoes	
1.2	37
a) $^{87}\text{Sr}/^{86}\text{Sr}$ vs. ϵ Nd b) $^{206}\text{Pb}/^{204}\text{Pb}$ vs. $^{208}\text{Pb}/^{204}\text{Pb}$ for Subaerial Tholeiites of Hawaiian Volcanoes with Shield-Building Stage Complete	
1.3	38
a) SiO_2 vs. Total Alkalis and b) CaO vs. TiO_2 for Hawaiian Subaerial Tholeiites (>7 wt% MgO) Grouped by Volcano-Type	
1.4	39
a) MgO vs. SiO_2 and b) MgO vs. TiO_2 for Hawaiian Subaerial Tholeiites Grouped by Volcano-Type	
1.4	40
(continued) c) MgO vs. FeO and d) MgO vs. CaO for Hawaiian Subaerial Tholeiites Grouped by Volcano-Type	
1.5	41
a) $^{87}\text{Sr}/^{86}\text{Sr}$ vs. ϵ Nd and b) $^{206}\text{Pb}/^{204}\text{Pb}$ vs. $^{208}\text{Pb}/^{204}\text{Pb}$ Tholeiite Isotopic Compositions Averaged for Individual Volcanoes and Grouped by Volcano-Type	
1.6	42
$^{87}\text{Sr}/^{86}\text{Sr}$ vs. $^{206}\text{Pb}/^{204}\text{Pb}$ Averaged Isotopic Compositions for a) Kohala-type and b) Haleakala-type Tholeiites and their Respective Alkali Basalt Caps	
1.7	43
Calculated Pearson Correlation Coefficients for Pb, Sr, Nd isotope ratios with each major element a) uncorrected for olivine and b) corrected for olivine accumulation	
1.8	44
$^{206}\text{Pb}/^{204}\text{Pb}$ vs. Calculated Average Pressure of Magma Segregation for Subaerial Tholeiites from Individual Volcanoes	
1.9	45
a) SiO_2 vs. Total Alkalis for Subaerial Hawaiian Tholeiites and Effects of Mineral Fractionation	
1.9	46
(continued) b) MgO vs. SiO_2 for Subaerial Hawaiian Tholeiites and Effects of Mineral Fractionation and Partial Melting	
1.9	47
(continued) c) MgO vs. TiO_2 for Subaerial Hawaiian Tholeiites and Effects of Mineral Fractionation and Partial Melting	
1.9	48
(continued) d) MgO vs. FeO for Subaerial Hawaiian Tholeiites and Effects of Mineral Fractionation and Partial Melting	
1.9	49
(continued) e) MgO vs. CaO for Subaerial Hawaiian Tholeiites and Effects of Mineral Fractionation and Partial Melting	

1.10 Schematic Model of Mantle Plume Variations that Produce Late-Shield Geochemical Differences between Koolau-type and Haleakala-type Volcanoes	50
2.1 Shaded Relief and Geologic Map Views of Waianae Volcano	74
2.2 Relations among Lithostratigraphic Boundaries (informal and formal), Magnetostratigraphic Boundaries, and Sample Locations of Waianae Volcano	75
3.1 SiO ₂ vs. Total Alkalis for Subaerial Basalts of Waianae Volcano	99
3.2 MgO vs. a) SiO ₂ b) TiO ₂ c) FeO d) CaO e) Na ₂ O and f) P ₂ O ₅ for Subaerial Basalts of Waianae Volcano	100
3.3 Representative Rare Earth Element (REE) Patterns for Subaerial Basalts of Waianae Volcano	101
3.4 La vs. a) La/Yb b) Sm/Yb c) Sr d) Pb e) Zr and f) Hf for Subaerial Basalts of Waianae Volcano	102
3.5 ²⁰⁶ Pb/ ²⁰⁴ Pb vs. ²⁰⁸ Pb/ ²⁰⁴ Pb for Subaerial Basalts of Waianae Volcano	103
3.6 ²⁰⁶ Pb/ ²⁰⁴ Pb vs. Stratigraphic Position for Basalts of Waianae Volcano	104
3.7 ⁸⁷ Sr/ ⁸⁶ Sr vs. ε Nd for Subaerial Basalts of Waianae Volcano	105
3.8 ⁸⁷ Sr/ ⁸⁶ Sr vs. Stratigraphic Position for Basalts Waianae Volcano	106
3.9 ⁸⁷ Sr/ ⁸⁶ Sr vs. ²⁰⁶ Pb/ ²⁰⁴ Pb for Hawaiian Basalts and Subaerial Basalts of Waianae Volcano	107
3.10 ²⁰⁶ Pb/ ²⁰⁴ Pb vs. SiO ₂ for Subaerial Hawaiian Tholeiites (MgO>6 wt%) Averaged for Individual Volcanoes	108
3.11 ²⁰⁶ Pb/ ²⁰⁴ Pb vs. a) SiO ₂ and b) Fe ₂ O ₃ (as total iron) for Subaerial Basalts of Waianae Volcano	109
3.12 ⁸⁷ Sr/ ⁸⁶ Sr vs. a) ²⁰⁶ Pb/ ²⁰⁴ Pb and b) ²⁰⁸ Pb/ ²⁰⁴ Pb for Hawaiian Basalts and Subaerial Basalts of Waianae Volcano with Model Mixing Lines between KOO and KEA Mantle Endmember Components	110
3.13 ⁸⁷ Sr/ ⁸⁶ Sr vs. ²⁰⁸ Pb/ ²⁰⁴ Pb for Hawaiian Basalts and Subaerial Basalts of Waianae Volcano with Model Mixing between KEA and an Isotopically Heterogeneous KOO Component	111
3.14 a) ⁸⁷ Sr/ ⁸⁶ Sr vs. Eu/Eu* b) ²⁰⁶ Pb/ ²⁰⁴ Pb vs. Eu/Eu* for Subaerial Pre-caldera Basalts of Waianae Volcano	112
4.1 Shaded Relief and Geologic Map Views of East Molokai Volcano	127

4.2	Sample Locations by Stratigraphic Section for East Molokai Volcano	128
5.1	SiO ₂ vs. Total Alkalis for Subaerial Basalts of East Molokai Volcano	153
5.2	Alkalinity vs. Stratigraphic Position for Basalts of East Molokai Volcano	154
5.3	MgO vs. Alkalinity for Subaerial Basalts of East Molokai Volcano	155
5.4	MgO vs. a) SiO ₂ b) TiO ₂ c) FeO d) CaO e) Na ₂ O and f) P ₂ O ₅ for Subaerial Basalts of East Molokai Volcano	156
5.5	Representative Rare Earth Element (REE) Patterns for Subaerial Basalts of East Molokai Volcano	157
5.6	⁸⁷ Sr/ ⁸⁶ Sr vs. ε Nd for Subaerial Hawaiian Basalts and Basalts of East Molokai Volcano	158
5.7	²⁰⁶ Pb/ ²⁰⁴ Pb vs. ²⁰⁸ Pb/ ²⁰⁴ Pb for Subaerial Hawaiian Basalts and Basalts of East Molokai Volcano	159
5.8	²⁰⁶ Pb/ ²⁰⁴ Pb vs. Stratigraphic Position for Basalts of East Molokai Volcano	160
5.9	⁸⁷ Sr/ ⁸⁶ Sr vs. ²⁰⁶ Pb/ ²⁰⁴ Pb for Subaerial Hawaiian Basalts and Basalts of East Molokai Volcano	161
5.10	Alkalinity vs. a) La/Ce and b) La/Lu for Subaerial Basalts of East Molokai Volcano and Other Haleakala-Types (Haleakala and Mauna Kea Volcanoes)	162
5.11	⁸⁷ Sr/ ⁸⁶ Sr vs. ²⁰⁶ Pb/ ²⁰⁴ Pb for East Molokai with Model for KOO-KEA Mantle Mixing as Hawaiian Shield Source	163
5.12	⁸⁷ Sr/ ⁸⁶ Sr vs. a) La/Ce and b) La/Lu for Subaerial Basalts of East Molokai Volcano and Other Haleakala-types (Haleakala and Mauna Kea Volcanoes) with Model for Mixing between Shield Source and Small Degree Melts of Depleted Mantle	164
5.13	²⁰⁶ Pb/ ²⁰⁴ Pb vs. La/Lu for Subaerial Basalts of East Molokai Volcano and Other Haleakala-types (Haleakala and Mauna Kea Volcanoes) with Model for Mixing between Shield Source and Small Degree Melts of Depleted Mantle	165
5.14	⁸⁷ Sr/ ⁸⁶ Sr vs. La/Ce for Subaerial Basalts of East Molokai Volcano and Other Haleakala-types (Haleakala and Mauna Kea Volcanoes) with Alternative Models for Mixing between Shield Source and Depleted Mantle (both as solids, both as melts)	166

LIST OF TABLES

Number

1.1 Hawaiian Volcano-type Classification	51
1.2 Calculated Average Isotopic Compositions for Hawaiian Subaerial Tholeiites	52
1.3 Calculated Primary Magma Compositions and Melt Segregation Conditions	53
3.1 a) Major and Trace Element and Isotopic Compositions - Puu Heleakala	113
3.1 a) (continued) Major and Trace Element and Isotopic Compositions - Puu Heleakala	114
3.1 b) Major and Trace Element and Isotopic Compositions - Nanakuli Ridge	115
3.1 c) Major and Trace Element and Isotopic Compositions - Kamaileunu Ridge	116
3.1 d) Major and Trace Element and Isotopic Compositions - Palehua Alkali Cap	117
3.2 Mixing Parameters for Model Mantle Source of Waianae Lavas	118
5.1 a) Major and Trace Element and Isotopic Compositions - Haupu Section	167
5.1 b) Major and Trace Element and Isotopic Compositions - Hakaaano Section	168
5.1 b) (continued) Major and Trace Element and Isotopic Compositions - Hakaaano Section	169
5.1 c) Major and Trace Element and Isotopic Compositions - Kamalo Section	170
5.1 c) (continued) Major and Trace Element and Isotopic Compositions - Kamalo Section	171
5.1 d) Major and Trace Element and Isotopic Compositions - Kamalo Alkali Cap	172
5.2 Melting and Melt Mixing Parameters for Model Mantle Source of East Molokai Lavas	173

INTRODUCTION

Geochemical characteristics of ocean island basalts provide information for identifying geochemical reservoirs and processes of melt generation in mantle material not sampled by other types of volcanism. Major and trace element chemistry carry information on pressure, temperature, and other physical parameters of the sources, whereas ratios of radiogenic isotopes (Sr, Nd, Pb), which are not fractionated by crystallization or melting processes, reflect the composition of the sources. Variations in lava isotope ratios are described by mixing between mantle isotopic reservoirs (i.e., mantle regions with long-term differences in parent/daughter ratios). The variety of mantle components needed to describe overall geochemical variations in ocean island lavas is testimony to heterogeneity of the mantle. However, the physical characteristics and locations of the sources represented by isotopic endmembers are unresolved issues.

Although subaerially-exposed lavas record only a small fraction of the eruptive history of any volcano, they include a period in which rapid geochemical changes accompany extinction of the volcano as it is carried away from the magma source. One of the significant changes is the shift from the voluminous volcanism of the shield-building stage to the declining volcanism of the post-shield stage. Distinct isotopic and incompatible element differences between shield and post-shield lavas at many ocean island volcanoes imply that variations in the proportions of isotopically distinct source components also accompany the transition to low magma generation rates. The transition from shield to post-shield volcanism is a common feature of ocean island volcanoes and therefore must

reflect a fundamental process in plume evolution independent of which mantle components dominate a particular plume.

The Hawaiian mantle plume has long been a focus of petrologic and geochemical studies. It is one of the most productive sources of ocean island basalts (Sleep, 1990) and is isolated from present day continental or mid-ocean ridge processes that might alter the geochemical signature of the mantle source. The stage of declining volcanism in the evolution of Hawaiian volcanoes, preserved in the subaerial lavas, is marked by a transition from tholeiitic to alkalic basalt volcanism, although there is a full spectrum in the extent to which any particular volcano undergoes this transition. The potential is great for highly-detailed sampling and geochemical studies of individual volcanoes, and studies are gradually turning toward this approach. However, most published studies of Hawaiian volcanoes are reconnaissance in nature and not related to a well-documented stratigraphic context. Detailed studies of tholeiitic to alkalic basalt transitions are especially rare.

OBJECTIVES

This report describes an investigation of the geochemical nature of the tholeiite to alkali basalt transition of Hawaiian volcanoes, with the intent to understand mantle sources and processes associated with melt generation at this stage within the Hawaiian plume. The approach is two-fold; 1) to compare and contrast the geochemistry of Hawaiian volcanoes as a group and present a model that generalizes the observations to identify a common mechanism involved in producing the wide range, both chemical and physical, of late-shield volcanic character, and 2) to present the results of detailed, stratigraphically-controlled geochemical studies of two Hawaiian volcanoes, Waianae and East Molokai, with interpretations consistent with the model describing the late-shield evolution of

Hawaiian volcanoes. These case studies include results of field stratigraphic research that provide the basis for interpretation of the geochemical evolution of each volcano. The Waianae Volcano field research, in particular, is presented in detail to show the benefit of supplementing traditional lithologic stratigraphic subdivision with field-determined magnetostratigraphy in order to provide an accurate volcanologic context for geochemical interpretation.

CHAPTER 1

Characteristics of the Hawaiian Plume: Systematic Relations Between Major Element Variability, Isotopic Variability, and Eruptive Evolution of Hawaiian Volcanoes

ABSTRACT

Systematic intershield geochemical relations exist among those Hawaiian volcanoes that have completed shield growth. Intershield major element differences among subaerial tholeiitic basalts correlate with intershield isotopic differences, which in turn relate to the extent to which a volcanic system subsequently undergoes the transition to alkalic basalt volcanism in the late-shield stage. An evaluation of subaerial tholeiite data, both published and new, shows that correlations between isotope ratios of Pb, Sr, and Nd and abundances of SiO₂, TiO₂, FeO, CaO, and Na₂O are statistically significant at the 99% confidence level. The correlations indicate that, for any particular volcano, the proportion of the two identified endmember isotopic components of the Hawaiian shield-building stage, the KOO and KEA components, is related to whether and to what extent eruptions subsequently shift from tholeiitic to alkalic basalt. The spectrum of late-shield volcanic behavior is described by a model in which lavas dominated by the KOO component result from melting of a plume with a steep marginal temperature gradient, which accounts for production of large degrees of melt followed by an abrupt termination as the volcano moves off of the plume. Lavas dominated by the KEA component result from melting of a plume that has developed

a long lateral temperature gradient, where large degree melts are followed by continued melt production of increasingly smaller degree. Longer temperature gradients develop during periods of lesser source buoyancy through increased conductive heat loss to the surrounding mantle, which results in greater ambient mantle entrainment. In this model, the KOO component dominates the initial mantle plume and the KEA component is entrained in amounts proportional to variations in initial plume buoyancy, resulting in a general correlation between major element and isotope compositions among shields. In summary, the model generalizes the geochemical observations to identify a single mechanism - variation in buoyancy flux - that relates major element variability to isotopic variability to eruptive evolution of Hawaiian plume volcanoes.

INTRODUCTION

The geochemical characteristics of plume-derived lavas, particularly ocean island basalts, provide evidence for the composition and melting behavior of mantle not sampled by other types of volcanism. Consequently, much effort has gone into detailing the compositions of ocean island lavas in the quest to identify geochemical reservoirs of the mantle and describe processes of melt generation. Variability in isotopic compositions reflects mixing between mantle isotopic reservoirs (i.e., mantle regions with long-term differences in parent/daughter ratios), yet the physical characteristics and locations of the sources represented by isotopic endmembers are unresolved issues. Because major and trace element chemistry carries information on pressure, temperature, and other physical parameters of melt production in the sources, correlation of elemental with isotopic data provides strong constraints on associating an isotopic source with a physically-characterized part of the mantle and its associated post-melting history.

A large amount of data exists for volcanoes of the Hawaiian plume (Fig. 1.1), and allows identification of intershield geochemical discriminants (e.g., Frey and Rhodes, 1993). Intershield geochemical differences are larger than most identified intrashield variations (Frey and Rhodes, 1993) and, therefore, constrain the identity of relatively large scale variations in source and processes generating the shields. Correlations between intershield differences in isotopic composition are well-documented and reflect the isotopic sources contributing to shield genesis. However, only recently have correlations been described between isotopic and major element compositions (Hauri, 1996), which may reflect association of different mantle sources with characteristic processes of magma genesis.

OBJECTIVES

The research described here shows that statistically significant correlations exist between intershield isotopic (Pb, Sr, Nd) and major element (SiO_2 , TiO_2 , FeO, CaO, Na_2O) discriminants of the subaerial (i.e., late-shield) tholeiitic portion of Hawaiian volcanoes that have completed their shield evolution, and that these correlations are systematically associated with the spectrum of late-shield eruptive styles apparent in lava sequences that record the transition from tholeiitic to alkalic basalt volcanism. Specifically, the evolutionary characteristics of late-shield volcanism, as defined by major element evidence for whether and to what extent a volcanic system undergoes a transition from tholeiitic to alkalic basalt volcanism, are correlated with the isotopic variation among shields.

PREVIOUS OBSERVATIONS

Isotopic and major element differences among Hawaiian shield volcanoes are well-documented. The Pb, Sr, and Nd isotopic heterogeneity in subaerial tholeiitic lavas spans a

relatively wide range of compositions compared to the range known for any particular volcano (Fig. 1.2). The correlations among isotope ratios suggest two endmember mantle sources, identified as KOO and KEA components (Stille et al., 1986), are involved in generating the range of subaerial tholeiite compositions. At least a third endmember, PE, is involved in genesis of Hawaiian post-erosional and some post-shield alkalic basalts.

Distinct intershield differences in some major element abundances of Hawaiian tholeiites may reflect differences in source composition or conditions of melting. The lower total FeO of Mauna Loa lavas relative to Kilauea lavas (Langmuir and Hanson, 1980) and the anomalously low FeO content of Koolau lavas (Roden et al., 1994) have been attributed to depleted source material, although the depletion would have to be a recent event because $^{87}\text{Sr}/^{86}\text{Sr}$ and $^{143}\text{Nd}/^{144}\text{Nd}$ of the lavas reflect long term high Rb/Sr and Nd/Sm (Roden et al., 1994). The distinct intershield differences in SiO_2 , TiO_2 , CaO, and K_2O for the adjacent volcanoes Kilauea and Mauna Loa, and in SiO_2 and CaO for Koolau and Waianae (Frey and Rhodes, 1993), and the geochemical differences between Koolau, Mauna Loa, and Kilauea shield lavas (Frey et al., 1994) have been attributed to variations in mean depth and extent of melting, although the lack of experimental data for compositions of partial melts in equilibrium with garnet peridotite preclude definitive conclusions.

Frey et al. (1994) noted that Koolau lavas define an extreme for Hawaiian tholeiites in isotope ratios as well as in the content of several major elements, yet Lanai and some Kahoolawe lavas, also isotopically extreme, are not similar to Koolau in major element composition. They concluded that no correlations exist between major element composition and isotope ratios. However, more recent studies suggest otherwise. Broad correlations between major element composition and isotope ratios were proposed by Lassiter et al. (1996), who compared the volcano groups of the parallel structural

lineaments, the Loa- and Kea-trends. They argued that major element differences are consistently observed between the trends and that, although there is significant overlap in isotope composition between Loa and Kea volcanoes, Kea-trend volcanoes on average have lower $^{87}\text{Sr}/^{86}\text{Sr}$ and higher $^{206}\text{Pb}/^{204}\text{Pb}$ and $^{143}\text{Nd}/^{144}\text{Nd}$. They showed that the average olivine-corrected tholeiite composition of Kea-trend volcanoes (Kilauea, Mauna Kea, Kohala, Haleakala, West Maui, East Molokai) compared to that of Loa-trend volcanoes (Mauna Loa, Hualalai, Lanai, West Molokai, Koolau) has lower SiO_2 and higher TiO_2 and CaO , from which they concluded that Kea-trend tholeiites result from smaller degrees of melting at higher pressures. More detailed relations among individual volcanoes were reported by Hauri (1996), who showed that statistically significant intershield correlations exist between Pb, Sr, and Nd isotope ratios and fractionation-corrected SiO_2 , TiO_2 , Al_2O_3 , FeO , CaO , Na_2O , and $\text{CaO}/\text{Al}_2\text{O}_3$ for eight volcanoes, with endmembers defined by Koolau and Loihi volcanoes. Based on experimental data, he argued that Koolau lava compositions are too high in SiO_2 at a given FeO content to originate from partial melting of peridotite, and that an eclogitic mantle component in the Koolau source may supply the SiO_2 -rich contribution to the melt. Intershield correlations are extended here with additional data and, more significantly, shown to vary systematically with the nature of the subsequent tholeiitic to alkalic basalt transition.

INTERSHIELD CONTRASTS AND CORRELATIONS

The data set for this study comprises major element and Pb, Sr, and Nd isotopic data for lavas from all Hawaiian volcanoes, except as noted below, and includes unpublished results for Waianae (Chap. 3) and East Molokai (Chap. 5) volcanoes. Major element compositions are recalculated to convert all iron to FeO , eliminate volatiles, and normalize to 100% total. To minimize effects of obvious multiphase fractionation, only samples with

MgO greater than approximately 7 weight percent are considered. The statistical analysis of relations between isotope and major element compositions involves all subaerial tholeiites, as defined by total alkalis and silica content (Macdonald and Katsura, 1964), from each volcano where shield-building volcanism has ended. The data are necessarily limited to samples with both isotopic and major element analyses. Because many more tholeiites are characterized only by isotopic or major element composition, all geochemical data are included when comparing the overall isotopic, major element, and evolutionary character of each volcano.

STYLE OF LATE-SHIELD VOLCANIC EVOLUTION

Hawaiian volcanoes are generally described in terms of typical growth stages (e.g., Clague and Dalrymple, 1987) from pre-shield to shield to post-shield, followed by a rejuvenated stage at some volcanoes. Shield-building volcanism is characterized by voluminous eruptions of tholeiitic lavas that make up the bulk of each volcano. Tholeiites may be interbedded with transitional and alkalic basalts in the late shield before a transition to alkalic capping lavas of the post-shield. However, this growth sequence does not describe every volcano. Much evidence exists for a systematic spectrum of late-shield volcanic behavior (Table 1.1). Macdonald and Katsura (1964) argued that those volcanoes that erupted alkalic rocks can be distinctly subdivided into a Haleakala-type and a Kohala-type. The Haleakala-type volcano has a succession of tholeiitic basalts passing, without apparent erosional break, into a series of interbedded basalts, ankaramites, and hawaiites. Alkalic basalts occur in the middle or late caldera-filling sequence and are commonly preceded by interbedded tholeiitic and transitional basalts. Macdonald and Katsura (1964) included in this category West Maui, Mauna Kea, and Kauai Volcanoes. The Kohala-type volcano has a sequence of tholeiitic basalts that in places are interbedded with alkalic basalts below an

erosional unconformity that separates them from an overlying thin cap of mugearite and trachyte. Included in this category is Waianae Volcano. Macdonald and Katsura (1964) concluded that only minor compositional differences exist among tholeiitic shields and that they are not related to volcano type as defined by differences in late-stage eruptive history.

Based on further observations of variations in the character of the mildly alkalic rock series, Wright and Helz (1987) refined the subdivisions into four categories: the Haleakala-type, Kohala-type, Hualalai-type, and Koolau-type. The Haleakala-type volcano, similar to that of Macdonald and Katsura (1964) but comprising a different set of volcanoes, is characterized by a thick transitional zone of interbedded tholeiite, transitional basalt, and ankaramite, and is capped by hawaiiite and mugearite. The other volcanoes of this type are Mauna Kea and East Molokai. The Kohala-type volcano lacks abundant mafic alkalic rocks. Hawaiiite and mugearite dominate, forming a thin cap of lava erupted from vents scattered around the tholeiitic shield. Included in this type are Waianae, West Molokai, and West Maui Volcanoes. The Hualalai-type volcano is unusual in that Wright and Helz (1987) included no other volcano in this group. Hualalai alkalic rocks are characterized by nepheline-normative alkaline basalts and trachytes. The Koolau-type volcano either lacks an alkalic cap or has a few alkalic flows at the top of the tholeiitic sequence. This type includes Lanai, Kauai, Niihau, and Kahoolawe Volcanoes.

The previous summary shows that the spectrum of late-shield evolutionary character can be subdivided into categories, although there is apparent overlap in characteristics. The discussion here focuses on Haleakala, East Molokai, and Mauna Kea as Haleakala-type volcanoes; Kohala, Waianae, West Maui, and Kahoolawe as Kohala-type volcanoes; and Koolau and Lanai as Koolau-type volcanoes (Table 1.1). West Maui has been categorized as both Haleakala-type (Macdonald and Katsura, 1964) and Kohala-type (Wright and Helz,

1987), but apparently is best described as Kohala-type in either classification. Kahoolawe is here shifted from the Koolau-type to Kohala-type category because more recent studies (Fodor et al., 1992; Leeman et al., 1994) showed that Kahoolawe erupted intercalated tholeiitic and alkalic basalts during late-shield growth, and that a thin cap of post-caldera lavas erupted from at least eight major vents. Two of the post-caldera flows have been analyzed and are hawaiite in composition (Leeman et al., 1994). Therefore, these recent studies best describe Kahoolawe as a Kohala-type volcano according to the definitions of Wright and Helz (1987). Excluded from the discussion are the volcanoes West Molokai, Niihau, and Hualalai because there are no or very few published major element or isotopic analyses for subaerial tholeiites, and Kauai because it may comprise more than one shield volcano (Holcomb et al., 1995; 1997) where the evolutionary character of each is unresolved. The volcanoes Mauna Loa and Kilauea have not yet completed their evolution and can not be categorized in Wright and Helz (1987) fashion. Discussion concerning the tholeiite compositions of these volcanoes is deferred to a later section.

Wright and Helz (1987) suggested that the subdivision of volcanoes indicates that the groups reflect significant differences in either source, or plumbing, or both. Whereas Macdonald and Katsura (1964) found no differences in tholeiitic lava compositions that are systematically related to volcano type, as defined by late-stage eruptive history, it is shown here that intershield major element differences among subaerial tholeiites reflect the extent to which a particular volcanic system underwent the transition to alkalic basalt volcanism and that these differences are correlated with intershield isotopic differences.

INTERSHIELD GEOCHEMICAL VARIATIONS IN SUBAERIAL THOLEIITES

Whether considered as individual volcanoes or grouped by type, as defined above, one can discern systematic differences in concentrations of SiO_2 vs. total alkalis and CaO vs. TiO_2 (Fig. 1.3). Specifically, the trend of decreasing SiO_2 and increasing TiO_2 from Koolau-type to Haleakala-type subaerial tholeiites defines compositions that are increasingly transitional to alkalic basalt. Intershield differences in SiO_2 , TiO_2 , CaO , and FeO content are also apparent when lavas of similar MgO are compared (Fig. 1.4 a-d). The compositional spectrum, for a given MgO content, spans a range from Koolau-type to Kohala-type to Haleakala-type volcanoes, where Koolau-type subaerial tholeiites have the highest SiO_2 and the lowest TiO_2 , FeO , and CaO content.

Because intrashield isotopic variations are smaller than most intershield variations, a predominant isotopic characterization of subaerial tholeiites may be approximated by computing an average with standard deviation for each volcano (Table 1.2; Fig. 1.5 a,b). As is the case for major element content, the volcano types are distinguished by isotope composition. Specifically, the sequence Koolau-type to Haleakala-type volcanoes is a trend toward radiogenic Pb and Nd and nonradiogenic Sr isotope compositions. This trend is well-defined for Pb isotope ratios, but there is overlap between Haleakala-type and Kohala-type volcanoes in Sr and Nd isotope ratios because the West Maui composition is within the range of Haleakala-type volcanoes and the Haleakala composition is within the range of Kohala-type volcanoes.

Systematic intershield differences among volcano types extend to isotope compositions of alkalic basalt capping-lavas relative to underlying tholeiites, particularly for Sr and Pb

isotope ratios which provide the clearest discrimination among the Hawaiian isotopic endmembers KOO, KEA, and PE (Fig. 1.6 a,b). The average composition of tholeiites from each shield-type is systematically offset from the isotope composition of their respective alkalic cap rocks. Whereas the Koolau-type volcanoes erupt no alkalic lavas, the Kohala-type volcanoes erupt alkalic cap lavas that are either isotopically similar to the tholeiites or trend toward the KEA isotopic endmember, and the Haleakala-type volcanoes erupt alkalic cap lavas that trend toward the PE isotopic endmember. Late-shield alkalic lavas (not shown), which are particularly abundant in Haleakala-type volcanoes, are isotopically distinct from alkalic cap lavas and isotopically similar to tholeiites with which they are interbedded (e.g., Mauna Kea: Frey et al., 1991; Haleakala: Chen et al., 1991).

Statistical evaluation of the subaerial tholeiite data confirms that correlations exist at the 99% confidence level between isotope ratios of Pb, Sr, and Nd and abundances of SiO_2 , TiO_2 , FeO, CaO, and Na_2O (Fig. 1.7 a,b). The correlations are significant among data uncorrected for mineral accumulation and fractionation (Fig. 1.7 a) because low pressure phenocryst effects, which may partially mask isotopic-major element correlations associated with source processes, are minimized by restricting the database to compositions with greater than approximately 7% MgO. The restricted data fall along olivine control lines (e.g., Fig. 1.4), indicating olivine accumulation, which primarily affects MgO content in basaltic lavas.

The isotopic-major element correlations are generally improved using data corrected for olivine accumulation (Fig. 1.7 b). Major element compositions are corrected by subtracting the composition of average accumulated olivine in a suite of lavas from the bulk rock compositions until 7% MgO is reached. It is common practice to determine average accumulated olivine for any particular suite of tholeiites by projecting olivine control lines

in a plot of MgO vs. FeO. However, the amount of scatter in the data is significantly reduced by using a plot of $Al/(Mg+Fe)$ vs. $Mg/(Mg+Fe)$, where the axis intercept of a line through the data is the forsterite (Fo) content of the accumulated olivine (e.g., Rhodes, 1996). This is the correction scheme adopted here.

Hauri (1996) reported correlations between Pb, Sr, and Nd isotope ratios and fractionation-corrected SiO_2 , TiO_2 , Al_2O_3 , FeO, CaO, Na_2O , and CaO/Al_2O_3 for eight volcanoes, subdivided into those of the Loa trend (Loihi, Mauna Loa, Kahoolawe, Koolau) and the Kea trend (Kilauea, Mauna Kea, Kohala, Haleakala). He showed that isotopic and major element correlations are best among the Loa-trend volcanoes, and that addition of the Kea-trend volcanoes increases the scatter in the correlations. The data set of Hauri (1996) includes pre-shield and shield stage tholeiitic and alkalic basalts, and excludes basalts from intercalated tholeiitic and alkalic sections, which he considers of the post-shield stage. The data set used here is considerably different, including only subaerial tholeiites from those volcanoes that have completed the shield-building stage. This allows intershield comparison of tholeiites at a similar and specific stage of evolution, i.e. the end-of-shield. The data set additionally includes volcanoes East Molokai, Lanai, Waianae, and West Maui.

In the Hauri (1996) data set, exclusion of tholeiites that are interbedded with alkalic basalts removes much of the chemically-transitional aspect of subaerial tholeiite compositions that characterize Haleakala-type volcanoes. Furthermore, as shown later, subaerial tholeiites from volcanoes in the active shield-stage (Kilauea, Mauna Loa) and many sampled submarine tholeiites have higher SiO_2 content than subaerial tholeiites at volcanoes where shield-building is complete. Inclusion of these lavas in the Hauri (1996) data set again obscures the relatively transitional nature of Haleakala-type end-of-shield tholeiites.

Subaerial tholeiite compositions range from strongly tholeiitic (Koolau-type) to more chemically transitional (Haleakala-type), and correlations between major element and isotopic compositions indicate a relation between the proportion of isotopic components in the mantle source and the extent to which a volcano makes a transition to alkalic eruptions.

INTERPRETATION

The available data suggest that major element compositions of subaerial tholeiites from Hawaiian volcanoes are related to the extent to which a volcanic system develops an end-of-shield transition to alkalic basalt volcanism, and that certain intershield major element differences correlate with intershield isotopic differences. Because intershield major element differences reflect spatial variability of melting processes and conditions on a large scale, and isotopic heterogeneity reflects variable sources, it is proposed here that relatively restricted conditions of melting are discernibly and consistently associated with different mantle source regions. Discussion focuses on what melt conditions and processes may produce the observed intershield major element differences, and then on how isotopic variations are related to these conditions.

ISOTOPIC CORRELATION WITH MELT SEGREGATION CONDITIONS

Albarède (1992) proposed conditions of melting for various ocean island basalt magmas by using calculated primary magma compositions in equations derived from empirical relations between the composition, temperature, and pressure of experimentally-produced partial melts. He calculated an average fractionation-corrected composition for each volcano and used it as a proxy for a possible primary magma, from which he inferred an average

temperature and pressure of magma segregation. The method of Albarède (1992) is used here to infer melt conditions producing the late-shield tholeiites of the Hawaiian volcanoes.

Obtaining an estimate for the primary magma composition requires correction for olivine fractionation. Equilibrium olivine is added to a representative parental liquid composition to achieve a primary liquid in equilibrium with olivine of Fo 91 content, which is assumed to be fertile mantle olivine. The uncorrected parental liquid, to which olivine is added, is that which is in equilibrium with the calculated average accumulated olivine composition for the subaerial suite of tholeiites from any particular volcano. This liquid is assumed to be the average magma composition erupted as subaerial tholeiitic lava from that volcano. Although Albarède (1992) determined average accumulated olivine from projected trends in the MgO vs. FeO plot, the accumulated olivine compositions used here are determined from the linear regressions in Al/(Mg+Fe) vs. Mg/(Mg+Fe) and shown in Table 1.3.

The composition of accumulated olivine from any particular volcano should be in equilibrium with a parental liquid of a particular FeO/MgO content (assuming K_D of 0.3 between olivine and liquid; Roeder and Emslie, 1970). This corresponds to a particular parental MgO content and, therefore, an average parental major element composition determined from MgO variation plots. Equilibrium olivine is added in 0.5% increments and recalculated until the equilibrium olivine reaches Fo 91 content. The resultant liquid composition is assumed to be representative of the primary magma of the particular tholeiite suite. Table 1.3 presents the calculated primary magma composition for each volcano.

The melt condition equations express temperature and pressure as a function of a limited number of chemical parameters:

$$T (^{\circ}\text{C}) = \left[2000 \frac{\text{MgO}}{(\text{SiO}_2 + \text{MgO})} \right] + 969$$

$$\ln P (\text{kbar}) = 0.00252 T - 0.12 \text{ SiO}_2 + 5.027 \quad (\text{Albarède, 1992})$$

The calculated temperatures and pressures of melt segregation for each volcano are shown in Table 1.3.

The calculated melt segregation pressures for late shield Hawaiian magmas range from 16 - 35 kbar. This range can be shifted to higher or lower pressures depending on the method used to calculate primary magma compositions. Therefore, the relative melt segregation pressures among the volcano types are more significant than the actual calculated pressures. Based on the model, the magmas supplying the late-shield tholeiites of Koolau-type volcanoes segregate at the shallowest depths and those supplying the late-shield tholeiites of Haleakala-type volcanoes segregate at the deepest levels. The previously noted correlation between Pb isotope composition and SiO₂ translates to a correlation between depth of magma segregation and isotope composition (Fig. 1.8).

The preceding discussion addresses the character of the late-shield tholeiites. Kilauea and Mauna Loa volcanoes are in the active shield stage and, therefore, are not classified according to end-of-shield character; however, consideration of Kilauea and Mauna Loa tholeiitic compositions is important. The pressures of melt segregation calculated for lavas from these two volcanoes are not related to their Pb isotope composition in the same pattern manifested in the other volcanoes (Fig. 1.8). The relatively lower pressures reflect the high calculated SiO₂ and low calculated MgO content of the primary magmas. It is probable that this contrast with other volcanoes reflects the earlier main shield stage of evolution at Kilauea and Mauna Loa. This conclusion is consistent with the relatively high SiO₂ and,

therefore, comparatively low melt segregation pressures calculated for apparent main shield lavas from submarine rift zones (Table 1.3). Differences in late-shield evolution, which generate the distinct subaerial intershield differences, might possibly be predicted by main shield isotope composition.

SOURCE OF INTERSHIELD MAJOR ELEMENT DIFFERENCES

The melt conditions model of Albarède (1992) suggests that subaerial intershield major element differences might be generated by variations in temperature and pressure of melt segregation. Comparison of the intershield data with compositional trends generated by variations in fractional crystallization and parameters of melt generation allows further speculation on what processes may control the intershield major element differences, and therefore relate to the intershield isotopic differences.

The Role of Fractional Crystallization Processes

The effects of fractional crystallization on major element compositions (Fig. 1.9 a-e) are calculated for the proposed average Puna Ridge (submarine Kilauea) primary magma (Clague et al., 1995) using the MELTS thermodynamic potential minimization algorithm of Ghiorso and Sack (1993). Fractional crystallization is possible during transit in magma conduits and during residence in magma chambers or other stagnation points that may exist at various depths. Therefore, the liquid lines of descent and the effects of fractionation of individual minerals are shown for pressures of 1 bar, 2 kbar, and 15 kbar to simulate fractionation at the surface, in an intervolcanic magma chamber, and near the base of the lithosphere. The crystallization sequence is orthopyroxene followed by clinopyroxene at 15 kbar, olivine followed by orthopyroxene and clinopyroxene at 2 kbar, and olivine

followed by clinopyroxene at 1 bar. This indicates the magma is in equilibrium with harzburgite at some pressure between 2 and 15 kbar. The subject of discussion here is not whether this magma is representative of Hawaiian primary magmas, but whether the characteristic major element variations among the three volcano types can be simply explained by variations in fractional crystallization.

Starting from the average (16.5% MgO) Puna Ridge primary magma (Fig. 1.9 a-e), the lower SiO₂ and higher TiO₂, FeO, CaO, and total alkalis that characterize the Haleakala-type tholeiites compared to the Koolau-type tholeiites apparently can be generated by early fractionation of orthopyroxene. However, whereas relatively high magma SiO₂ content is required to stabilize orthopyroxene in the fractionating mineral assemblage, the Haleakala-type tholeiites are characterized by the lowest SiO₂ content among the volcano types.

Furthermore, orthopyroxene phenocrysts are relatively rare in Hawaiian lavas.

Orthopyroxene occurs in lavas from Koolau and Mauna Loa (Frey et al., 1994), which are two volcanoes characterized by high SiO₂ compositions. Therefore, major element differences among the volcano types are not simply explained by orthopyroxene fractionation.

The Role of Melt Generation Processes

Clague et al. (1995) used the range of FeO found in Puna Ridge glass sands containing greater than 8% MgO to calculate a range of primary liquid compositions in equilibrium with olivine Fo 90.7, which is the most forsteritic phenocryst analyzed in the glasses.

They attributed the range of compositions to variation of approximately 20% relative degree of melting; therefore, this range (Fig. 1.9 b-e) is an example of the relative effect melt fraction variation can have on major element compositions. The most MgO-rich

composition is similar to, but contains less MgO than, the submarine Kilauea primary magma composition calculated here.

Kushiro (1996) melted a fertile garnet peridotite at various pressures and presented melt compositions in term of melt fractions, which he estimated from K_2O content of the melts. His work is one of the very few that includes compositions produced in the garnet stability field at melt fractions small enough, less than approximately 15-20%, to preserve clinopyroxene \pm garnet and/or spinel in the residue. However, he reports results from only one experimental pressure within the garnet stability field, at 30 kbar. His results for melts formed at 20, 25, and 30 kbar indicate the effect melt fraction variation at different pressures can have on major element compositions (Fig. 1.9 b-e). According to Kushiro (1996) data, for each pressure shown, the smaller degree melts (6.4-7.5% melting) generate alkalic basalts and leave residual garnet. The larger degree melts (11.3-16.3% melting) produce tholeiitic basalts and consume the source garnet. The lower MgO of Kushiro's experimental melts compared to that of primary magma compositions calculated here is a result of the experimental liquid in equilibrium with approximately Fo 87.5 olivine compared to the calculated liquid in equilibrium with Fo 91 olivine. The calculated primary magmas are of similar MgO content to the experimental magmas when recalculated in equilibrium with Fo 87.5 olivine (not shown). The other compositional differences are most likely due to differences between the Hawaiian source and the garnet lherzolite used by Kushiro (1996). However, the point of discussion here is not whether the Kushiro (1996) garnet lherzolite is representative of the Hawaiian source, but whether the intersield trend in calculated primary magma composition may be explained by variable degree or depth of melting.

Kushiro (1996) concluded that TiO_2 content can be used to estimate the degree of melt because TiO_2 content is relatively invariable for pressure differences at a given degree of melt. For each experimental pressure, Kushiro (1996) data decrease in TiO_2 (and therefore increase in melt fraction) with increases in MgO, similar to the trend of calculated Puna Ridge primary magmas (lightweight arrow, Fig. 1.9 c: Clague et al., 1995). However, neither this constant pressure trend (lightweight arrow, Fig. 1.9 c: Clague et al., 1995) nor the constant melt fraction trend (dashed line, Fig. 1.9 c: Kushiro, 1996) is similar to that of the calculated subaerial tholeiite primary magmas. The calculated intershield trend of increasing TiO_2 with increasing MgO is best modeled by differences between a higher pressure, smaller fraction melt and a lower pressure, larger fraction melt (heavyweight arrow, Fig. 1.9 c: Kushiro, 1996). A similar situation holds for MgO vs. SiO_2 (Fig. 1.9 b). The calculated intershield trends in MgO vs. Al_2O_3 (not shown) and MgO vs. FeO (Fig. 1.9 d) are similar to both the constant pressure trends and the constant melt fraction trends. However, if considering combined pressure and temperature effects, as is necessary to describe relative differences in calculated intershield TiO_2 and SiO_2 , then compositional differences between a lower pressure, larger fraction melt and a higher pressure, smaller fraction melt also describe the relative differences in calculated intershield Al_2O_3 and FeO. The implication is that subaerial Haleakala-type tholeiites are produced by smaller melt fractions at higher pressures than Koolau-type tholeiites. The higher MgO content of the calculated primary magmas for the Haleakala-type tholeiites, which would typically be attributed to larger degrees of melting, may instead reflect higher pressures of melt generation (Kushiro, 1996).

The calculated subaerial tholeiite primary magmas do not form a distinct trend in MgO vs. CaO (Fig. 1.9 e) as they do for SiO_2 , TiO_2 , and FeO in the MgO variation plots. The trend that represents effects of combined pressure and melt fraction variations (heavyweight

arrow in Fig. 1.9 e: Kushiro, 1996) is also indistinct. Magma CaO content apparently decreases with increased pressure of melting (dashed line in Fig. 1.9 e: Kushiro, 1996). However, the effect of melt fraction variations on CaO content is unclear. Many experimental data show that CaO increases with extent of melt at pressures in spinel stability field, and the Kushiro (1996) data show this trend for pressures in both the spinel and garnet stability field (compare same pressure data symbols in Fig. 1.9 e). In contrast, Clague et al. (1995) conclude for Puna Ridge magmas that CaO content decreases with increased degree of melt (lightweight arrow in Fig. 1.9 e). Other recent experimental data show a negative correlation between CaO and degree of melt, but only in the garnet stability field (e.g., Walter and Presnall, 1994). Kinzler (1992) attributed the reversal in CaO melting behavior at increased pressure to the change in the melting assemblage, comprising dominantly clinopyroxene at pressures in the spinel stability field, but roughly equal proportions of clinopyroxene and garnet at higher pressures.

The simple trends shown by the experimental MgO, SiO₂, TiO₂, and FeO data of Kushiro (1996) compare well with the calculated subaerial tholeiite primary magmas. However, more data apparently are needed to describe the complex melting relations among melt pressure, melt fraction, and CaO content. At similar melt fractions, there is agreement that higher pressure results in a decrease in melt CaO content (Walter and Presnall, 1994; Kushiro, 1996). Therefore, if a decrease in CaO with increased melt fraction is assumed, as shown by the calculated Puna Ridge primary magmas, and if this same trend is duplicated at lower CaO content (i.e., increased pressure), then the trend for calculated subaerial tholeiite primary magmas can again be accounted for by differences between lower pressure, larger degree melts and higher pressure, smaller degree melts.

The calculated subaerial tholeiite primary melt segregation pressures range to as shallow as 16 kbar (Table 1.3), but these results give no indication of the amount of melting that took place in the garnet stability field. Hawaiian magmas are thought to be derived from melting in the garnet stability field based on uniformly low Al_2O_3 contents compared to MORB compositions (Frey and Rhodes, 1993), relatively high Sm/Yb, and uniform Yb and Lu with variable trace element contents (Hofmann et al., 1984), all of which indicate garnet in the melt residue (Frey et al., 1994). The trends in Kushiro (1996) experimental compositions (Fig. 1.9 b-e) mainly reflect conditions with garnet absent. It is not well known whether compositional trends observed in the spinel stability field are representative of trends at pressures where garnet is stable because experimental data for melts formed under conditions of variable temperature and pressure and with garnet in the residue are few and inconsistent. In addition, Hawaiian magmas are most likely a result of polybaric melting, where a fraction of the total melt is in the garnet stability field. Therefore, comparison of experimental data trends with Hawaiian compositional trends is limited. However, existing experimental data support the conclusion that late-shield major element differences are produced by differences in pressure and temperature of melt generation, and reflect the differing late-shield evolution among the volcano types.

SOURCE OF INTERSHIELD CORRELATIONS

Correlations between major element content and isotope ratios imply an association between processes controlling intershield major element differences and mantle sources of different isotopic compositions. The issue is to determine why and how melting processes correlate with isotopic compositions of these sources. The discussion has shown that variations in temperature and pressure of melting may generate relative major element differences similar to Hawaiian intershield differences, an observation that relies on

comparison of Hawaiian tholeiite compositions and calculated primary magmas with experimental melt compositions. Because the experimental data are for melts derived from peridotite sources (Albarède, 1992; Kushiro, 1996), this model assumes a general homogeneity in the major element content of the magma sources. Although major element heterogeneity in the source, addressed in a later section, cannot be ruled out (e.g., Hauri, 1996), it is not a requirement in the following model in which a single mechanism provides the correlative link between major element and isotopic variability of subaerial tholeiitic lavas as well as with the subsequent eruptive evolution of the volcanoes.

Linking Tholeiite Chemistry to Late-Shield Eruptive Style

Clues to source character and processes of melt generation are not only in magma chemistry, but also in late-shield eruption rates and petrogenetic diversity of the volcanoes. As each volcano is carried away from the plume, there is an observed range in potential for eruption of the decreased degrees of melting that mark the transition from tholeiitic to alkalic basalt volcanism. Three main styles are represented in the subaerial suites of Hawaiian volcanoes; 1) these smaller degree melts may not erupt at all (Koolau-type), 2) they may erupt with significantly decreased rates in the late-shield, producing a thin transitional section that is separated from the overlying alkalic cap by an eruption hiatus (Kohala-type), or 3) they may erupt at sufficiently high rates early in the late-shield, producing a thick transitional section that grades without apparent pause into the alkalic cap (Haleakala-type). Two endmember processes are considered that may control differences in extrusion volumes of late-shield, smaller degree melts; there is either a range in efficiency of magma transport to the surface or simply a range in the amount of small degree melts produced.

If small degree melts are ubiquitously and abundantly produced at the outer regions of the plume, then they must have a variable capacity to erupt as the volcano moves off of the plume. In this case, late-shield melts below the Koolau-type volcanoes do not reach the surface, whereas those below Haleakala-type volcanoes erupt readily. There is no evidence for differences in magma pathways, such as distinct variations in lithospheric thickness or composition, below different volcanoes to explain the contrast. In fact, adjacent volcanoes are typically of different types (e.g., Koolau-Waiaanae), which would require relatively small scale lithospheric differences. There is also no evidence for density differences that would affect magma transport between small degree melts of a heterogeneous source. According to calculations based on the MELTS algorithm (Ghiorso and Sack, 1993), 5% batch melts of a variety of fertile and depleted mantle compositions show essentially no density differences and 2% batch melts show a maximum density difference of 0.1 gm/cm³, with pyrolite yielding the melt of least density. Therefore, it is unlikely that differences in transport efficiency of late-shield magmas determine whether or not the magmas erupt.

Alternatively, intershield variations in the volume flux of late-shield magmas, rather than eruptive capacity, might produce the spectrum of late-shield evolutionary character. In this case, melt production following shield-building volcanism below Koolau-type volcanoes is weak, whereas that below Haleakala-type volcanoes is vigorous. Moore and Clague (1992) considered Koolau and Lanai to be weak systems without adequate magma supply to enable small degree melts to reach the surface, whereas the robust systems of Mauna Kea and Haleakala had sufficient amounts of small degree melts supplied at shield-building rates. Geochemical data for Lanai tholeiites indicate the lavas could not have been formed by smaller degrees of partial melting than that supplied to other Hawaiian volcanoes (West

et al., 1992); therefore, the idea of weak and robust systems apparently must apply only to production of small degree melts as a volcano moves away from the plume source.

If the production volume of small degree melts is variable, then the correlation of eruptive style with source isotope composition implies that the source dominated by the KOO isotopic component does not produce small degree melts at the end of shield-building, whereas the source dominated by the KEA isotopic component produces small degree melts at a high rate. As discussed in a later section, it is unlikely that differences in melt production volume are controlled by differences in the composition/fertility of the sources; therefore, differences in the supply of late-shield melts may be determined by physical parameters of source melting. Specifically, it is proposed here that production volumes of late-shield melts are determined by the temperature gradient at the plume margin. In this model, Koolau-type magmas are supplied by a plume where the temperature gradient at the plume margin is steep, whereas Haleakala-type volcanoes are supplied by a plume with a long lateral temperature gradient. As a volcano forms and moves away from the magma source, a plume with a steep marginal temperature gradient may supply shield volcanism then abruptly terminate melt production. This is consistent with a narrow hot plume suggested as the source of Lanai lavas to explain large melt fractions, required by geochemistry, and a small shield volume (West et al., 1992). In contrast, a plume with a long lateral temperature gradient may supply shield volcanism followed by continued melt production with increasingly smaller degrees of melt. The implication is that different proportions of KOO and KEA components are associated with physical differences at the plume margins that affect the character of late-shield volcanism.

Sources of the KOO and KEA Isotopic Components

The proportion of KOO and KEA isotopic components in the late-shield source of a particular volcano is associated with the extent to which a source will generate a transition to alkalic basalt volcanism. A reasonable model predicts that intershield major element differences, well-developed in tholeiites of the late-shield stage, are generated by differences in the average temperature and pressure of melting, which are determined by dynamic variability in the plume source. I propose that Koolau-type volcanoes are supplied by a plume with a steep marginal temperature gradient, whereas Haleakala-type volcanoes are supplied by a plume with a long lateral temperature gradient.

Furthermore, there are possible conditions under which a range of marginal temperature gradients might develop along the length of a plume conduit (Fig. 1.10). If different sources upwell at different rates, the more slowly rising source may lose more heat through conduction to the surroundings, and therefore develop a longer, gentler lateral temperature gradient. Conceptually, a stream of pulses, each with a characteristic upwelling rate and with sufficient magma to supply an individual volcano, may develop from large-scale temporal variations in buoyancy at the plume source. In this model, greater initial buoyancy could result from initially higher temperatures. Variations in compositional buoyancy cannot be ruled out; however, the suggestion by Hauri (1996) that the 'Koolau' melt component comes from subducted oceanic crust is not consistent with the model where Koolau-type volcanoes require a source that upwells more rapidly than another and, therefore, develops a steep marginal temperature gradient due to less conductive heat loss. Because eclogite is more dense than fertile peridotite (Hofmann and White, 1982), subducted oceanic crust would not be a source of compositional buoyancy.

In the model where Koolau-type volcanism is supplied by a plume with a steep marginal temperature gradient and Haleakala-type volcanism by a plume with a long lateral temperature gradient, and where the temperature gradient is produced through radial conductive heat loss, the amount of ambient mantle entrainment caused by heat conduction into the surrounding mantle (Griffiths and Campbell, 1991) should be associated with the different volcano types and, therefore, greatest in the KEA-enriched Haleakala-type source (Fig. 10). This implies that the KOO component is associated with the initial plume and that the KEA component is entrained material.

The Question of Mantle Major Element Heterogeneity

Hauri (1996) compared Hawaiian major element data to experimental melts and argued that the SiO₂ content of most lavas are too high at a given FeO content to have been produced by melting of garnet and clinopyroxene-bearing mantle peridotite. He concluded that SiO₂-rich melt derived from small amounts of subducted oceanic crust, as quartz eclogite, in the peridotite source contributes to the resultant lava compositions, and that the largest mass proportion of the eclogitic 'Koolau' component (at least 5%) was in the source of Koolau lavas. Hauri et al. (1996) showed that isotope correlations in Hawaiian shield lavas include ¹⁸⁷Os/¹⁸⁸Os, and proposed that, because the negative Os-Pb isotope correlation trends toward the EM1 mantle component, the isotope composition of the eclogite endmember is dominated by a sedimentary component associated with subducted crust.

The Os isotope correlation is strong evidence for a subducted component in the Koolau lava source. If the SiO₂ content of a melt can be significantly increased by a small contribution from eclogite in the source, then melt segregation pressure calculations, which are not formulated from an experimental database containing eclogite melt compositions (Albarède,

1992), may result in pressures lower than for lavas with no eclogite contribution. However, it is unlikely that the entire range of observed SiO_2 in Hawaiian lavas, and therefore the range of calculated melt segregation pressures, is controlled by small variable proportions of eclogite in the source. Although Hauri (1996) reasoned that the SiO_2 content of subaerial Koolau lavas is higher than any produced by experimental melting of peridotite at appropriate pressures, the narrow compositional range of many earlier-shield submarine samples, including those from KEA-dominated volcanoes Kilauea (Clague et al., 1995; Garcia et al., 1989) and Mauna Kea (Garcia et al., 1989; Yang et al., 1994), overlap the Koolau SiO_2 field at similar FeO/MgO and at similar total alkali content. This suggests that the relatively high SiO_2 end of the Hawaiian compositional range may simply be representative of main shield tholeiite compositions, and that experimental compositions have not approximated the Hawaiian source. The wide range of SiO_2 developed in subaerial tholeiitic basalts represents the varying extent to which any particular volcanic system has undergone a transition to alkalic basalt in the late-shield stage of volcanism (Fig. 1.3 a).

Furthermore, if the composition of the KOO component reflects an eclogite contribution, the implication is that the KOO component is more fertile than the KEA component. If the isotopic source of shield magmas is a mixture of KOO and KEA in varying proportions, then differences in source fertility would favor contribution from the more fertile source in smaller degree melts. Because late-shield interbedded tholeiitic and alkalic rocks of individual volcanoes do not show systematic isotopic differences (e.g., Haleakala: Chen et al., 1991; Mauna Kea: Frey et al., 1990; 1991; Kennedy et al., 1991), no particular isotopic component dominates the smaller degree melts on an intrashield scale of melting. Instead, a greater proportion of KEA component in a source is associated with a more robust and prolonged period of smaller degree melt production. In the present model, this

association is the result of a sequence of events in which lesser initial source buoyancy allows greater conductive heat loss at the margin of the rising plume, resulting in higher degrees of KEA entrainment and development of a long lateral temperature gradient at the plume margin, which is the region in which late-shield melts are formed.

CHARACTER OF THE HAWAIIAN PLUME

The ability to provide strong constraints on the character of the Hawaiian plume using lava chemistry is presently hampered by a lack of main shield lava data. Intersield correlations exist between isotope ratios, major elements, and the evolution of late-shield volcanism, yet it is unknown whether the observed correlations apply to entire volcanoes or are manifested only during late-stage volcanism. Submarine rocks have been sampled with the intent to recover lavas older than those exposed subaerially. For those portions of shields that have been sampled, intersield major element differences apparently exist (Garcia et al., 1989). These subtle major element differences develop into distinct differences among subaerial tholeiites, reflecting the relatively different compositional evolution taken by Koolau-, Kohala-, and Haleakala-type volcanoes at the late-shield stage. However, a fundamental limitation to data interpretation is the uncertainty in the span of shield history represented by sampled submarine lavas. Available submarine geochemical data are for samples taken along rift zones, of which large portions may correlate stratigraphically with subaerial lavas (e.g., Moore and Clague, 1992). Samples of unambiguous main shield origin may be accessed from large submarine scarps or deep drill core, but such sampling has only been initiated at one volcano. The Hawaii Scientific Drilling Project (HSDP) has sampled flows to 1056 meters depth on the flank of Mauna Kea and will presumably core through the entire shield. Although the deepest recovered samples are all tholeiitic and stratigraphically lower than the present subaerially-exposed intercalated tholeiitic and alkalic basalts

(Rhodes, 1996), they were subaerially-erupted (Stolper et al., 1996) and probably represent only a small fraction of the volcanic pile. The point is that the entire available Hawaiian data set probably represents only a small portion of each shield.

Regardless of the severe need for additional main shield lava data, observations show that the sampled portion of each volcano has a characteristic average isotope composition, or proportion of KOO and KEA components. The proportions of the components are variable within lava sequences at any particular volcano, but this variability is small enough to maintain intershield distinctions at this late-shield stage of evolution. Isotope compositions are correlated with the style of late-shield volcanism, which is characterized by major element compositions. The implication is that mixtures of different proportions of KOO and KEA components produce different sources via a mechanism such that corresponding different late-shield characteristics are also produced. These observations constrain physical models of the Hawaiian plume.

Hauri et al. (1994) examined entrainment by a laminar, vertical, steady-state plume conduit. In this case, entrained mantle is incorporated as radially concentric zones surrounding a core of plume material. Their model predicts slow radial inflow of entrained material, which creates juxtaposition of different mantle parcels but not mixing on a small scale as would be the case in turbulent flow. The scale of mixing in the plume conduit is constrained by the observation that, based on the available data, intershield geochemical differences are larger than most intrashield differences (Frey and Rhodes, 1993). This requires mixing of KOO and KEA components on a small scale with respect to the volume of the source, but preservation of variable KOO and KEA proportions on a large scale. A steady-state, concentrically-zoned plume will satisfy these requirements if different volcanoes are samples of different regions of the plume, in which case the plume diameter

is larger than the distance between adjacent volcanoes. This type of plume was proposed to explain the geochemical differences between volcanoes of the Loa- and Kea-trends, where Loa-trend volcanoes have formed over the core of the plume and Kea-trend volcanoes have formed over a zone of entrained material off center of the plume (e.g., Lassiter et al., 1996; Hauri et al., 1996). This model predicts that Kea-trend volcanoes are derived from smaller degrees of melting (Lassiter et al., 1996) and should average slightly shorter life spans and total volumes than Loa-trend volcanoes (DePaolo and Stolper, 1996). However, the volcanoes that attained the greatest height at the end of shield-building, Mauna Kea and Haleakala (Moore and Clague, 1992), are Kea-trend volcanoes. The model also does not account for the differences between adjacent Waianae and Koolau volcanoes, which grew prior to the apparent development of the Loa- and Kea-trends, nor is it consistent with the observation that Loa-trend volcanoes do not all produce smaller degree melts nor transition to Kea-trend compositions as each volcano moves off center of the plume.

An alternative model is a heterogeneously buoyant plume, or individual mantle diapirs, with a diameter on the order of distance between adjacent volcanoes. A deflected plume conduit can entrain and mix surroundings through conductive heat coupling and non-axisymmetric flow within the conduit (Griffiths and Campbell, 1991). Of modern plumes, Hawaii has the highest buoyancy flux (Sleep, 1990), and is presumably least deflected and least altered by stirring. However, the plume is predicted to be diluted 20-30% through entrainment (Griffiths and Campbell, 1991). Non-axisymmetric flow within the conduit ensures mixing of entrained material into the interior of the conduit and the resultant source region may therefore have a characteristic isotope composition dependent on the particular proportions of plume and entrained mantle. Temporal (vertical) variations in buoyancy flux and, therefore, the amount of conductive heat loss and entrainment, provide individual volcanoes with a characteristic proportion of KOO and KEA components. Mixing of the

components is on a small scale with respect to the source volume. The amount of conductive heat loss at the plume margins determines the extent to which a temperature gradient will develop and the subsequent extent to which a transition to alkalic volcanism will develop in the eruptive products, thus identifying variable buoyancy flux in the plume source as the possible mechanism that links isotope composition, major element composition, and late-shield volcanic evolution at any particular shield.

Davies (1992) proposed much larger scale variations in plume buoyancy flux to account for observed undulations in the magnitude of the Hawaiian seafloor swell along approximately 3000 kilometers of the volcanic chain. Smaller scale variations in buoyancy flux, as proposed here, may not produce significant differences in surface uplift, but may best be expressed by variations in the eruptive products of the plume.

ENTRAINED MANTLE SOURCES OF ALKALIC CAP BASALTS

Entrained material that has not yet become mixed into the plume conduit may upwell as a sheath. Hauri et al. (1994) suggested that mantle material viscously coupled to plume flow may provide a mechanism for generating post-shield alkalic capping basalts, and this mechanism works well in the present model. During periods of lesser entrainment and, therefore, lesser viscous coupling as well, the plume produces Koolau-type volcanism, which is noted for the lack of alkalic capping basalts. Intermediate amounts of entrainment produce the characteristic KOO-KEA isotopic mixtures of Kohala-type volcanism, where the alkalic capping lavas, if at all isotopically distinct from shield lavas, are offset toward the KEA component (Fig. 1.6 a). The greatest amount of entrainment, which produces the strongest KEA isotopic signature, is characteristic of Haleakala-type volcanism and associated with alkalic cap lavas that trend toward the PE isotopic component (Fig. 1.6 b).

Because material is progressively entrained from deep to more shallow regions of the ambient mantle (Hauri et al., 1994), the KOO isotopic component is the lowermost mantle feeding the plume and the KEA component is entrained from more shallow mantle. During Kohala-type volcanism, additional KEA material upwells through viscous coupling to plume flow to supply alkalic capping lavas. During Haleakala-type volcanism, entrainment continues to levels where MORB-like mantle (PE component) is available as viscously-coupled material.

CONCLUSIONS

Intershieldd major element differences among Hawaiian subaerial tholeiitic basalts are correlated with intershieldd isotopic differences and are associated with the extent to which a volcano underwent the transition to alkalic basalt volcanism. Statistical analysis shows that correlations between isotope ratios of Pb, Sr, and Nd and abundances of SiO₂, TiO₂, FeO, CaO, and Na₂O are significant at the 99% confidence level. The correlations indicate that the proportion of KEA and KOO components in the late-stage tholeiitic magma source of a volcano is related to whether and to what extent the volcano will undergo the transition from tholeiitic to alkalic volcanism. At endmembers of the compositional spectrum are Koolau-type and Haleakala-type volcanoes, which are products of the sources dominated by the KOO and KEA components, respectively. It is suggested here that Koolau-type volcanoes are the result of melting of a plume with the steep marginal temperature gradient, which accounts for production of large degrees of melt followed by an abrupt termination as the volcano moves off of the plume. Haleakala-type volcanoes are the result of melting of a plume with a long lateral temperature gradient, where large degree melts are followed by continued melt production of increasingly smaller degree. Variations in source buoyancy can account for the different temperature gradients that develop within the plume.

The largest temperature gradient is developed during periods of lesser source buoyancy, through increased conductive heat loss to the surrounding mantle. Because heat conducted into surrounding mantle causes entrainment, maximum entrainment is associated with the KEA component. In this model, the KOO component dominates the initial mantle plume, and the KEA component is entrained in amounts proportional to variations in initial plume buoyancy. The model implies that the KOO component represents the initial source for all plumes; however, the lowermost mantle may comprise a variety of isotopic components, where KOO is the main one in lowermost Hawaiian mantle. In contrast, the KEA component, in its various forms (PHEM, C, FOZO), is an ubiquitous isotopic endmember in most plumes that produce ocean island volcanoes and, therefore, is apparently a common entrained component (Hart et al., 1992; Hauri et al., 1994).

In this model, temporal variations originating in the deep mantle result in lateral variations at the surface, which provide for systematic differences in late-stage evolution of volcanoes. Although deep mantle major element heterogeneity cannot be ruled out, it is not required. Variations or pulses in the initial source temperature can create variations in source buoyancy, and thus the subsequent variations in conduit deflection, entrainment, melt conditions, and melt geochemistry. The model generalizes the geochemical observations to identify a single mechanism that relates major element variability to isotopic variability to eruptive evolution of Hawaiian plume volcanoes.

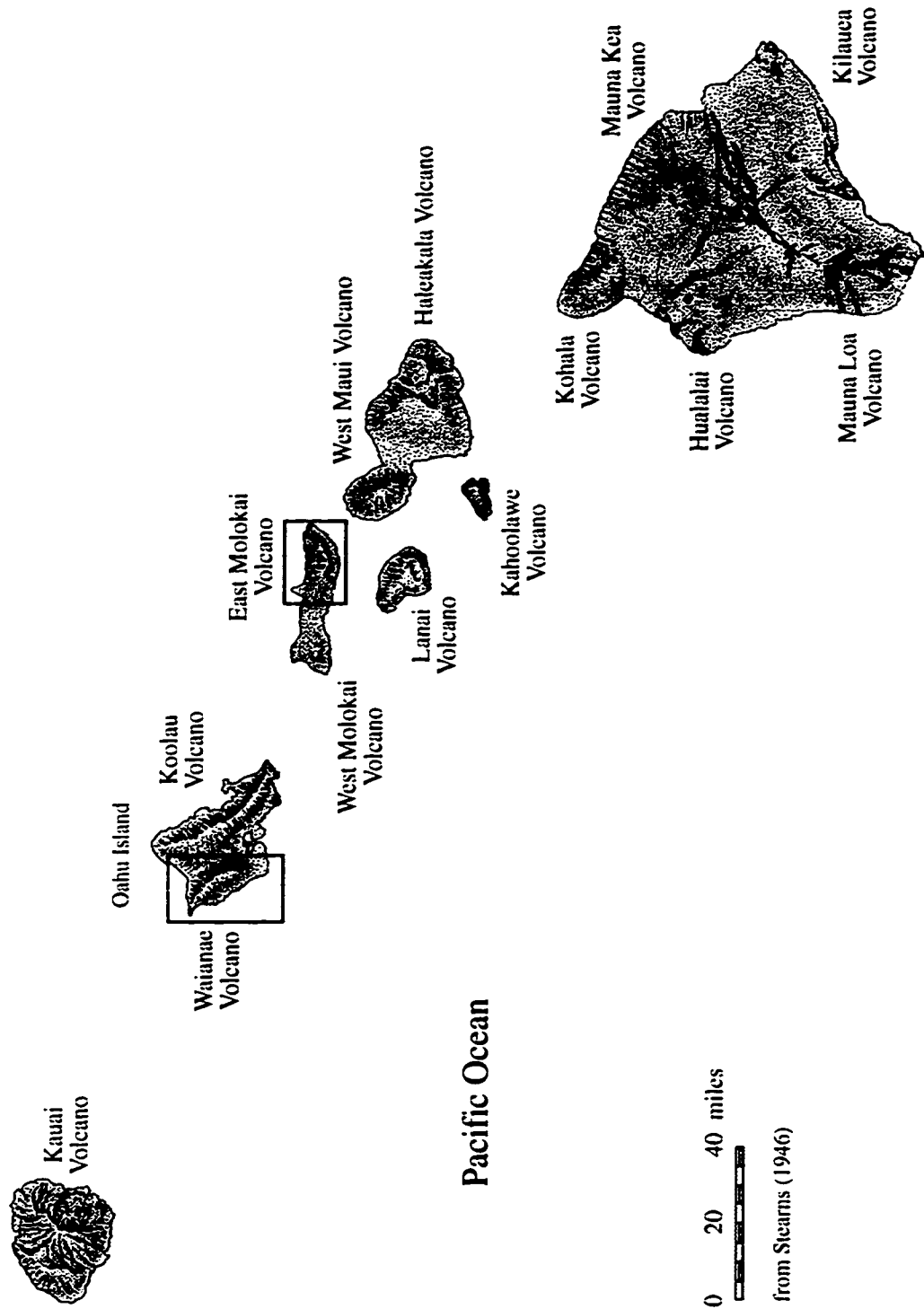


Figure 1.1 Hawaiian Islands with Case Study Areas Identified - Waianae and East Molokai Volcanoes

KOO, KEA, and PE component data after Stille et al. (1986) and West and Leeman (1987). Some East Molokai and Waianae data from Chapters 3, 5. Other data from Chen and Frey (1985), Chen et al. (1991), Hart (1988), Hegner et al. (1986), Hofmann et al. (1987), Kennedy et al. (1991), Roden et al. (1984; 1994), Stille et al. (1983), Stille et al. (1986), Tatsumoto (1978), West and Leeman (1987), West et al. (1987).

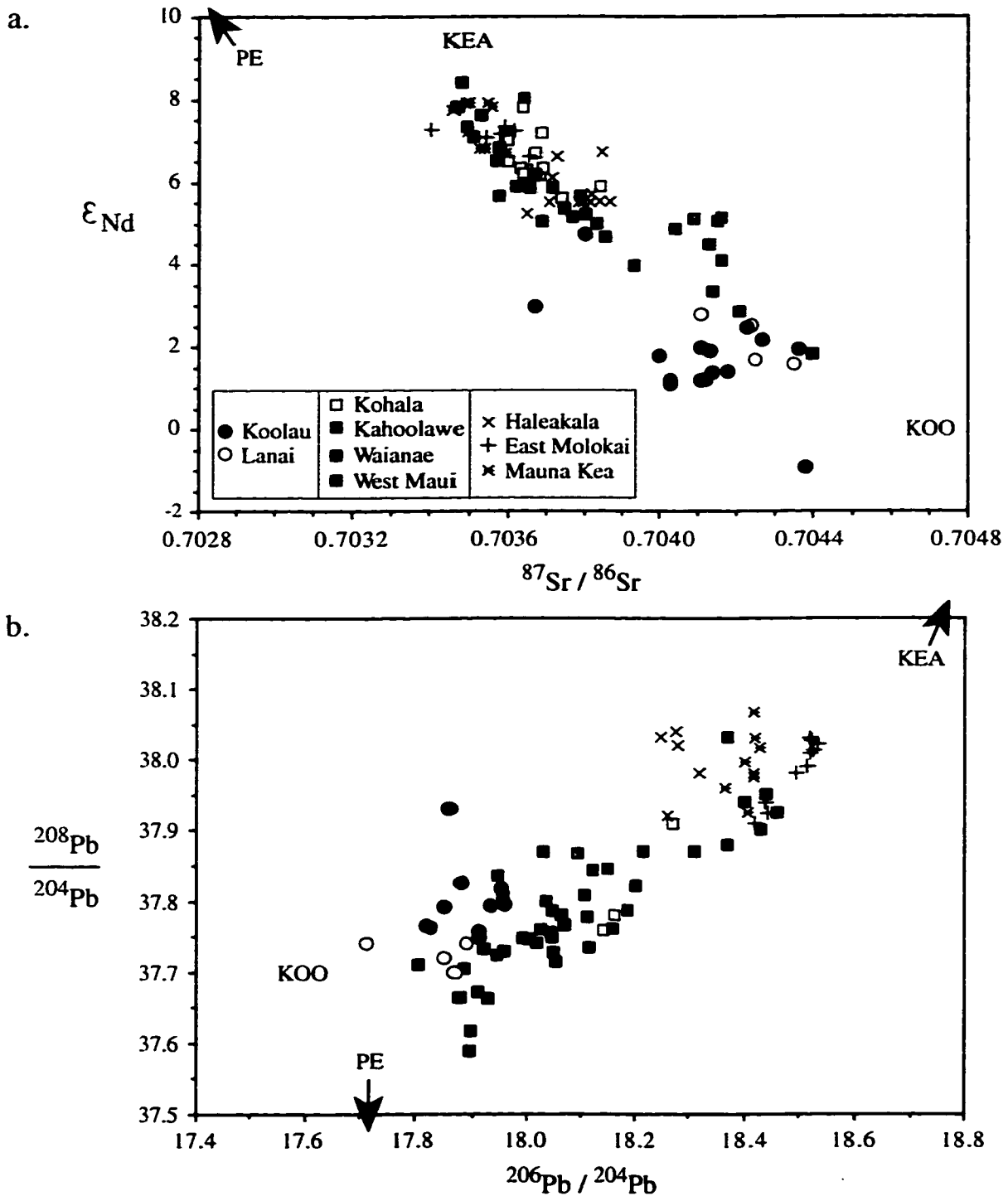


Figure 1.2 a) $^{87}Sr/^{86}Sr$ vs. ϵ_{Nd} b) $^{206}Pb/^{204}Pb$ vs. $^{208}Pb/^{204}Pb$ for Subaerial Tholeiites of Hawaiian Volcanoes with Shield-Building Stage Complete (see text for exclusions)

Data from sources listed in Fig.1.1 and from Macdonald and Katsura (1964), Beeson (1976), Bonhommet et al. (1977), Feigenson et al. (1983), Frey et al. (1990), Frey et al. (1991) Lanphere and Frey (1987), Fodor et al. (1992), West et al. (1992), Frey et al. (1994), Leeman et al. (1994).

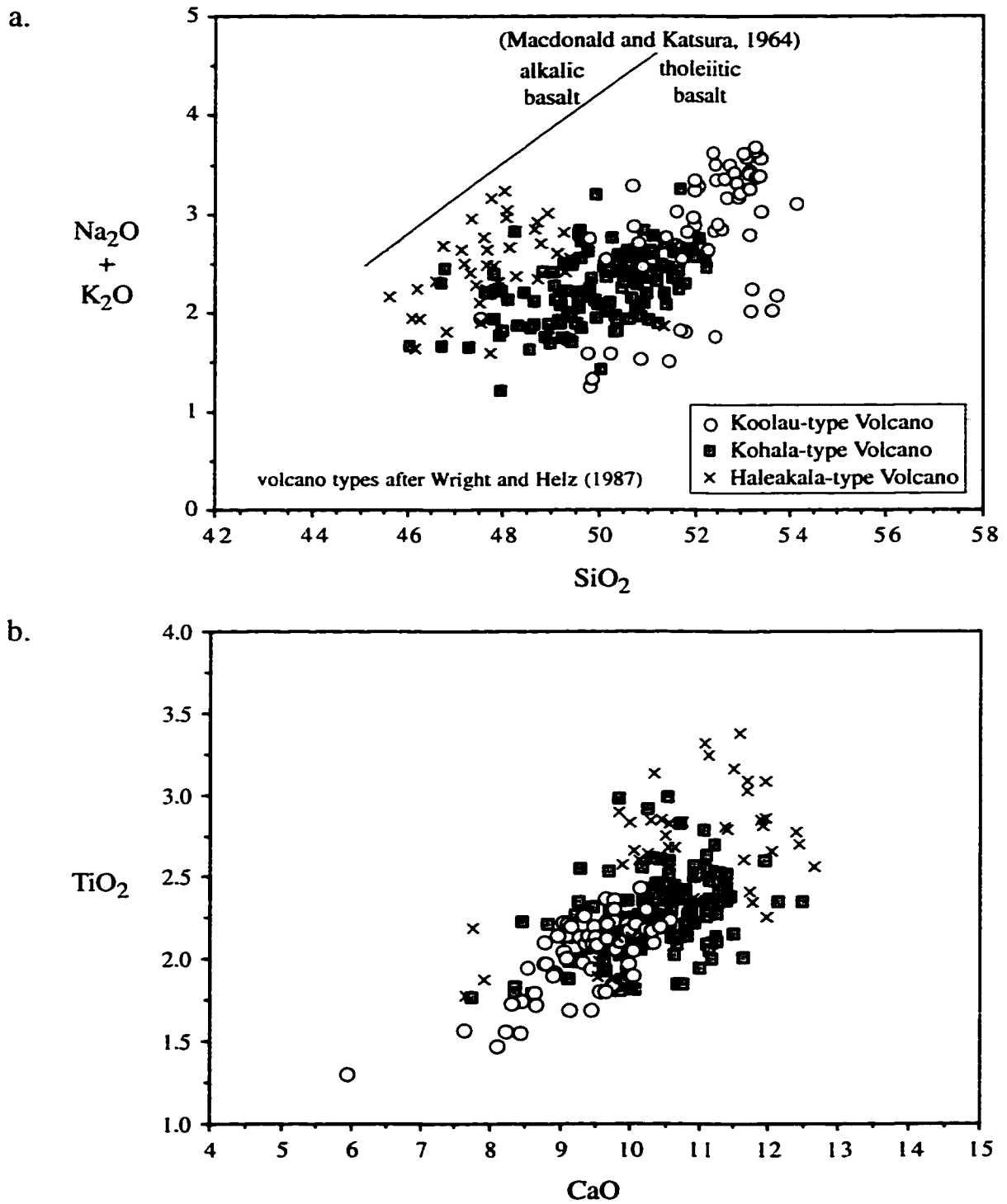


Figure 1.3 a) SiO₂ vs. Total Alkalis and b) CaO vs. TiO₂ for Hawaiian Subaerial Tholeiites (>7 wt% MgO) Grouped by Volcano-Type

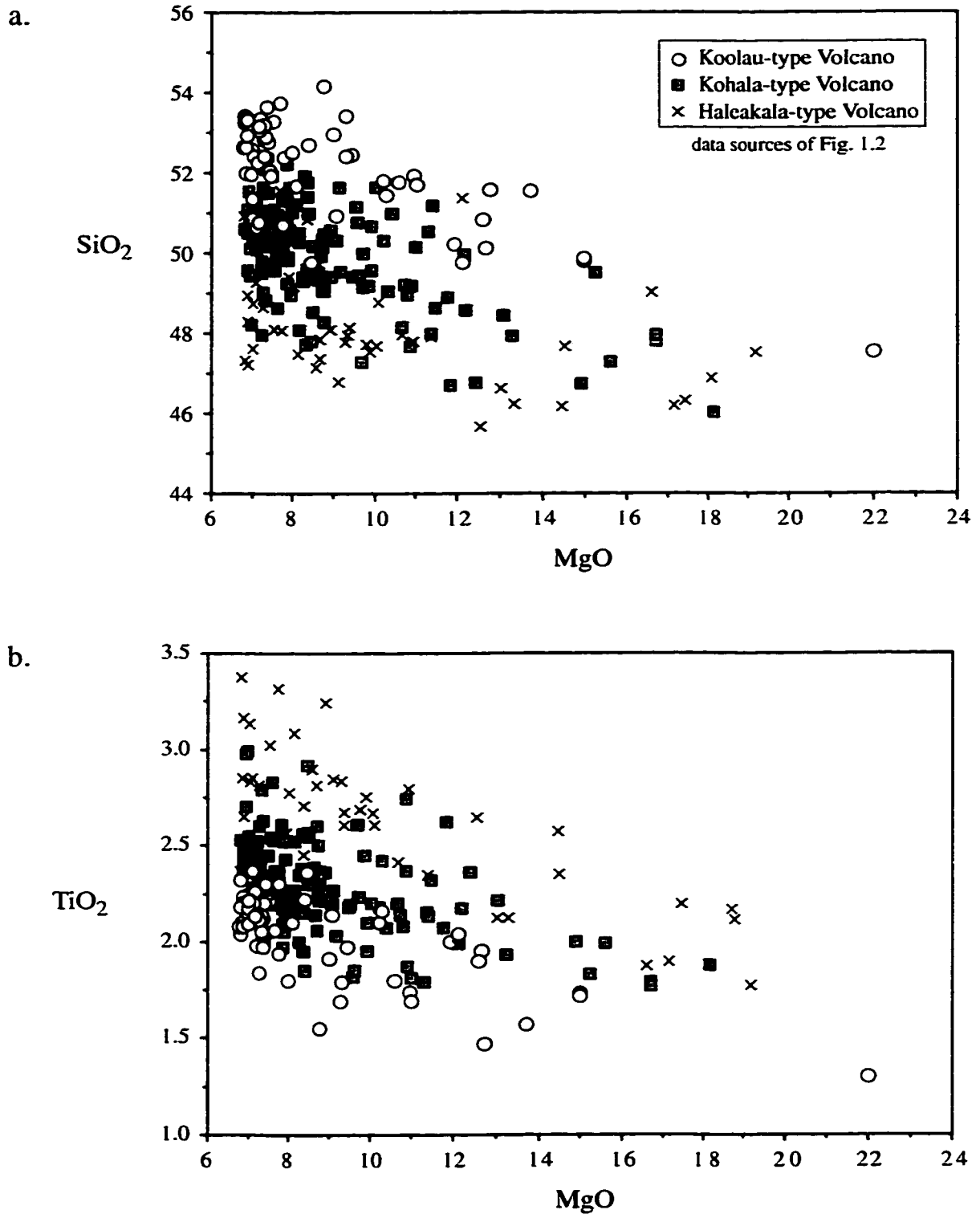


Figure 1.4 a) MgO vs. SiO₂ and b) MgO vs. TiO₂ (wt%) for Hawaiian Subaerial Tholeiites Grouped by Volcano-Type

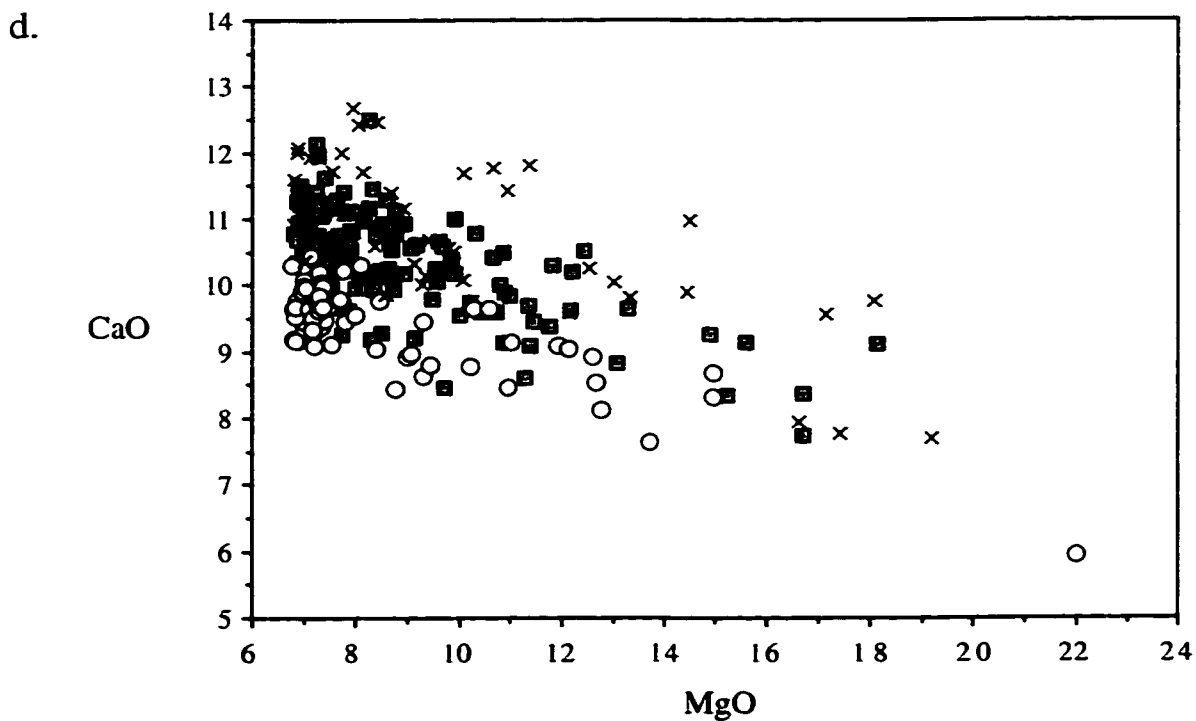
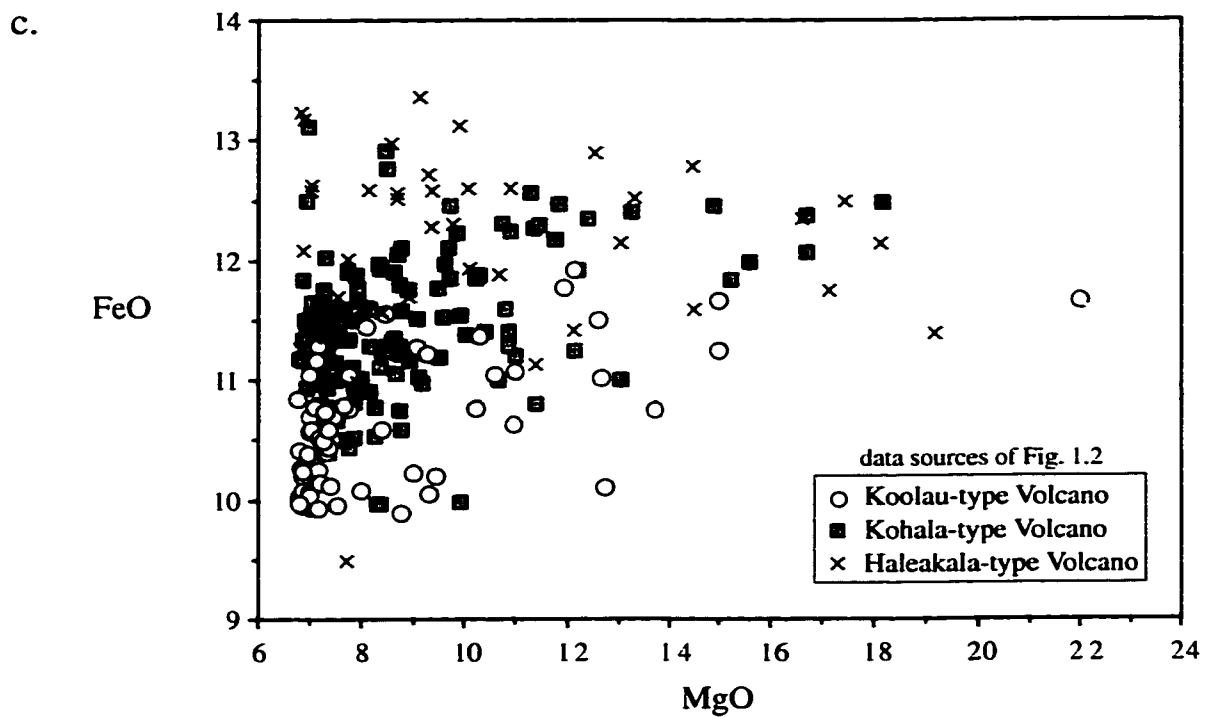
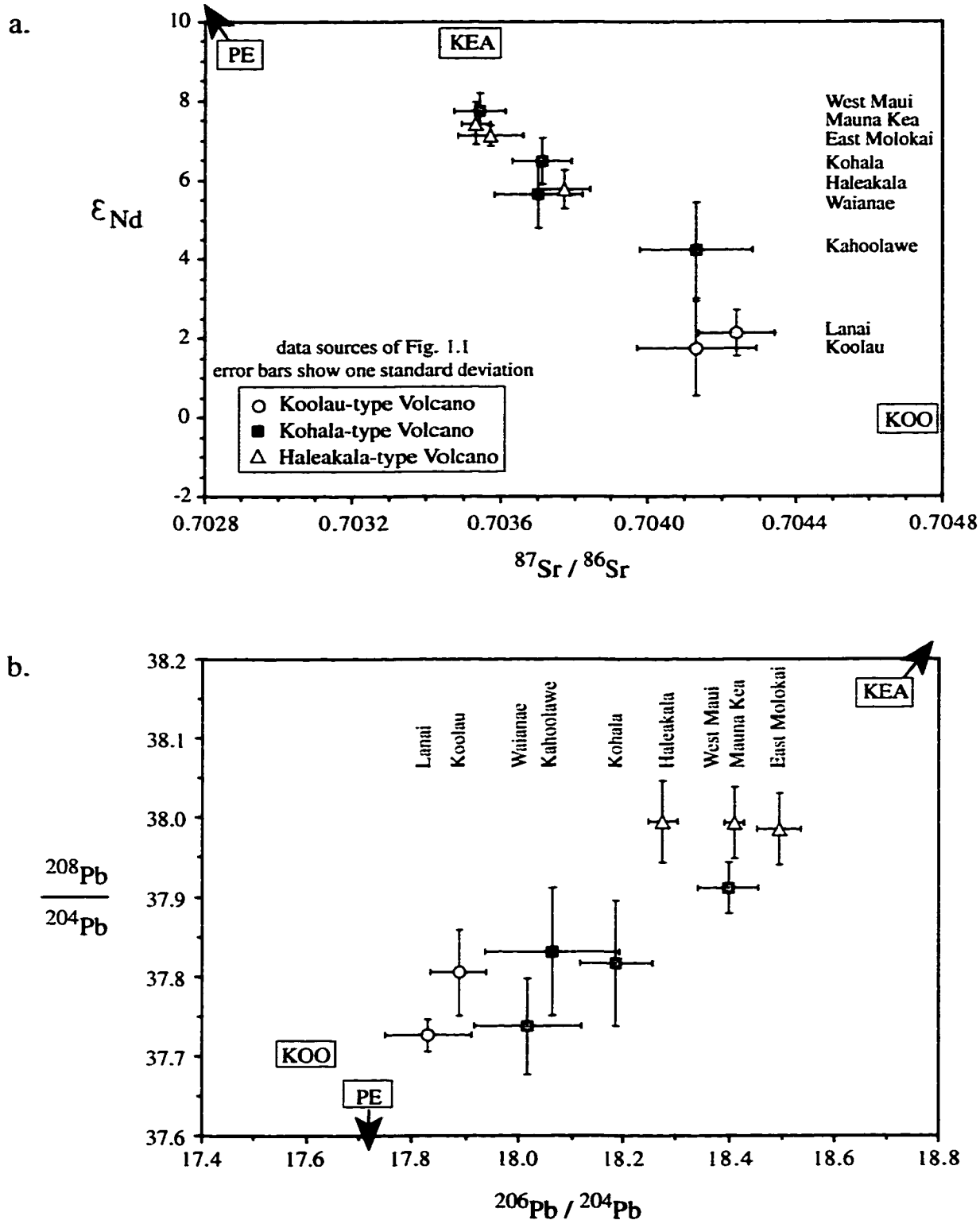


Figure 1.4 (continued) c) MgO vs. FeO and d) MgO vs. CaO (wt%) for Hawaiian Subaerial Tholeiites Grouped by Volcano-Type



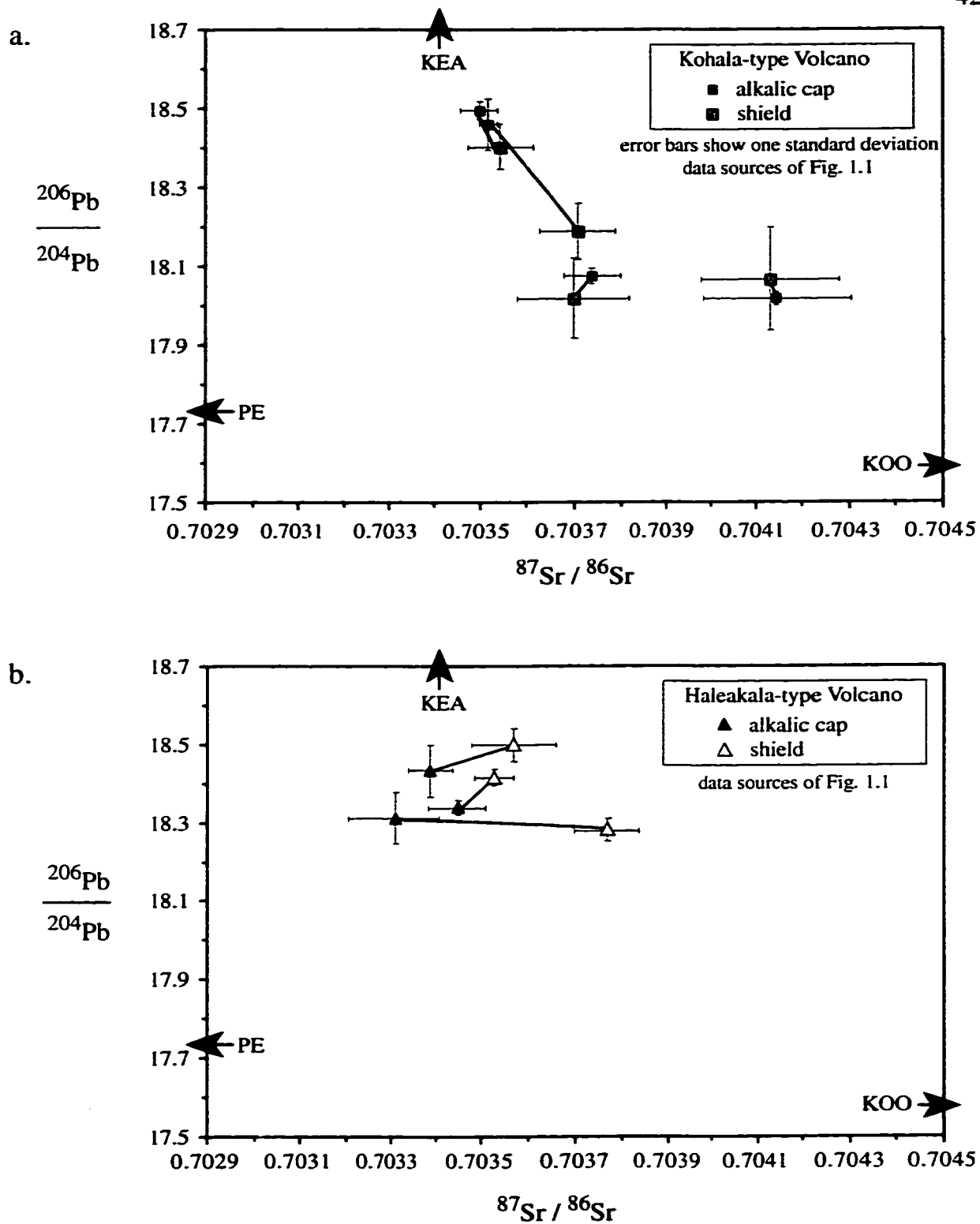
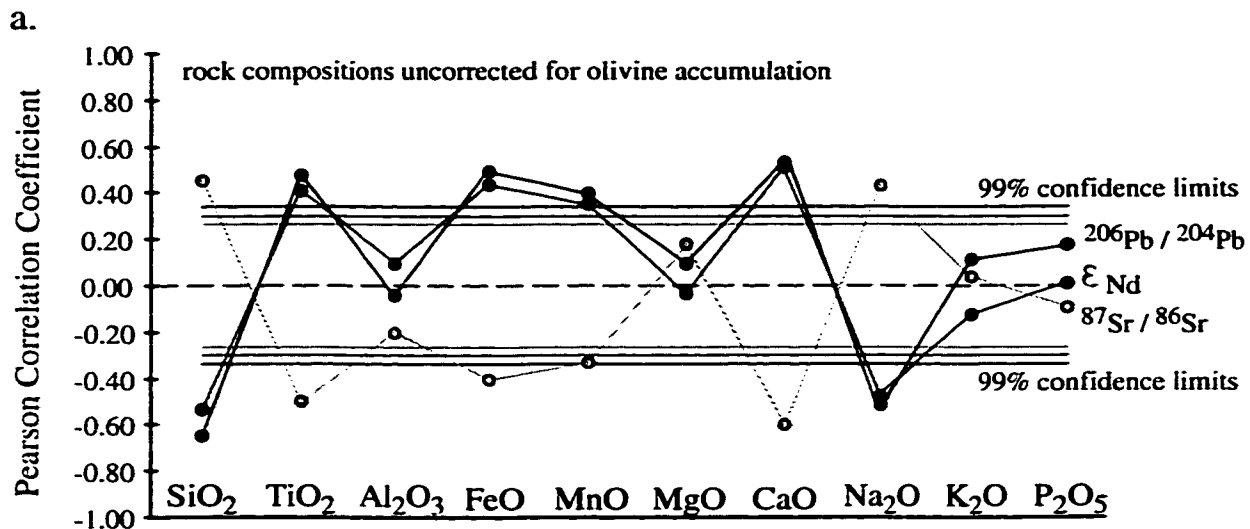


Figure 1.6 $^{87}\text{Sr}/^{86}\text{Sr}$ vs. $^{206}\text{Pb}/^{204}\text{Pb}$ Averaged Isotopic Compositions for a) Kohala-type and b) Haleakala-type Tholeiites and their Respective Alkali Basalt Caps



Data sources of Figs. 1.1 and 1.2. 99% confidence limits are values above which the relationship between a particular major element content and a specified isotope ratio is a statistically significant correlation at the 99% confidence level (Rollinson, 1993). The database is weighted according to number of samples from each volcano with analyses of both major element compositions and isotope ratios of Sr, Nd, or Pb (East Molokai: 2, 2, 3; Haleakala: 10, 10, 3; Kahoolawe: 7, 7, 7; Kohala: 23, 12, 3; Koolau: 12, 6, 3; Lanai: 3, 3, 3; Mauna Kea: 7, 6, 5; West Maui: 4, 4, 4; Waianae: 9, 9, 16).

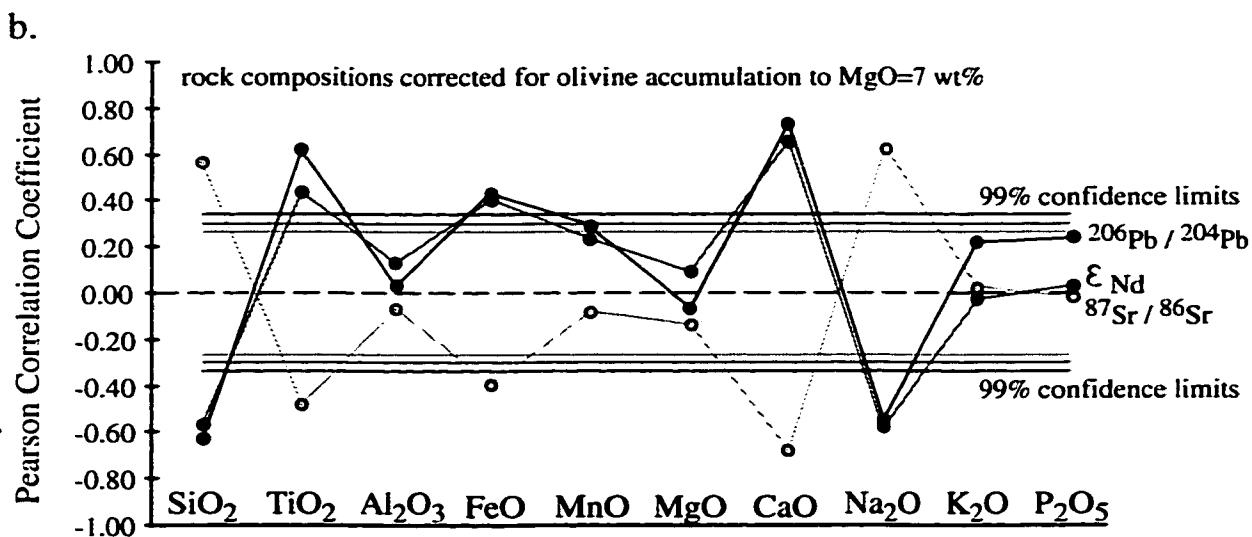


Figure 1.7 Calculated Pearson Correlation Coefficients for Pb, Sr, Nd isotope ratios with each major element a) uncorrected for olivine and b) corrected for olivine accumulation.

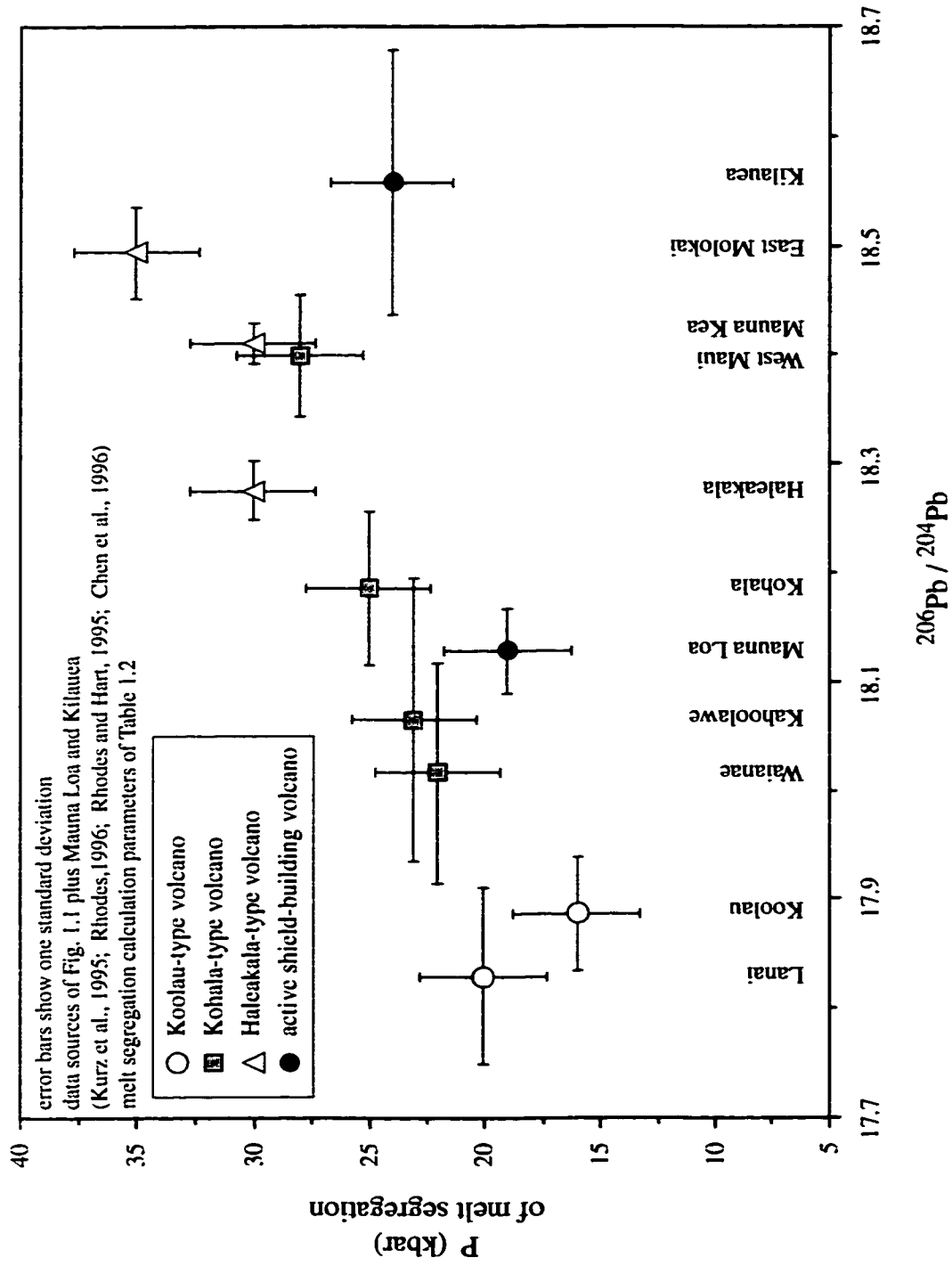


Figure 1.8 $^{206}\text{Pb}/^{204}\text{Pb}$ vs. Calculated Average Pressure of Magma Segregation for Subaerial Tholeiites from Individual Volcanoes

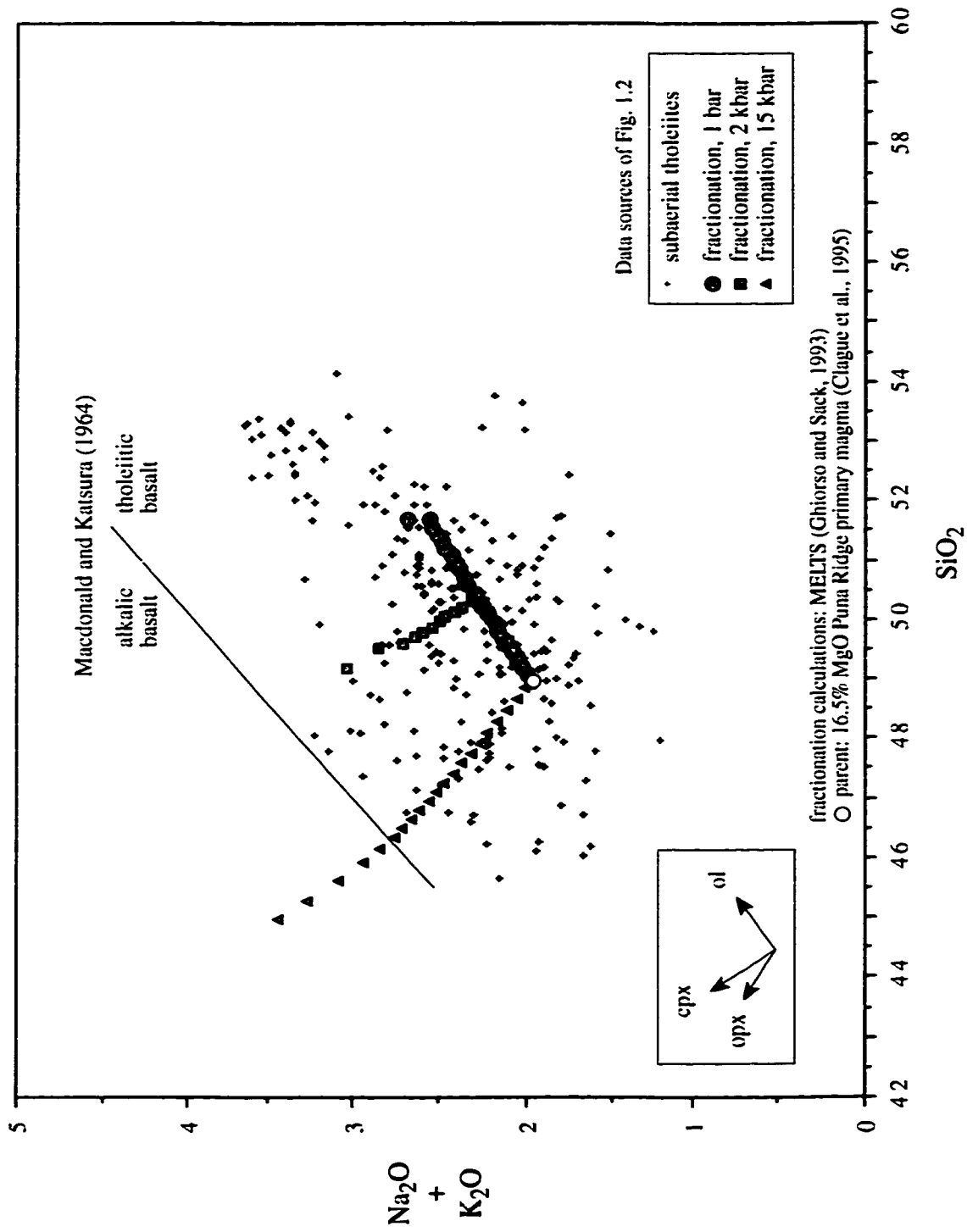


Figure 1.9 a) SiO_2 vs. Total Alkalis for Subaerial Hawaiian Tholeiites and Effects of Mineral Fractionation

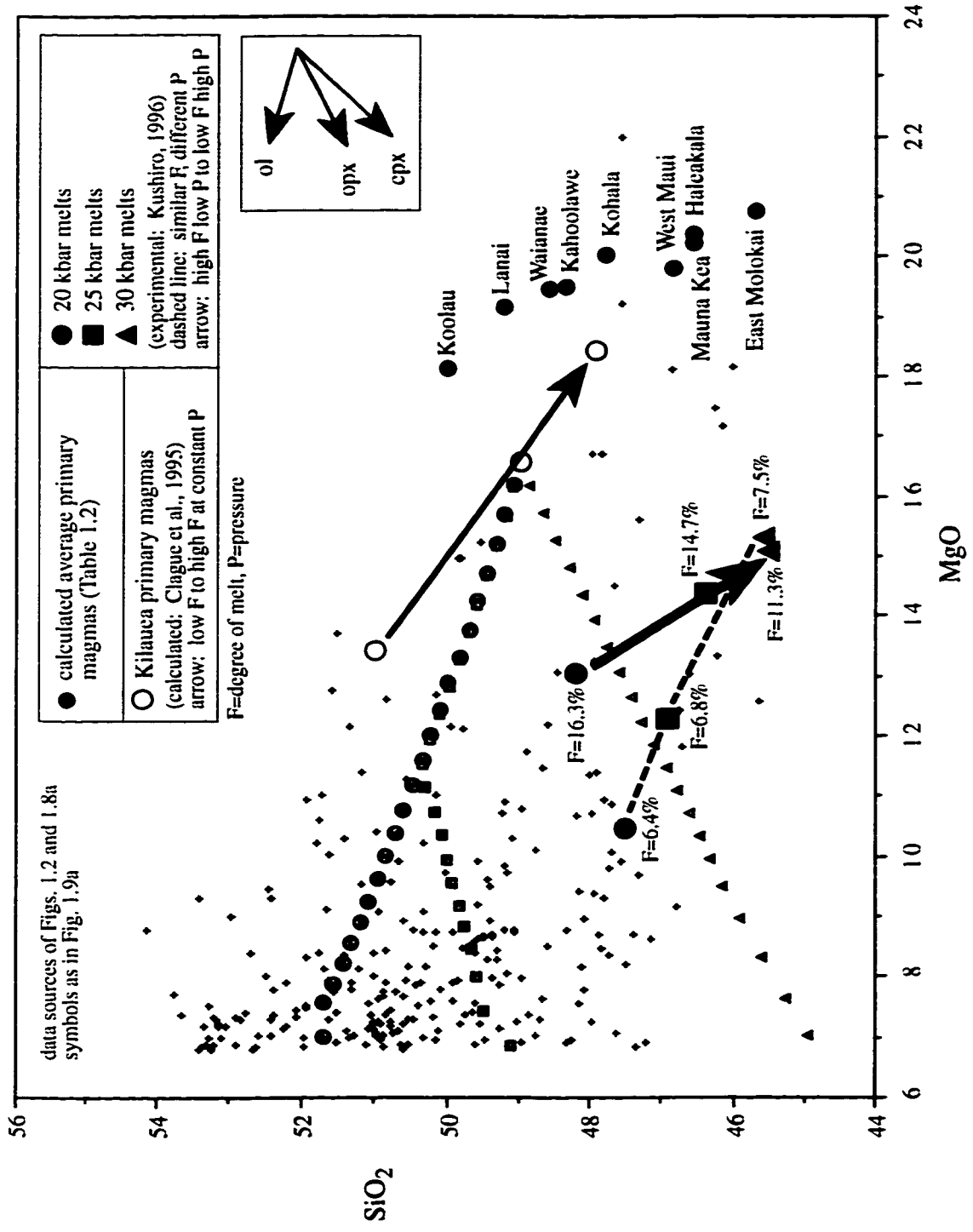


Figure 1.9 (continued) b) MgO vs. SiO₂ for Subarcial Hawaiian Tholeiites and Effects of Mineral Fractionation and Partial Melting 46

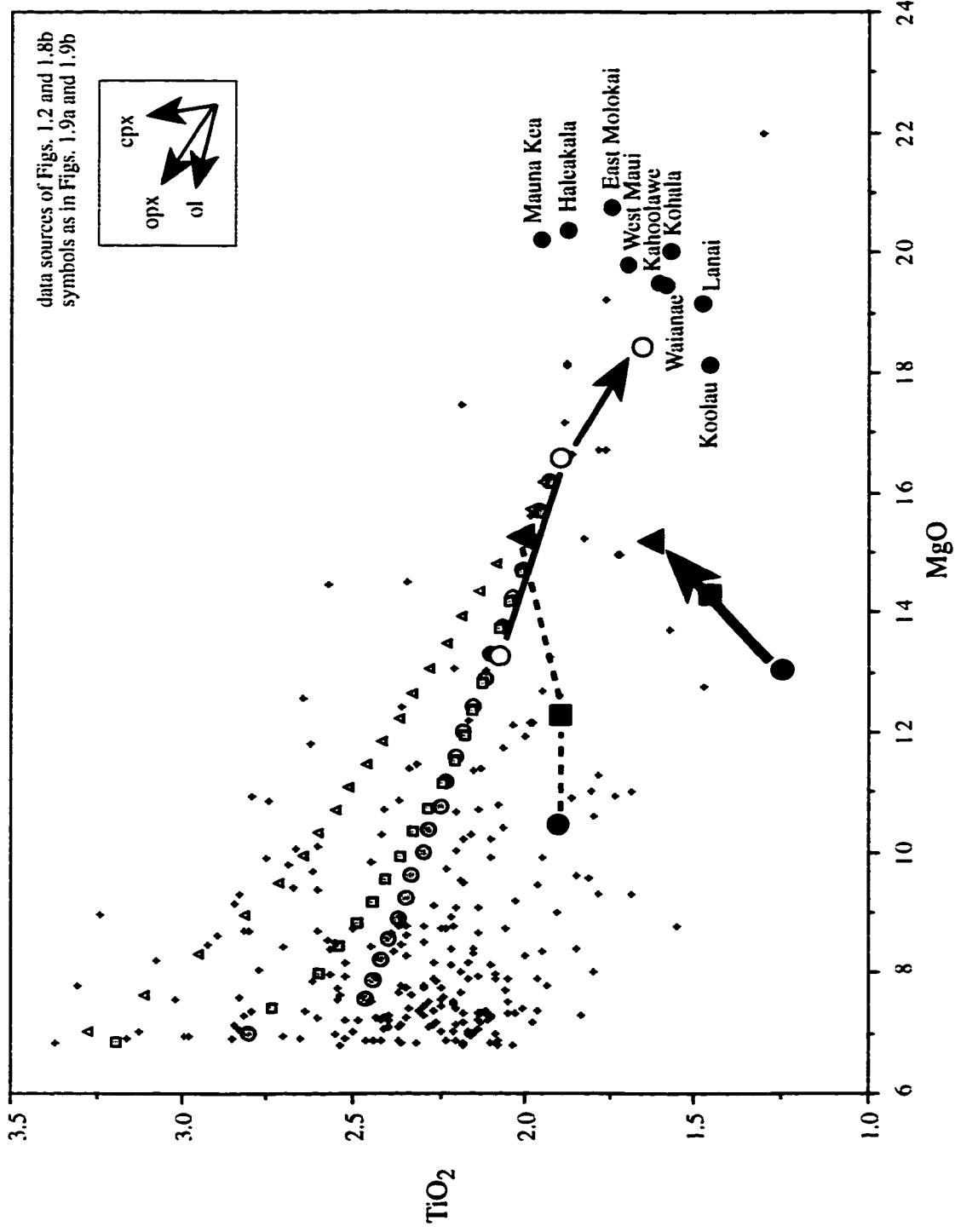


Figure 1.9 (continued) c) MgO vs. TiO_2 for Subaerial Hawaiian Tholeiites and Effects of Mineral Fractionation and Partial Melting

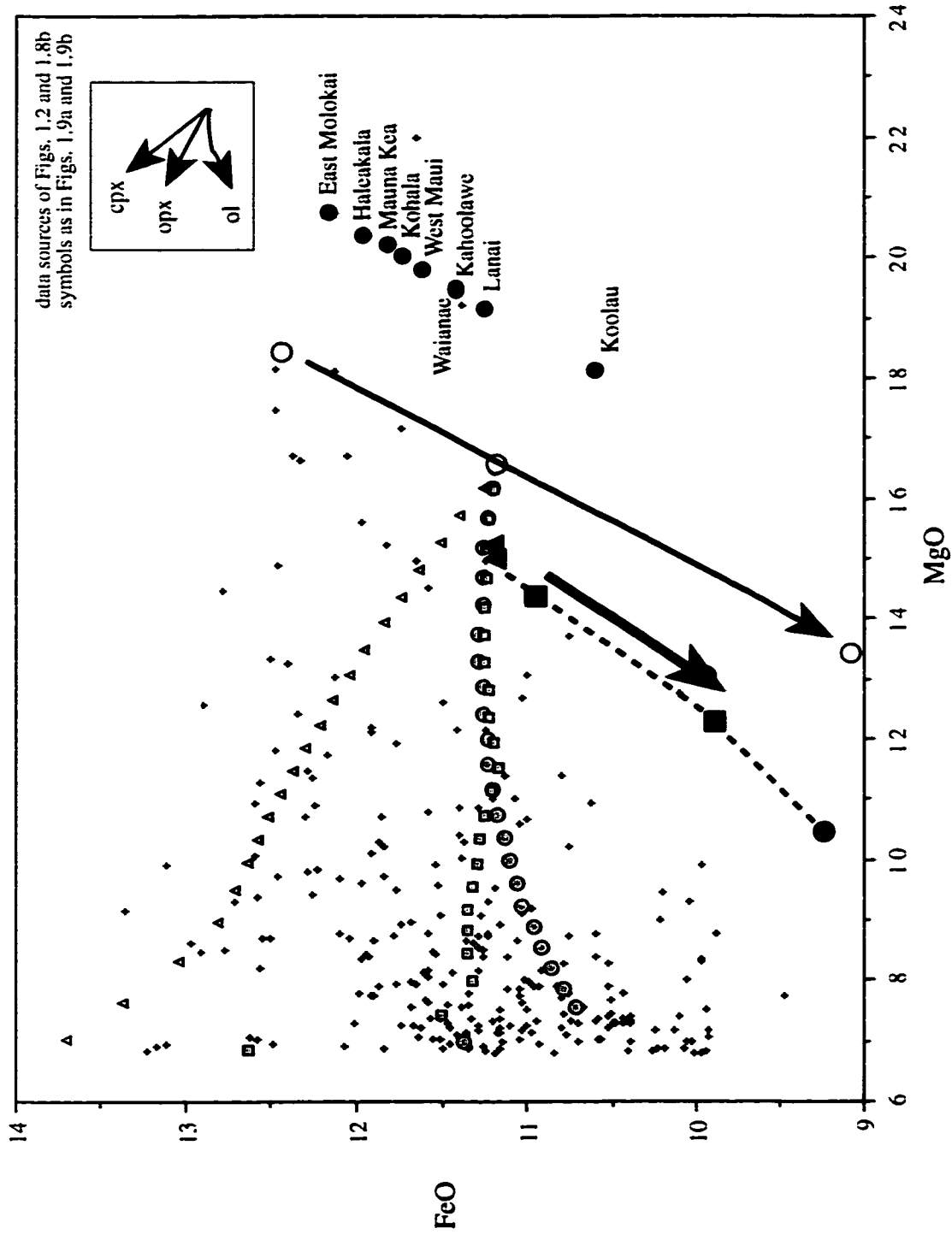


Figure 1.9 (continued) d) MgO vs. FeO for Subaerial Hawaiian Tholeiites and Effects of Mineral Fractionation and Partial Melting

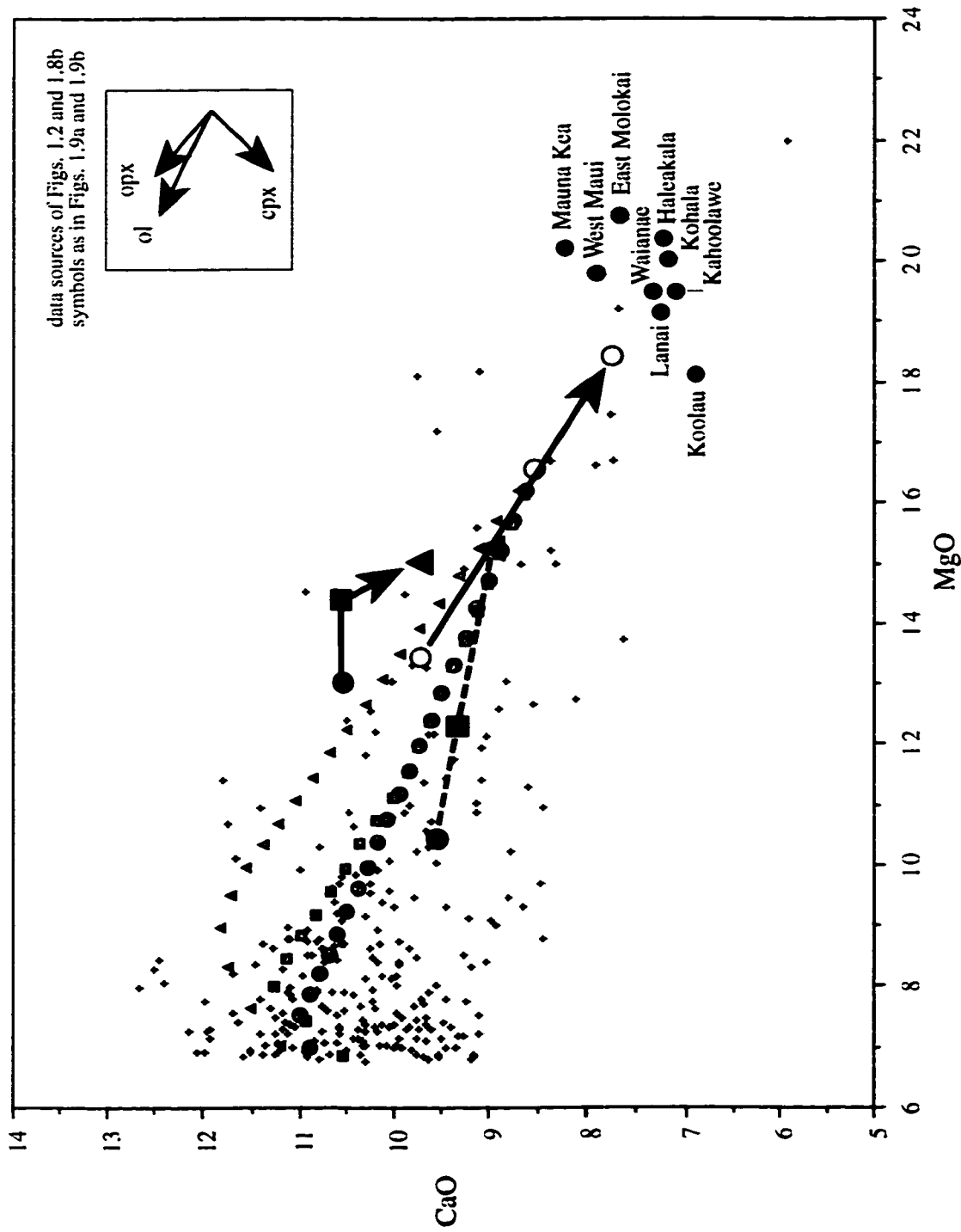


Figure 1.9 (continued) e) MgO vs. CaO for Subaerial Hawaiian Tholeiites and Effects of Mineral Fractionation and Partial Melting

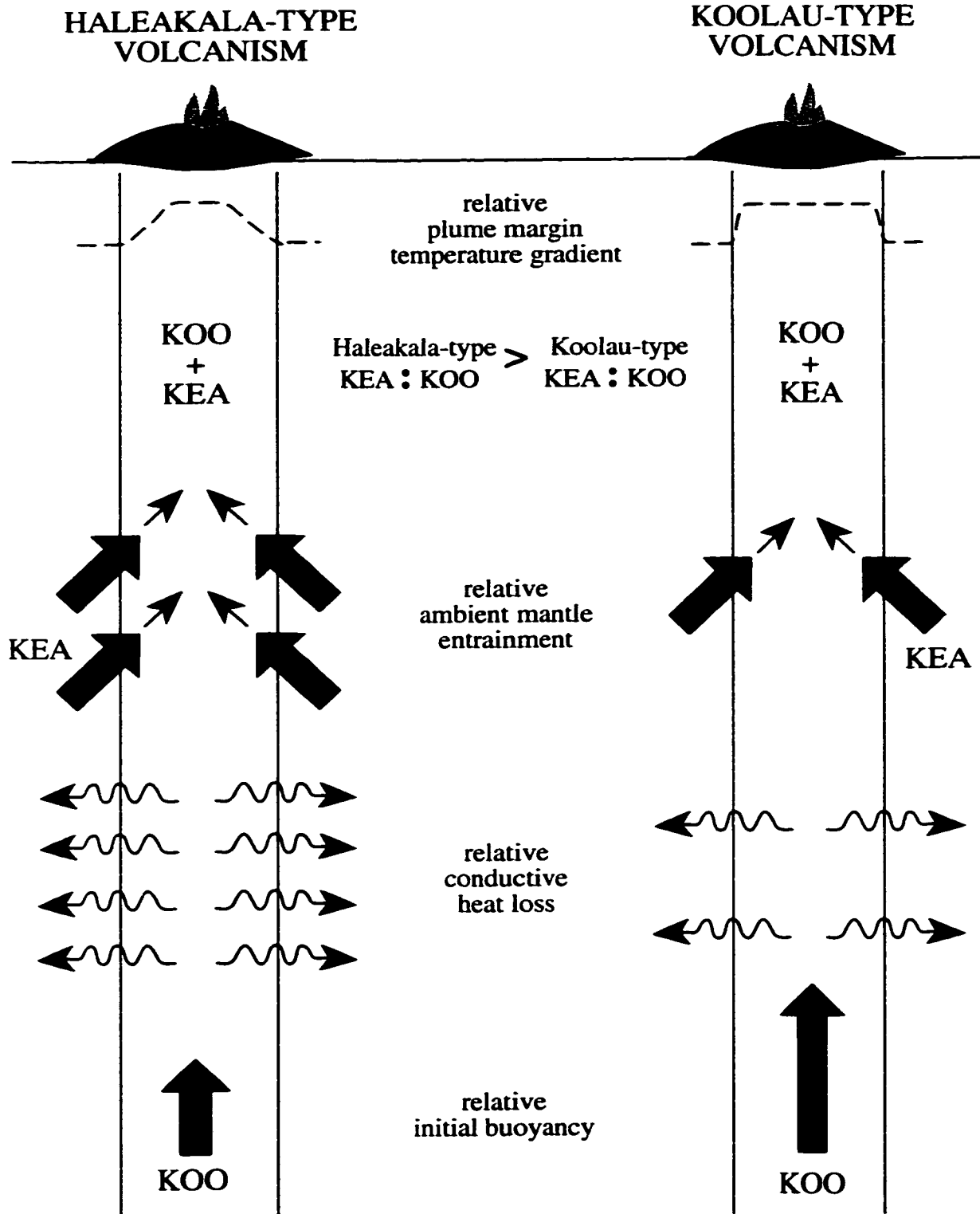


Figure 1.10 Schematic Model of Mantle Plume Variations that Produce Late-Shield Geochemical Differences between Koolau-type and Haleakala-type Volcanoes

Table 1.1 Hawaiian Volcano-type Classification

Category	Late shield description	Volcanoes ^a
Haleakala-type	The tholeiitic sequence passes into a thick transitional zone of interbedded tholeiite, transitional basalt, and ankaramite, with no apparent erosional break separating it from the overlying cap of hawaiite and mugearite.	Haleakala Mauna Kea East Molokai
Kohala-type	Lacks abundant mafic alkalic rocks. The tholeiitic sequence in places is interbedded with alkalic basalts below an erosional unconformity separating it from an overlying thin cap of hawaiite and mugearite.	Kohala Waianae West Maui Kahoolawe
Koolau-type	Lacks or has few alkalic flows at the top of the tholeiitic sequence.	Koolau Lanai
Other	Shield volcanism active	Mauna Loa Kilauea

Modified after Macdonald and Katsura (1964), Wright and Heiz (1987).
^aExcluded due to lack of data: Niihau, Kauai, West Molokai, Hualalai (see text).

Table 1.2 Calculated Average Isotopic Compositions for Hawaiian Subaerial Tholeiites

	Calculated Average $^{206}\text{Pb}/^{204}\text{Pb}$	s.d.	Calculated Average $^{208}\text{Pb}/^{204}\text{Pb}$	s.d.	n	Calculated Average $^{87}\text{Sr}/^{86}\text{Sr}$	s.d.	n	Calculate Average ϵ_{Nd}	s.d.	n
Koolau	17.888	0.052	37.804	0.054	9	0.70413	0.00016	22	1.77	1.19	15
Lanai	17.831	0.080	37.725	0.020	4	0.70424	0.00010	4	2.15	0.59	4
Kohala	18.187	0.071	37.816	0.079	3	0.70371	0.00008	27	6.47	0.58	14
Kahoolawe	18.066	0.130	37.830	0.080	10	0.70413	0.00015	10	4.23	1.20	10
Waianae	18.017	0.102	37.736	0.061	36	0.70370	0.00012	15	5.62	0.84	15
West Maui	18.401	0.056	37.911	0.032	7	0.70354	0.00006	7	7.72	0.44	7
Haleakala	18.277	0.027	37.994	0.051	5	0.70377	0.00007	13	5.75	0.49	11
East Molokai	18.495	0.042	37.984	0.045	10	0.70357	0.00009	6	7.10	0.26	6
Mauna Kea	18.412	0.019	37.993	0.045	8	0.70353	0.00004	10	7.41	0.53	9

s.d. = standard deviation, n = number of samples. Some Waianae and East Molokai data from Chapters 3, 5. Other data from Chen and Frey (1985); Chen et al. (1991); Hegner et al. (1986); Hofmann et al. (1987); Kennedy et al. (1987); Lanphere and Frey (1987); Roden et al. (1984); Roden et al. (1994); Stille et al. (1983); Stille et al. (1986); Tatsumoto (1978); West and Leeman (1987); West et al. (1987)

Table 1.3 Calculated Primary Magma Compositions and Melt Segregation Conditions

Volcanic suite of tholeiitic basalts	Fo content average accumulated olivine	Calculated primary magma compositions (wt%)										Calculated melt segregation conditions		
		SiO ₂	TiO ₂	Al ₂ O ₃	FeO	MnO	MgO	CaO	Na ₂ O	K ₂ O	P ₂ O ₅	T (°C)	P (kbar)	
Subaerial late shield														
Koolau	86.4	50.1	1.44	10.6	10.7	0.13	18.1	6.97	1.94	nd	0.18	1501	16	
Lanai	85.7	49.2	1.47	10.2	11.3	0.13	19.1	7.30	1.13	0.05	0.08	1529	20	
Kohala	83.5	47.8	1.57	10.2	11.7	0.13	20.0	7.19	1.22	nd	0.14	1559	25	
Kahoolawe	83.9	48.3	1.61	9.9	11.4	0.13	19.5	7.35	1.62	nd	0.14	1544	23	
Waianae	83.0	48.5	1.57	9.7	11.4	0.12	19.5	7.16	1.54	0.34	0.16	1541	22	
West Maui	82.1	46.9	1.70	10.2	11.6	0.13	19.7	7.93	1.39	0.21	0.17	1561	28	
Haleakala	86.5	46.6	1.88	9.9	12.0	0.15	20.4	7.26	1.61	0.10	0.18	1577	30	
East Molokai	86.5	45.7	1.75	10.1	12.2	0.15	20.7	7.72	1.47	nd	0.18	1593	35	
Mauna Kea	83.2	46.6	1.96	9.4	11.8	0.13	20.2	8.21	1.41	0.05	0.21	1574	30	
Subaerial active shield														
Mauna Loa	86.7	49.4	1.48	9.8	11.0	0.14	18.7	7.55	1.55	0.25	0.16	1519	19	
Kilauea	86.2	48.0	1.79	9.4	11.4	0.14	19.4	7.86	1.64	0.28	0.16	1545	24	
Submarine														
Mauna Loa glass		49.4	1.53	10.1	10.7	0.12	18.2	7.93	1.61	0.23	0.13	1508	18	
Kilauea glass		48.6	1.69	9.8	11.2	nd	19.1	7.67	1.53	0.28	0.17	1533	21	
Haleakala glass		48.5	1.81	9.7	11.1	0.16	18.9	7.73	1.67	0.27	0.16	1530	21	
Fo = forsterite, nd = not determined														

CHAPTER 2

Magnetostratigraphic Subdivision and Stratigraphic Relations at Waianae Volcano, Oahu, Hawaii

ABSTRACT

The composite subaerial stratigraphic sequence of Waianae Volcano is based on magnetic polarity reversals identified in lava flow sequences. The magnetic polarity units are described in detail at the type sections for the existing lithostratigraphy. The detail provided by the coupled lithostratigraphic and magnetostratigraphic subdivision makes Waianae the most stratigraphically well-understood of the Hawaiian volcanoes. The time-stratigraphic nature of the units and the distinct nature of the boundaries allow correlation between sections, thus providing an unambiguous basis for stratigraphic relations and interpretations. Precaldera flows comprise a nearly 800 meters-thick composite (two parts) subaerial section, the upper approximately 200 meters of which is previously unrecognized in formal type or reference section. The relation between the precaldere lithostratigraphic and magnetostratigraphic boundaries indicates previous lithologic mapping is incomplete and future mapping can be better constrained. The stratigraphic resolution provided by the magnetostratigraphy at Waianae evidences the need to supplement the traditional lithologic subdivision of Hawaiian volcanoes.

INTRODUCTION

The stratigraphic sequences of Hawaiian volcanoes traditionally have been subdivided by lithology, aided in many cases by the early recognition that a volcano evolves from a tholeiitic basalt shield to an alkalic basalt cap, and by obvious structural evidence, such as flow orientations. However, boundaries between lithologic members are arbitrary because changes in the magma system generally are not abrupt. Consequently, it can be extremely difficult to define a distinct, correlatable boundary between rock lithologies. Various exposed sections of a particular volcano may be assigned to a particular lithologic member, but the relative position of any particular section in the overall volcanic stratigraphy can be ambiguous. Understanding relations between stratigraphic sections is crucial to any interpretation of the growth history of a Hawaiian volcano, particularly as studies at individual volcanoes become increasingly detailed.

This report emphasizes the utility of magnetostratigraphic subdivision where accumulation of basaltic material, as at many Hawaiian volcanoes, creates thick sections of lithologically similar flows, yet records several reversals of the earth's magnetic field. Preserved magnetic polarity reversals are easily located and readily correlated over different parts of the volcano, and are good approximations to isochronous surfaces, giving temporal significance to magnetostratigraphic units. Magnetostratigraphy has been used previously in stratigraphic studies at Hawaiian volcanoes (e.g., Holcomb, 1985; Bogue, 1987), but has generally been viewed as an informal aid to lithostratigraphic subdivision. The results of this study show that magnetostratigraphic subdivision can provide an additional, effective means of defining relations among stratigraphic sections at an individual volcano.

OBJECTIVES

This report is the result of a field study of Waianae Volcano (Figure 2.1), the westernmost of two volcanoes that make up the island of Oahu (Fig. 1.1). The study is based on previous work in lithostratigraphy (Sinton, 1987) and magnetostratigraphy (Holcomb et al., 1993). Sinton (1987) revised the original volcanic subdivision (Stearns, 1935) by formally recognizing the Lualualei Member (tholeiite shield stage), Kamaileunu Member (transitional late-shield stage), and Palehua Member (hawaiiite postcaldera stage).

However, as is typical for Hawaiian volcanoes, the descriptions of the Members and their boundaries provide little detail to assemble a composite stratigraphic column or to relate the various exposed sections of the volcano. Greater detail in stratigraphic relations was provided by Holcomb et al. (1993), who used a portable fluxgate magnetometer to identify a series of magnetic polarity reversals preserved in the flows, and subdivided the stratigraphic sequence into magnetic polarity units. These works are extended here with the results of a detailed lithologic and magnetostratigraphic field study of Kamaileunu Ridge, Puu Paheehē, and the bounding ridges of Nanakuli Valley (Figure 2.1), in order to describe the composite stratigraphy for the subaerial portion of Waianae Volcano. The importance of the study is threefold:

1. Waianae Volcano is the focus of a study on volcanic geochemical evolution (Chap. 3) for which a detailed understanding of the stratigraphic sequence in the sampling area is necessary.
2. The study area contains the identified magnetic polarity intervals of Holcomb et al. (1993), which are described here. This work emphasizes the importance of magnetic

polarity units as easily located, readily mapped units with unambiguous time-stratigraphic significance.

3. The study area contains the formal type sections for the Lualualei, Kamaileunu, and Palehua Members (Sinton, 1987). Because the magnetic polarity units are described at the Member type sections (except the Nanakuli (N) unit; see Results), the time-stratigraphic relations of Members to each other and to other sections of the volcano are clarified based on relations to the polarity units. In addition, field descriptions of the polarity units (Appendix B) provide greater lithologic detail than currently available for the Members.

PREVIOUS WORK

STRATIGRAPHY

Stearns (1935) ascribed the structural features of Waianae Volcano to a growth history typical of Hawaiian volcanoes. The bulk of the volcano was built by frequent, voluminous fissure eruptions of olivine basalt, culminating in decreased flank eruptions and caldera collapse. As lavas were impounded by caldera walls, a weathering horizon developed over the flanks of the volcano consisting of windblown ash from caldera fire fountains and soil. When lava overflowed the caldera walls, the outer slopes of the volcano were covered again. The structural features of Waianae volcano prompted Stearns (1935) to subdivide the Waianae Volcanic Series into lower, middle, and upper members. The lower member, comprising shallow-dipping shield-building flows, is separated from the horizontal impounded flows of the middle member by ancient buried cliffs and talus breccias. The upper member consists of flows that overtopped the impoundments and capped the upper parts of the volcano. The boundary between the middle and upper members occurs within

impounded flows, where, using nomenclature of Macdonald (1940), the predominantly olivine basalts of the middle member and basaltic andesites of the upper member are interbedded and intergradational at the boundary. The boundary arbitrarily was placed as close as possible to the change from one rock type to the other. Stearns (1935) and Macdonald (1940) stated that this boundary coincides with the horizon exposed in the head of Nanakuli Valley below Mauna Kapu (Fig. 2.1) where upper member lavas pass over the talus breccia of the caldera margin and onto the soil and ash unconformity that marks the top of the lower member.

Sinton (1979) concluded that the lower and middle members of Stearns (1935) lacked time-stratigraphic significance, citing results of chronological studies at the time (Doell and Dalrymple, 1973 and references therein) that reported K-Ar dates of 3.6-3.0 Ma for both the lower and middle members and 3.0-2.6 Ma for the upper member. Within the precision of the ages, the lower and middle members are approximately contemporaneous, and upper member lavas are younger at the 90%, but not 95%, confidence level (Garcia, 1979). Sinton (1979) remapped the area by rock lithology in order to better define stratigraphic relationships and concluded that, although individual lithologies also do not have time-stratigraphic significance, individual lithologic sections help define the evolution of the volcano in terms of rock type produced. The work led to Sinton's (1987) proposed revisions to the Waianae stratigraphic nomenclature. The Waianae Volcanic Series was renamed Waianae Volcanics, and was formally subdivided into the Lualualei, Kamaileunu, and Palehua Members.

The map in Figure 2.1 shows the areal extent of the Members as mapped by Sinton (1987). The Lualualei Member constitutes part of Stearns's (1935) lower member. Whereas lower and middle members were distinguished by structural criteria, the distinction between

Lualualei and Kamaileunu Member flows are lithologic, resulting in a generally conformable boundary located outside the margins of impounded flows. Sinton (1987) arbitrarily placed the boundary at the lowermost clinopyroxene-saturated flow, determined by petrographic analysis. Sinton (1987) specified that the Palehua Member is equivalent to the upper member except for some young cones and flows on the south end of the range that have been included in the rejuvenated stage Kolekole Volcanics.

MAGNETOSTRATIGRAPHY

Doell and Dalrymple (1973) reported results of rock magnetic polarity for cored flows on the large west-trending ridge at the head of Nanakuli Valley (here called Nanakuli Ridge, Fig. 2.1) and on the small ridge, intersected by a breccia outcrop, on the north side of Nanakuli Valley (their site O). They reported reversed polarity flows at their site O, both below and above the breccia, and normal polarity flows at Nanakuli Ridge. Coe et al. (1984) extended the study with a detailed assessment of magnetic polarity excursions, one of which was reported by Doell and Dalrymple (1973) to be preserved in the lowermost section of Nanakuli Ridge. Coe et al. (1984) concluded that this excursion was most likely the fragment of an actual reversal.

Holcomb et al. (1993) identified a series of magnetic polarity reversals and proposed to refine and further subdivide the stratigraphic sequence into a sequence of magnetic polarity units. Their magnetostratigraphic nomenclature, proposed in abstract, included Member names of the lithologic subdivision, but was later presented in modified form with unique nomenclature. Figure 2.2 shows the relations between the various stratigraphic subdivisions and the nomenclature of the magnetostratigraphic units described here.

FIELD OBSERVATIONS

Kamaileunu Ridge, Puu Paheehee, and the bounding ridges of Nanakuli Valley (Fig. 2.1) were densely sampled in order to compile field lithologic descriptions and field measurements of rock magnetic polarity (Appendix B).

FAULTS AND TALUS BRECCIA

Fault scarps identified on the maps of Stearns (1939) and Sinton (1987), and shown in Figure 2.1, are walls of collapse structures that subsequently impounded lava flows. Whereas the proposed caldera margins of Sinton (1987) do not correspond to the outermost fault scarps, but reflect a rounded structure roughly centered around Mauna Kuwale, the caldera margins of Holcomb (personal communication) do correspond to the outermost scarps and reflect an elongate caldera (Holcomb et al., 1993). The caldera lavas described (Appendix B) and sampled (Chap. 3) for the present study are within the caldera margins of both Sinton (1987) and Holcomb et al. (1993).

The only described collapse margin in the study area is well-exposed in the saddle east of Puu Heleakala (Fig. 2.1). This is the southern margin of Holcomb's (1993) elongate caldera, but in the interpretation of Sinton (1979) it is the wall of a pit crater situated south of the main caldera. The collapse margin separates south-dipping reversed polarity flows on the southwest from nearly horizontal reversed polarity flows on the northeast. Breccia that accumulated against the fault scarp contains lithic fragments of aphyric and plagioclase- and/or olivine-phyric basalt. The upper surface of the breccia dips approximately 40° NE beneath the horizontal flows; the fault scarp is presumed to be near vertical. The breccia

strikes eastward to additional outcrops, not found in this study but shown on the geologic map of Stearns (1939) and described by Stearns (1935) and Macdonald (1940).

SOIL AND ASH UNCONFORMITY

The soil and ash unconformity that separates Stearns's (1935) lower and upper members outside the collapse margins is well-exposed at 543 meters elevation on Nanakuli Ridge below Palehua (Fig. 2.1). Below the soil horizon are thin-bedded (0.15-1.5 meters), normal polarity flows with abundant small plagioclase phenocrysts. Above the horizon are thick (~ 2-3 meters), gray, aphyric, normal polarity hawaiite flows of the Palehua Member. The soil layer itself is approximately 1 meter thick with abundant pieces of platy plagioclase-phyric rocks, which apparently are relic thin-bedded flows. The soil horizon dips 5° E and extends north on the geologic map of Stearns (1939) to the top of a collapse margin in the valley headwall and south along the south-bounding ridge of the valley.

MAGNETIC POLARITY UNITS

Reversals in rock magnetic polarity, previously identified by Holcomb et al. (1993), were located in the described sections with a portable fluxgate magnetometer. Within the mapped area, a single reversal occurs in precaldera lavas, separating Heleakala (R) flows from overlying Nanakuli (N) flows. Within caldera lavas, two reversals separate the lowermost Paheehee (N) from the overlying Kepauula (R) and the uppermost Kaala (N) flows. The Paheehee (N) to Kepauula (R) transition is preserved at Kamaileunu Ridge in a sequence thick enough to be identified as a unit. The magnetic polarity units are described at Sinton's (1987) Member type and reference sections, except for the Nanakuli (N) unit which is a previously undefined extension of his precaldera section. The descriptions for

each sampled section (Appendix B) include field-determined lithology, elevation, and magnetic polarity.

The magnetostratigraphy of the sampled sections spans a composite of approximately 1800 meters of subaerial flows (Fig. 2.2). A stratigraphic gap between the uppermost sampled precaldera flow and the lowermost sampled caldera flow is represented by the unconformity of the collapse margin, but the amount of eroded or buried stratigraphy, if any, is unknown. The composite precaldera section was compiled by correlation of the common magnetic reversal boundary in the Nanakuli Ridge and Puu Heleakala sections.

Precaldera Magnetic Polarity Units

The reversed to normal polarity transition in precaldera flows defines the boundary between the Heleakala (R) and Nanakuli (N) flows. On the northwest ridge of Puu Heleakala (Fig. 2.1), the transition occurs between 490 and 500 meters elevation, which is 90-100 meters above the boundary between Lualualei and Kamaileunu Members. The transition is also located on the northeast ridge of Puu Heleakala at approximately the same elevation. On the south-bounding ridge of Nanakuli Valley, the transition was found near 135 meters elevation. This location is approximately 245 meters below the soil and ash unconformity identified in the same ridge by Stearns (1935). Based on the polarity reversal locations, the calculated dip of the magnetic reversal surface is 8-9° S, consistent with the measured 8-12° S flow dips of Stearns (1935).

At the head of Nanakuli Valley in Nanakuli Ridge, the transition was found between 260 and 290 meters elevation, which is approximately 275 meters below the soil and ash

unconformity. At each of the sites where the reversal was measured, rocks on either side are mainly olivine-phyric, with lesser plagioclase and some pyroxene. Through correlation of the precaldera magnetic polarity transition, the bounding ridges of Nanakuli Valley comprise a precaldera section nearly 800 meters thick.

Heleakala (R) flow unit. The Heleakala (R) unit is described (Appendix B.1) at the northwest ridge of Puu Heleakala, coincident with Sinton's (1987) Lualualei Member type section. The Heleakala (R) unit comprises the subaerial Lualualei Member and the lower approximately 90 meters of the precaldera Kamaileunu Member. The lower boundary of the Heleakala (R) unit, presumably a transition to an underlying normal polarity unit, is not exposed in the study area. The upper boundary of the Heleakala (R) unit is the transition to the Nanakuli (N) unit between 490 and 500 meters elevation. Notable outcrops in the section are olivine-rich. Flows containing 30-50% phenocrysts occur in the Heleakala (R) unit at 85 and 140 meters elevation, and in the Nanakuli (N) unit at 510 meters elevation.

Nanakuli (N) flow unit. The Nanakuli (N) unit is described (Appendix B.2) in the segment of Nanakuli Ridge below the soil and ash unconformity. The lower boundary of the Nanakuli (N) unit is the transition from the Heleakala (R) unit between 260 and 285 meters elevation. The upper boundary is the soil and ash unconformity, which is then overlain by the described section of the Kaala (N) unit (Appendix B.6). A notable flow in the Nanakuli (N) section occurs at 323 meters elevation, where an outcrop contains up to 50% olivine. This outcrop was noted by Macdonald and Katsura (1964) as an oceanite containing up to 60% olivine near 320 meters elevation. The Nanakuli Ridge segment, which contains the entire precaldera Kamaileunu Member, does not coincide with any of Sinton's (1987) recognized sections because the type and reference Kamaileunu Member sections are in flows impounded within collapse margins.

Intracaldera Magnetic Polarity Units

The stratigraphically lowest polarity transition within impounded flows is best preserved in the study area at Kamaileunu Ridge spur (Figure 2.1). The change from normal to transitional polarity flows and from transitional to reversed polarity flows occurs at 230 meters and 330 meters elevation, respectively. The reversal defines the boundary between the Paheehee (N) and Kepauula (R) flow units but, at this location, the thick magnetically transitional sequence itself can be identified as a unit. In contrast, the transition is preserved as an abrupt change from normal to reversed polarity flows at 250 meters elevation on the northern spur (here called Ulehawa ridge) of the ridge separating Nanakuli and Lualualei Valleys and at 100 meters elevation on the north side of Puu Paheehee (Fig. 2.1). Rocks on either side of the transition are mainly olivine- and plagioclase-phyric, with plagioclase commonly occurring in clusters with or without pyroxene.

The stratigraphically highest magnetic polarity reversal is a reversed to normal transition preserved within impounded lavas and defining the boundary between the Kepauula (R) and Kaala (N) flow units. The transition was identified on Kamaileunu Ridge above Puu Kepauula (Figure 2.1) at 870 meters elevation. In the Nanakuli Valley region, the transition is located on the ridge extending southwest into the valley from Palikea between 580 and 640 meters elevation. Rocks on either side of the transition are mainly aphyric or plagioclase-phyric with lesser pyroxene.

The Paheehee (N) and Kepauula (R) units, with the intervening thick transition unit, are well exposed on Kamaileunu Ridge spur. This multi-unit section overlaps the Kamaileunu Member type section of Sinton (1987). The described multi-unit section (Appendix B.5)

extends beyond Puu Kepauula through the upper boundary of the Kepauula (R) unit at 870 meters elevation, whereas the Kamaileunu Member type section of Sinton (1987) terminates at the 816 meters elevation of Puu Kepauula, approximately 30 meters into the Palehua Member. The Ulehawa Ridge and the north ridge of Puu Paheehee, which are Kamaileunu Member reference sections (Sinton, 1987), are described as Paheehee (N) subsections (Appendices B.3 and B.4, respectively).

Paheehee (N) flow unit. The Paheehee (N) flows outcrop for 88 meters in the northern ridge of Puu Paheehee, but the unit has greater exposure in the lower Kamaileunu Ridge spur (135 meters) and in Ulehawa ridge (207 meters). The Paheehee (N) unit is entirely within the Kamaileunu Member of Sinton (1987). The lower boundary of the Paheehee (N) unit is not identified at any of the described sections. This unit may represent a continuation of the normal polarity interval in which the precaldera Nanakuli (N) unit accumulated, but the structural separation requires identification of individual units (Holcomb, personal communication). The upper boundary of the Paheehee (N) unit is at 230 meters elevation in the Kamaileunu Ridge spur, at the first magnetically transitional measurements. Notable outcrops in the Paheehee (N) unit are at 165 meters elevation, where flows contain 30% olivine, and at 125 and 216 meters elevation, where flows contain 20% clusters of plagioclase and pyroxene up to 10 mm wide. The olivine-rich outcrops may be those that Stearns (1935) noted at 155 meters elevation as pahoehoe with up to 40% olivine.

Transition unit at Kamaileunu Ridge. The 100 meters-thick magnetically transitional sequence of flows separating the Paheehee (N) and Kepauula (R) units was measured only at the multi-unit Kamaileunu spur. The transition unit is not found at the Puu Paheehee and Ulehawa Ridge sections, where the observed transition from Paheehee (N) to Kepauula (R)

units is abrupt. Magnetically transitional directions were measured at Kamaileunu Ridge spur from 230 to 330 meters elevation, which places the unit entirely within the Kamaileunu Member of Sinton (1987). Within this unit, there are flows containing 20 mm wide clusters of plagioclase and pyroxene, most notably near 300 meters elevation where the clusters constitute 30% of the rock. These may be the flows that were noted by Stearns (1935) at 296 meters elevation as pahoehoe with feldspars 1 inch across.

Kepauula (R) flow unit. The Kepauula (R) unit comprises the upper 540 meters-thick dog-leg segment of the described Kamaileunu Ridge section (Appendix B.5). The Kepauula (R) unit is 119 meters thick in the north ridge of Puu Paheehee, where erosion has removed the upper boundary, and approximately 435 meters thick in the Ulehawa ridge, where the upper boundary is still intact. The Kepauula (R) unit at Kamaileunu Ridge extends from 330 to 870 meters elevation, the lower boundary of which is within the Kamaileunu Member of Sinton (1987) and the upper within the Palehua Member. Notable outcrops contain 40% olivine at 494 meters elevation with phenocrysts a few mm in size, and at 588 meters elevation with phenocrysts up to 15 mm in size. This latter flow fits the description, except for elevation, of a dense aa flow with 50% olivine noted by Stearns (1935) at 646 meters elevation.

Kaala (N) flow unit. The Kaala (N) unit is described (Appendix B.6) at the 237 meters-thick exposure in Nanakuli Ridge above the soil and ash unconformity. Although this section lies outside the collapse margins, unconformably overlying the Nanakuli (N) unit, it is chosen for description because it is readily accessible, located on the same ridge as the Nanakuli (N) described section, and coincides with Sinton's (1987) Palehua Member type section. The unconformable lower boundary of the Kaala (N) unit outside the collapse margins is typical. Within impounded flows, such as at 870 meters elevation at

Kamaileunu Ridge, the lower boundary is abrupt within hawaiite flows. The upper boundary of the unit was not observed in the study area. Notable outcrops within the described section are dense flows containing 20 mm clusters of plagioclase and pyroxene forming up to 40% of the rock, at 607 and 680 meters elevation.

STRATIGRAPHIC RELATIONS

The traditional subdivision of Hawaiian volcanoes into tholeiitic shield, late-shield, and alkalic cap conveys the overall evolutionary character of the basaltic flow sequence, but generally does not provide the stratigraphic groundwork necessary for detailed studies of volcanic evolution. A particular section may be assigned to a particular lithologic member, but any relation between sections within the member is ambiguous. Distinct flows may be traced among nearby sections but, because individual flows do not cover the entire volcano, are generally useless in overall stratigraphic correlations. Soil and ash layers can be useful as time-stratigraphic markers if they can be correlated, but they may be only locally exposed. The time-stratigraphic nature of magnetic polarity units allows correlation between various sections, particularly those in which a unit boundary occurs. Combined with lithology and structural features, magnetic polarity units are powerful tools for unraveling stratigraphic relations.

PRECALDERA

The boundary between Lualualei and Kamaileunu Members is defined at Puu Heleakala at approximately 396 meters elevation, in accordance with Sinton's (1987) specification that the boundary is at the lowest pyroxene-saturated flow. Because of the nature of magma systems, the appearance of pyroxene in a volcanic pile is generally not abrupt and the

location of such a horizon is not unambiguously verifiable. Furthermore, boundaries between rock lithologies based on petrographic analysis are not easy to find in the field. The difficulty in mapping the boundary may be one of the reasons that the Lualualei and Kamaileunu Members are undivided on the northern flanks of the volcano. These Members have been divided only in the Nanakuli Valley region, where the Lualualei Member is shown to outcrop only on Puu Heleakala below 396 meters elevation and at Puu O Hulu to the northwest (Sinton, 1987).

The Nanakuli Valley stratigraphy is refined using the magnetostratigraphy. The boundary between the Heleakala (R) and the Nanakuli (N) polarity units is located between 490 and 500 meters elevation at Puu Heleakala and has been located down dip at various other places around Nanakuli Valley. Therefore, the boundary between the Lualualei and Kamaileunu Members, stratigraphically about 90 meters lower, also projects around the valley such that the Lualualei Member is exposed in the lower precaldera flows of the other bounding ridges of the valley rather than just at Puu Heleakala. This observation implies a constancy in stratigraphic thickness, which may not be a reasonable assumption on a more regional scale.

The extent of the precaldera Kamaileunu Member is refined using magnetostratigraphy. The precaldera Kamaileunu Member, although mapped, is not formally recognized through a type or reference section in Sinton's (1987) stratigraphy. However, based on correlation of the polarity boundary, the precaldera Kamaileunu Member makes up approximately 375 meters of the 800 meters-thick composite section of precaldera flows in the mapped region. This segment is best exposed in Nanakuli Ridge where the Nanakuli (N) polarity unit is described.

INTRACALDERA

The Kamaileunu Member of Sinton (1987) comprises nearly the entire pile of impounded flows as well as nearly half of the precaldera subaerial section. The exposed 690 meters-thick intracaldera section of this Member, except for some unusual flow compositions at Mauna Kuwale, is overall lithologically indistinct. Without magnetostratigraphy, there is essentially no basis for relating the thick sections of horizontal flows. The identification of a multi-unit sequence Paheehee (N), transition, and Kepauula (R) not only allows sections to be related to one another, but variations in the thickness of these units and locations of the boundaries provide evidence for multiple caldera collapses (Holcomb et al., 1993).

The boundary between Sinton's (1987) Kamaileunu and Palehua Members, like that between the Lualualei and Kamaileunu Members, is arbitrarily defined within a gradual change in rock lithology. Sinton (p. A13: 1987) stated that the Palehua Member is equivalent to the upper member of Stearns (1935), the lower boundary of which separates mainly olivine basalts from mainly basaltic andesites (Macdonald, 1940). However, Sinton (Fig. 2: 1987) indicated that the base of the Palehua Member is near 660 meters elevation in the north-bounding ridge of Nanakuli Valley and showed on his map that Palehua Member crops out on this ridge at the unnamed peak NE of Puu Heleakala, whereas Stearns (p. 73: 1935) placed the base of the upper member at 565 meters elevation in this location, in which case upper member rocks should crop out along the entire ridge. However, on the geologic maps of Macdonald (1940) and Takasaki (1971), which are based on Stearns' work, upper member rocks do not crop out anywhere along the ridge until about 760 meters elevation just below Palikea. Inconsistencies are eliminated in the magnetostratigraphy, where unit boundaries are unambiguous. The boundary between the

Kepauula (R) and the Kaala (N) polarity units is located in the upper part of both the Nanakuli Valley ridge and Kamaileunu Ridge, and presumably can be located within hawaiites at all of the impounded flow sections.

UNFINISHED MAPPING

There is potential to readily map the entire north flank of the volcano, which is presently undivided into Lualualei and Kamaileunu Members (Sinton, 1987). A great amount of work will go into locating the lowest pyroxene saturated flow by petrographic analysis at any section under study. However, the transition from Heleakala (R) to Nanakuli (N) magnetic polarity units should be easily located in the field. The location of the unit boundary can be predicted based on reconnaissance polarity measurements of the stratigraphically lowest flows in sections along the northern coast. Flows are reversed polarity along the shoreline at Kaneana Cave in the south-bounding ridge of Makua Valley and at the mouth of Kaluakauila Stream in the north-bounding ridge of Makua Valley (Doell and Dalrymple, 1973). Flows are normal polarity at Kaena Point. Therefore, the reversed to normal polarity transition intersects sea level along the shoreline in flows between these two locations. Assuming 10° N dip of flows, the transition should be located near 215 meters elevation in the bulk of the north-bounding ridge of Makua Valley and near 685 meters elevation in the south-bounding ridge. Reconnaissance measurements on this latter ridge confirmed reverse polarity flows to at least 500 meters elevation.

There is potential to map the margins of collapse structures of the caldera, or at least the extent of the flows that filled the structures. Holcomb et al. (1993) implied that the abrupt transition between the Paheehee (N) and Kepauula (R) units at Puu Paheehee and the Ulehawa ridge represents a hiatus, where filling of an outer caldera was interrupted during

Paheehee (N) time by a central caldera collapse which filled through the transition to Kepauula (R) time before overflowing and continuing to fill the outer caldera. The central caldera lavas are represented by the Kamaileunu Ridge section, which preserves the 100 meters-thick transition unit, whereas flows of the outer collapse record an abrupt boundary between the Paheehee (N) and Kepauula (R) polarity units. The extent of the central caldera, preliminarily constrained by identification of outer collapse lavas at the Ulehawa ridge and at Puu Paheehee, can be identified in the field by the presence of the thick magnetically transitional sequence. The difference in elevation of the abrupt transition at these latter two locations may be evidence for separate collapses in the outer impounded flows (Holcomb, personal communication), in which case tracing the transition may delineate the extent of discrete fill sequences.

CONSTRAINTS AND IMPLICATIONS

Magnetostratigraphic relations at Waianae Volcano provide stratigraphic constraints for past and future studies. The results of two past studies are discussed here with new stratigraphic perspective.

Doell and Dalrymple (1973) determined that Nanakuli Ridge contained normal polarity flows, but that the small ridge, cut by a breccia outcrop, on the north side of the valley (their site O) contained reversed polarity flows both below and above the breccia. These results implied there was a polarity discontinuity across the axis of the valley. Coe et al. (1984) subsequently concluded that an excursion in the lower segment of Nanakuli Ridge was more likely a fragment of an actual magnetic reversal. The results presented here confirm that the Nanakuli Ridge flows preserve a reversal and show that it can be traced to other sections of precaldern flows, in particular to the reversal preserved at Puu Heleakala.

In this interpretation, the reversed polarity flows below the breccia at Doell and Dalrymple's (1973) site O are part of the Heleakala (R) unit, stratigraphically lower in a section continuous with Puu Heleakala and Nanakuli Ridge. The nearly horizontal flows above the breccia at their site O are part of the intracaldera Puu Kepauula (R) unit.

The work of Macdonald and Katsura (1964) on the chemical compositions of Hawaiian lavas included analyses of flows from the two ridges in Nanakuli Valley which were subsequently studied by Doell and Dalrymple (1973). They concluded for Waianae Volcano that the shift from tholeiitic to alkalic basalts is in the middle or late caldera fill preceded by chemically transitional rocks interbedded with tholeiites. The Waianae caldera rocks of Macdonald and Katsura (1964) are from the small ridge on the north side of Nanakuli Valley (Doell and Dalrymple's, 1973, site O), above the breccia, between 400 and 585 meters elevation. According to magnetostratigraphic relations, this segment is a thin section within the upper Kepauula (R) unit. There are approximately 490 meters of stratigraphically lower intracaldera flows, best exposed at Kamaileunu Ridge. Additional chemical analyses from these flows will better describe the evolution of caldera lavas.

CONCLUSIONS

Magnetostratigraphy divides the exposed flows of Waianae Volcano into easily located, readily mapped magnetic polarity units with unambiguous time-stratigraphic significance. Magnetostratigraphic correlations make it possible to define relations among the various sections of the volcano and, consequently, to construct a composite subaerial section. Magnetostratigraphic relations within impounded flows allow interpretation of multiple collapses where structural evidence apparently no longer exists. The detail provided by the individual, yet coupled, lithostratigraphic and magnetostratigraphic subdivision makes

Waianae the most stratigraphically well understood of the Hawaiian volcanoes, and shows potential for establishing magnetostratigraphic foundations at other Hawaiian volcanoes that have preserved reversals.

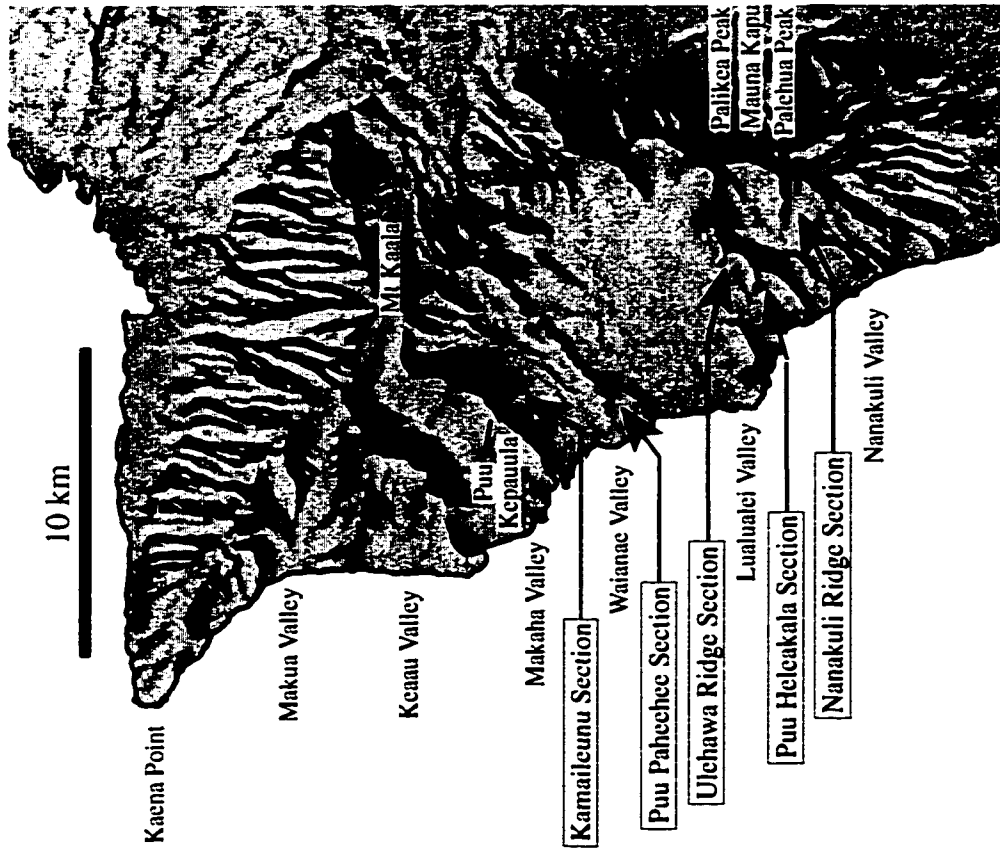
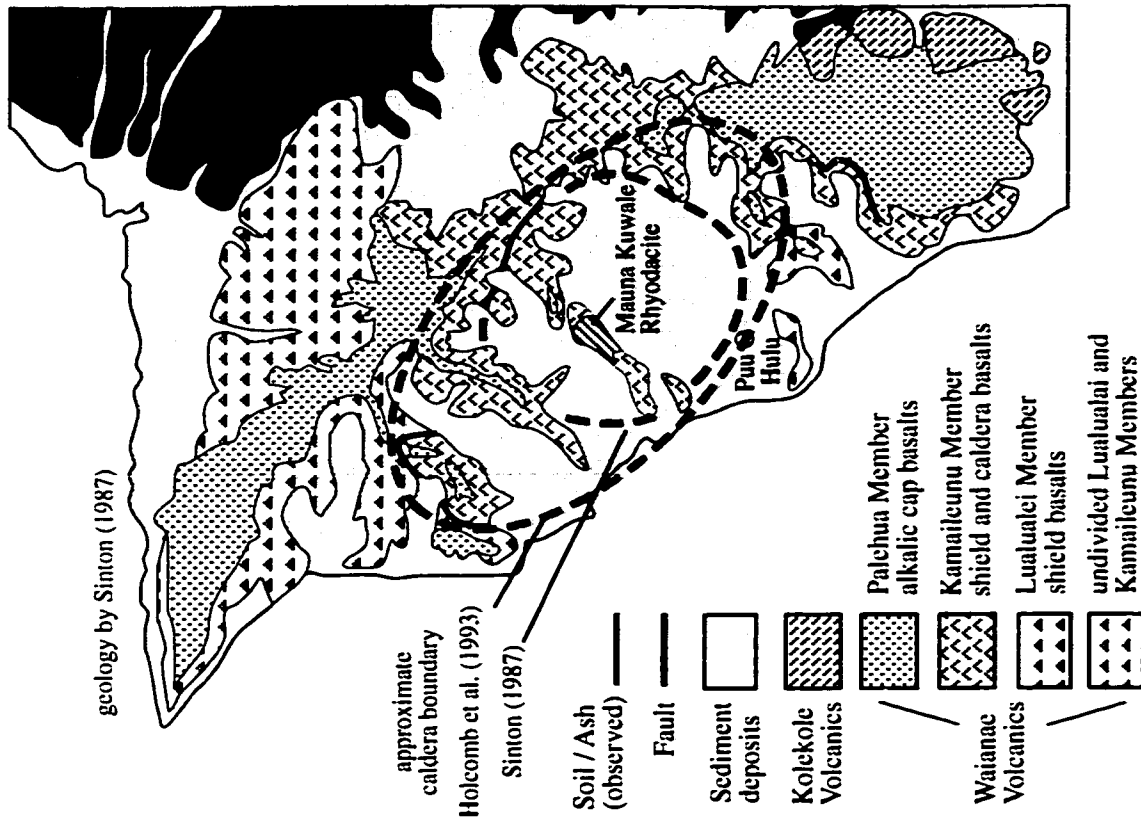


Figure 2.1 Shaded Relief and Geologic Map Views of Waianae Volcano

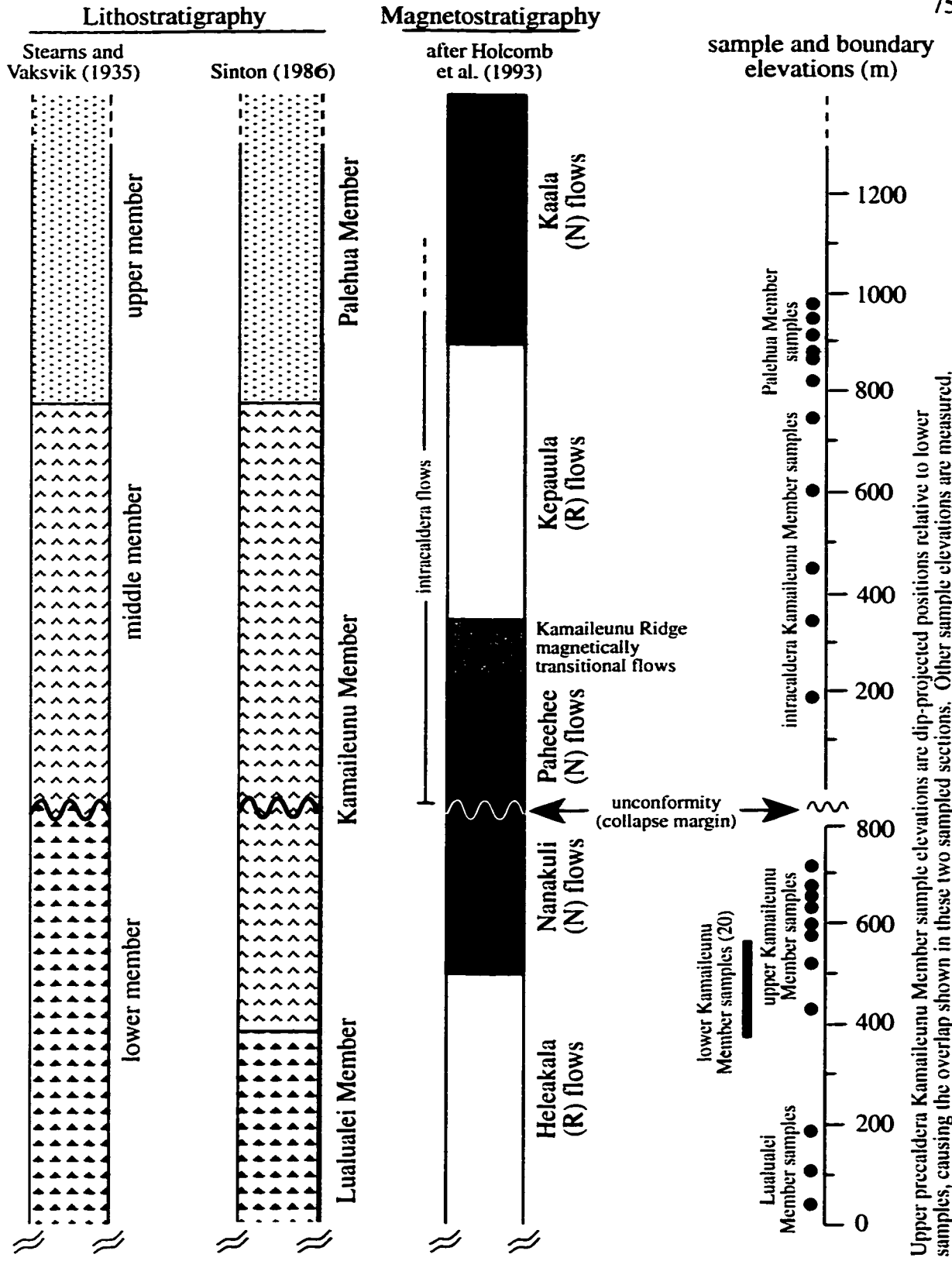


Figure 2.2 Relations among Lithostratigraphic Boundaries (informal and formal), Magnetostratigraphic Boundaries, and Sample Locations of Waianae Volcano

CHAPTER 3

The Geochemistry of Waianae Volcano, Hawaii: Isotopic and Major Element Correlations in Late-Shield Lavas and the Identification of an Extreme Koolau Component in the Source

ABSTRACT

One of the most limiting factors in detailed geochemical studies of individual Hawaiian volcanoes is the stratigraphic understanding necessary for detailed sampling. The stratigraphy of Waianae Volcano is very well understood from mapping of lithologies and a series of magnetic reversals, and was the basis for a dense sampling to determine the detailed geochemical characteristics of the waning stage of volcanism. New data for subaerial lavas of Waianae show that significant Pb isotopic variability exists only in the late precaldera lavas, which comprises a large proportion of the late-shield sequence. Nd and Sr isotopic variations also appear in these lavas, but the range of Nd and Sr isotope ratios is small compared to that of Pb. In contrast, the alkalic cap, caldera fill, and oldest precaldera flows have nearly identical isotope compositions. KEA and KOO isotopic source components, apparently otherwise well-mixed in the source of subaerial Waianae lavas, are systematically sampled by late-shield lavas, where isotopic compositions vary with stratigraphy from increased KEA component to increased KOO component. These isotopic variations are accompanied by correlated variations in the major element content of the lavas. Correlations between isotopic and major element compositions have been previously recognized, but on a larger scale, in Hawaiian intershield geochemical

differences. As is the case for intershield correlations, the Waianae correlations are attributed to variations in source isotopic components which generate magmas under different conditions of melting. The robust appearance of the KOO component in Waianae late-shield lavas, previously identified only in lavas of Koolau, Lanai, and Kahoolawe, provides an opportunity to further characterize this isotopically-extreme endmember of the Hawaiian plume. The new data associated with the KOO component in Waianae lavas require heterogeneity at the KOO end of mixing. This heterogeneity is not likely due to variable Sr/Pb concentration ratios in the KOO component, but is better explained by an isotopically-depleted ingredient in the KOO mixing endmember.

INTRODUCTION

Among the subaerial tholeiitic basalts of Hawaiian volcanoes, systematic relations exist in major element compositions which reflect a spectrum of volcanic behavior during the transition from shield-building to post-shield volcanism. The character of the transition ranges from those volcanoes that produce no alkalic volcanism to those that produce a stratigraphically lengthy and extensive transition from tholeiitic to alkalic volcanism. Intershield correlations between average tholeiite major element compositions and radiogenic isotope ratios indicate that different mantle sources are associated with different late-shield melt segregation conditions such as pressure, temperature, and degree of melting. These chemical systematics are, in turn, correlated with the character of the transition to post-shield volcanism.

In the model describing the late-shield volcanic spectrum (Chap. 1), the isotopic composition of late-shield tholeiites from any particular volcano reflects a constant (i.e.,

well-mixed) proportion of source components because intrashield isotopic variations are smaller than most intershield variations. Although isotopic variability does exist among tholeiites from individual volcanoes, and has been attributed to changes in proportions of source components, correlations between isotopic variability and major element composition, such as those found for intershield differences (Hauri, 1996; Chap. 1), have not been reported for tholeiites of individual Hawaiian volcanoes.

OBJECTIVES

Waianae Volcano is an excellent candidate for detailed geochemical study because erosion has exposed thick stratigraphic sequences, the remnant magnetic character of which provides good stratigraphic control and, therefore, a composite stratigraphy describing the entire subaerially-exposed portion of the volcano (Chap. 2). This report describes new major element, trace element, and isotopic data for Waianae Volcano, and the geochemical character of the volcano as it relates to the spectrum of Hawaiian volcanoes. It is shown that the intershield isotope-major element correlations identified among the subaerial tholeiitic suites (Chap. 1) is also present within the late-shield lavas of Waianae Volcano itself. These systematic variations reflect sampling of a source region where the two isotopically distinguishable components of Hawaiian shield lavas, the KEA and KOO components, are poorly mixed. The marked presence of the KOO component in Waianae late-shield lavas provides a particularly good opportunity to further characterize this endmember Hawaiian plume component. There are two main conclusions:

- 1.) The few preexisting data for Waianae Volcano implied isotopic homogeneity of subaerial lavas. New data show a similarly narrow range of isotopic compositions among alkalic cap, caldera, and the oldest subaerial precaldera lavas; however, there is a wide

range of compositions in the late-shield precaldera lavas. The isotopic composition of late-shield lavas varies systematically with stratigraphy and is correlated with major element variability. Correlations between isotopic and major element compositions have been identified in intershield geochemical variability (Hauri, 1996; Chap. 1), but this study presents correlations discerned in the compositional variability of an individual volcano. The correlations between isotopic and major element compositions in Waianae lavas are consistent with the model describing the late-shield intervolcanic variation (Chap. 1), where sources dominated by the different isotopic components generate magmas under different conditions of melting. Specifically, a source dominated by the KOO component generates larger degrees of melt (i.e., larger F) at lower pressures than a source dominated by the KEA component.

2) Waianae isotopic data are distinct when compared to isotopic compositions of lavas from other Hawaiian volcanoes. Whereas isotopic variability of Hawaiian shields imply mixing between relatively isotopically-discrete KEA and KOO components, the addition of Waianae isotope ratios to the Hawaiian data set requires isotopic heterogeneity at the KOO end of mixing. This isotopic heterogeneity may represent heterogeneity within the KOO endmember, or a discrete KOO component mixed with variable amounts of depleted mantle.

PREVIOUS OBSERVATIONS

Macdonald and Katsura (1964) reported major element analyses for a fairly large suite of Waianae lavas. Their principal section of sampled lavas is a sequence of precaldera flows at the head of Nanakuli Valley. The analyzed samples are tholeiites. According to new stratigraphic detail (Chap. 2), this section is the upper approximately 360 meters of the 800

meters-thick exposed precaldera section. A smaller section sampled by Macdonald and Katsura (1964), in the north wall of Nanakuli Valley, encompasses the upper flows of the caldera and the alkalic cap. The few analyzed samples from this section comprise a mixed group of tholeiitic, alkalic, and chemically transitional basalt, and hawaiiite.

Sinton (1987) formally divided the flows of Waianae into the Waianae Volcanics and the Kolekole Volcanics. The Waianae Volcanics include the Lualualei Member (shield-building stage), the Kamaileunu Member (late shield-building and caldera-filling stage), and the Palehua Member (alkalic cap stage). The rejuvenated stage Kolekole Volcanics, consisting of a series of cinder cones, are the youngest lavas of the volcano. Major element and some trace element analyses of lavas from the Waianae Volcanics are unpublished by Sinton but available from the Bishop Museum database. Major element variations in dikes sampled from the caldera and rift zones of Waianae are reported in Zbinden and Sinton (1988). Analyses of hawaiiites from the Palehua Member and alkalic basalts from the Kolekole Volcanics are reported in Presley et al. (1997).

Analyses of isotope ratios in Waianae lavas are few. Sr and Nd isotope ratios are published for two tholeiites and two alkali basalts (Stille et al., 1983; 1986). Pb isotope ratios are published for one tholeiite and one alkali basalt (Stille et al., 1986). In addition, unpublished Sr isotope ratios are available from the Bishop Museum database for one precaldera tholeiite, one caldera tholeiite, and one alkalic cap hawaiiite from the Macdonald and Katsura (1964) collection.

For this study, a set of 31 precaldera samples were analyzed for Pb isotope ratios, 24 for major and trace element composition, and 12 for Sr and Nd isotope ratios (Table 3.1 a-d). In addition, a set of 14 intracaldera and alkalic cap samples were analyzed for Pb isotope

ratios, 8 for major and trace element composition, and 5 for Sr and Nd isotope ratios (Table 3.1 a-d). Analytical methods are described in Appendix A.

SAMPLING AND RESULTS

In addition to the lithostratigraphy of Sinton (1987), the stratigraphic sequence has been divided into six magnetic polarity units based on polarity of flows as measured in the field with a portable magnetometer (Holcomb et al., 1993; Chap. 2). The units are defined and described in detail at the type sections for the existing lithostratigraphy (Appendix B). The time-stratigraphic nature of the units and the distinct nature of the boundaries allow correlation between sections, thus providing an unambiguous basis for stratigraphic relations. The precaldera magnetic polarity units encompass the Lualualei and precaldera Kamaileunu Members, and extend the formally recognized precaldera Kamaileunu Member by 200 stratigraphic meters. At the studied sections (Chap. 2), the precaldera flows comprise a nearly 800 meters-thick composite (two parts) subaerial section.

NOMENCLATURE AND GENERAL ROCK DESCRIPTION

The sampled lavas of the precaldera section are tholeiitic basalts (Fig. 3.1), except for one chemically transitional sample, PH-29. This sample was collected from a flow located near the transition between the Lualualei and Kamaileunu Members, the boundary of which is defined as the lowermost clinopyroxene-saturated flow, determined by petrographic analysis (Sinton, 1987). According to available published and unpublished data, all other analyzed precaldera flows are also tholeiites. The Lualualei Member lavas contain olivine as the dominant phenocryst, occasionally with plagioclase. Pyroxene and plagioclase phenocrysts are common in addition to olivine in the precaldera Kamaileunu Member lavas.

The sampled caldera lavas include tholeiites, one transitional basalt, and one alkalic basalt (Fig. 3.1). According to available published and unpublished data, other analyzed caldera flows also span the range from tholeiite to alkali basalt, where alkali basalts are interbedded with tholeiites in the upper portions of the caldera fill (Macdonald and Katsura, 1964). Plagioclase and pyroxene phenocrysts are dominant in the caldera lavas. The sampled alkalic cap lavas are hawaiites, although other flows can be classified as alkali basalt or mugearite (Presley et al., 1997). These lavas are mainly aphyric or contain plagioclase phenocrysts up to 20 mm in length.

ALTERATION

Previous studies have shown that K may be lost in weathering, whereas P is immobile (e.g., Lipman et al., 1990; Frey et al., 1991). Therefore, relatively low values of K_2O/P_2O_5 have been viewed as a measure of rock alteration. This is consistent with studies that report $K_2O/P_2O_5 > 1.3$ in submarine glasses (Moore et al., 1990; Garcia et al., 1989) and in recent Kilauea and Mauna Loa lavas (Wright, 1971). Although nearly half of the precaldera samples in this study are in the range $K_2O/P_2O_5 = 0.5 - 1.0$, this ratio shows no correlation with element abundances, nor with other indices of alteration such as Ba/Rb (Hofmann and White, 1983; White and Duncan, 1996) or loss-on-ignition (LOI). Furthermore, although not perfect, K_2O abundances vary with immobile incompatible element abundances. Therefore, data have not been eliminated based on K_2O/P_2O_5 content.

Fodor et al. (1992) showed that weathering can mobilize REE and Y without Ce, which is less soluble in the oxidized state. This can result in REE and Y enrichment and Ce anomalies in nearby lavas without an increase in immobile incompatibles. The

stratigraphically-highest precaldera sample in this study, NANA-31.31, contains anomalously high REE and Y relative to other samples, and is the only sample with a pronounced Ce anomaly ($Ce/Ce^* = 0.83$). Therefore, the REE and Y abundances of this sample are eliminated from further discussion.

MAJOR ELEMENT COMPOSITIONS

The tholeiite to alkali basalt transition at Waianae Volcano is characterized by a stratigraphically short interval of interbedded tholeiitic and alkalic basalts in the upper caldera-filling lavas, underlying a mantle of predominantly hawaiitic lavas. Lower caldera and precaldera flows are tholeiitic. Tholeiite differentiates, such as icelandite and rhyodacite, are rare in Hawaiian lavas but are found at some localities within the Waianae caldera (e.g., Sinton, 1987). These evolved compositions are not considered in this study.

Major element variation diagrams (Fig. 3.2 a-f) characterize the general evolution of the subaerial lavas. The data presented here focus on the late-shield lavas of Waianae and, therefore, include few of the highly evolved range of compositions found in the post-shield and some caldera lavas; however, this range is well characterized by existing data (Macdonald and Katsura, 1964; Presley et al., 1997). Disregarding detailed variations for the moment, the overall data set (Fig. 3.2 a-f) shows a distinct increase at approximately 7% MgO in the incompatible elements TiO_2 and P_2O_5 (also Na_2O , K_2O), and a distinct decrease in CaO (and increase in Al_2O_3/CaO). These inflections apparently indicate a change in the fractionating mineral assemblage from olivine control to multiple saturation, which also is reflected in the lava samples. Samples containing moderate amounts of pyroxene and plagioclase phenocrysts are within the range 6.0-6.5% MgO. The inflections in the data trends at 4-5% MgO are mainly generated by the hawaiites of the Palehua

Member. At this MgO content, there is a sharp increase in SiO₂ and decrease in TiO₂ and FeO (and V, Sc, not shown), consistent with Fe-Ti oxide fractionation.

Within the cluster of data at 6-8% MgO, which are for the lavas of the precaldera Kamaileunu Member section, there is obvious variability in SiO₂ and FeO. Of particular interest is the trend in data to higher SiO₂ and lower FeO, which is in contrast to the overall trend with MgO. A particular group of dike compositions (Zbinden and Sinton, 1988) shows a similar inflection to higher SiO₂ and lower FeO compared to the overall data trends, but these samples have a slightly lower MgO content than the precaldera Kamaileunu samples (Fig. 3.2 a-f). Zbinden and Sinton (1988) refer to this group of dike compositions as “strongly tholeiitic”, based on the range of silica saturation in their samples. They state that these tholeiitic magmas, richer in silica than their fractionating plagioclase, follow a strong silica enrichment trend.

TRACE ELEMENT ABUNDANCES

This study presents the first rare earth element (REE) data for Waianae lavas. Representative REE patterns (Fig. 3.3) for the various stratigraphic sections of the volcano show that the precaldera tholeiites have a similar range in abundance. The upper caldera lavas and the sample PH-29, which are more transitional in major element composition (Fig. 3.1), are within the same range of heavy REE (HREE) as the precaldera tholeiites, but are offset to relatively higher light REE (LREE) content. The hawaiites of the alkalic cap are offset to higher REE overall, and more so for the LREE. A distinct feature of the REE patterns is a positive Eu anomaly in all the samples.

The abundance of the incompatible element La correlates with the REE fractionation ratios La/Yb and Sm/Yb (Fig. 3.4 a,b). The fractionation of REE, particularly HREE, increases in the stratigraphic order Lualualei, precaldera Kamaileunu, intracaldera Kamaileunu, and Palehua. La correlates positively with TiO₂, P₂O₅, and LREE (not shown), and Pb, Sr, Hf, and Zr (Fig. 3.4 c-f), indicating that these elements behave incompatibly. These positive correlations exist for the entire precaldera, caldera, and alkalic cap sections. Other correlations (not shown) are not as uniform. The correlations between La and HREE and Y are also positive, but the trend of the precaldera sample data has a more steeply positive slope than that of the caldera and alkalic cap data. Sc is positively correlated with La for most of the precaldera tholeiites, but apparently decreases in the upper precaldera and continues to decrease through the caldera and alkalic cap sections. Ba and Rb correlate well with La in the caldera and alkalic cap sections, but only show a fair correlation with one another in the precaldera section.

RADIOGENIC ISOTOPE RATIOS

Pb, Nd, and Sr isotopic data for Hawaiian lavas have been described by mixing between three isotopic endmembers. Following Stille et al. (1986), the terminology adopted here is KEA for the Kilauea endmember, KOO for the Koolau endmember, and PE for the post-erosional (rejuvenated stage) endmember.

The very few existing isotopic data for Waianae lavas show little variability. However, the new data show that Pb isotope ratios span the widest range known for Hawaiian shields and trend to the least radiogenic ²⁰⁸Pb/²⁰⁴Pb found for Hawaiian lavas (Fig. 3.5). Waianae compositions extend far into the field of Kahoolawe, Lanai, and Koolau, which have the only lavas previously found to contain the extreme KOO component composition. This

wide range of Pb isotope compositions is found mainly in the upper 500 meters of the precaldera tholeiites; specifically, in the precaldera Kamaileunu Member. Furthermore, Pb isotope ratios vary systematically with stratigraphy (Fig. 3.6). Whereas lowermost precaldera lavas, caldera lavas, and alkalic cap lavas have similar Pb isotope compositions (e.g., $^{206}\text{Pb}/^{204}\text{Pb} = 18.0\text{-}18.1$), precaldera Kamaileunu Member lavas sample increased KEA component (0-400 m) followed by increased KOO component (400-700 m).

In contrast to the wide range of Pb isotope compositions, Nd and Sr isotope ratios have a more restricted range relative to overall isotopic variability in Hawaiian lavas (Fig. 3.7). Whereas Pb isotopic compositions of Waianae extend far into the Koolau field, the Nd and Sr compositions show only partial overlap. However, even with relatively restricted composition, there is also a Nd-Sr stratigraphic trend of increased KEA component followed by increased KOO component (Fig. 3.8).

A plot of $^{206}\text{Pb}/^{204}\text{Pb}$ vs. $^{87}\text{Sr}/^{86}\text{Sr}$ best displays the isotopic variability within and among Hawaiian volcanoes, and the need for at least three isotopic endmembers to describe the entire data set (Fig. 3.9). Whereas the PE component is apparently involved in the post-erosional (rejuvenated) stage and the post-shield stage at some volcanoes (e.g., Haleakala), it has been argued that, for shield lavas, the relatively linear trend of data between the KEA and KOO components and the lack of any trends toward the PE component indicate shield compositions are generated by mixing between the KEA and KOO endmembers (e.g., West et al., 1987). However, in Waianae lavas, the relatively narrow range of Sr (and Nd) isotope ratios coupled with the wide range of Pb isotope ratios gives Waianae a relatively unique composition. With the addition of the new Waianae data set, the shield array is best described as fan-shaped, which rules out simple two-component mixing as an explanation

for shield isotope compositions. The fanned array toward the KOO component indicates heterogeneity at the KOO end of mixing.

Identifying correlations among isotopic and elemental data provides strong constraints on inferring the origin, history, and overall geochemical character of mantle isotopic endmembers. Among Waianae data, correlations of isotopic compositions with Th/La and Th/Ba suggest that the greatest Th depletion is associated with KOO component, as implied by Hofmann and Jochum (1996) and Hofmann (1999) for Hawaiian lavas. Correlation of Eu anomalies with Sr isotope ratios, but not with those of Pb, suggest Eu anomalies are related to KOO isotopic heterogeneity.

DISCUSSION

Wright and Helz (1987) subdivided Hawaiian volcanoes into Haleakala-type, Kohala-type, and Koolau-type volcanoes, based on observations of variations in the character of the mildly alkalic rock series on each volcano. They classified Waianae Volcano as a Kohala-type, i.e. one which lacks abundant mafic alkalic rocks and erupts a thin alkalic cap of hawaiite and mugearite. In comparison, a Koolau-type volcano erupts few or no alkalic rocks and a Haleakala-type volcano erupts a thick transitional unit of interbedded tholeiite, transitional basalt, and ankaramite, followed by a cap of hawaiite and mugearite.

The identification of intershield correlations between isotopic and major element compositions (Hauri, 1996) was expanded (Chap. 1) by focusing on correlations among the subaerial (late-shield) tholeiitic stage of volcanoes and showing that these correlations were related to the subsequent late-shield volcanic behavior, as subdivided by volcano type. Specifically, for any particular volcano, the proportion of KEA and KOO

components in the late-shield tholeiite source is related to the pressure and temperature of magma generation, and to what extent eruptions subsequently shift from tholeiitic to alkalic basalt.

The intershield correlations between major element and isotopic compositions can be summarized by SiO_2 and Pb isotopic relations among volcano types (for those volcanoes where shield-building volcanism is completed) (Fig. 3.10). Based on calculations for the pressure of magma segregation (Chap. 1), a source dominated by the KOO isotopic component generates larger degrees of melting (i.e. larger F) at shallower depths than a source dominated by the KEA component.

Because compositional variability in tholeiites at any particular volcano is small compared to the range of intershield variability, plume heterogeneities are considered well-mixed on the scale of the individual volcano, enabling some compositional averages to be used in intershield comparisons (e.g., Fig. 3.10). However, for the case of Waianae, the intershield correlations defined among shields are also discerned in the compositional variability within an individual volcano, and are evidence for incomplete mixing in the source of Waianae late-shield lavas.

GEOCHEMICAL VARIATIONS AND CORRELATIONS

Distinguishing compositional variations that are related to source heterogeneity, partial melting, and fractional crystallization is key to better understanding processes associated with Hawaiian volcanism, and ocean island volcanism in general. Because isotopic variations in lavas can be attributed to source heterogeneity with some confidence, one of the main objectives in identifying correlations of isotopic with other compositional

variations is to further characterize plume components originally identified only by isotopic composition and, therefore, provide constraints on theories of component origins.

Isotopic and Major Element Relations

The overall major element variation in Waianae lavas can be attributed to changes in the fractionating mineral assemblage (Fig. 3.2 a-f). Lava compositions are controlled by olivine fractionation and/or accumulation until approximately 7% MgO, below which a distinct decrease in CaO (and increase in CaO/Al₂O₃) indicates the addition of clinopyroxene to the fractionating assemblage. The positive correlation between La and Sr suggests that plagioclase is not a significant fractionating phase. The decrease in TiO₂ and FeO and increase in SiO₂ at approximately 4% MgO is evidence for Fe-Ti oxide fractionation in the more evolved lavas, particularly the hawaiites.

The major element variation in the precaldera tholeiites of the Kamaileunu Member is not readily associated with fractionation. The distinct inflections to higher SiO₂ and lower FeO (at 6-8% MgO) in this late-shield section of lavas (Fig. 3.2 a,c) contrast with the overall trend of Waianae data. Zbinden and Sinton (1988) reported similar inflections, although at slightly lower MgO content, in their "strongly tholeiitic" group of dike compositions, and attributed the increase in SiO₂ to plagioclase fractionation from a tholeiitic magma. However, the incompatible nature of Sr in the new data (Fig. 3.4) and the positive Eu anomalies (Fig. 3.3) are not consistent with plagioclase removal. Oxide fractionation can create SiO₂ enrichment in lavas, but is ruled out due to the incompatible behavior of TiO₂ (Fig. 3.2 b) in the precaldera Kamaileunu Member lavas.

A distinct compositional feature of the precaldera Kamaileunu Member lavas is the variability in isotope ratios, particularly those of Pb. Whereas the alkalic cap, caldera, and oldest precaldera lavas fall within a narrow range of Pb isotope compositions, the Kamaileunu precaldera lavas vary widely and systematically throughout the section, showing an increase in the proportion of KEA isotopic component followed by an increase in KOO component (Fig. 3.6). A significant feature of the SiO₂ and FeO variability in the precaldera Kamaileunu Member lavas, and another argument against involvement of post-melting processes, is that variability is correlated with differences in isotopic composition (Fig. 3.11). As is the case for intershield compositional variability, where two of the distinct major element discriminants are SiO₂ and FeO content, the SiO₂-rich end of the Waianae precaldera compositional range is associated with the increased KOO component, which is characterized by more radiogenic Sr, and less radiogenic Pb and Nd.

Although correlations between isotopic and major element variations in precaldera lavas are best graphically displayed for SiO₂ and FeO content, correlations also exist for other major elements. Statistical evaluation of precaldera data, adjusted by olivine addition and subtraction to 7% MgO and normalized, confirms that correlations exist at the 95% confidence level between isotope ratios of Pb, Nd, Sr and abundances of SiO₂, TiO₂, FeO, and P₂O₅. These correlations persist, and include CaO, when the few samples containing less than approximately 6.5% MgO are excluded. Interestingly, whereas Na₂O is included in intershield correlations, it is not in Waianae correlations. It is probable that the larger intershield database includes more chemically transitional lavas than those of the Waianae precaldera section.

Differences in source proportions of KOO and KEA at any particular volcano are associated with the average pressure of magma segregation in late-shield tholeiites (Chap. 1).

Tholeiitic magmas produced by a KOO-dominated source segregate on average at shallower depths than those from a KEA-dominated source, therefore generating differences in the content of major elements affected by the degree of melting (TiO_2 , P_2O_5) and the pressure of melting (SiO_2 , FeO). For Waianae Volcano, the isotopic and major element correlations and the systematic compositional variations with stratigraphy reflect sampling a source region where the KEA and KOO components are poorly mixed.

Isotopic and Trace Element Relations

The fractionation of the REE (La/Yb , Sm/Yb) in Waianae precaldera lavas is not correlated with isotopic or most major element variations, but rather with indicators of degree of melt, such as La content (Fig. 3.4 a,b) and TiO_2 . Certain other trace element pairs are not correlated with indicators of degree of melt among Waianae lavas. Ratios of elements with similar compatibility, such as Hf/Sm (0.75 ± 0.11) and Ce/Pb (28 ± 3) are relatively invariant, consistent with previous studies which found these ratios relatively constant for other volcanoes (Haleakala $\text{Hf/Sm} = 0.72 \pm 0.08$, Chen et al., 1991) or for most ocean island basalts ($\text{Ce/Pb} = 25 \pm 5$, Hofmann et al., 1986).

Some trace element pairs are thought to be related to source heterogeneity in the Hawaiian plume. Frey and Rhodes (1993) showed that, based on correlations with Sr isotope ratios, the trace element ratios Zr/Nb and Sr/Nb are intershield discriminants for the volcanoes Kilauea, Mauna Loa, Koolau, and Waianae. Without high quality Nb analyses, these correlations can not be tested for the Waianae suite of lavas. Hofmann and Jochum (1996) showed that Th depletion, as reflected by the ratios Th/Ba and Th/La , is a characteristic of the present-day Hawaiian plume source; these ratios are correlated with isotopic

compositions in Waianae lavas (discussed in the following section). Specifically, the greatest degree of apparent Th depletion is associated with the KOO component.

That some geochemical variations may reflect source heterogeneities while others reflect degree of melting has not been suggested only for the Hawaiian plume. White and Duncan (1996) showed that the Society plume, according to factor analysis, has certain trace element ratios associated with isotopic heterogeneity (e.g., Rb/Sr, Zr/Nb) and others associated with degree of melt (e.g., La/Sm, trace abundances).

NATURE OF THE MANTLE SOURCES

Systematic isotopic variations with stratigraphy show that Waianae late-shield lavas sampled increased KEA component followed by increased KOO component (Fig. 3.6). The isotopically-extreme KOO component, which makes a strong geochemical appearance in Waianae late-shield lavas, has previously been identified only in lavas of Koolau, Lanai, and Kahoolawe. The following discussion describes the distinct isotopic character of the KOO component, as it appears in Waianae lavas, and the implications for Hawaiian source component mixing.

Characteristics of KEA and KOO Component Mixing

Isotopic compositions of Hawaiian shield lavas imply mixing in the mantle source between the KEA component and an isotopically heterogeneous KOO component (Fig. 3.9). The apparent isotopic heterogeneity of the KOO component can be explained by two possible endmember scenarios; mixing between KEA and 1) a KOO endmember with variable Sr/Pb (and Nd/Pb) concentration ratios, or 2) a KOO endmember with variable isotopic

composition that extends to less radiogenic Sr ratios than previously inferred. Each of these possibilities is considered here by calculating and comparing mixtures of KEA and KOO components as the source of Hawaiian shield isotopic compositions.

For calculation purposes, the KEA component is assigned isotope ratios within the range suggested for this component by Stille et al. (1986) and West and Leeman (1987), the KOO component near bulk earth isotope ratios, and the PE component MORB source isotope ratios (Table 3.2). Both KOO and KEA are assigned Pb and Sr abundances similar to primitive mantle (Table 3.2). It has been argued that the KOO component is not primitive mantle, based on the constant and non-chondritic character of certain incompatible element ratios unaffected by melting processes (Nb/U, Nb/Th, Pb/Ce) in MORB and OIB, including Koolau lavas (Hofmann et al., 1986). However, West et al. (1992) argue that OIB and MORB do not have constant Ce/Pb and Nb/U, based on variability of highly incompatible element ratios in Lanai lavas. They show, for example, that some Lanai data approach primitive Ce/Pb and chondritic La/Th. Despite this debate, the bulk earth isotopic character of KOO lavas prompts the choice of primitive mantle Pb and Sr concentrations in calculations involving the KOO component.

The undepleted isotopic character of KEA lavas compared to upper mantle compositions indicates a relatively trace element enriched source, and primitive mantle values are chosen for simplicity. If more enriched Sr and Pb compositions are assumed for the KEA component, such as those suggested by West and Leeman (1987), then model calculations would be affected as described in the following model analysis.

Assuming variable Sr/Pb ratios in the KOO endmember, calculated mixing curves show that Hawaiian shield $^{87}\text{Sr}/^{86}\text{Sr}$ and $^{206}\text{Pb}/^{204}\text{Pb}$ data can be generated by mixing between a

KEA component and a KOO component that ranges from a primitive Sr/Pb ratio to a 15-fold decrease in the Sr/Pb ratio (Fig. 3.12 a). In this case, Kahoolawe isotopic data are described by mixing between KEA and the primitive KOO Sr/Pb ratio, and Waianae data by mixing between KEA and KOO with decreased Sr/Pb ratio. However, in a plot of $^{87}\text{Sr}/^{86}\text{Sr}$ and $^{208}\text{Pb}/^{204}\text{Pb}$ (Fig. 3.12 b), the mixing curve calculated for a 15-fold decrease in the KOO Sr/Pb ratio barely overlaps the Waianae data field. A mixing curve calculated for a 50-fold decrease in primitive Sr/Pb ratio still does not describe the Waianae data. If a more trace element enriched KEA component is used (West and Leeman, 1987), the mixing curves overlap the Waianae data field even less. Furthermore, depletion of a mantle source, as suggested by isotopic compositions for the KOO component in the Waianae source, implies an increase in the Sr/Pb ratio rather than a decrease.

Because variable Sr/Pb at the KOO end of mixing does not explain isotopic relations between $^{87}\text{Sr}/^{86}\text{Sr}$ and both $^{206}\text{Pb}/^{204}\text{Pb}$ and $^{208}\text{Pb}/^{204}\text{Pb}$, the more likely explanation for the array of shield compositions is mixing with an isotopically heterogeneous KOO component, where the mixing endmember ranges from near bulk earth to a more depleted composition. The extent of variability can be arbitrarily chosen so as to encompass the shield compositions. For example, a reasonable choice might be a KOO component that ranges in $^{87}\text{Sr}/^{86}\text{Sr}$ from 0.7038 to 0.7046 along an isotopic trend similar to that of the Koolau Volcano lavas (Fig. 3.13). In this case, Kahoolawe isotopic data are characterized by mixing between KEA and the isotopically primitive KOO component, and Waianae data by mixing between KEA and the more depleted KOO component.

Although the KOO mixing endmember may range from near bulk earth to more depleted isotopic compositions, this may not reflect the KOO component itself. If the KOO component is accepted as a discrete isotopically primitive endmember, then the trend of

isotopic variability at this end of mixing can also be explained by a mixture of KOO component and depleted mantle. For $^{87}\text{Sr}/^{86}\text{Sr}$ and $^{208}\text{Pb}/^{204}\text{Pb}$, a calculated mixing curve suggests that 0-50% DM mixing with the KOO component will satisfy the heterogeneity requirements at the KOO end of mixing (Fig. 3.13). In this case, Kahoolawe isotopic data are characterized by mixing between KEA and KOO components and Waianae data by mixing between KEA and a KOO-DM mixture.

In summary, the new data for Waianae Volcano add significant heterogeneity to Hawaiian isotope compositions. Whereas the relatively linear trend of preexisting Hawaiian shield Sr and Pb isotopic compositions indicated mixing between the KEA and KOO components, the new Waianae data give definition to a fan-shaped mixing array, and so require heterogeneity at the KOO end of mixing. This heterogeneity is not likely due to variable Sr/Pb concentration ratios in the KOO component, but is better explained by isotopic variability at the KOO end of mixing.

Characteristics of KOO Component Heterogeneity

There is a depleted aspect to the KOO end of mantle mixing that appears with the addition of Waianae data to the existing Hawaiian shield data set. Whereas the evidence for incomplete mixing of KOO and KEA components in the Waianae late-shield lavas is best displayed by the range of Pb isotope ratios, the evidence for a depleted component associated with KOO is most obvious in the range of Sr isotope ratios. The magnitude of the positive Eu anomaly, found in all Waianae samples, is not correlated with Pb isotope ratios, but with Sr isotope composition (Fig. 3.14); therefore, there is an apparent association of Eu anomaly variability with KOO heterogeneity. Although there are many more Pb than Sr isotope analyses for Waianae samples, and the correlation between the Eu

anomaly and Sr isotope ratios may be affected by more data, this correlation is statistically significant at the 99% confidence level for existing data.

Eu anomalies are not unique to Waianae lavas. West et al. (1992) reported Eu anomalies in some Lanai lavas and concluded that they were a characteristic of the source and possibly related to high degrees of melting. Hofmann and Jochum (1996) showed that negative Th (and U) anomalies, as seen in fractionation-corrected and primitive-mantle-normalized Th/Ba and Th/La ratios, were a characteristic of the Hawaiian plume and represented strongly-fractionated material. They speculated that the Hawaiian source contains a significant amount of oceanic gabbros and predicted that low Th/Ba and Th/La ratios, and positive Eu and Sr anomalies could be the signature of a gabbroic component, depending on the relative amount of initial cumulate feldspar.

The fractionation-corrected and primitive-mantle-normalized ratios Th/La and Th/Ba for Waianae precaldera lavas do not correlate solely with Sr isotope ratios, as do Eu anomalies, but show correlations (not shown) with both Sr and Pb isotope ratios that are statistically significant with 99% confidence for Th/Ba and with 95% confidence for Th/La. Based on the correlations, the relative Th depletion in Waianae lavas is greatest at the KOO end of mixing. This is consistent with the comparison of Th/Ba and Th/La ratios among six Hawaiian volcanoes (Hofmann and Jochum, 1996) that shows the greatest relative Th depletion for the lavas of Koolau volcano. However, in Waianae lavas, Th depletion is not associated with the largest magnitude Eu anomalies nor is it accompanied by positive Sr anomalies, as represented by Sr/Nd ratios (Hofmann and Jochum, 1996).

The presence of a gabbroic ingredient in the KOO component cannot be ruled out by the lack of predicted correlations with Eu and Sr anomalies in Waianae lavas. The partitioning

of Ba and La relative to Th, and Sr relative to Nd, is different in gabbro than in the high pressure equivalent eclogite. Whereas Ba, La, and Sr are mildly compatible to compatible in the plagioclase of gabbro, all of the elements are incompatible in eclogite (compilation in Rollinson, 1993). In contrast, Eu compatibility is similar in plagioclase and garnet. If eclogite layers or pods undergo variable melt extraction before being incorporated into the Hawaiian plume, it is possible that Th and Sr anomalies in the residue could be eliminated or reduced while Eu anomalies are retained. Therefore, if the KOO component carries shreds of gabbro-turned-eclogite mixed in with mantle peridotite, as speculated by Hofmann and Jechum (1996) and Hofmann (1999), a wide range of Th and Sr anomalies may be associated with Eu anomalies. Furthermore, if the gabbroic contribution to the KOO component has an upper mantle isotopic signature, then variability in the relative amount of gabbroic ingredient should result in an association between the greatest positive Eu anomaly and the least radiogenic Sr, which is what is observed in Waianae lavas.

CONCLUSIONS

Waianae late-shield lavas show a wide range of isotopic compositions, in contrast to the homogeneity found for the oldest precaldera, caldera, and alkalic cap lavas. The variability is particularly evident in Pb isotope ratios, which span the widest range of compositions yet published for an individual Hawaiian volcano. The KEA and KOO isotopic source components, apparently otherwise well-mixed in the source of subaerial Waianae lavas, are systematically sampled by late-shield lavas, in which isotopic compositions vary with stratigraphy from increased KEA to increased KOO component. The isotopic variations are correlated with variations in the major element content of the lavas.

Correlations between isotopic and major element compositions have been previously recognized, but on a larger scale, in Hawaiian intershield geochemical differences (Hauri, 1996; Chap. 1). As is the case for intershield correlations, the Waianae correlations are attributed to variations in the source between a KOO-dominated endmember, from which magmas segregate at lower pressures, to a KEA-dominated endmember, from which magmas segregate at higher pressures.

The robust appearance of the KOO component in Waianae late-shield lavas, previously identified only in lavas of Koolau, Lanai, and Kahoolawe, provides an opportunity to characterize further this isotopically-extreme endmember of the Hawaiian plume. Whereas the relatively linear trend of preexisting Hawaiian shield Sr and Pb isotope compositions indicated mixing between relatively discrete KEA and KOO components, new Waianae data give definition to a fan-shaped mixing array and require heterogeneity at the KOO end of mixing. This heterogeneity is not likely due to variable Sr/Pb concentration ratios in the KOO component, but is better explained by an isotopically-depleted ingredient that adds heterogeneity to the KOO endmember. In this case, the array of Hawaiian volcanoes that sample a large proportion of KOO component in their source range from Kahoolawe at the relatively primitive isotopic end of the KOO mixing endmember to Waianae at the relatively depleted end.

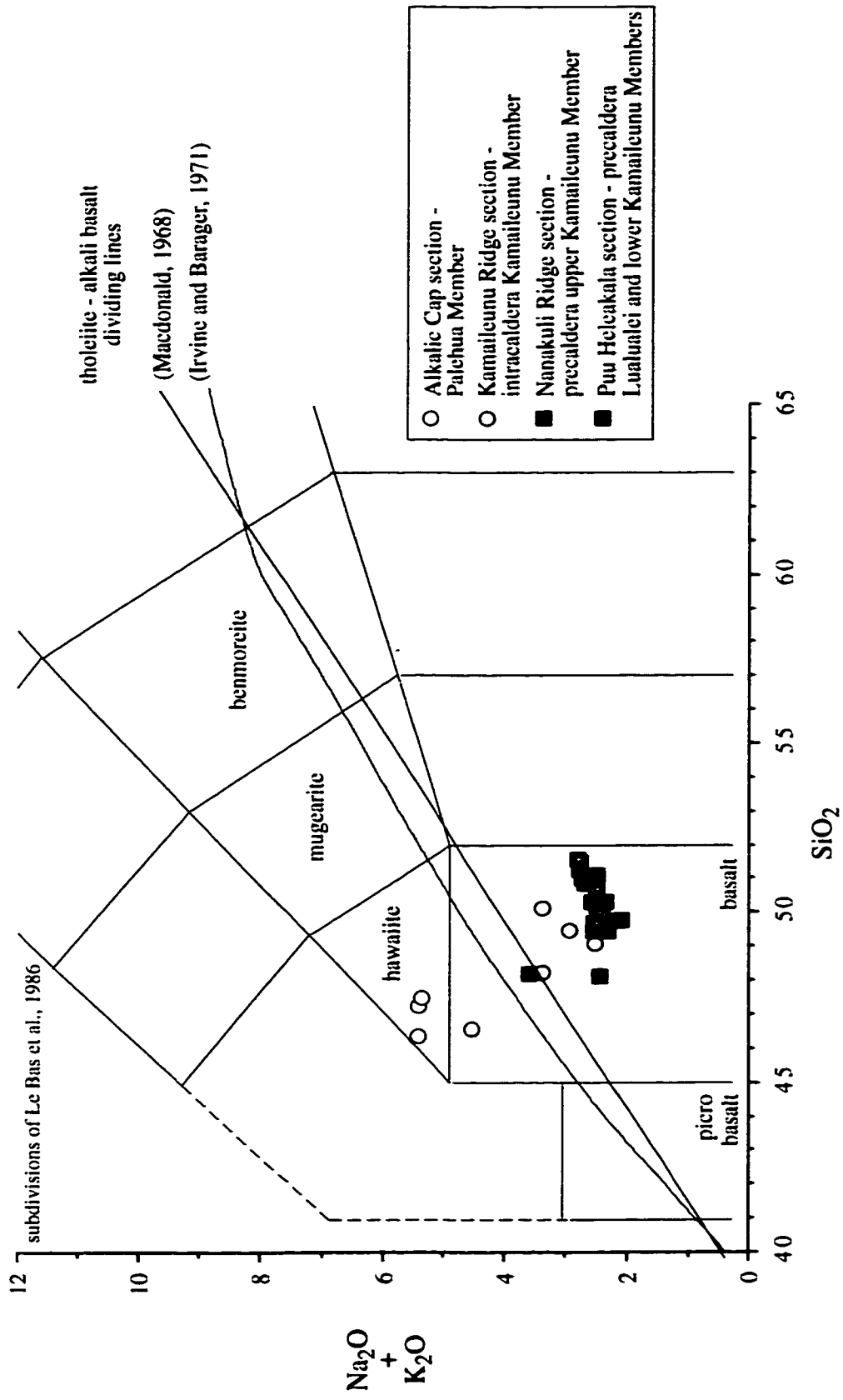


Figure 3.1 SiO₂ vs. Total Alkalis (wt. %) for Subaerial Basalts of Waianae Volcano

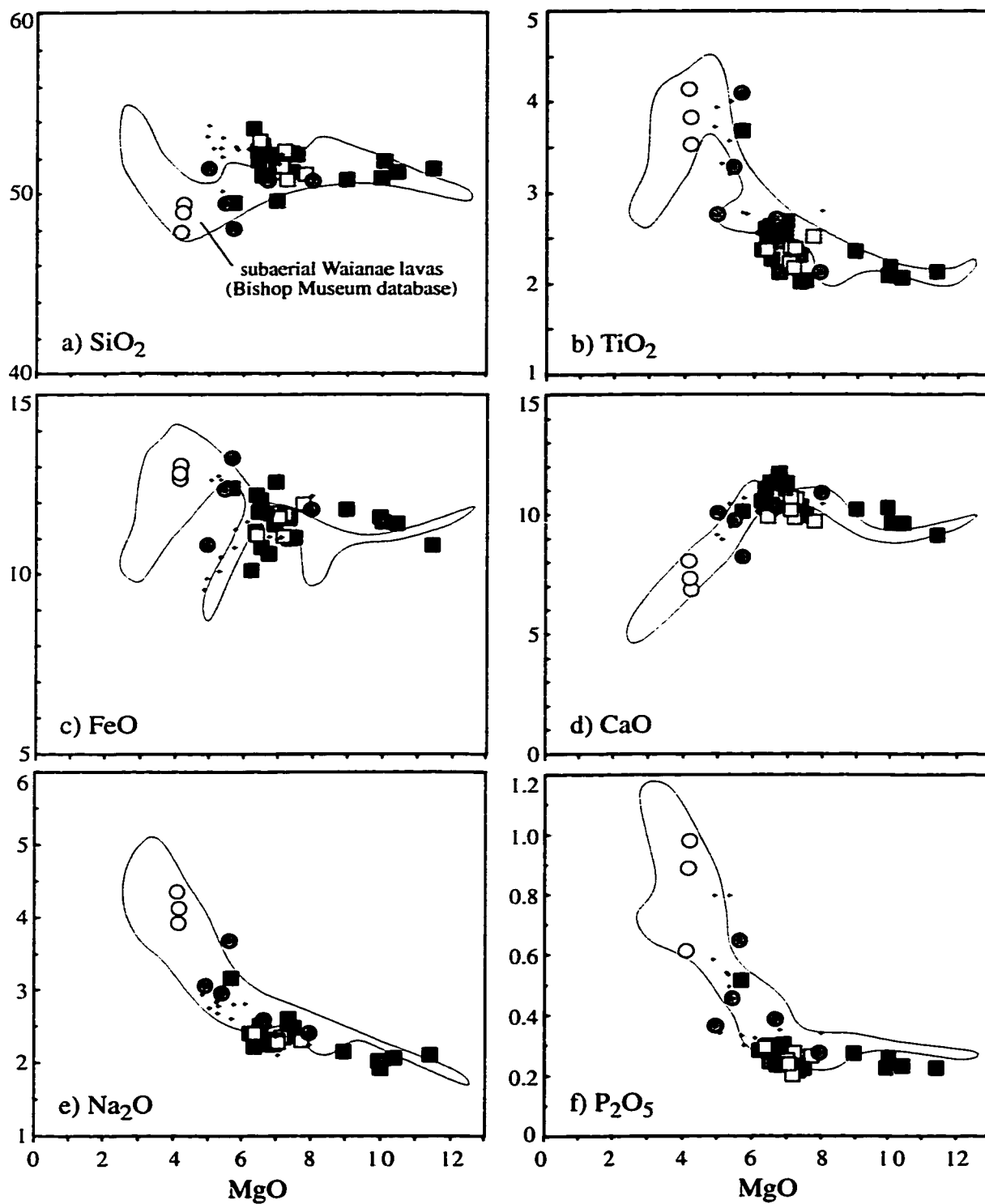
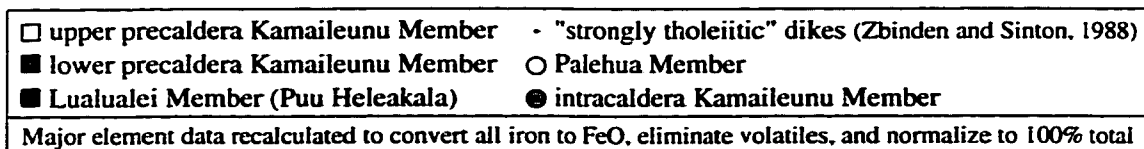


Figure 3.2 MgO vs. a) SiO_2 b) TiO_2 c) FeO d) CaO e) Na_2O and f) P_2O_5 (wt%) for Subaerial Basalts of Waianae Volcano

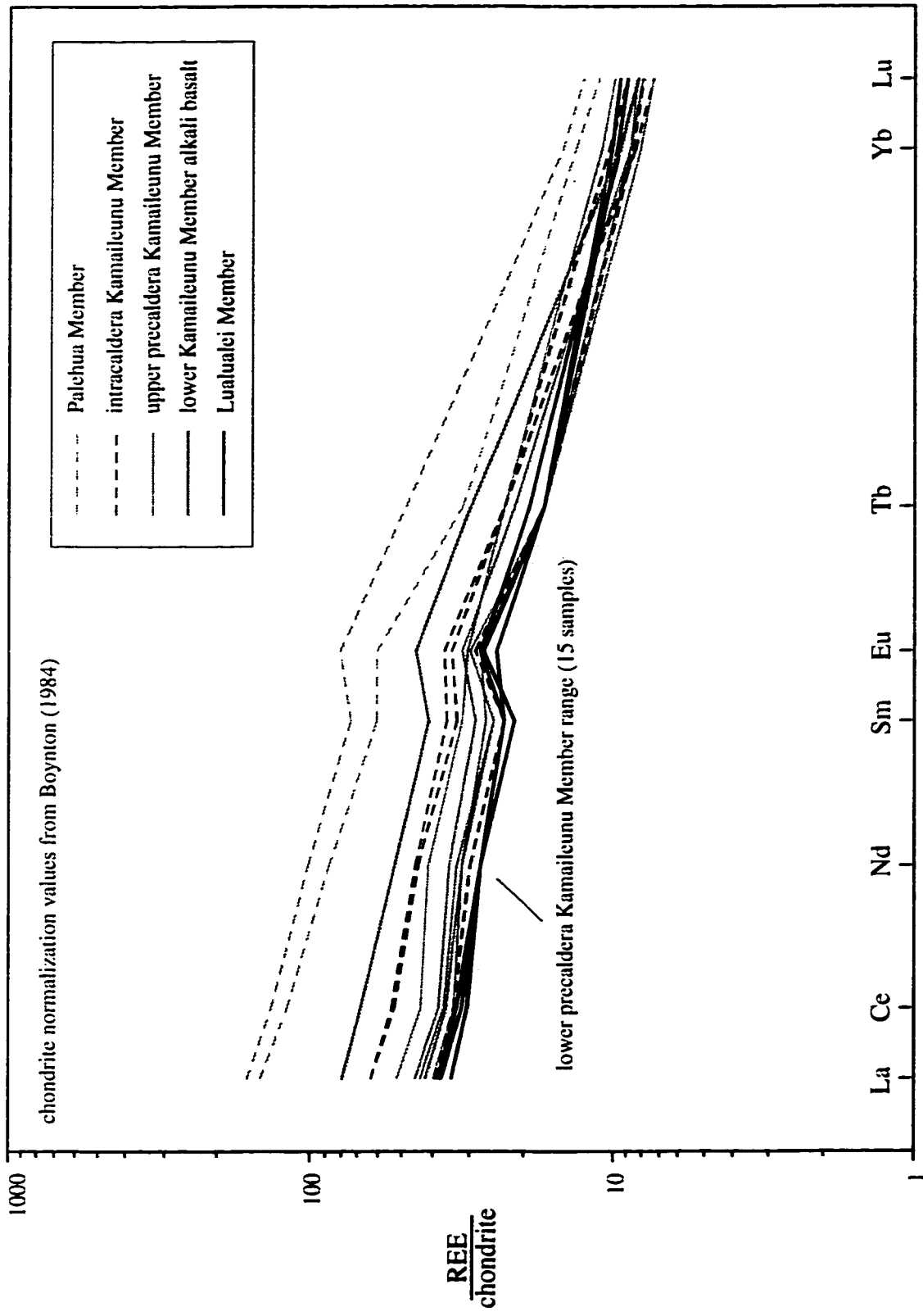


Figure 3.3 Representative Rare Earth Element (REE) Patterns for Subaerial Basalts of Waianae Volcano

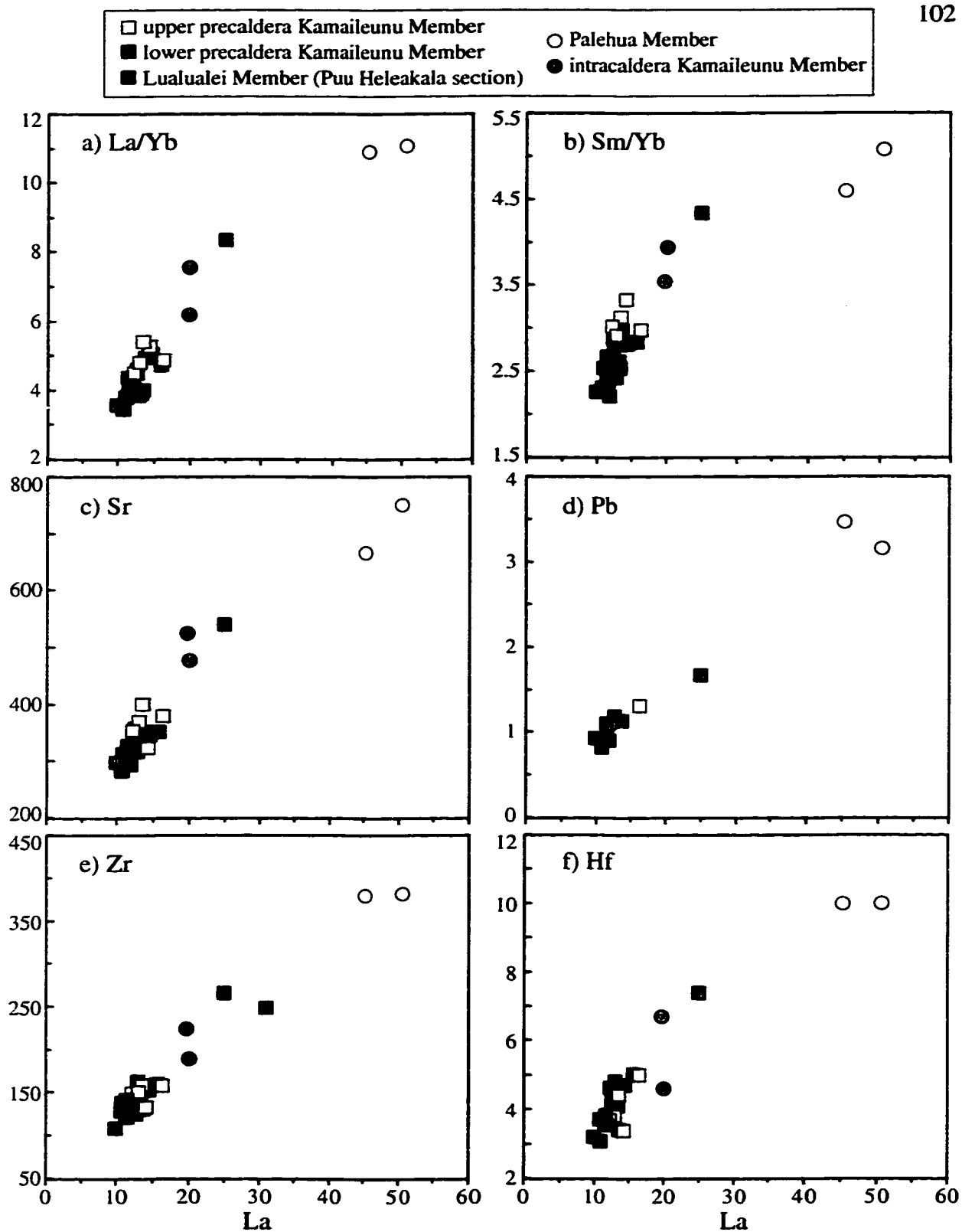


Figure 3.4 La vs. a) La/Yb b) Sm/Yb c) Sr d) Pb e) Zr and f) Hf (ppm) for Subaerial Basalts of Waianae Volcano

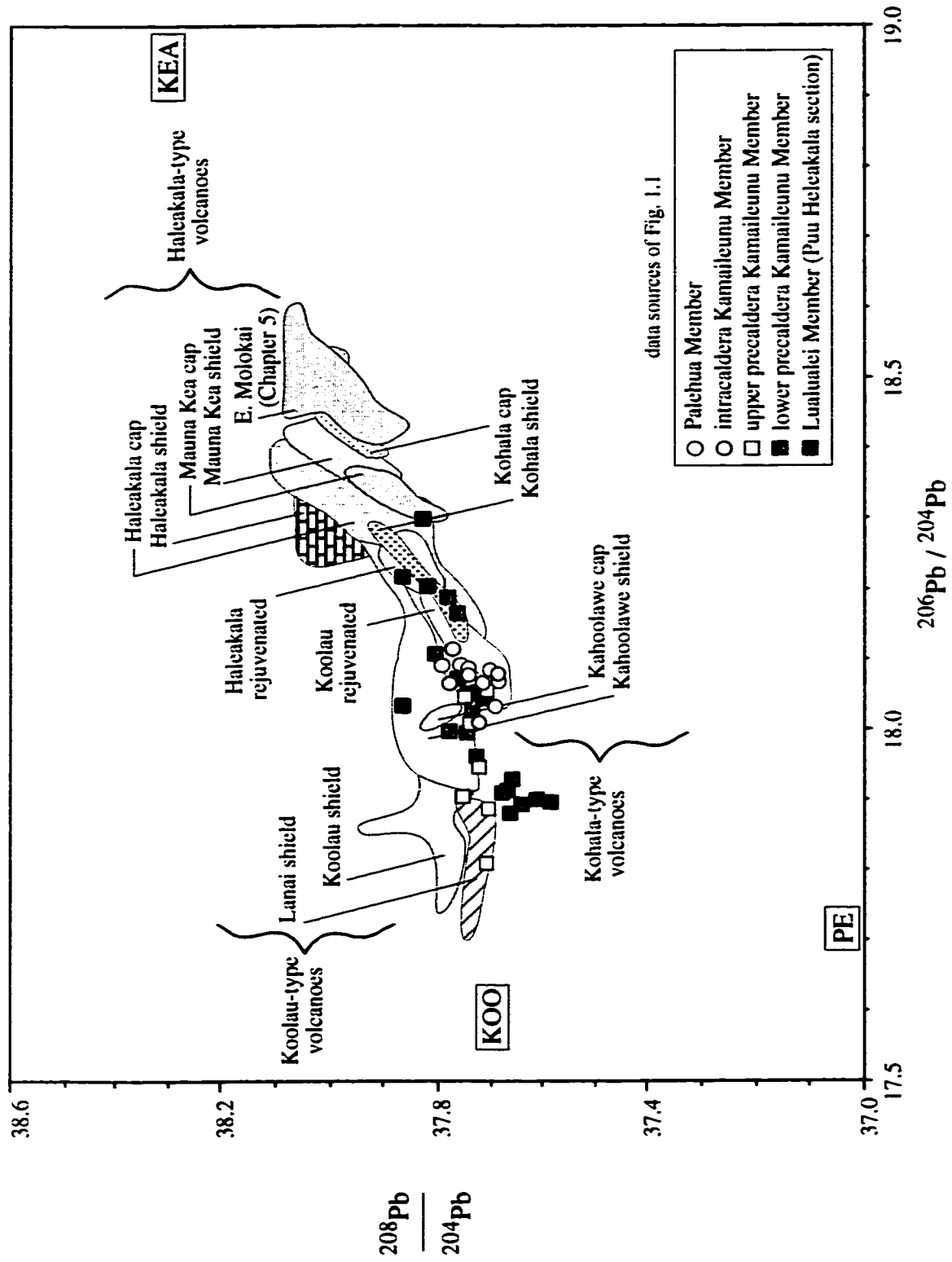


Figure 3.5 $^{206}\text{Pb}/^{204}\text{Pb}$ vs. $^{208}\text{Pb}/^{204}\text{Pb}$ for Subaerial Basalts of Waianae Volcano

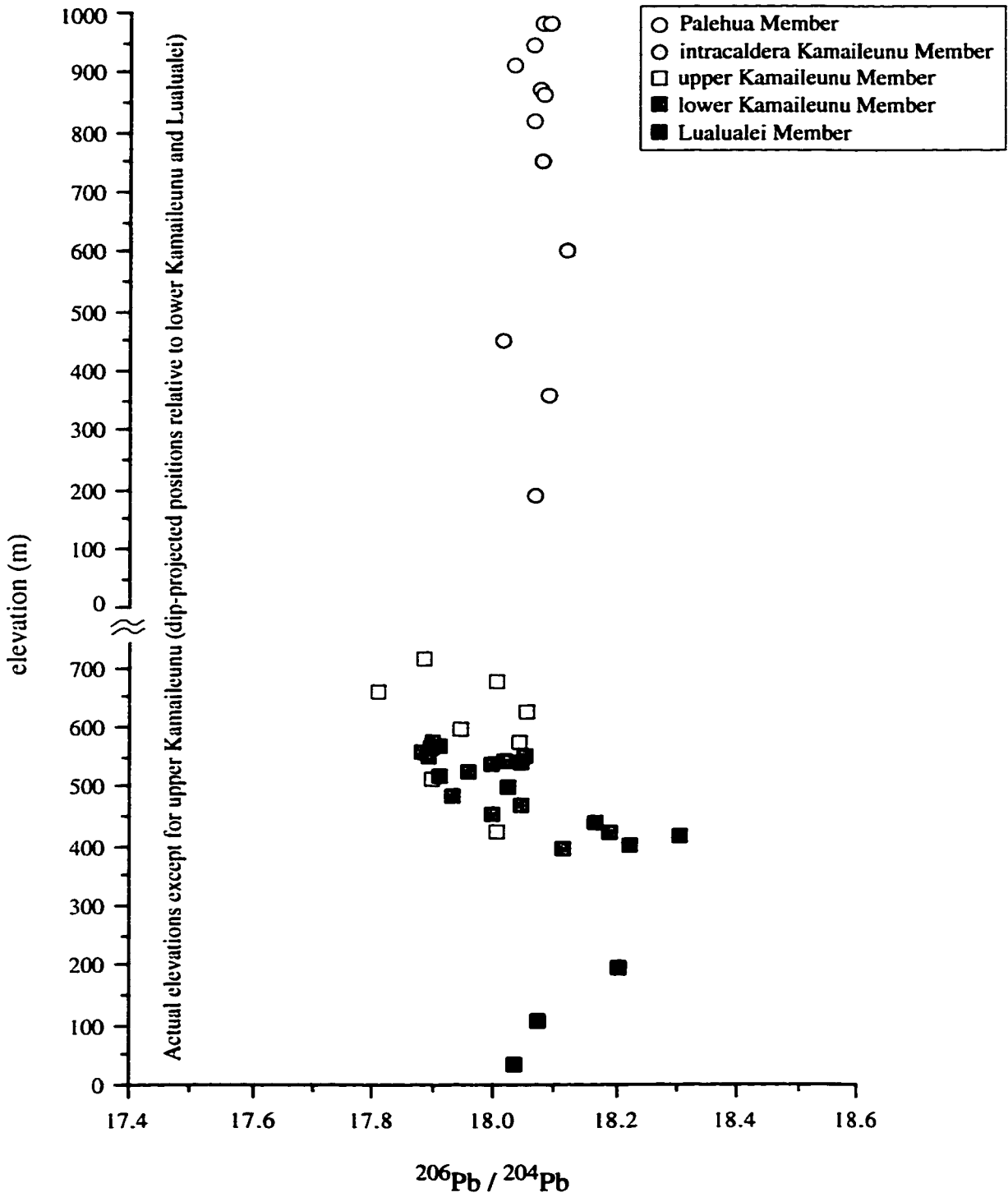


Figure 3.6 $^{206}\text{Pb}/^{204}\text{Pb}$ vs. Stratigraphic Position for Basalts of Waianae Volcano

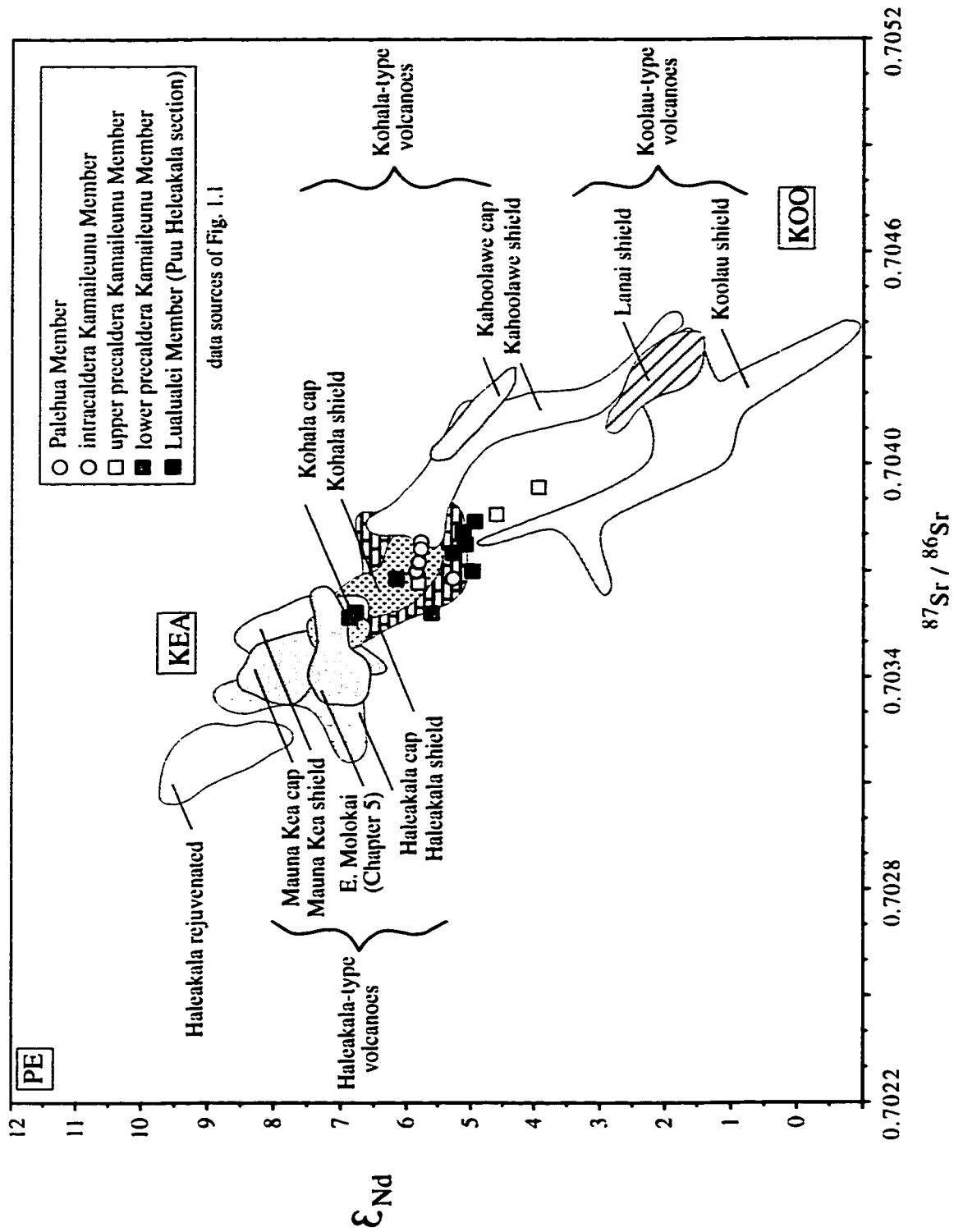


Figure 3.7 $^{87}Sr/^{86}Sr$ vs. ϵ_{Nd} for Subaerial Basalts of Waianae Volcano

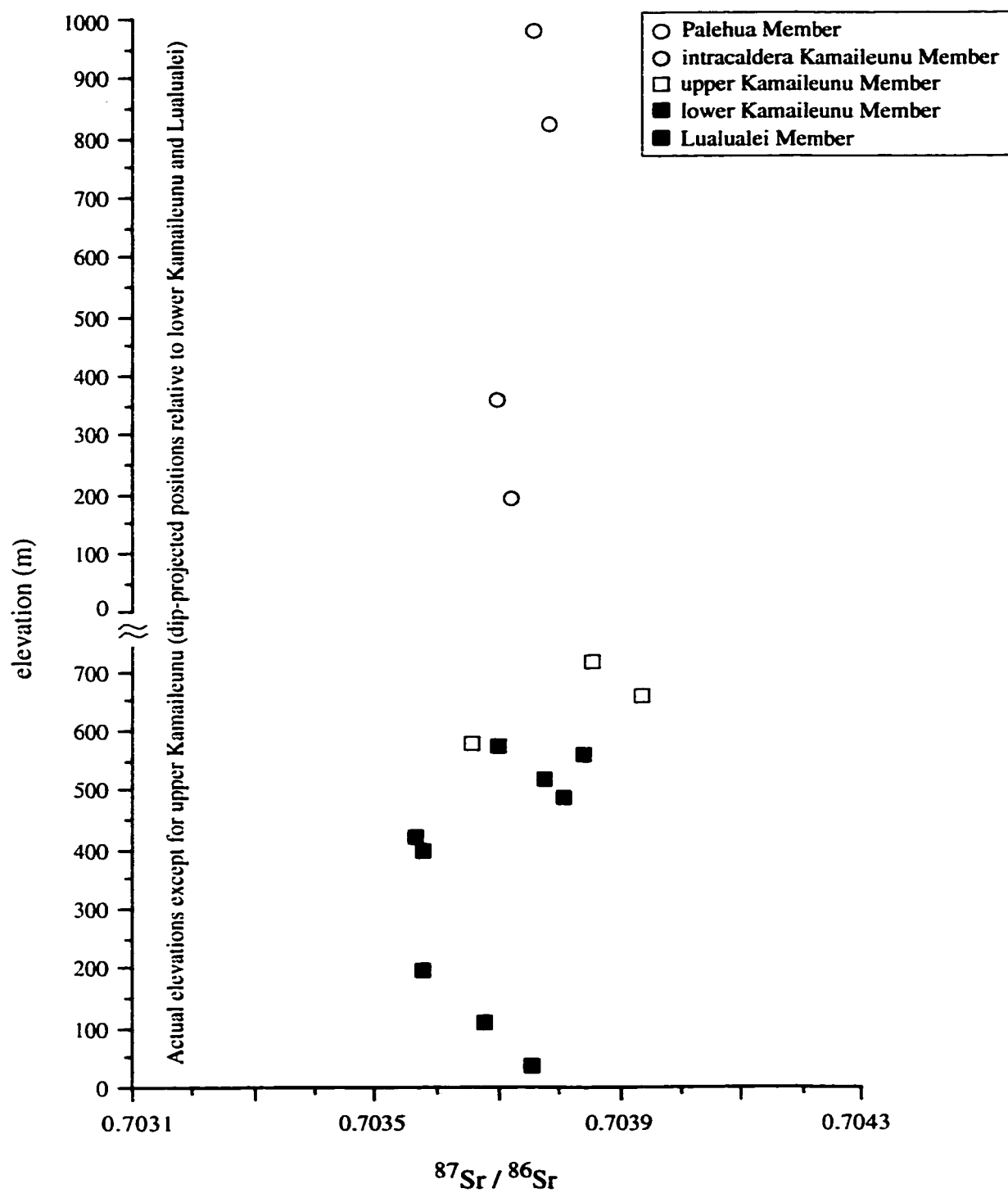


Figure 3.8 $^{87}\text{Sr}/^{86}\text{Sr}$ vs. Stratigraphic Position for Basalts Waianae Volcano

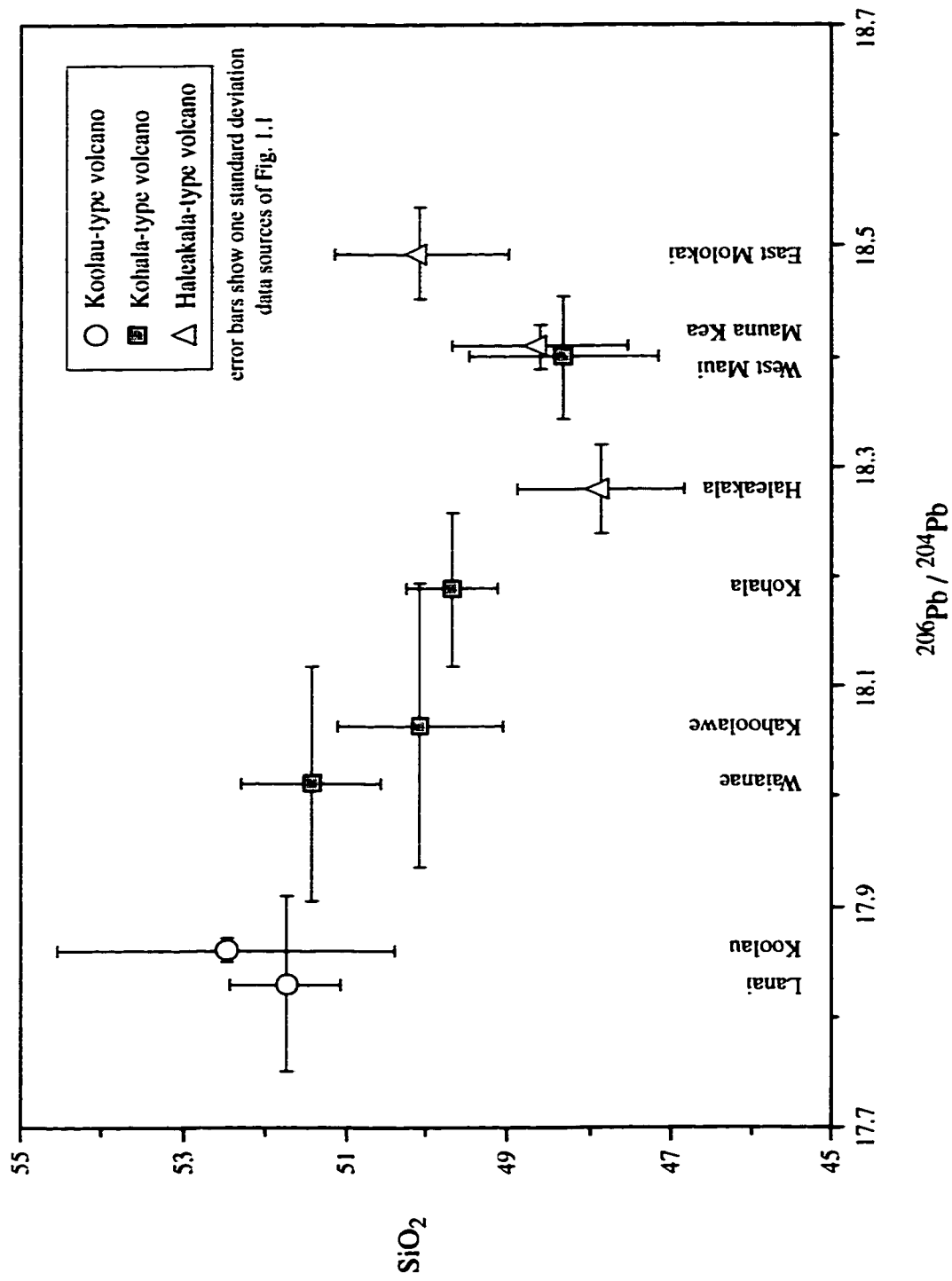


Figure 3.9 $^{206}\text{Pb}/^{204}\text{Pb}$ vs. SiO_2 for Subaerial Hawaiian Tholeiites ($\text{MgO} > 6 \text{ wt}\%$) Averaged for Individual Volcanoes

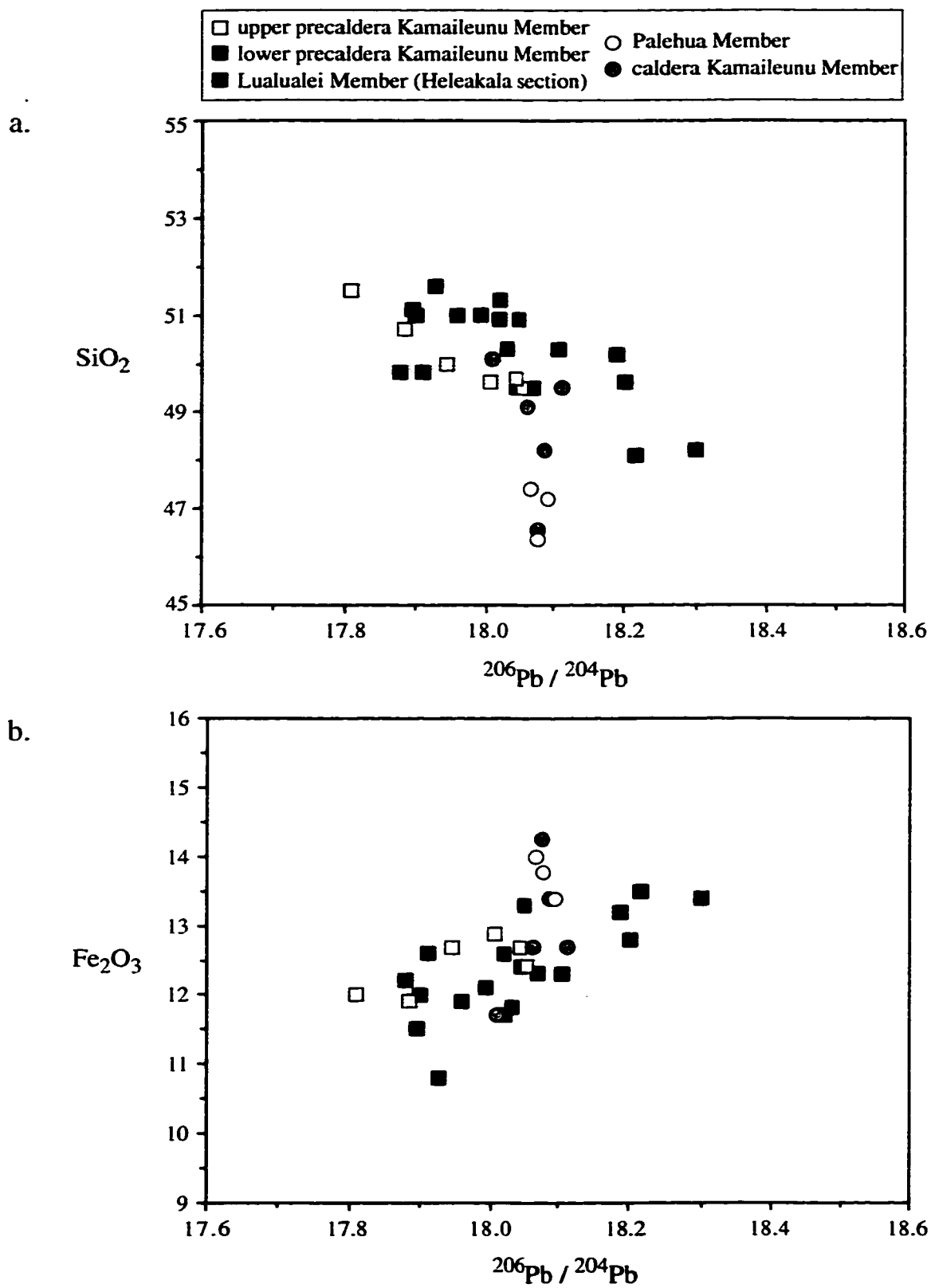


Figure 3.10 $^{206}\text{Pb}/^{204}\text{Pb}$ vs. a) SiO₂ and b) Fe₂O₃ (as total iron) for Subaerial Basalts of Waianae Volcano

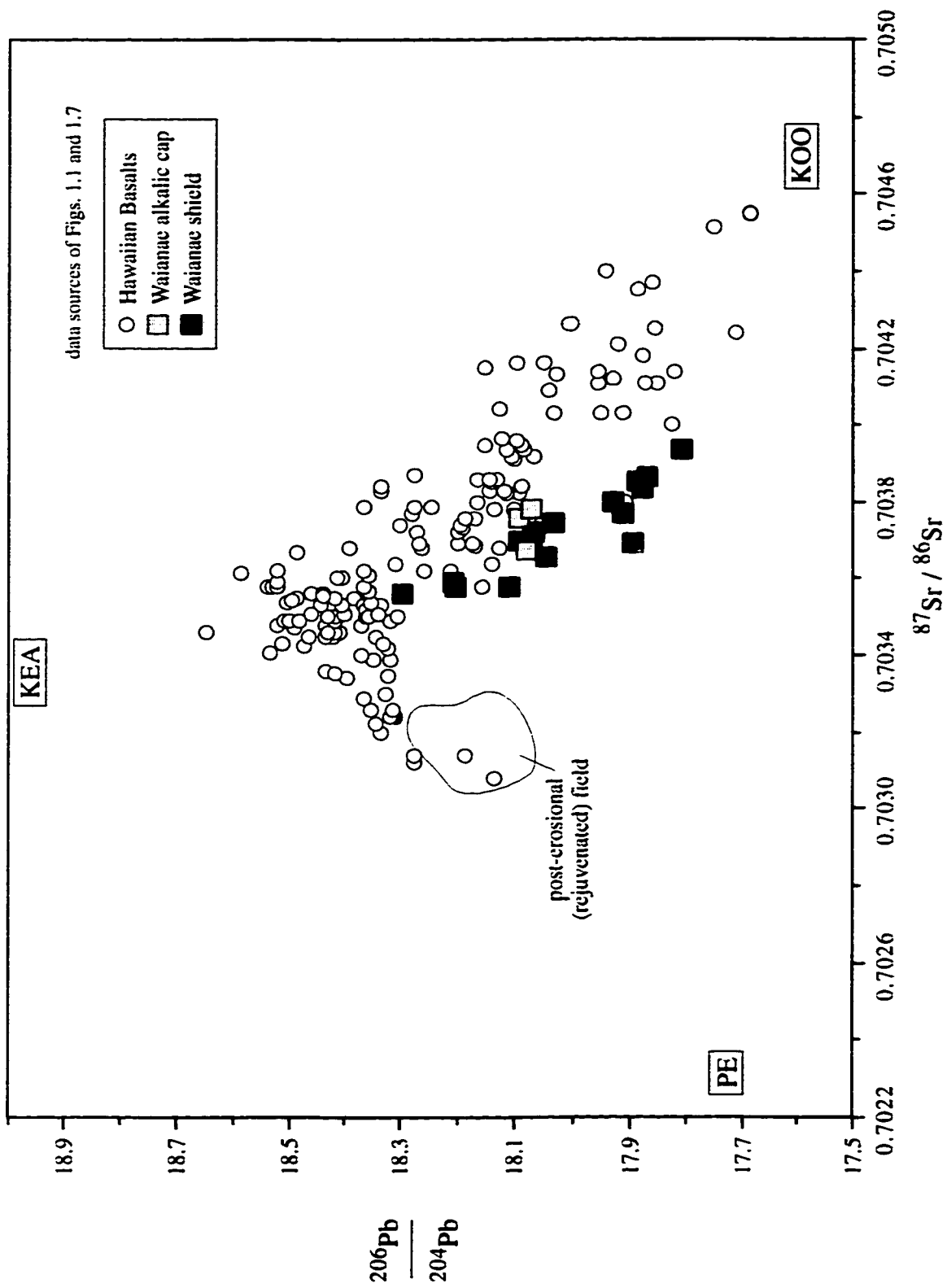


Figure 3.11 $^{87}\text{Sr}/^{86}\text{Sr}$ vs. $^{206}\text{Pb}/^{204}\text{Pb}$ for Hawaiian Basalts and Subaerial Basalts of Waianae Volcano

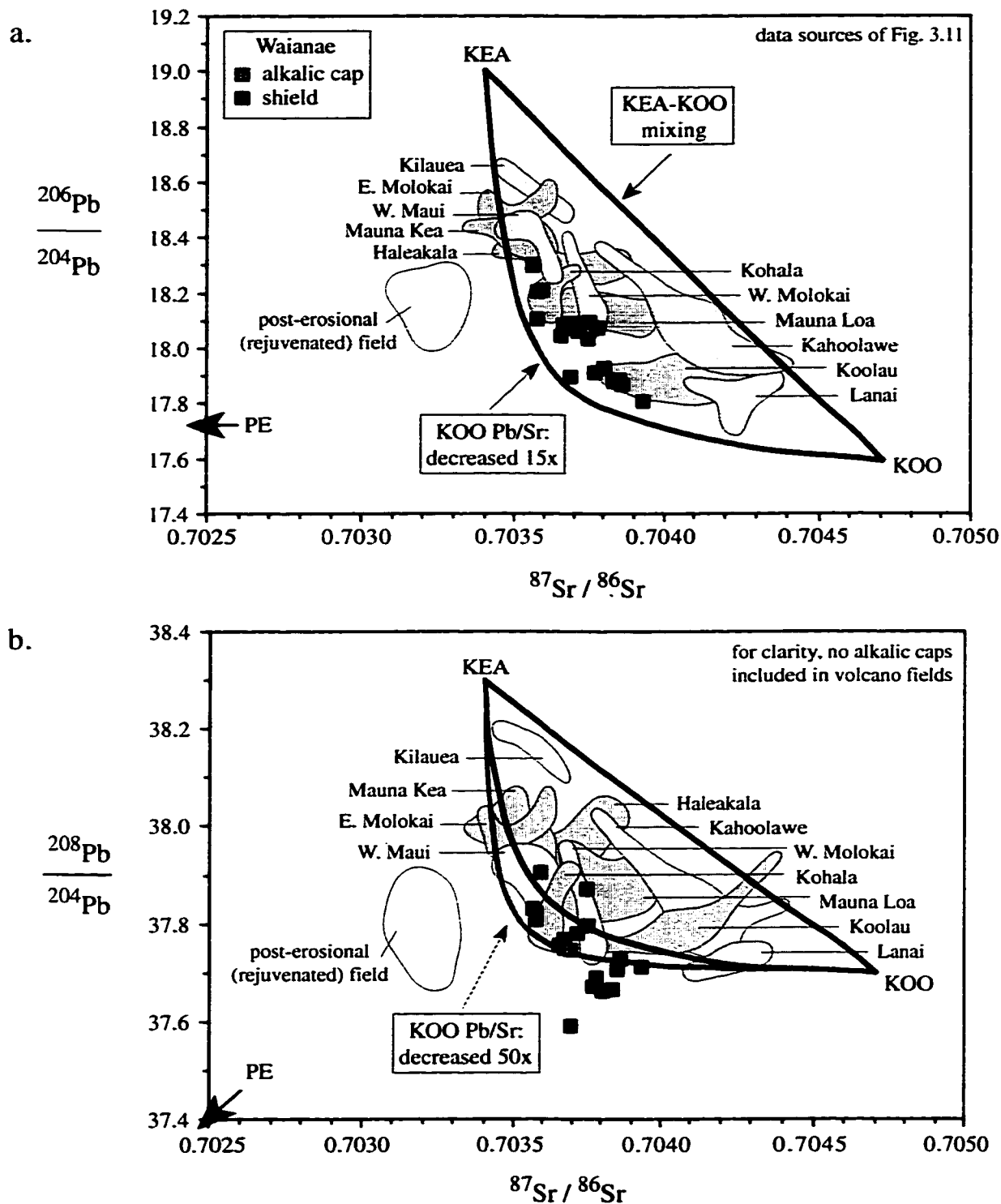


Figure 3.12 $^{87}\text{Sr}/^{86}\text{Sr}$ vs. a) $^{206}\text{Pb}/^{204}\text{Pb}$ and b) $^{208}\text{Pb}/^{204}\text{Pb}$ for Hawaiian Basalts and Subaerial Basalts of Waianae Volcano with Model Mixing Lines between KOO and KEA Mantle Endmember Components

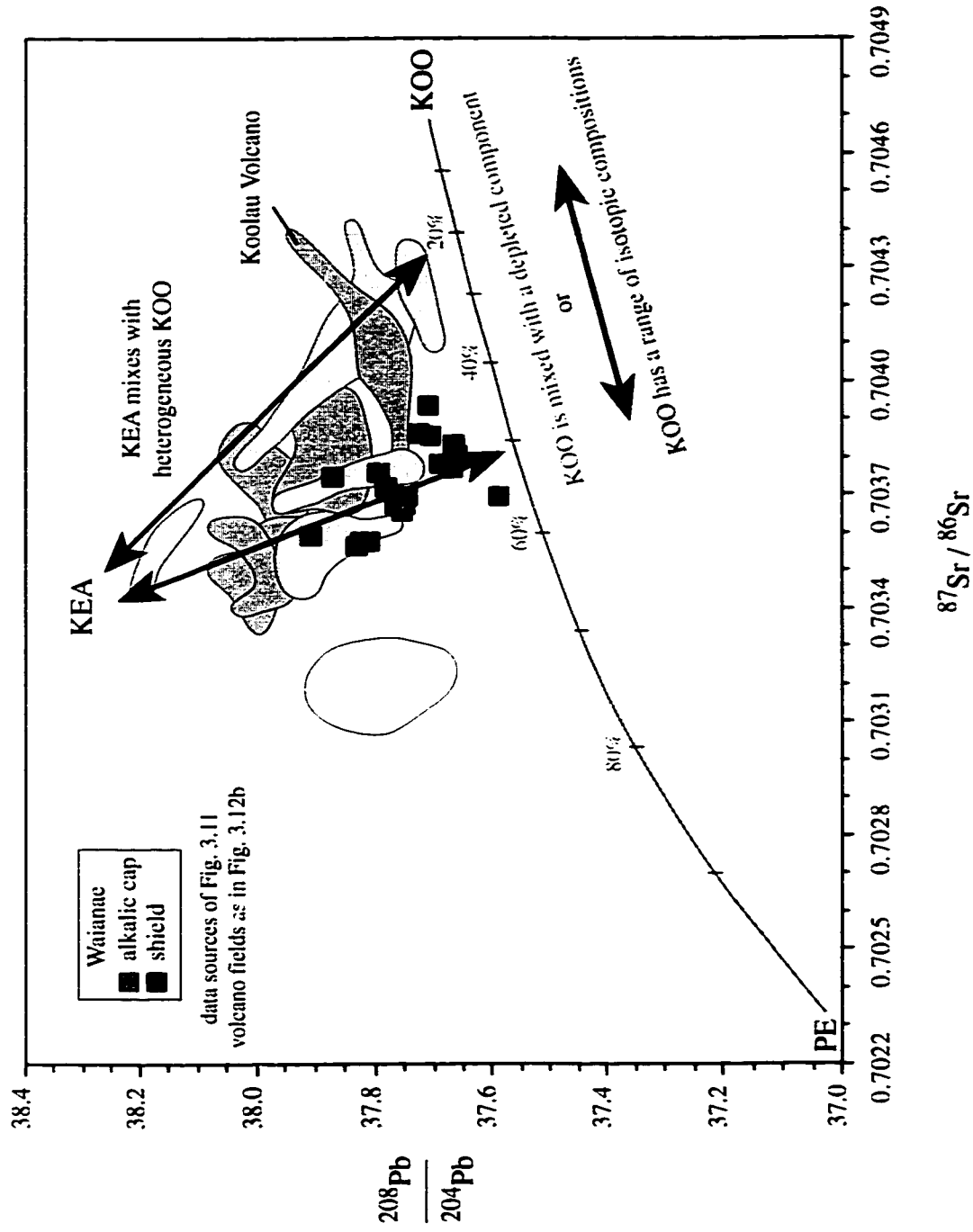
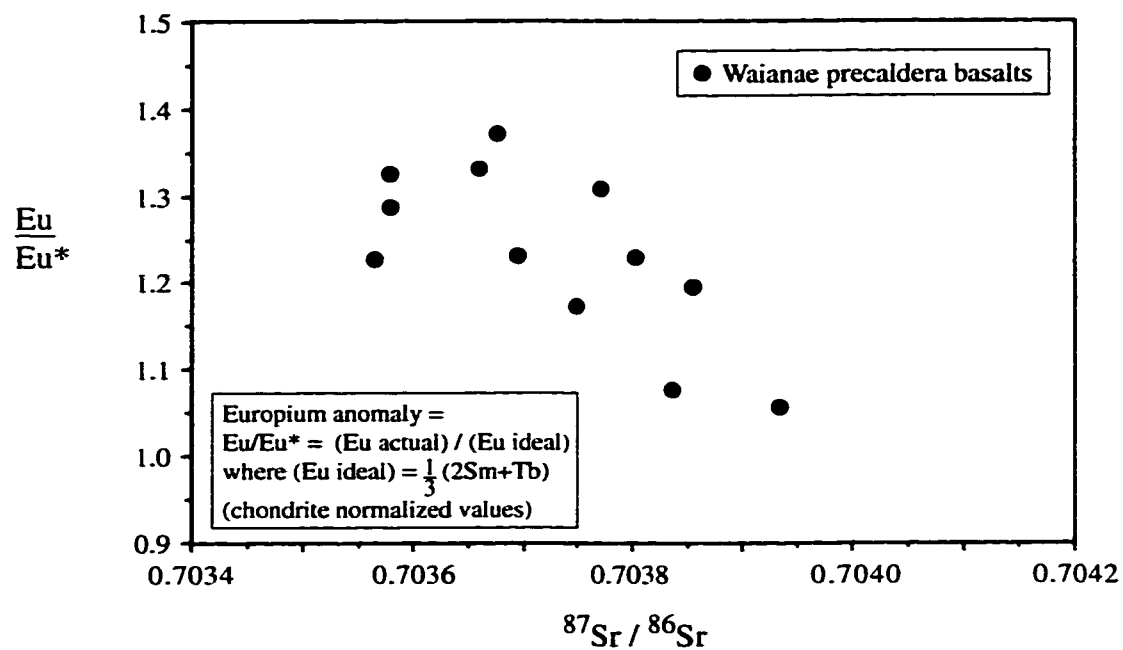


Figure 3.13 $^{87}\text{Sr}/^{86}\text{Sr}$ vs. $^{208}\text{Pb}/^{204}\text{Pb}$ for Hawaiian Basalts and Subaerial Basalts of Waianae Volcano with Model Mixing between KEA and an Isotopically Heterogeneous KOO Component

a.



b.

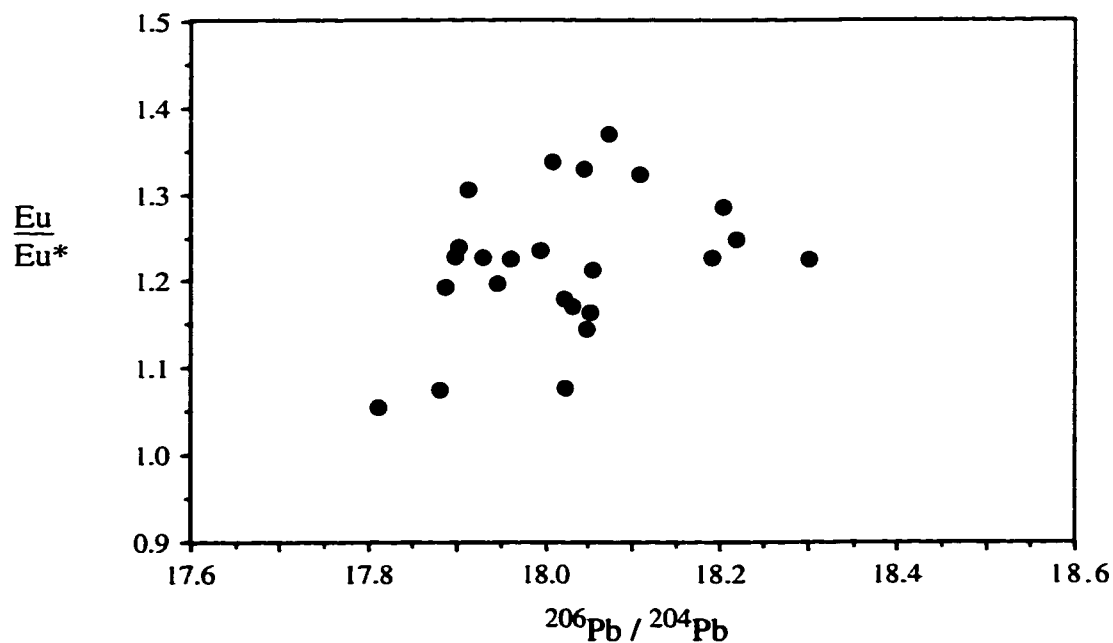


Figure 3.14 a) $^{87}\text{Sr}/^{86}\text{Sr}$ vs. Eu/Eu^* b) $^{206}\text{Pb}/^{204}\text{Pb}$ vs. Eu/Eu^* for Subaerial Precaldera Basalts of Waianae Volcano

TABLE 3.1 a) Major and Trace Element and Isotopic Compositions - Puu Heleakala

Puu Heleakala Sampled Section - Precaldera Lualualei and Kamaileunu Members								
sample rock type Member elevation (m)	RTH93-K12 tholeiite Lualualei 38	93HELE-22 tholeiite Lualualei 107	RTH93-K8 tholeiite Lualualei 198	92PH-31 tholeiite Kamaile 396	92PH-30 tholeiite Kamaile 405	92PH-29 trans Kamaile 418	92PH-28 tholeiite Kamaile 427	92PH-27 Kamaile 442
SiO ₂	50.3	49.5	49.6	50.3	48.1	48.2	50.2	
TiO ₂	2.09	2.01	2.31	2.46	2.63	3.60	2.61	
Al ₂ O ₃	12.4	12.4	13.0	13.3	13.8	14.2	13.6	
Fe ₂ O ₃	11.8	12.3	12.8	12.3	13.5	13.4	13.2	
MnO	0.16	0.17	0.17	0.17	0.18	0.16	0.18	
MgO	11.2	10.1	8.76	6.75	6.75	5.54	6.41	
CaO	8.93	9.31	9.98	10.7	10.9	9.83	11.1	
Na ₂ O	2.06	2.00	2.10	2.20	2.25	3.09	2.22	
K ₂ O	0.30	0.30	0.35	0.36	0.20	0.50	0.24	
P ₂ O ₅	0.22	0.22	0.26	0.28	0.29	0.50	0.29	
Pb	0.83	0.91	0.93			1.66		
Rb	15	20	14		12	19		
Sr	284	295	314	346	342	540	350	
Ba		90	79	116	52	182	109	
La	10.8	11.9	11.6	14.5	13.1	25.0	13.4	
Ce	25	27	26	33	31	56	32	
Nd	17	17	17	20	20	32	20	
Sm	4.54	4.25	4.56	5.09	5.53	8.17	5.37	
Eu	1.82	2.03	2.07	2.17	2.44	3.40	2.29	
Tb	0.8	0.8	0.9	0.7	1.1	1.4	1.0	
Yb	2.11	2.06	2.02	1.94	2.27	2.02	2.27	
Lu	0.31	0.29	0.27	0.27	0.30	0.27	0.31	
Y	24	23	22	22	21	30	14	
Zr	129	133	142	152	162	266	149	
Hf	3.1	3.6	3.8	4.7	4.8	7.4	4.1	
Ta	0.5		0.8	1.1	0.7	1.5	1.2	
Th	0.6	0.7	0.6	1.1	0.7	1.5	0.7	
Ni	360	220	130	80	80	80	120	
Cr	560	710	490	310	130	61	150	
Sc	27.7	29.3	29.6	30.3	33.0	25.9	32.9	
²⁰⁶ Pb/ ²⁰⁴ Pb	18.031	18.070	18.202	18.107	18.217	18.298	18.188	18.163
²⁰⁷ Pb/ ²⁰⁴ Pb	15.456	15.440	15.456	15.437	15.454	15.441	15.439	15.434
²⁰⁸ Pb/ ²⁰⁴ Pb	37.871	37.767	37.822	37.809	37.871	37.831	37.787	37.769
⁸⁷ Sr/ ⁸⁶ Sr	0.70375	0.70368	0.70358	0.70358		0.70356		
ε Nd	5.35	6.18	6.84	5.68		6.91		

Major element oxides in wt%. Fe₂O₃ = total iron. Trace element abundances in ppm.

TABLE 3.1 a) (continued) Major and Trace Element and Isotopic Compositions - Puu Heleakala

Puu Heleakala Sampled Section (continued) - Precaldera Kamaileunu Member Tholeiitic Basalts		92PH-24	92PH-22	92PH-20	92PH-17	92PH-15	92PH-13	92PH-11	92PH-10	92PH-9	92PH-8	92PH-7	92PH-6	92PH-5	92PH-4	92PH-3
sample elevation (m)		457	472	488	503	518	527	536	543	546	552	555	561	567	570	576
SiO ₂		51.0	49.5	51.6	51.3	49.8	51.0	50.9	50.9	546	552	555	49.8	567	570	576
TiO ₂		2.56	2.24	2.31	2.23	2.06	1.99	2.4	2.4	546	552	555	2.12	567	570	576
Al ₂ O ₃		13.5	14.0	13.6	14.6	12.8	14.3	13.1	13.1	546	552	555	12.1	567	570	576
Fe ₂ O ₃		12.1	12.4	10.8	11.7	12.6	11.9	12.6	12.6	546	552	555	12.2	567	570	576
MnO		0.16	0.17	0.16	0.16	0.17	0.17	0.17	0.17	546	552	555	0.17	567	570	576
MgO		6.21	7.14	6.03	6.42	9.76	7.19	6.29	6.29	546	552	555	9.66	567	570	576
CaO		10.7	9.98	10.1	10.1	10.0	9.63	9.90	9.90	546	552	555	9.20	567	570	576
Ni ₂ O		2.17	2.37	2.33	2.46	1.99	2.54	2.31	2.31	546	552	555	1.84	567	570	576
K ₂ O		0.36	0.17	0.47	0.32	0.12	0.17	0.36	0.36	546	552	555	0.32	567	570	576
P ₂ O ₅		0.27	0.22	0.27	0.24	0.22	0.21	0.28	0.28	546	552	555	0.24	567	570	576
Pb				1.17		0.92							1.14			
Rb		12	12	19	19	19	12	12	12				18			
Sr		337	319	358	314	297	317	325	325				351			
Ba		106	68	98	88	105	105	97	97				83			
La		12.3	12.0	12.7	11.0	10.0	12.8	12.6	12.6				13.8			
Ce		29	28	30	25	24	29	28	28				31			
Nd		18	17	19	17	14	19	19	19				20			
Sm		5.11	4.79	4.98	4.57	3.99	5.07	4.92	4.92				5.19			
Bu		2.16	1.85	2.17	1.84	1.78	2.13	1.83	1.83				1.90			
Tb		0.9	0.8	1.0	0.8	0.7	0.9	0.9	0.9				0.9			
Yb		2.05	1.94	1.86	1.94	1.89	2.24	1.87	1.87				1.87			
Lu		0.29	0.28	0.26	0.28	0.26	0.30	0.26	0.26				0.27			
Y		23	23	10	21	21	20	20	20				25			
Zr		146	138	128	138	109	125	145	145				130			
Hf		4.6	3.8	4.4	3.7	3.2	3.8	4.1	4.1				3.4			
Ta		0.8	0.8	0.8	0.6	0.9	0.6	0.7	0.7				0.7			
Th		0.6	0.3	0.7	0.6	0.5	0.6	0.7	0.7				0.2			
Ni		50	130	120	130	320	90	80	80				160			
Cr		290	340	360	270	630	350	260	260				650			
Sc		32.9	29.0	28.6	28.0	28.8	30.3	28.1	28.1				27.5			
²⁰⁶ Pb/ ²³⁸ Pb		17.992	18.046	17.928	18.020	17.910	17.959	17.995	18.019	18.042	17.893	18.050	17.879	17.909	17.899	17.895
²⁰⁷ Pb/ ²³⁵ Pb		15.426	15.435	15.424	15.445	15.436	15.447	15.465	15.445	15.452	15.429	15.454	15.418	15.442	15.418	15.414
²⁰⁸ Pb/ ²³² Pb		37.748	37.751	37.663	37.741	37.671	37.729	37.782	37.74	37.718	37.642	37.727	37.664	37.682	37.616	37.589
⁸⁷ Sr/ ⁸⁶ Sr				0.70380		0.70377							0.70384			
ε _{Ni}				5.20		5.16							4.99			

TABLE 3.1 b) Major and Trace Element and Isotopic Compositions - Nanakuli Ridge

Nanakuli Ridge Sampled Section - Precaldera Kamaileunu Member								
sample	93Nana-4	93Nana-21	93Nana-28	93Nana-30.2	93Nana-30.12	93Nana-31.12	93Nana-31.22	93Nana-31.31
rock type			tholeiite	tholeiite	tholeiite	tholeiite	tholeiite	tholeiite
Member	Kamaile	Kamaile	Kamaile	Kamaile	Kamaile	Kamaile	Kamaile	Kamaile
elevation (m)	232	323	366	390	424	454	475	546
SiO ₂			49.7	50.0	49.5	51.5	49.6	50.7
TiO ₂			2.36	2.36	2.17	2.34	2.48	2.12
Al ₂ O ₃			14.3	14.2	14.3	14.1	13.9	14.3
Fe ₂ O ₃			12.7	12.7	12.4	12.0	12.9	11.90
MnO			0.17	0.17	0.16	0.16	0.16	0.15
MgO			7.09	6.91	6.79	6.24	7.54	6.95
CaO			10.4	10.4	9.79	9.64	9.44	9.48
Na ₂ O			2.31	2.25	2.19	2.35	2.24	2.27
K ₂ O			0.20	0.12	0.20	0.43	0.30	0.23
P ₂ O ₅			0.27	0.24	0.24	0.28	0.25	0.19
Pb						1.31		1.14
Rb			15	12	10	14	13	
Sr			367	353	324	380	399	321
Ba			77	87	76	109	66	
La			13.1	12.3	14.3	16.4	13.6	17.4
Ce			29	28	31	36	30	33
Nd			19	19	21	25	20	26
Sm			5.00	5.24	5.72	6.34	4.96	6.60
Eu			2.22	2.07	2.37	2.28	2.22	2.72
Tb			0.8	0.8	1.0	1.1	0.8	1.2
Yb			1.84	1.86	1.84	2.28	1.70	3.12
Lu			0.27	0.26	0.26	0.32	0.24	0.45
Y			22	20	24	25	19	51
Zr			149	149	133	157	159	137
Hf			3.8	3.7	3.4	5.0	4.4	3.5
Ta			0.8	0.7	0.8	0.5	0.8	0.6
Th			0.4	0.5	0.5	0.6	0.7	0.6
Ni			80	120	80	100	65	60
Cr			300	300	350	270	340	280
Sc			30.8	30.8	29.1	29.8	29.3	28.1
²⁰⁶ Pb/ ²⁰⁴ Pb	18.004	17.903	18.043	17.944	18.054	17.808	18.006	17.884
²⁰⁷ Pb/ ²⁰⁴ Pb	15.445	15.449	15.466	15.454	15.449	15.435	15.461	15.423
²⁰⁸ Pb/ ²⁰⁴ Pb	37.744	37.760	37.755	37.724	37.714	37.711	37.746	37.706
⁸⁷ Sr/ ⁸⁶ Sr			0.70366			0.70393		0.70385
εNd			5.85			3.97		4.66

TABLE 3.1 c) Major and Trace Element and Isotopic Compositions - Kamaileunu Ridge

Kamaileunu Ridge Spur Sampled Section - Intracaldera Kamaileunu Member					
sample rock type Member elevation (m)	93KR-23 tholeiite Kamaile 195	93KR-16A trans Kamaile 357	93KR-13 tholeiite Kamaile 457	93KR-8 tholeiite Kamaile 610	93KR-4 tholeiite Kamaile 817
SiO ₂	49.1	48.2	50.1	49.5	46.6
TiO ₂	2.08	3.22	2.70	2.66	4.00
Al ₂ O ₃	13.3	15.5	15.9	14.3	15.0
Fe ₂ O ₃	12.7	13.4	11.7	12.7	14.3
MnO	0.17	0.16	0.15	0.16	0.18
MgO	7.71	5.32	4.82	6.52	5.50
CaO	10.5	9.51	9.79	10.0	7.98
Na ₂ O	2.34	2.89	2.99	2.53	3.57
K ₂ O	0.21	0.52	0.43	0.39	0.98
P ₂ O ₅	0.26	0.44	0.35	0.37	0.62
Pb	1.09				
Rb		21		22	
Sr	359	526		477	
Ba	106	186		124	
La	12.1	19.8		20.0	
Ce	28	45		43	
Nd	18	28		27	
Sm	4.62	7.10		6.59	
Eu	2.16	2.74		2.58	
Tb	0.8	1.1		1.1	
Yb	1.82	2.15		1.79	
Lu	0.26	0.29		0.24	
Y	18	26		25	
Zr	134	225		189	
Hf	3.3	6.7		4.6	
Ta		0.9		1.1	
Th	0.7	1.2		1.2	
Ni	150	80		90	
Cr	510	130		260	
Sc	30.9	25.3		28.8	
²⁰⁶ Pb/ ²⁰⁴ Pb	18.063	18.088	18.009	18.113	18.077
²⁰⁷ Pb/ ²⁰⁴ Pb	15.453	15.450	15.443	15.449	15.440
²⁰⁸ Pb/ ²⁰⁴ Pb	37.781	37.746	37.727	37.779	37.690
⁸⁷ Sr/ ⁸⁶ Sr	0.70372	0.70370			
εNd	5.86	5.89			

TABLE 3.1 d) Major and Trace Element and Isotopic Compositions - Palehua Alkali Cap

Alkalic Cap at Kamaileunu Ridge								at Mauna Kapu		
sample	93KR 1	RTH93 K6	RTH93 K1	RTH93 K5	RTH93 K4	RTH93 K3	RTH93 K2	93PALIK 12	93PALIK 11	
rock type	hawaiite							hawaiite		hawaiite
Member	Palehua							Palehua	Palehua	Palehua
elevation (m)	817	862	872	914	945	975	978	793	793	
SiO ₂	47.4						47.2		46.4	
TiO ₂	3.72						3.40		4.04	
Al ₂ O ₃	15.8						16.1		16.4	
Fe ₂ O ₃	14.0						13.4		13.8	
MnO	0.19						0.19		0.18	
MgO	4.04						3.99		4.01	
CaO	7.09						6.53		7.77	
Na ₂ O	3.99						3.75		4.22	
K ₂ O	1.44						1.71		1.27	
P ₂ O ₅	0.85						0.93		0.59	
Pb	3.15						3.46			
Rb	36						46			
Sr	751						665			
Ba	381						493			
La	50.6						45.3			
Ce	110						98			
Nd	62						53			
Sm	14.60						12.00			
Eu	6.00						4.50			
Tb	2.3						1.5			
Yb	3.08						2.80			
Lu	0.41						0.36			
Y	45						37			
Zr	382						379			
Hf	10.0						10.0			
Ta	2.8						2.8			
Th	2.9						3.6			
Ni										
Cr	14						10			
Sc	16.0						15.6			
²⁰⁶ Pb/ ²⁰⁴ Pb	18.067	18.083	18.079	18.031	18.063	18.084	18.091	18.089	18.076	
²⁰⁷ Pb/ ²⁰⁴ Pb	15.442	15.461	15.460	15.450	15.454	15.446	15.471	15.466	15.457	
²⁰⁸ Pb/ ²⁰⁴ Pb	37.691	37.747	37.747	37.693	37.718	37.704	37.795	37.763	37.749	
⁸⁷ Sr/ ⁸⁶ Sr	0.70378						0.70376		0.70367	
εNd	5.82						5.81		5.34	

Table 3.2 Mixing Parameters for Model Mantle Source of Waianae Lavas

		Sr	Pb	$\frac{87\text{Sr}}{86\text{Sr}}$	ϵ_{Nd}	$\frac{206\text{Pb}}{204\text{Pb}}$	$\frac{208\text{Pb}}{204\text{Pb}}$
compositions	KOO ^a	23.0	0.071	0.7047	0.23	17.6	37.7
	KEA ^b	23.0	0.071	0.7034	+9.4	19.0	38.3
	PE ^c	12.9	0.018	0.7023	+12.0	17.72	37.0
^a Sr and Pb concentrations from primitive mantle compilation in Rollinson (1993). Sr and Nd isotope compositions from EM of Reiners and Nelson (1998). Pb isotope composition consistent with Stille et al. (1986) and West and Leeman (1987). ^b Sr and Pb concentrations from primitive mantle compilation in Rollinson (1993). Isotope compositions consistent with Stille et al. (1986) and West and Leeman (1987). ^c Sr and Pb concentrations from Geochemical Earth Reference Model. Sr and Nd isotope compositions of Reiners and Nelson (1998). Pb isotope composition of West and Leeman (1987) and data trends.							

CHAPTER 4

Field Investigation and Composite Stratigraphy of East Molokai Volcano, Hawaii

ABSTRACT

The composite subaerial stratigraphic sequence of East Molokai Volcano is based on dip projection of sampled sections. Although there are no common magnetic polarity reversal boundaries identified in the sampled sections, the composite is consistent with the relative positions of identified reversals and with major element geochemical trends identified in Chapter 5. Extracaldera flows are approximately 1280 meters thick in composite (three parts), including a stratigraphic gap of approximately 250 meters.

INTRODUCTION

The remnant of East Molokai Volcano forms the eastern two-thirds of the island of Molokai (Fig. 1.1). The north coast of East Molokai is a series of spectacular sea cliffs, locally more than 1000 meters high. The sea cliffs, and the large deep valleys of the north coast, provide excellent exposure of subaerial lava flows in cross-section. The southern flank of the volcano approximates the original surface of the volcano, but also offers excellent interior exposures in erosional valleys such as the deep Kamalo Gulch.

OBJECTIVES

To establish geologic content for lava sampling and subsequent geochemical study of the evolution of the volcano (Chap. 5), a composite stratigraphy of the subaerial flows of East Molokai was constructed, based on flow orientation and remnant magnetic polarity determined by a portable fluxgate magnetometer in the field. Although none of the sections have an identified common magnetic polarity reversal boundary, requiring projection of the stratigraphic sections into composite based solely on structural criteria, the composite stratigraphy is consistent with relative magnetic polarities and boundaries identified in the field. Whereas the lithologic similarity of the subaerial shield flows provides little information in constructing a composite, the major element geochemistry (Chap. 5) reveals a trend in the alkaline character of the lavas that correlates with the lava position in the composite stratigraphy.

PREVIOUS WORK

Stearns and Macdonald (1947) presented a detailed account of the geology of East Molokai Volcano and the only geologic map. They subdivided the lavas into the East Molokai Volcanic Series, informally divided into the basaltic lower member and the andesitic upper member (nomenclature of Stearns and Macdonald, 1947), and the Kalaupapa Basalt (Fig. 4.1). Langenheim and Clague (1987) revised the names to the East Molokai Volcanics and Kalaupapa Volcanics. The Kalaupapa Volcanics are the lavas of a rejuvenated stage shield that surfaces as the Kalaupapa Peninsula on the north coast of Molokai (Fig. 4.1).

The identification of debris avalanche deposits on the seafloor north of Molokai (Moore, 1964; Moore et al., 1989) and stratigraphic study of the subaerial East Molokai lavas (Holcomb, 1985; 1990) indicate a giant landslide issued from the north flank of the volcano, removing the entire northern half of the shield. Holcomb (1985, 1990) compiled a general magnetostratigraphy for the subaerial flows and argued that the seacliffs along the north coast of Molokai bisect a caldera about 12 km wide. Whereas Stearns and Macdonald (1947) mapped the caldera complex as a crescent-shaped body extending from the heads of Wailau to Pelekunu valleys, the reinterpretation by Holcomb (1985) places the Stearns and Macdonald caldera at the southern end of a much larger structure centered along the north coast between the mouths of Haupu Bay and Papalaua Valley (Fig. 4.1). The caldera fill comprises more than 600 meters of flat-lying to gently-dipping normal magnetic-polarity flows, which overlie talus that accumulated against caldera walls exposed in the head of Haupu Bay and along the southwest wall of Pelekunu Valley (Holcomb, 1985; 1990; unpublished data).

Two magnetic polarity boundaries are distinguished in extracaldera flows (Holcomb, 1985; 1990; unpublished data). The lowermost subaerial polarity boundary is exposed west of the caldera margin in cliffs west and south of Haupu Bay (Fig. 4.1), where it separates the reversed polarity flows of the oldest exposed unit from overlying normal polarity flows. The oldest unit is subaerially about 200 meters thick, but has limited exposure as it dips southwest below sea level. This unit is not subaerially exposed east of the caldera, probably due to tilting of the bulk of East Molokai under the weight of younger volcanoes (Holcomb, 1985).

The younger extracaldera polarity boundary separates the normal polarity unit from an overlying reversed polarity unit. The normal polarity unit is 200-300 meters thick and,

consistent with flow dip, is exposed west of the caldera from Haupu Bay to Kalaupapa Peninsula and east of the caldera from Papalaua Valley to just past the Puahaunui Peninsula (Fig. 4.1). Holcomb (1990) suggested that this unit accumulated during the Olduvai epoch (1.88-1.66 Ma). The overlying reversed polarity unit, which includes the alkalic capping basalts, was the focus of geochemical studies by Beeson (1976) and Clague and Beeson (1980), who sampled the 300 meters-thick section in the cliff above Kalaupapa Peninsula. Holcomb (1990) summarized ages of dated flows in this reversed polarity unit, reporting alkalic cap lavas at 1.49-1.35 Ma and underlying lavas at slightly greater than 1.5 Ma.

The normal polarity caldera flows are younger, by superposition, than the two extracaldera polarity boundaries. Holcomb (personal communication) suggested that caldera lavas may have accumulated during an interval of normal polarity at 1.55 Ma, although normal polarity lavas of this interval have not yet been identified in extracaldera flows.

Rejuvenated stage Kalaupapa Basalts built a small shield that surfaces as the Kalaupapa Peninsula below the cliffs of the north coast (Fig. 4.1). The rejuvenated stage lavas, with an eruption age of about 0.5 Ma (Clague et al., 1982) and a lack of significant marine erosion, is consistent with a time frame that indicates origin of the East Molokai sea cliffs by landsliding rather than erosion (Holcomb, 1985).

STRATIGRAPHIC SECTIONS

Haupu Section

The Haupu section, located just outside of the western caldera margin exposed in the head of Haupu Bay (Fig. 4.1), comprises the oldest subaerial flows of East Molokai. Reversed

polarity flows were sampled near sea level, and overlying normal polarity flows were sampled between 215-305 meters elevation (Nelson, personal communication). Sample locations are shown in Figure 4.2 and sample descriptions are in Appendix C.1.

Hakaaano Section

The Hakaaano section is the sea cliff above Hakaaano Peninsula, east of Papalaua Valley and just outside of the eastern caldera margin (Fig. 4.1). The normal polarity flows of the lower Hakaaano section were sampled between sea level and 122 meters elevation, where the normal to reversed polarity boundary was identified, consistent with the boundary located in the 1981 field expedition of Holcomb (personal communication). The reversed polarity flows of the upper Hakaaano section were sampled between 140-323 meters elevation by a team of climbers on the 1981 expedition. Sample locations are shown in Figure 4.2 and sample descriptions are in Appendix C.2.

Kamalo Gulch Section

The Kamalo Gulch section is a thick sequence of flows exposed in Kamalo Gulch on the southern slope of East Molokai (Fig. 4.1). The reversed polarity flows, including the alkalic basalt cap of the volcano, were sampled between 198-591 meters elevation on the west wall of the Gulch, just south of the canyon constriction. Four samples (90KAM) were collected from high in the stratigraphic sequence at the mouth of the canyon (Nelson, personal communication), and one sample (EKAM) was collected from high on the east wall of the canyon. Sample locations are shown in Figure 4.2 and sample descriptions are in Appendix C.3.

Caldera Samples

The two caldera samples were collected from normal polarity flows at sea level and at 220 meters elevation at the mouth of Pelekunu Valley (Nelson, personal communication) (Appendix C.4).

Rejuvenated Stage Samples

Samples of the Kalaupapa Basalt were collected from the crater wall (90KAL-1, 2) and adjacent lava tube (90KAL-4) on Kalaupapa Peninsula (Nelson, personal communication) (Appendix C.5).

COMPOSITE STRATIGRAPHY

The identification of magnetic polarity boundaries among the subaerial lava flows of East Molokai provides for a general composite magnetostratigraphy. Stratigraphic projection of the sampled sections, although interpretive, gives more detailed relations between samples. The sampled sections were projected according to dip slope to an intersection in the center of Holcomb's (1985, 1990) proposed caldera, which is the hypothetical central axis of the shield (Fig. 4.1). The caldera is centered approximately at the Wailele Falls at Puukaoku Peninsula on the north coast. Stearns and Macdonald (1947) measured a dip of 10° in flows of Kamalo Gulch, and dips between $8-15^\circ$ in flows surrounding Haupu Bay. No flow dips are indicated on their map in the vicinity of Hakaaano Peninsula. For these three sampled sections, a dip of 10° is assumed for the projection calculations. The sampled sections are similar distances from the intersection of projection, which supports the assumption of a similar flow dip for the three sections.

The stratigraphic projections suggest that the sampled Hakaano section directly overlies the Haupū section, but that there is an approximate gap of 250 meters between the sample highest in the Hakaano section and lowest in the overlying Kamalo Gulch section.

Because flows are much less steeply dipping further out on the volcano flanks, the reversed polarity section in the cliff above Kalaupapa Peninsula (Beeson, 1976; Clague and Beeson, 1980), with a dip of approximately 2°, may not be projected with confidence into the composite stratigraphy. However, the new composite major element geochemistry displays a geochemical trend (Chap. 5), in which the major element geochemistry of the Kalaupapa section (Beeson, 1976) overlaps the projected stratigraphic gap between the north coast and Kamalo Gulch lavas.

The Haupū, Hakaano, and Kamalo Gulch sections project to a composite subaerial extracaldera stratigraphic height of nearly 1280 meters. The overall lithology of the three sections is similar, with olivine, pyroxene, and plagioclase in various combinations, even in the lowermost subaerial flows (Appendix C). Although major element analyses (Chap. 5) show a gradual change with stratigraphic height from tholeiitic to transitional to alkalic basalt compositions, evidence of the change is not obvious in the field. However, there is a distinct lithologic change at about 480 meters elevation in the Kamalo Gulch section (1160 meters composite height) to aphyric or finely plagioclase-phyric, where plagioclase laths are visibly oriented in the uppermost flows. This change apparently corresponds to the boundary between the lower and upper member of Stearns and Macdonald (1947). Major element analyses show these upper lavas to be mugearites and benmoreites.

CONCLUSIONS

The subaerial shield and alkalic cap lavas of East Molokai Volcano are represented by a composite extracaldera stratigraphic column approximately 1280 meters thick and consisting of three sections projected along dip planes to a common intersection, presumably the central axis of the volcano. Although the sections share no correlatable stratigraphic markers, such as magnetic polarity reversal boundaries or distinct changes in rock lithology, the composite column is consistent with relationships between the three identified extracaldera magnetic polarity units and with the gradual change in major element compositions of the lavas (Chap. 5).

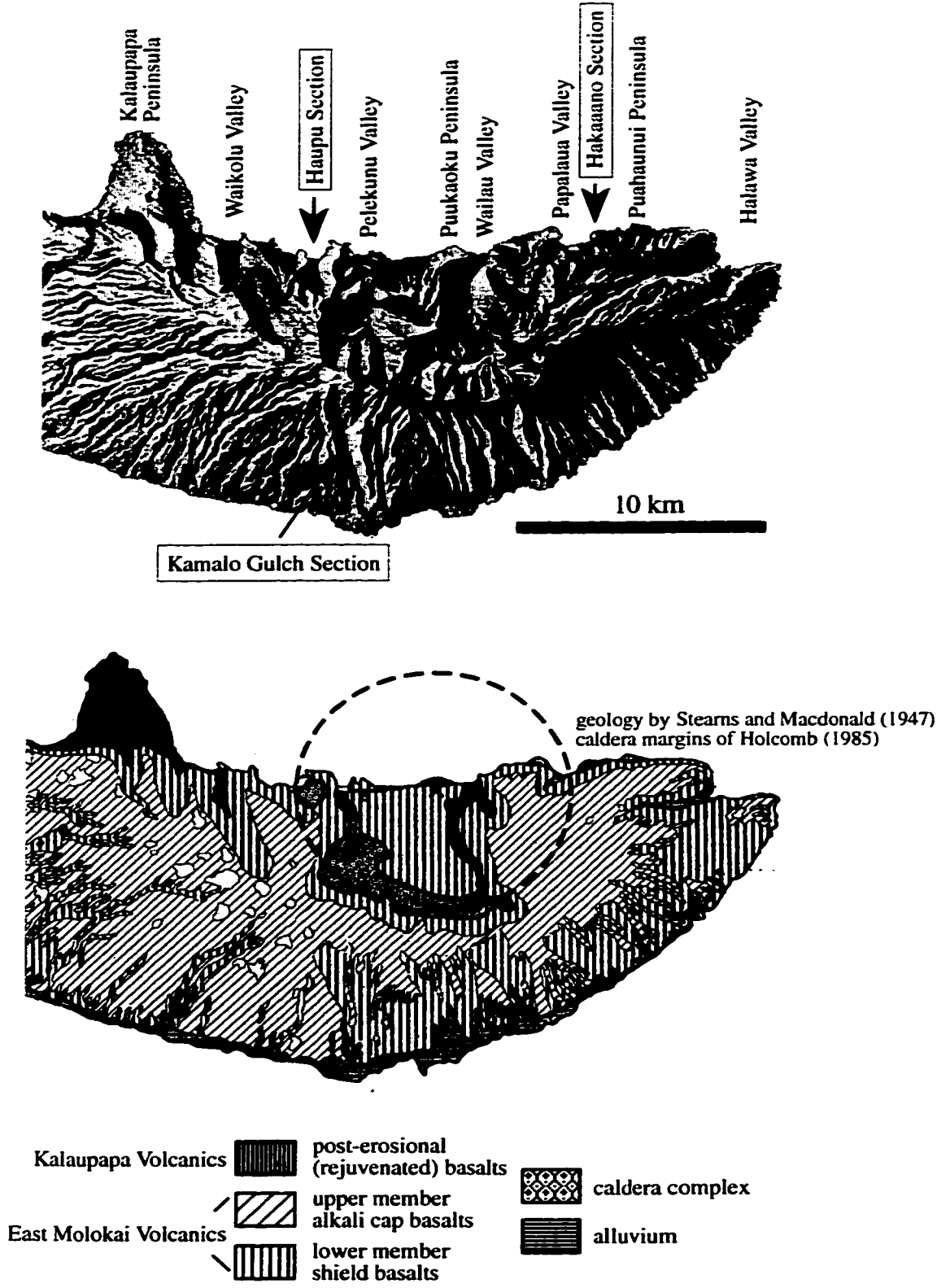


Figure 4.1 Shaded Relief and Geologic Map Views of East Molokai Volcano

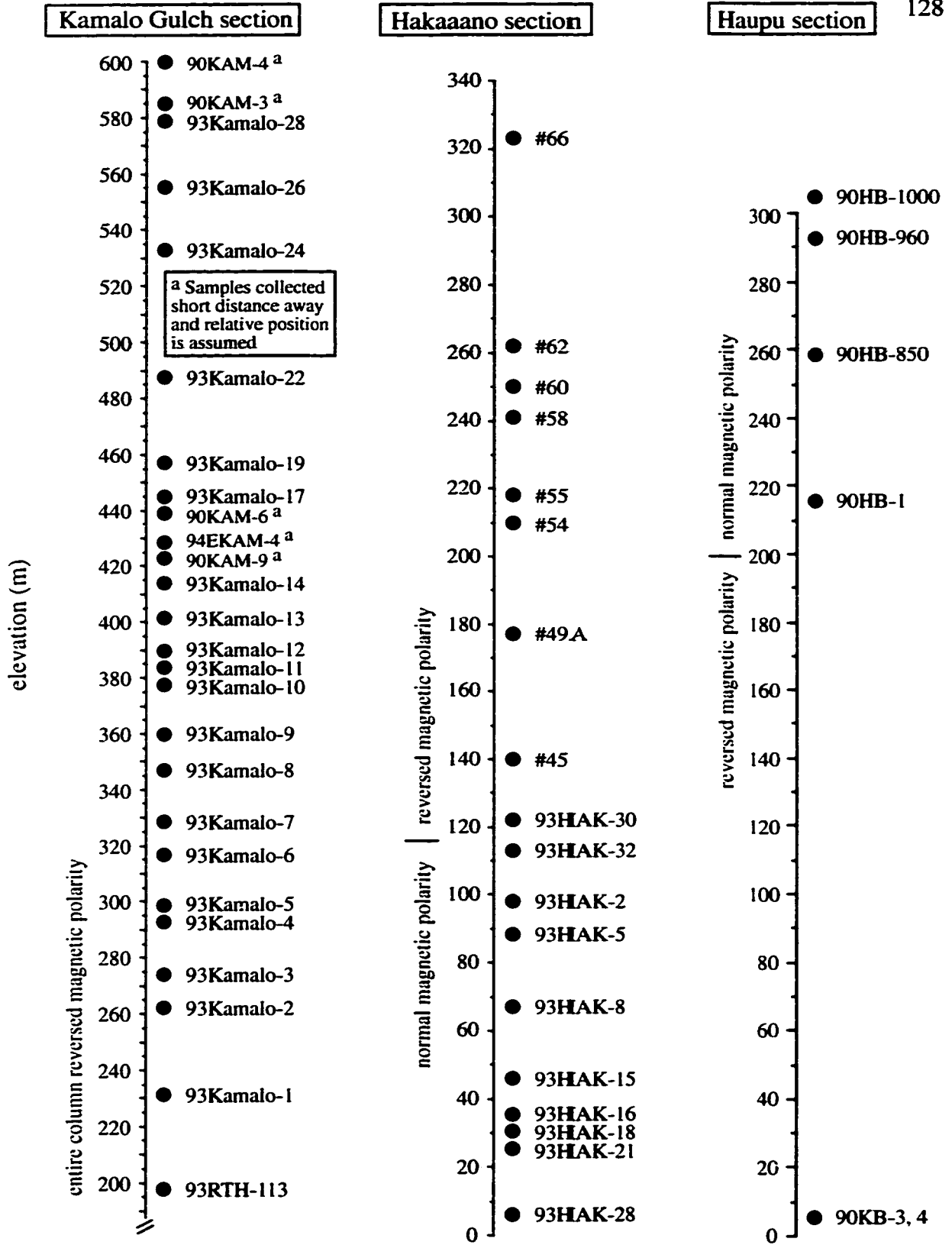


Figure 4.2 Sample Locations by Stratigraphic Section for East Molokai Volcano

CHAPTER 5

The Geochemistry of East Molokai Volcano, Hawaii: Evidence for Common Mantle Processes in the Tholeiite to Alkali Basalt Transition of Haleakala-Type Volcanoes

ABSTRACT

One of the significant geochemical events recorded in subaerially-exposed lavas of Hawaiian volcanoes is the transition from shield stage to post-shield stage that marks the decline in volcanism as the vent is carried away from the mantle plume source. The character of this transition varies among the volcanoes, producing a spectrum of late-shield petrologic and isotopic characteristics. East Molokai Volcano is an excellent example of a Haleakala-type volcano, one extreme of the spectrum, characterized by a thick transitional sequence of interbedded tholeiitic and alkalic basalt capped by hawaiite and mugearite. The subaerial stratigraphy of East Molokai reveals a lengthy and extensive end-of-shield evolution from shield to alkalic cap to rejuvenated stage. East Molokai tholeiites are dominated by the KEA isotopic source component, and compositions shift toward the isotopically depleted (MORB-related) PE component in the late-shield stage. Haleakala-type volcanoes are the only ones where the PE isotopic component contributes to melts prior to the rejuvenated stage. The isotopic shift accompanies the transition from tholeiitic to alkalic basalt volcanism, correlates with decreased degrees of source melting, and is consistent with increased PE component at the perimeter of the mantle plume source. Conclusions

drawn from mixing models that describe introduction of the PE component agree with previous studies that call on metasomatism of the Hawaiian plume by small degree MORB-source melts at the plume margin. The model accounts for both Sr and Pb isotopic variation, and is consistent with the model describing processes contributing to a spectrum of late-stage volcanic evolution (Chap. 1).

INTRODUCTION

Geochemical variations throughout the life of an individual Hawaiian volcano provide information about heterogeneities and melt processes within mantle material supplied by the Hawaiian plume. Although subaerial lavas record only a brief fraction of the eruptive history of each volcano, this record preserves the geochemical changes that accompany extinction of the volcano as it is carried away from the magma source. One of the significant changes associated with declining volcanism, and the shift from shield stage to post-shield stage, is a transition from tholeiitic to alkalic basalt eruptions.

The character of the tholeiite to alkali basalt transition varies for Hawaiian volcanoes, ranging from volcanoes with no transition to those with an extensive transition to alkalic basalt. Correspondingly, the major element compositions of subaerial tholeiites range from strongly tholeiitic to more chemically transitional. Intershield correlations among major element and isotopic compositions of subaerial tholeiites suggest that different late-shield tholeiitic melt segregation conditions are associated with different mantle isotopic sources (Chap. 1). Specifically, for any particular volcano, the proportion of the two identified isotopic components that contribute to Hawaiian shield volcanism, the KEA and KOO

components, is related to the pressure and temperature of magma generation and to what extent eruptions subsequently shift from tholeiitic to alkalic basalt.

The volcanic spectrum ranges from Koolau-type volcanoes, where a KOO-dominated mantle source produces only tholeiitic volcanism, to Haleakala-type volcanoes, where a KEA-dominated mantle source produces an extensive transition from tholeiitic to alkalic basalt volcanism. The model describing the late-shield volcanic spectrum suggests that temporal variations in the initial buoyancy of a KOO mantle plume result in different degrees of entrainment of KEA lower mantle. This produces temporal variations in the plume compositional mixture and radial temperature gradient at the depth of melting. A third isotopic mantle component, the MORB-related PE component, becomes significant in the late-shield stage of Haleakala (Chen et al., 1991) and Mauna Kea (Lassiter et al., 1996), which indicates entrainment continues into the uppermost mantle during periods of Haleakala-type volcanism.

Detailed stratigraphic and geochemical studies of individual volcanoes are necessary to improve and constrain the model describing late-shield petrologic and isotopic correlations. East Molokai is an excellent candidate for detailed geochemical study. Early field studies revealed a long stratigraphic transition to alkalic volcanism (Stearns and Macdonald, 1947; Beeson, 1976; Langenheim and Clague, 1987) which, combined with the isotopic composition of a single East Molokai tholeiite (Tatsumoto, 1978; Stille et al., 1986), suggests that East Molokai is a Haleakala-type volcano. The morphology of the volcano is ideal for detailed, stratigraphically-controlled sampling. The northern half of the volcano was removed by a giant landslide (Moore, 1964; Moore et al., 1989), exposing the interior of the subaerial volcano within sea cliffs of the north coast. Erosion of deep gulches has exposed additional thick stratigraphic sequences. The remnant magnetic character of

various stratigraphic sections provides important constraints on establishing a composite stratigraphy that spans the entire subaerially-exposed portion of the volcano (Chap. 4).

OBJECTIVES

This report describes the major element, trace element, and Nd, Sr, and Pb isotope compositions of the subaerial East Molokai shield, alkalic cap, and rejuvenated stage lavas within a detailed stratigraphic context. This is the first detailed geochemistry presented for the entire subaerial section of East Molokai. Previous geochemical studies have focused on a specific section, such as the transitional stage (Beeson, 1976; Clague and Beeson, 1980) or the rejuvenated stage (Clague et al., 1982). Published rare earth element (REE) compositions exist for two rejuvenated stage lavas (Clague et al., 1982). Published isotopic compositions include Nd, Sr, and Pb isotope ratios for a single shield tholeiite (Tatsumoto, 1978; Stille et al., 1986) and Sr isotope ratios for four rejuvenated stage basalts (Clague et al., 1982).

The new data presented here are consistent with identification of East Molokai as a Haleakala-type volcano and, as such, its geochemistry is related to the spectrum of Hawaiian volcanoes, particularly to the two relatively well-studied Haleakala-type volcanoes of Haleakala and Mauna Kea. It is shown that East Molokai tholeiites are dominated by the KEA isotopic component and that compositions shift toward the isotopically-depleted PE component in the late-shield stage. This isotopic shift accompanies the transition from tholeiitic to alkalic basalt volcanism, correlates with decreased degrees of source melting, and is consistent with increased PE component at the perimeter of the mantle plume source. The end-of-shield geochemistry of East Molokai is

consistent with the model describing processes contributing to a spectrum of late-stage volcanic evolution (Chap. 1).

PREVIOUS INVESTIGATIONS

Stearns and Macdonald (1947) subdivided the rocks into the East Molokai Volcanic Series, which includes the informal lower and upper members, and the Kalaupapa Basalt, which is the rejuvenated stage shield that surfaces as Kalaupapa Peninsula. Langenheim and Clague (1987) formally subdivided the rocks into the East Molokai Volcanics and the Kalaupapa Volcanics. The lower and upper member type locality of Stearns and Macdonald (1947) is the sea cliff above Kalaupapa Peninsula, described as a 550 meters-thick sequence of basalt flows that includes three or more upper member flows aggregating 60 meters thickness. Stearns and Macdonald (1947) identified lower member lavas as predominantly tholeiites, and upper member lavas as hawaiites, mugearites, and benmoreites, respectively (contemporary classification of Le Bas et al., 1986).

Beeson (1976) and Clague and Beeson (1980) examined the major and trace element content of the flows above Kalaupapa Peninsula, and described the geochemistry as a discontinuous upsection progression from tholeiitic to alkalic compositions. They considered this sequence of flows representative of the transitional stage from tholeiitic to alkalic volcanism.

RESULTS

Holcomb (1985, 1990) identified two magnetic polarity boundaries in flows of the northern sea cliffs and valleys and subsequently identified a composite stratigraphy (Chap. 4). East

Molokai extracaldera lavas were sampled from the reversed to normal magnetic polarity sequence of the northwest sea cliffs (Haupu section), the normal to reversed polarity sequence of the northeast sea cliffs (lower and upper Hakaaano sections), and the reversed polarity Kamalo Gulch section on the south slope of the volcano. The caldera fill and the rejuvenated stage Kalaupapa Basalt were also sampled. Stratigraphic projections (Chap. 4) suggest that the sampled Hakaaano section directly overlies the Haupu section, but that there is an approximate gap of 250 meters between these and the stratigraphically lowest samples in the overlying Kamalo Gulch section. The major element geochemistry of the reversed polarity basalts in the cliff above Kalaupapa Peninsula (Beeson, 1976; Clague and Beeson, 1980) suggests that this section overlaps the projected gap in the composite stratigraphy between the north coast and Kamalo Gulch lavas.

All samples were analyzed for major elements. A subset of the samples, which includes representatives from each stratigraphic section except the upper Hakaaano tholeiites and Kamalo Gulch mugearites, was analyzed for trace elements, including REE, and for Pb isotope ratios. A smaller subset of the samples was analyzed for Sr and Nd isotope ratios. Analytical results are in Table 5.1. Analytical methods are described in Appendix A.

ALTERATION

Previous studies indicate that weathering may mobilize K, whereas P is unaffected (e.g., Lipman et al., 1990; Frey et al., 1991). Therefore, values of $K_2O/P_2O_5 < 1.0$ are thought to be a possible indication of rock alteration, consistent with studies that report $K_2O/P_2O_5 > 1.3$ in fresh submarine glasses (Moore et al., 1990; Garcia et al., 1989) and in recent Kilauea and Mauna Loa lavas (Wright, 1971). Some East Molokai tholeiites have $K_2O/P_2O_5 < 1.0$, but also have low concentrations of other trace elements. It is therefore

difficult to differentiate K_2O weathering from melt processes. However, very low ratios ($K_2O/P_2O_5 < 0.5$) in tholeiite samples 90HB-850, 90HB-1000, #45, and #58 probably indicate weathering effects. Major and trace element abundances (but not incompatible trace element ratios) of these samples are excluded from further discussion. Leaching of sample 90HB-850 suggests Pb isotope compositions were not significantly affected by weathering, and isotopic compositions of the low K_2O/P_2O_5 samples are similar to other tholeiites with no evidence of alteration. Therefore, isotopic compositions will remain in the discussion.

Fodor et al. (1992) showed that weathering can mobilize REE and Y without Ce, which is less soluble in the oxidized state. This can result in REE and Y enrichment and Ce anomalies in nearby lavas without an increase in immobile incompatibles. East Molokai tholeiites 90HB-1 and 90HB-850, and transitional basalt 93Kamalo-2, have significant Ce anomalies ($Ce/Ce^* = 0.76, 0.83, 0.82$, respectively), and high La/Ce relative to the overall data trends. Samples 90HB-850 and 93Kamalo-2 have relatively low Hf/Sm and high Lu/Hf (and non-anomalous Zr/Hf), which might suggest REE influx. However, the sample 90HB-1, with the greatest Ce anomaly, has no unusual ratios involving REE other than high La/Ce. Although evidence for REE transport is not consistent, Ce anomalies are suspect and typically associated with weathering; therefore, samples with anomalous Ce will be excluded from the discussion of La/Ce variations in East Molokai lavas.

MAJOR ELEMENT COMPOSITIONS

The samples from the northern sea cliffs, including the caldera fill, are tholeiitic basalts, except for two samples in the Hakaaano section that are transitional and alkalic basalts (Fig. 5.1). Within the tholeiites, higher overall alkali content reflects the more transitional

character of upper Hakaano compared to lower Hakaano, and lower Hakaano compared to the Haupu section. The Kamalo Gulch lavas are interlayered transitional, alkalic, and hawaiitic basalts, with mugearites and benmoreites in the uppermost flows. The Beeson (1976) section, stratigraphically located between the Hakaano and Kamalo Gulch sections, is a sequence of tholeiitic, transitional, and alkalic basalts. The rejuvenated stage basalts are tholeiitic to transitional basalts, consistent with previous identification of transitional to alkalic basalt lavas sampled from the Kalaupapa Peninsula (Clague et al., 1982).

Previous studies indicated that the tholeiite to alkali basalt transition in East Molokai is characterized by a stratigraphically thick interval of lavas (e.g., Beeson, 1976). The new data show that the transition from tholeiitic to alkalic basalt spans nearly the entire subaerial section. In the composite stratigraphy, there is an overall gradual trend of increasing alkalinity with height (Fig. 5.2). Interlayering of differing alkalinities is most pronounced in the Kamalo Gulch section.

The tholeiitic and transitional basalts, and some of the alkalic basalts, overlap in MgO content (Fig. 5.3). The trend of increasing alkalinity, in stratigraphic order from the tholeiites of the Haupu section to the transitional basalts of Kamalo Gulch, is within the relatively narrow range 5-8% MgO, consistent with decreasing degrees of mantle melting rather than mineral fractionation. The hawaiites and most of the alkalic basalts of Kamalo Gulch are in the range 3-5% MgO, and most of the mugearites and benmoreites have less than 3% MgO. The decreasing MgO content of hawaiites, mugearites, and benmoreites is consistent with alkali basalt differentiation.

MgO variation diagrams (Fig. 5.4 a-f) show accumulation and fractionation trends defined by the Beeson (1976) and Kamalo Gulch samples. CaO starts to decrease at less than 6-

7% MgO, where pyroxene is expected to join the fractionating assemblage. Nearly all of the Haupū and Hakaaano tholeiites are within the range 5-7% MgO and pyroxene phenocrysts are present even in the stratigraphically lowest samples. One of the the caldera samples, with approximately 12% MgO, contains 20-30% phenocrysts of olivine and pyroxene. The distinct increase in SiO₂ at less than 4-5% MgO is accompanied by an increase in Na₂O and P₂O₅, and a decrease in TiO₂, FeO, and CaO, probably in response to Fe-Ti oxide fractionation. The benmoreites show a distinct decrease in P₂O₅ content, below about 2-3% MgO, consistent with apatite fractionation.

Within the range 5-8% MgO, the Haupū and Hakaaano samples deviate from the fractionation trends. Similar to trends in alkalinity, increasing SiO₂ correlates with successively deeper stratigraphic groups in the order from upper Hakaaano to lower Hakaaano to Haupū samples (including caldera fill). These samples also plot to slightly lower TiO₂, FeO, Na₂O, and P₂O₅.

TRACE ELEMENT COMPOSITIONS

This study presents the first REE data for East Molokai shield and alkalic cap lavas. Representative REE patterns are shown in Figure 5.5 for the various stratigraphic sections of the volcano. The tholeiitic, transitional, and alkalic basalts overlap in HREE, but increase in LREE in stratigraphic order from Haupū tholeiites to Hakaaano tholeiites to Kamalo Gulch transitional and alkalic basalts. The Kamalo Gulch hawaiites and benmoreites are offset to higher REE overall, but the benmoreites are LREE enriched in comparison. The rejuvenated stage lavas are also LREE enriched, but have overall REE in the range of the main shield tholeiites.

La correlates positively with TiO_2 , Na_2O , K_2O , P_2O_5 , Ta, Th, LREE, Sr, Pb, Hf, and Zr, (not shown) indicating that these elements behave incompatibly. However, TiO_2 decreases in the hawaiites and benmoreites, P_2O_5 decreases in the benmoreites, and Sr is variable in the alkali basalts, reflecting the effects of Fe-Ti oxide, apatite, and feldspar fractionation, respectively. Correlations between La and HREE and Y are positive, but the trend of the tholeiite data has a more steeply positive slope than that of the alkali basalts. Sc content is relatively invariable in tholeiites but correlates negatively with La and positively with CaO in the transitional and alkali basalts, consistent with pyroxene fractionation.

RADIOGENIC ISOTOPE COMPOSITIONS

Variations in Nd, Sr, and Pb isotope ratios in Hawaiian lavas have been attributed to mixing between three isotopic endmember components in the source. Following Stille et al. (1986), the terminology adopted here is KEA for the Kilauea endmember, KOO for the Koolau endmember, and PE for the post-erosional, or rejuvenated stage endmember. Isotopic compositions of Hawaiian shield and alkalic cap lavas represent varying proportions of KEA and KOO components. However, late-shield and alkalic lava compositions at Haleakala (Chen et al., 1991) and Mauna Kea (Lassiter et al., 1996) show evidence of the PE component, otherwise only detected in rejuvenated stage lavas.

East Molokai shield and alkalic cap lavas exhibit a narrow range of Nd and Sr isotopic compositions (Fig. 5.6). Nd isotope ratios are relatively invariable among the sampled lavas, ranging only from $\epsilon_{\text{Nd}} = 6.7-7.3$. In contrast, Sr isotope ratios show a shift toward less radiogenic compositions from tholeiites to alkali basalts, except for one caldera sample which is in the range of the alkalic lavas. There are no Nd isotope data for East Molokai

rejuvenated stage basalts, but the range of Sr isotope ratios (Clague et al., 1982) is characteristic of the rejuvenated stage depleted isotopic compositions.

Pb isotope ratios were measured for a much larger number of samples than for Nd and Sr isotope ratios, and also show a narrow range of composition in the shield and alkalic cap samples (Fig. 5.7). The rejuvenated stage compositions are like other isotopically-depleted basalts of this stage elsewhere in Hawaii (Fig. 5.7). The Pb and Sr isotope ratios show a shift toward less radiogenic composition. However, the more detailed Pb isotope data show that the isotopic shift is relatively abrupt in the stratigraphy, and accompanies the change from moderately tholeiitic to more transitionally tholeiitic lavas within the Hakaano section (Fig. 5.8). The less radiogenic compositions persist in the overlying samples, except in one Kamalo Gulch hawaiite which has Pb isotope ratios within the range of the lowermost tholeiites (Fig. 5.8). No trace element data are available for this particular sample.

Because the Nd isotope compositions of the KEA and PE components are relatively similar, the most descriptive plot showing involvement of the three isotopic source components in Hawaiian lavas is that of Pb and Sr isotope ratios (Fig. 5.9). The shift toward less radiogenic isotope composition within the 'ava sequence of Hakaano is a shift toward the PE component. A late-shield temporal trend toward the PE component is documented at only two other volcanoes, Haleakala (Chen et al., 1991) and Mauna Kea (Lassiter et al., 1996). The rejuvenated stage samples of East Molokai plot clearly toward the PE isotopic field, similar to all other identified and analyzed rejuvenated stage lavas.

DISCUSSION

The spectrum of characteristics during late-shield volcanism, for Hawaiian volcanoes that have completed their evolution, is categorized into Koolau-type, Kohala-type, and Haleakala-type (Macdonald and Katsura, 1964; Wright and Helz, 1987; Chap. 1). Wright and Helz (1987) summarized the general petrologic characteristics. The Koolau-type volcano erupts few or no alkalic rocks, the Kohala-type lacks abundant mafic alkalic rocks and erupts a thin alkalic cap of hawaiite and mugearite, and the Haleakala-type erupts a thick transitional unit of interbedded tholeiite, transitional basalt, and ankaramite, followed by a cap of hawaiite and mugearite.

Systematic relations in isotopic and elemental compositions are distinguished among the volcano-types (Chap. 1). The average isotopic composition of subaerial tholeiites, and the isotopic variations that accompany the tholeiite to alkali basalt transition, are related to the style of transition from tholeiitic to alkalic basalt described by Wright and Helz (1987). The Koolau-type tholeiites have the greatest proportion of KOO component and have no alkalic cap stage, the Kohala-type tholeiites have an isotopic composition intermediate to KEA and KOO, and an alkalic cap with a similar or more KEA-like composition, and the Haleakala-type tholeiites have the greatest proportion of KEA component, and an alkalic cap with a more PE-like composition (Fig. 1.6). The Haleakala-type volcanoes are the only ones for which the PE isotopic component is identified prior to the rejuvenated stage.

The East Molokai late-shield characteristics identify the volcano as Haleakala-type. The subaerial flows exhibit a relatively lengthy and extensive end-of-shield evolutionary sequence, including, although not specifically assigned to Haleakala-type volcanoes by Wright and Helz (1987), a significant rejuvenated stage. The transition from tholeiitic to

alkalic volcanism is first noted relatively low in the subaerial sequence, within the Hakaano section of the composite stratigraphy (Fig. 5.2), where the alkalinity of tholeiitic lavas becomes more transitional. There follows a thick transitional sequence, represented by a 230 meters-thick section within the cliff above Kalaupapa (Beeson, 1976), a very thick sequence of interbedded transitional, alkalic, and hawaiitic basalts, represented by a 300 meters-thick portion of the Kamalo Gulch section, and a cap of mugearites with some minor benmoreites. Also consistent with Haleakala-type character, the isotopic compositions of the East Molokai tholeiites are among those with the most pronounced KEA signature for Hawaiian tholeiites, and late-stage tholeiites and alkalic lavas show evidence of the PE component (Fig. 5.9).

LATE-SHIELD GEOCHEMICAL CHARACTERISTICS

The progressive increase in alkalinity (Fig. 5.2) and decrease in SiO_2 content (Fig. 5.4 a) within East Molokai tholeiites indicate decreasing degrees of mantle melting at increasing pressures, as expected for a decline in volcanism as a vent is carried away from the magma source. The stratigraphic increase in LREE within the tholeiites (Fig. 5.5) is also consistent with decreasing degrees of mantle melting. The relative uniformity of HREE, which is typical of Hawaiian tholeiites (Hofmann et al., 1984), reflects residual garnet in the source. East Molokai tholeiites with greater than 6% MgO, corrected for olivine fractionation to 17% MgO, have a range of $\text{Yb}_{17} = 1.4\text{-}2.1$, and an average $\text{Yb}_{17} = 1.78 \pm 0.25$. This relatively restricted compositional range is comparable to that of the tholeiitic basalts of Haleakala with $\text{Yb}_{17,2} = 1.2\text{-}1.8$ (Chen et al., 1991), and Mauna Kea with $\text{Yb}_{16} = 1.6 \pm 0.1$ (Yang et al., 1996).

Certain ratios of elements with similar compatibility, such as Hf/Sm and Ce/Pb, are relatively invariable among East Molokai tholeiites and alkali basalts. Excluding the benmoreite compositions, which are extensively fractionated, East Molokai lavas have an average Hf/Sm = 0.70 ± 0.06 , similar to the Haleakala subaerial shield average Hf/Sm = 0.72 ± 0.08 (Chen et al., 1991). The East Molokai average Ce/Pb = 36.8 ± 1.8 overlaps the Mauna Kea tholeiite range of Ce/Pb = 40 ± 4 (Kennedy et al., 1991), although most ocean island basalts have a reported range of Ce/Pb = 25 ± 5 (Hofmann et al., 1986).

The La/Ce ratio also involves elements of similar compatibility, but this ratio increases from East Molokai tholeiites to alkalic basalts (Fig. 5.10 a). Excluding the three samples with significant Ce anomalies, the tholeiite and transitional basalts have an average La/Ce = 0.40 ± 0.02 and La/Ce(N) = 1.03 ± 0.05 , which overlaps the tholeiite average La/Ce = 0.38 ± 0.02 of Haleakala (Chen et al., 1991) and La/Ce(N) ~ 1 of Mauna Kea (Yang et al., 1996). Similar to the East Molokai trend, the La/Ce ratio increases in the late-shield and alkalic caps of Haleakala and Mauna Kea.

The ratio La/Lu (or La/Yb), which involves elements of differing compatibility, is affected by degree of melting but is not very sensitive to post-melting processes such as mineral fractionation and accumulation. This ratio increases systematically with incompatible element abundance and alkalinity in East Molokai basalts, as it does in Haleakala and Mauna Kea basalts (Fig. 5.10 b). Of the East Molokai samples, three tholeiites and one alkali basalt show an inconsistent REE pattern at Lu (fig. 5.5), indicating a possibly greater analytical error on this element. However, there are no distinct differences in La/Lu between these samples and those with a consistent REE pattern at Lu, and the increase in La/Lu from tholeiite to alkali basalts is defined by the entire East Molokai data set.

THE NATURE OF THE MANTLE SOURCES

The transition from tholeiitic to alkalic basalt volcanism at East Molokai is characterized by increases in alkalinity, La/Ce, and La/Lu, all of which represent source processes, and a shift toward less radiogenic isotopic compositions, which indicates involvement of the PE source component. Therefore, correlations exist between these trace element and isotope ratios that represent a relation between the late-shield stage decline in volcanism and the change in source composition; specifically, the addition of the PE component. The correlations are used in the following sections to evaluate detailed mixing relations between the PE component mantle and the tholeiite source mantle.

PE Component Involvement in Hawaiian Volcanism

The shift toward the depleted PE component in late-shield to early post-shield is documented at Haleakala (Chen et al., 1991), Mauna Kea (Lassiter et al., 1996), and at East Molokai by the data presented here (Fig. 5.9). The association of the PE component with late-shield volcanism suggests that it has a spatial relation to the periphery of the plume (Lassiter et al., 1996). It is well accepted that the depleted PE component is MORB-source related. Chen et al. (1991) and West et al. (1987) attributed the temporal increase of the PE component in Haleakala lavas to progressive addition of an upper mantle component to the plume. Based on Os isotopic evidence, Martin et al. (1994) ruled out interaction of plume melts with MORB-source peridotite during the Haleakala late-shield stage, but suggested that the isotopic data support a model for progressive mixing between plume-derived melts and up to 30% of small degree partial melts of the MORB source. Lassiter et al. (1996) argued that Mauna Kea isotopic evidence supports post-shield involvement of an

increasing proportion of melt generated from a depleted upper mantle component, but they preferred a model of upper mantle entrained in the plume.

It was argued in Chapter 1 that upper mantle entrainment is the source of the PE component and lower mantle entrainment is the source of KEA component in Hawaiian lavas, and a model was proposed that explains the correlation between isotopic composition and late-shield character at any particular volcano. The model describes a spectrum of transient plume states ranging from that with a wide radial temperature gradient, which would allow a long period of decreasing degree melt production as the volcano is carried away from the plume center (Haleakala-type), to that with a narrow radial temperature gradient, where melt production ends abruptly after large degree tholeiitic volcanism (Koolau-type).

It was suggested in Chapter 1 that the development of a wide radial temperature gradient may be caused by a period of relatively low initial plume buoyancy resulting in relatively slow plume rise and, therefore, high peripheral heat conduction away from the rising plume and large peripheral entrainment of surrounding lower and upper mantle. On the other end of the spectrum is a period of relatively high initial plume buoyancy resulting in relatively rapid plume rise and, therefore, low peripheral heat conduction and little peripheral entrainment of surrounding mantle. The model is consistent with Haleakala-type volcanoes having the greatest proportion of KEA component (lower mantle entrainment) among Hawaiian subaerial tholeiites and having the PE component (upper mantle entrainment) appear in late-shield lavas. Because rejuvenated stage basalts are associated with examples of all three volcano-types, any of these plume states can apparently cause passive upwelling of MORB-source mantle through viscous coupling, a process suggested by Hauri et al. (1994) for producing rejuvenated stage basalts.

Model for the PE Component in East Molokai Basalts

The shift toward the depleted PE component in late-shield to early post-shield at the Haleakala-type volcanoes is associated with a general decrease in melt degree that produces alkalic basalts. Because earlier alkalic basalts at Haleakala and Mauna Kea have isotopic compositions similar to those of tholeiitic basalts with which they are interbedded (e.g., respectively, Chen et al., 1991; Frey et al., 1991), and because other volcano-types undergo transition to alkalic basalt volcanism without evidence of PE involvement (Fig. 5.9), the introduction of the PE component is not necessarily a consequence of smaller degrees of melting. Rather, the introduction of the PE component is related to smaller degrees of melting, specifically at Haleakala-type volcanoes, as a consequence of entrainment at the plume periphery. Because the introduction of an additional mantle source affects the geochemistry of the resultant lavas, the correlations between elemental and isotopic compositions provide information on mixing processes at the plume periphery.

Reiners and Nelson (1998) examined the covariation between $^{87}\text{Sr}/^{86}\text{Sr}$ and La/Lu among rejuvenated stage basalts of Kauai, and presented a mantle mixing and melting model to describe the relations between the degree of melting and the proportion of depleted isotopic component in the lavas. They showed that the model was generally applicable to other stages of Hawaiian volcanism. They supported the conclusions of Chen and Frey (1983, 1985), who examined relations between $^{87}\text{Sr}/^{86}\text{Sr}$ and La/Ce in different evolutionary stages of Haleakala lavas, that the presence of a depleted isotopic component in Hawaiian lavas reflects metasomatism of the plume source by very small degree MORB-source melts. However, Reiners and Nelson (1998) found that, during rejuvenated stage volcanism, lavas with the least incompatible element enrichment have the most depleted isotopic signature, whereas Chen and Frey (1983, 1985) determined that, in earlier stages of

volcanism, lavas with the greatest incompatible element enrichment have the most depleted isotopic signature. In summary, the overall Haleakala trend from shield to post-shield stages is best modeled by smaller degree melts of a progressively more metasomatized source (Chen and Frey, 1983; 1985), but the opposite trend evidenced within the rejuvenated stage lavas of Kauai indicates that, at some scale, there is a positive correlation between degree of melt and extent of metasomatism (Reiners and Nelson, 1998). The mixing models are expanded upon here to describe the addition of the depleted PE component to the source of East Molokai lavas, and to Haleakala-type volcanoes in general.

The mixing models of Reiners and Nelson (1998) and Chen and Frey (1983, 1985) relied on a plume source characterized by bulk earth $^{87}\text{Sr}/^{86}\text{Sr}$ composition. It is fairly well established that, for any particular Hawaiian volcano, the plume source does not necessarily have bulk earth $^{87}\text{Sr}/^{86}\text{Sr}$, but rather a composition that is an isotopic mixture of the KOO and KEA components (Fig. 5.9). The model presented here invokes a mixture of KOO and KEA to provide a plume source $^{87}\text{Sr}/^{86}\text{Sr}$ that is similar to actual shield lava compositions of the Haleakala-type volcanoes, and therefore reduces the amount of PE component necessary to account for the late-stage trend to depleted isotope compositions. In addition, the model accounts for variations in $^{206}\text{Pb}/^{204}\text{Pb}$ that can not be described by the same mixing parameters that describe $^{87}\text{Sr}/^{86}\text{Sr}$ if a bulk earth Pb isotopic composition is assumed for the plume source.

The East Molokai tholeiite source is a mantle component mixture in the calculated proportions 80% KEA and 20% KOO, which are representative of proportions for Haleakala-type volcanoes in general (Fig. 5.11). The calculation assumes that the KEA component has an isotopic composition within the range of many suggested for this component (e.g., Stille et al., 1986; West and Leeman, 1987), and that the KOO

component has near bulk earth isotope ratios (Table 5.2). The components are both assumed to have bulk earth trace element compositions (Table 5.2), although it has been argued that the KOO component is not primitive mantle (Hofmann et al., 1986), and that the KEA component has enriched trace element concentrations relative to the KOO component (e.g., West and Leeman, 1987). The calculated proportions of KEA and KOO components in the East Molokai tholeiite source are significantly affected by assuming a trace element enriched KEA component such as that of West and Leeman (1987), which has Sr and Pb concentrations approximately 5 and 10 times more abundant, respectively, than primitive mantle. However, the purpose here is to use the component mixture as the plume source endmember in calculating the amount of depleted PE component added to the source during the late-shield stage, and the simplification results in only small differences in the amount of the PE endmember required to explain late-shield evolution.

Figure 5.12 a,b shows the variation of $^{87}\text{Sr}/^{86}\text{Sr}$ with La/Ce and La/Lu in East Molokai lavas, and the outline of a mixing model described below. Also shown are shield and alkalic cap data fields for Haleakala and Mauna Kea, in which alkalic cap lavas are offset toward increased La/Ce and La/Lu and more depleted $^{87}\text{Sr}/^{86}\text{Sr}$. Although the Sr isotope data for East Molokai lavas are few, there are similar temporal increases in La/Ce , La/Lu , and depleted $^{87}\text{Sr}/^{86}\text{Sr}$. The rejuvenated stage of East Molokai, like that of Haleakala volcano, is offset from the main Haleakala-type trend along the rejuvenated stage trend, defined by Kauai data (Reiners and Nelson, 1998).

Figure 5.13 shows the variation of $^{206}\text{Pb}/^{204}\text{Pb}$ with La/Lu in East Molokai lavas. The fields for the shield and alkalic cap of Mauna Kea (Frey et al., 1990, 1991; Kennedy et al., 1991; West et al., 1988) represent the only published Haleakala-type data that include both REE and Pb isotope ratios for lavas of different volcanic stages. The East Molokai data,

like those of Mauna Kea, exhibit a distinct shift in compositions between the tholeiites and alkalic basalts toward increased La/Lu and less radiogenic $^{206}\text{Pb}/^{204}\text{Pb}$. Although no published data are available to define a rejuvenated stage trend in Pb isotope compositions, the East Molokai rejuvenated stage lavas are offset in the direction of a hypothetical trend consistent with that defined by Sr isotope compositions.

The model that best describes mantle mixing and melting in the East Molokai lava source, similar to models of Chen and Frey (1983, 1985) and Reiners and Nelson (1998), invokes metasomatism of the solid tholeiite source (plume) by very small degree (0.1%) MORB-source melts, followed by melting of the mixture (Figs. 5.12, 5.13). Whereas Chen and Frey (1983) and Reiners and Nelson (1998) described $^{87}\text{Sr}/^{86}\text{Sr}$ variations with metasomatism of a bulk earth composition (KOO) plume, the plume source used here for East Molokai is a mixture of 80% KEA and 20% KOO components. It is apparent in Figure 5.12 that either of these plume compositions can account for $^{87}\text{Sr}/^{86}\text{Sr}$ of the lavas by varying the amount of the metasomatism. However, when $^{206}\text{Pb}/^{204}\text{Pb}$ is taken into consideration (Fig. 5.13), mixing between a KOO-composition plume and MORB-source melts can not describe any of the lava compositions because the KOO and the PE components both have less radiogenic Pb than any of the lava samples. The plume must be a mixture of KEA and KOO components if the Haleakala-type lava compositions are to be described by plume and MORB-source mixing.

The mixing and melting parameters of the best-fit model provide a consistent and reasonable description of $^{87}\text{Sr}/^{86}\text{Sr}$ and $^{206}\text{Pb}/^{204}\text{Pb}$ variations in East Molokai lavas. Model parameters are those of Reiners and Nelson (1998), plus any additional noted in Table 5.2. East Molokai tholeiites are produced by 4-10% melting of a plume source that has been metasomatized by an extremely small amount (0.2%), if any, of small degree

MORB-source melts. The transitional and alkalic lavas are produced by 2-3% melting of a slightly more metasomatized plume. Although the amount of metasomatism is small, it is enough in the calculations to create the isotopic differences among tholeiitic, transitional, and alkalic lavas.

An example of sensitivity of assumed source compositions is given by comparison with Chen and Frey (1983, 1985). Their model for Haleakala, based on $^{87}\text{Sr}/^{86}\text{Sr}$ and La/Ce variations, allows mixing of the MORB-source melt with a large degree melt of the plume. The MORB-source La and Ce concentrations (0.31, 0.95 ppm) in their model yield calculated small degree melt compositions that extend to higher La/Ce than do the Haleakala data, such that mixing lines between MORB-source melts and a large degree plume melt encompass the Haleakala data (Chen and Frey, 1983: Fig. 3). In the model here, mixing between MORB-source melts and large degrees of plume melt cannot reproduce the high La/Ce compositions of the lavas (Fig. 5.14), due to an alternative choice of MORB-source La and Ce concentrations (0.206, 0.722 ppm) (Reiners and Nelson, 1998, using "depleted earth" values of McKenzie and O'Nions, 1991). This allows description of both La/Ce and La/Lu variations with a single model. Another alternative model, that of mixing between solid MORB source and plume source prior to melting, requires melt fractions much too small to reproduce the La/Ce compositions of the lavas, especially those of the alkalic cap basalts (Fig. 5.14).

The rejuvenated stage lavas of East Molokai are produced by a model 4% melting of a plume source metasomatized by 0.5-1% of the MORB-source melt (Figs. 5.12, 5.13). As is the case for Haleakala, the rejuvenated stage basalts of East Molokai do not plot along the trend of earlier stage basalts. The compositions are consistent with the proposal of a rejuvenated stage trend, where positive correlations between degree of melt and extent of

metasomatism may reflect the effects of source processes different than those supplying the shield and alkalic cap volcanism of Hawaiian volcanoes (Reiners and Nelson, 1998).

Hauri et al. (1994) suggested that rejuvenated stage basalts might be produced by mantle melting in response to passive upwelling at the plume margin. In this case, perhaps the transition from negative to positive correlations between degree of melting and extent of metasomatism is associated with the passage of the volcano over the transition from active upwelling, supplying shield and alkalic cap volcanism, to passive upwelling, supplying rejuvenated stage volcanism. If metasomatism is a significant process in the passively-upwelling region that is viscously coupled to the plume, then perhaps there is a certain degree of metasomatism above which chemical buoyancy is progressively added to the passively-upwelling mantle. In this model, the greatest degree of metasomatism is related to the greatest element of chemical buoyancy and contributes the greatest melt fractions in the eruptive products. This speculation implies that the active upwelling region, whether relatively rapid (Koolau-type) or relatively slow (Haleakala-type), has the ability to cause passive upwelling along the plume periphery.

CONCLUSIONS

This report describes the first detailed geochemistry for the entire subaerial section, nearly 1300 meters thick in composite, of East Molokai Volcano. East Molokai is a Haleakala-type volcano that exhibits an extensive evolutionary sequence from shield to alkalic cap to rejuvenated stage. The mantle source is dominated by the KEA isotopic component in the shield-building stage, but shows involvement of the isotopically-depleted PE component in the late-shield stage. This particular temporal trend was documented previously only at Haleakala (e.g., Chen et al., 1991) and Mauna Kea (e.g., Lassiter et al., 1996), the two

other identified Haleakala-type volcanoes. The PE component is otherwise significant only in rejuvenated stage lavas of Hawaiian volcanoes. The late-shield isotopic shift accompanies the transition from tholeiitic to alkalic basalt volcanism, correlates with decreased degrees of source melting, and is consistent with increased PE component at the perimeter of the mantle plume source.

A mixing model is proposed here that describes the addition of the PE component to the source of East Molokai lavas, and to the source of Haleakala-type volcanoes in general. In this model, East Molokai tholeiites are produced by 4-10% melting of a plume source that has been metasomatized by 0.2%, or less, of a very small degree (0.1%) MORB-source melt. The transitional and alkalic lavas are produced by 2-3% melting of a slightly more metasomatized plume. The negative correlation between degree of melt and extent of metasomatism is also a characteristic of the Chen and Frey (1983, 1985) model describing MORB-source involvement in the generation of Haleakala post-shield lavas.

The rejuvenated stage lavas of East Molokai are produced by a model 4% melting of a plume source that has been metasomatized by 0.5-1% of very small degree MORB-source melt. The positive correlation between degree of melt and extent of metasomatism is also a characteristic of the model describing MORB-source involvement in the generation of Kauai rejuvenated stage lavas, and may reflect the effects of source processes different than those supplying the shield and alkalic cap volcanism of Hawaiian volcanoes (Reiners and Nelson, 1998).

Chen and Frey (1983, 1985) and Reiners and Nelson (1998) examined $^{87}\text{Sr}/^{86}\text{Sr}$ variations in their mixing models describing Haleakala post-shield lavas and Kauai rejuvenated stage lavas, and called on metasomatism of a plume source with bulk earth composition. The

model presented here relies on a plume that is a mixture of KEA and KOO isotopic components, which best describes the isotopic composition of the Haleakala-type tholeiite source. The model then accounts for variations in $^{206}\text{Pb}/^{204}\text{Pb}$, which cannot be described by the same mixing parameters that describe $^{87}\text{Sr}/^{86}\text{Sr}$ if bulk earth Pb isotopic composition is assumed for the plume. The late-shield geochemistry of East Molokai, and the mixing model for involvement of the PE component in the late-shield of Haleakala-type volcanoes, are consistent with the generalized plume model describing processes contributing to the spectrum of Hawaiian late-stage volcanic evolution (Chap. 1).

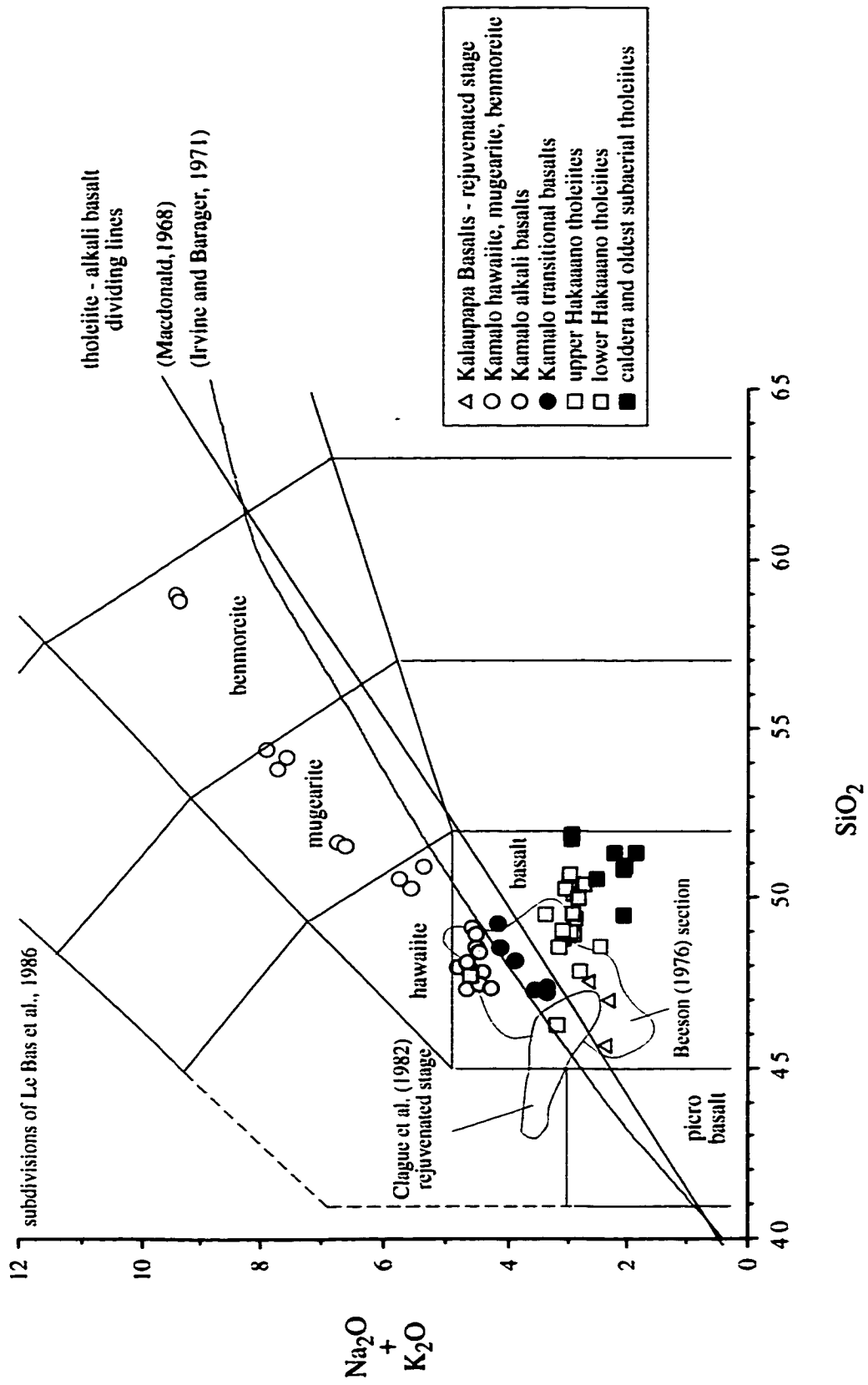


Figure 5.1 SiO₂ vs. Total Alkalis (wt%) for Subaerial Basalts of East Molokai Volcano

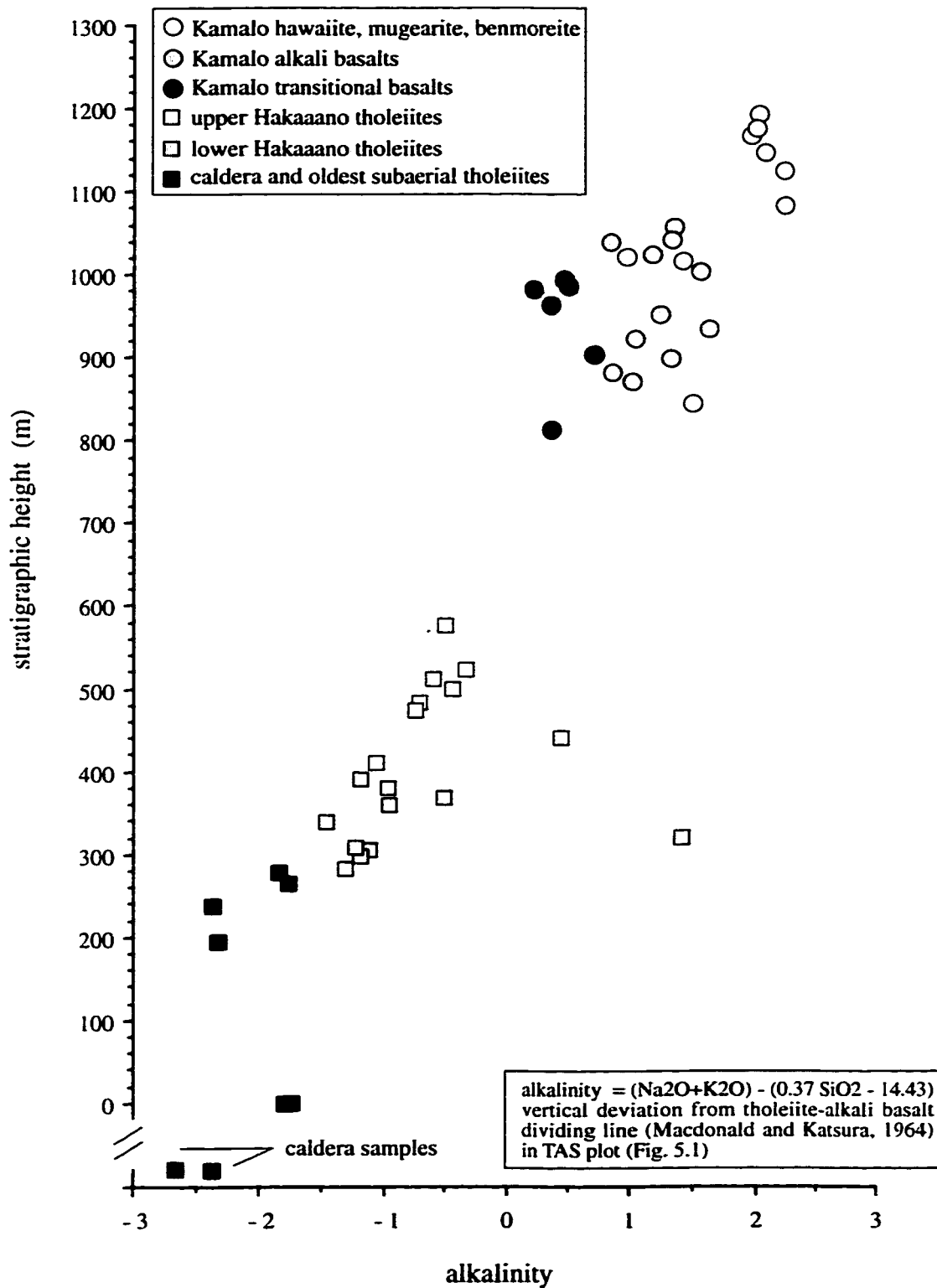


Figure 5.2 Alkalinity vs. Stratigraphic Position for Basalts of East Molokai Volcano

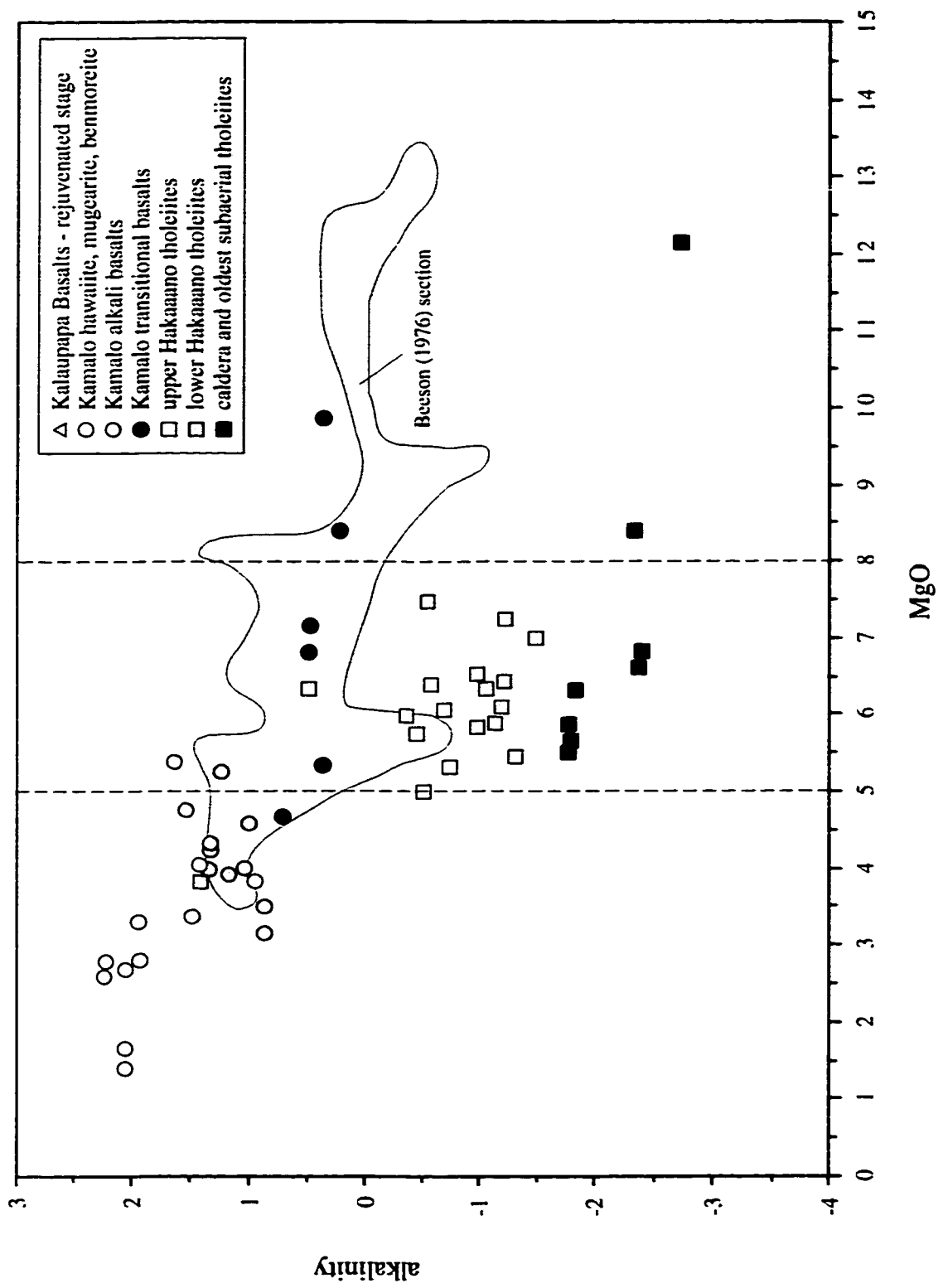


Figure 5.3 MgO vs. Alkalinity for Subaerial Basalts of East Molokai Volcano

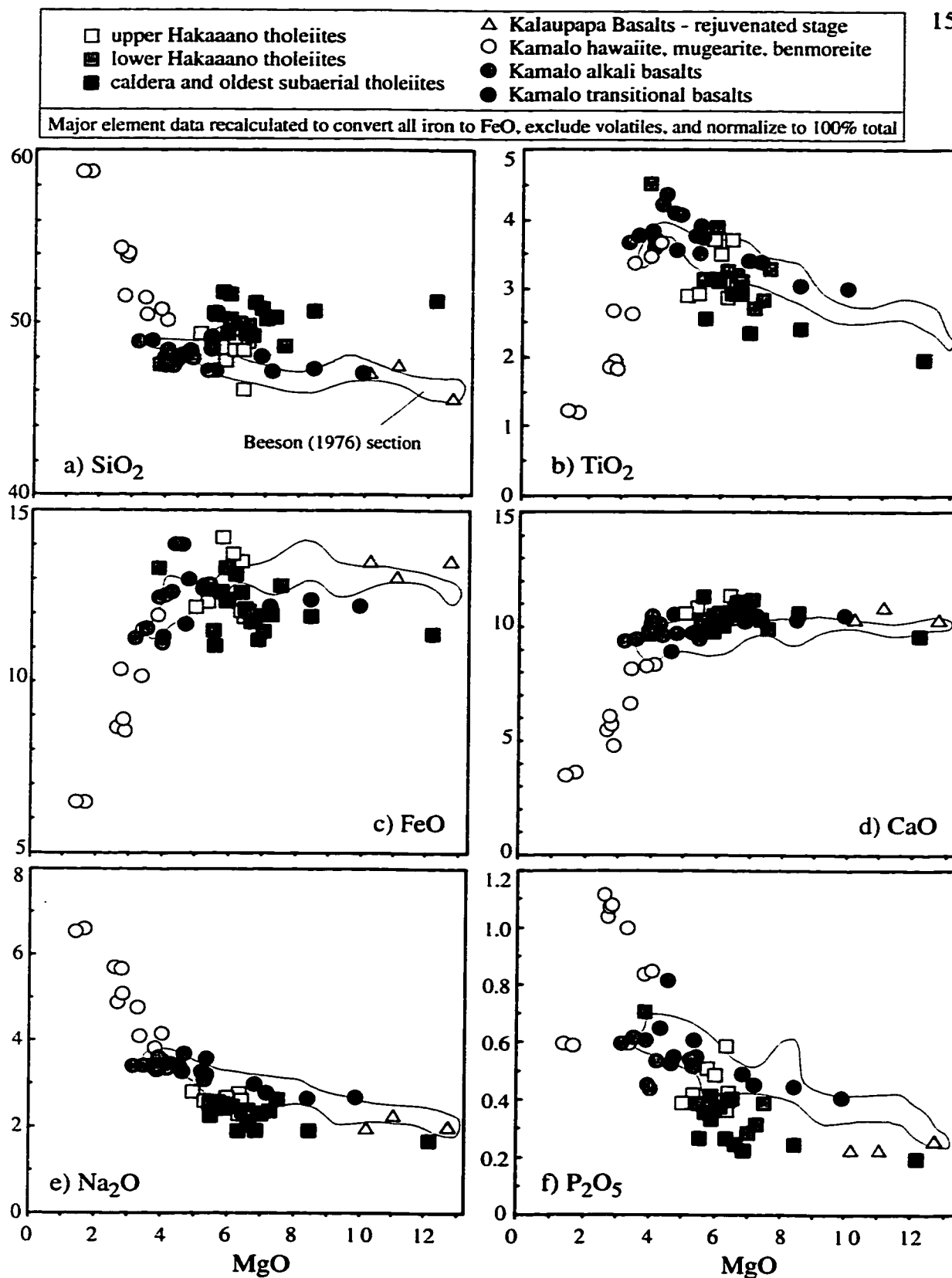


Figure 5.4 MgO vs. a) SiO_2 b) TiO_2 c) FeO d) CaO e) Na_2O and f) P_2O_5 (wt%) for Subaerial Basalts of East Molokai Volcano

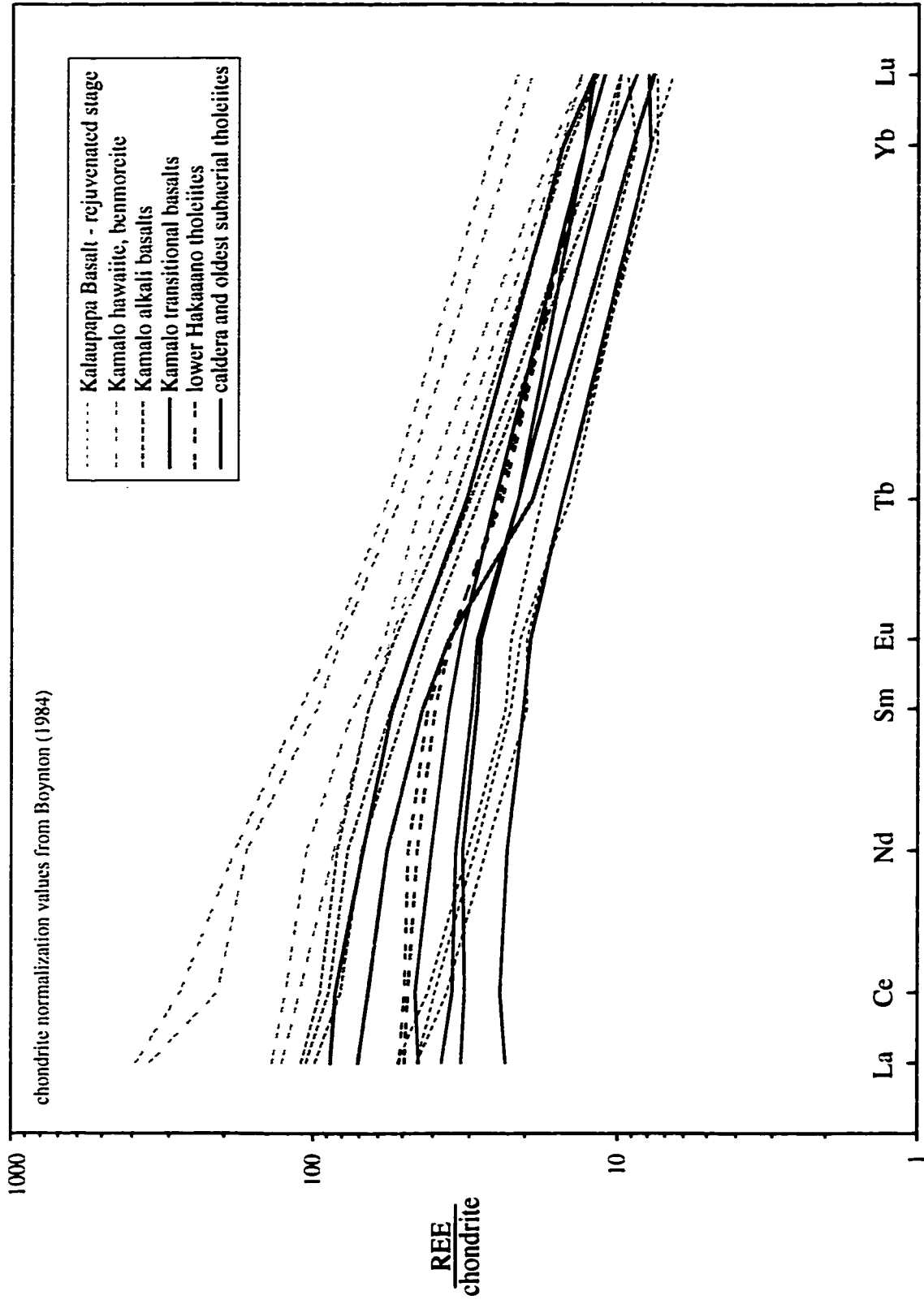


Figure 5.5 Representative Rare Earth Element (REE) Patterns for Subaerial Basalts of East Molokai Volcano

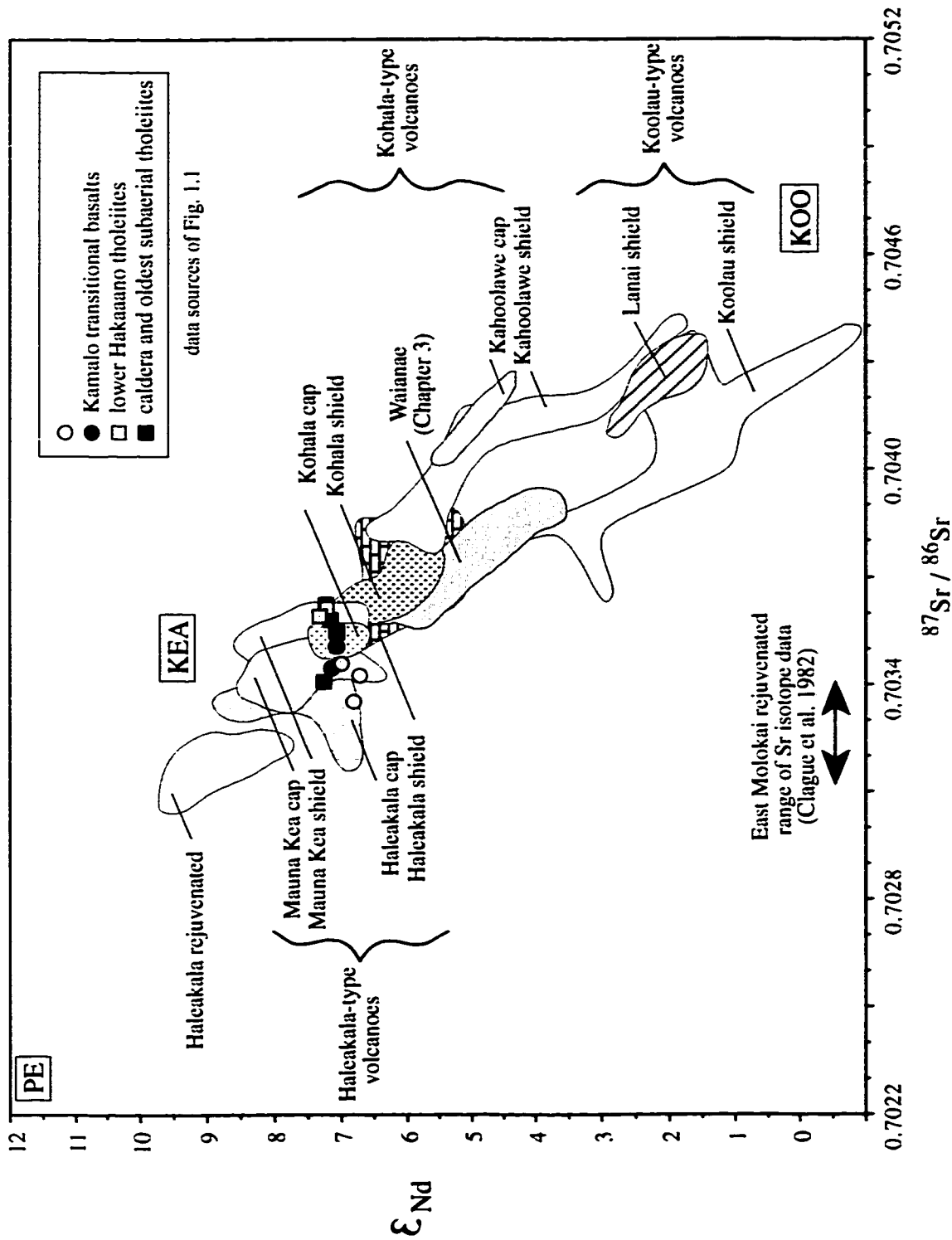


Figure 5.6 $^{87}Sr / ^{86}Sr$ vs. ϵ_{Nd} for Subaerial Hawaiian Basalts and Basalts of East Molokai Volcano

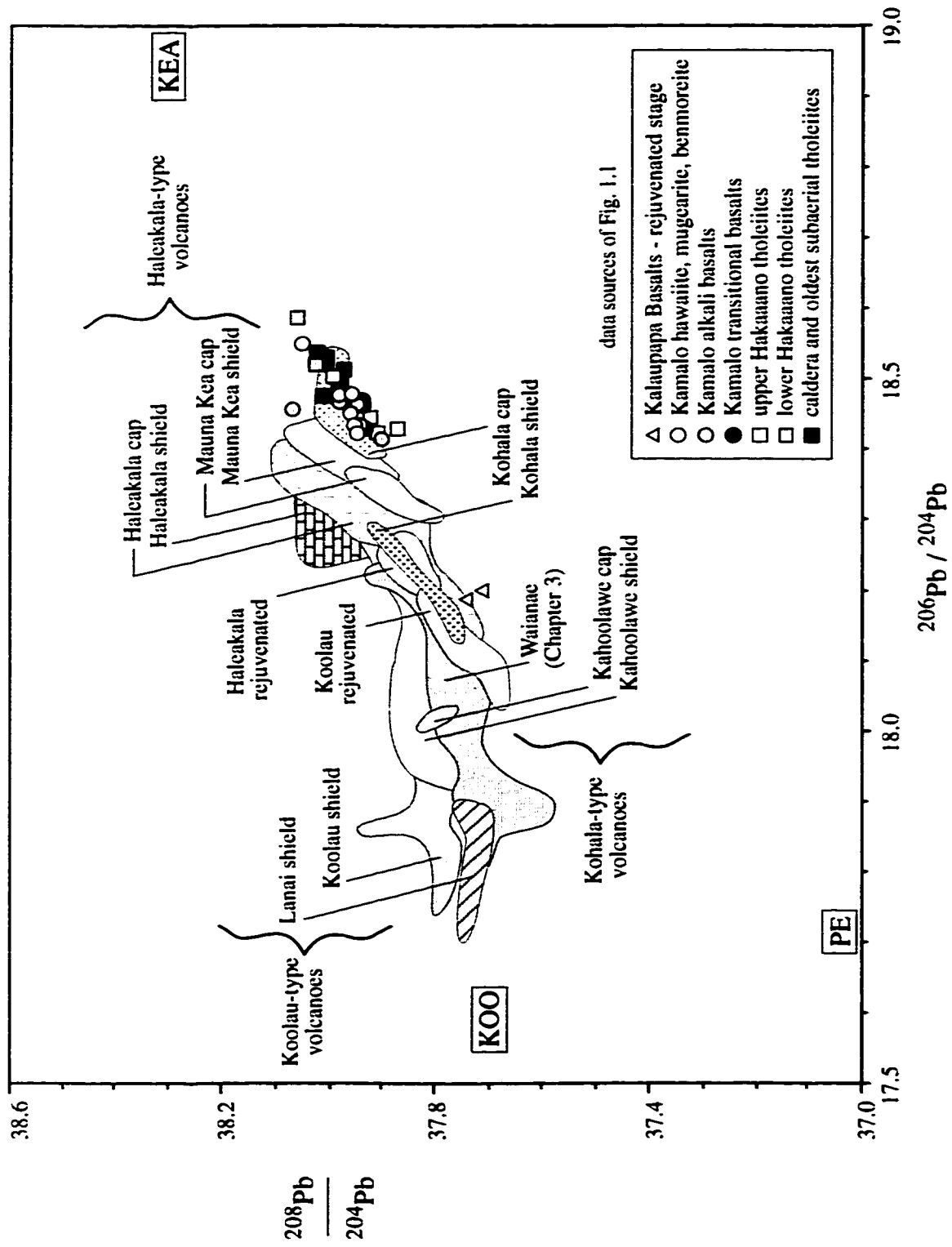


Figure 5.7 $^{206}\text{Pb}/^{204}\text{Pb}$ vs. $^{208}\text{Pb}/^{204}\text{Pb}$ for Subaerial Hawaiian Basalts and Basalts of East Molokai Volcano

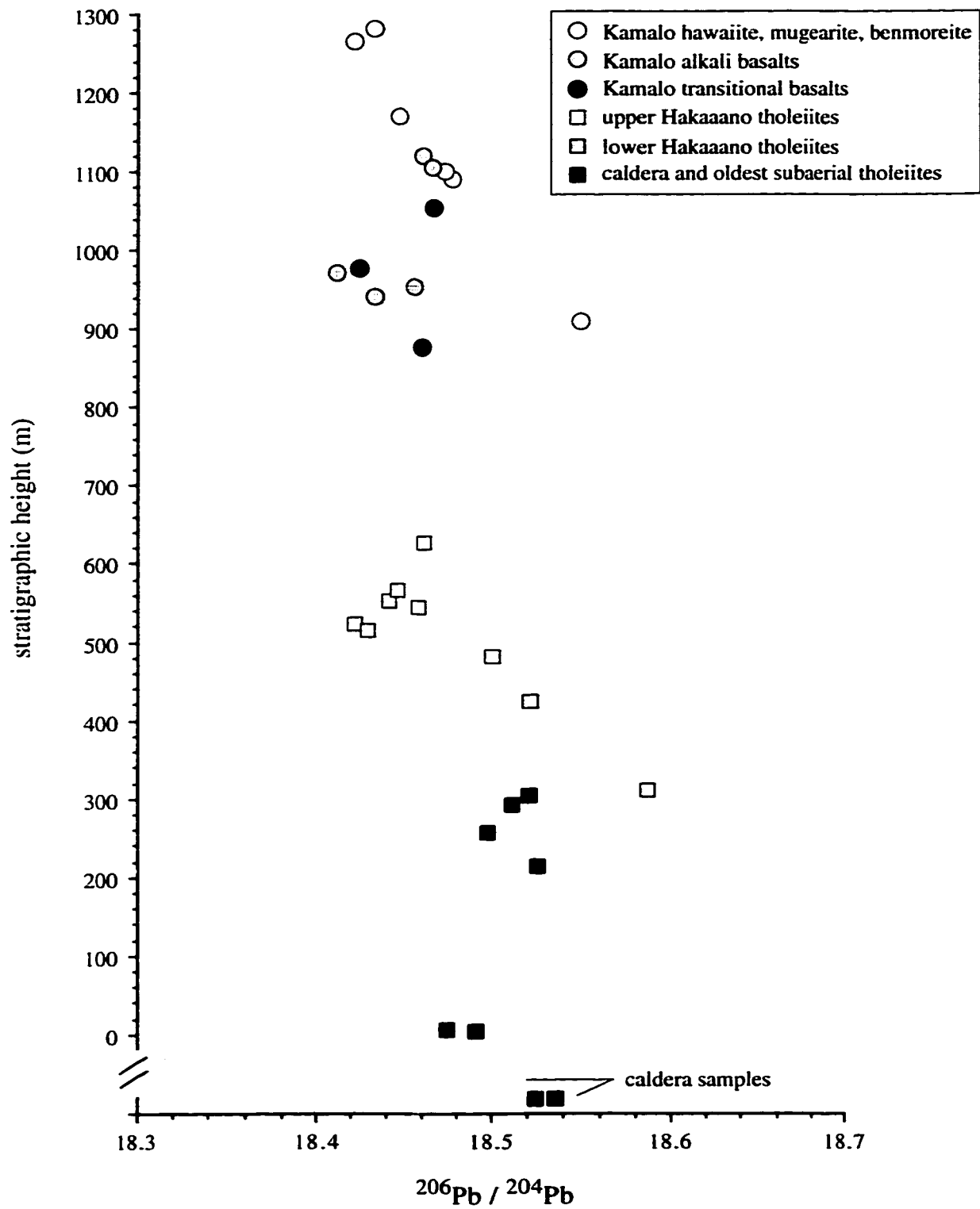


Figure 5.8 $^{206}\text{Pb}/^{204}\text{Pb}$ vs. Stratigraphic Position for Basalts of East Molokai Volcano

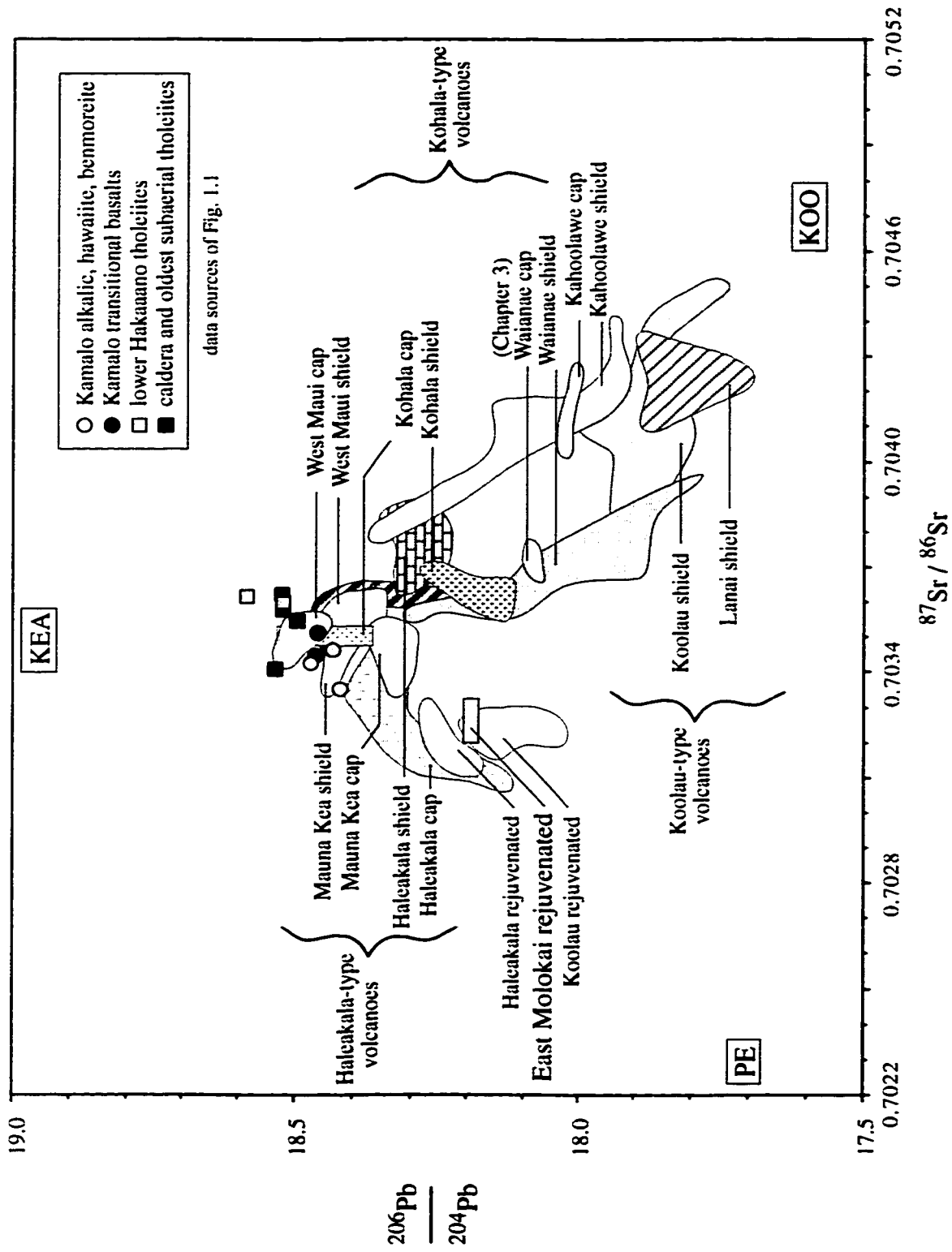


Figure 5.9 $^{87}\text{Sr}/^{86}\text{Sr}$ vs. $^{206}\text{Pb}/^{204}\text{Pb}$ for Subaerial Hawaiian Basalts and Basalts of East Molokai Volcano

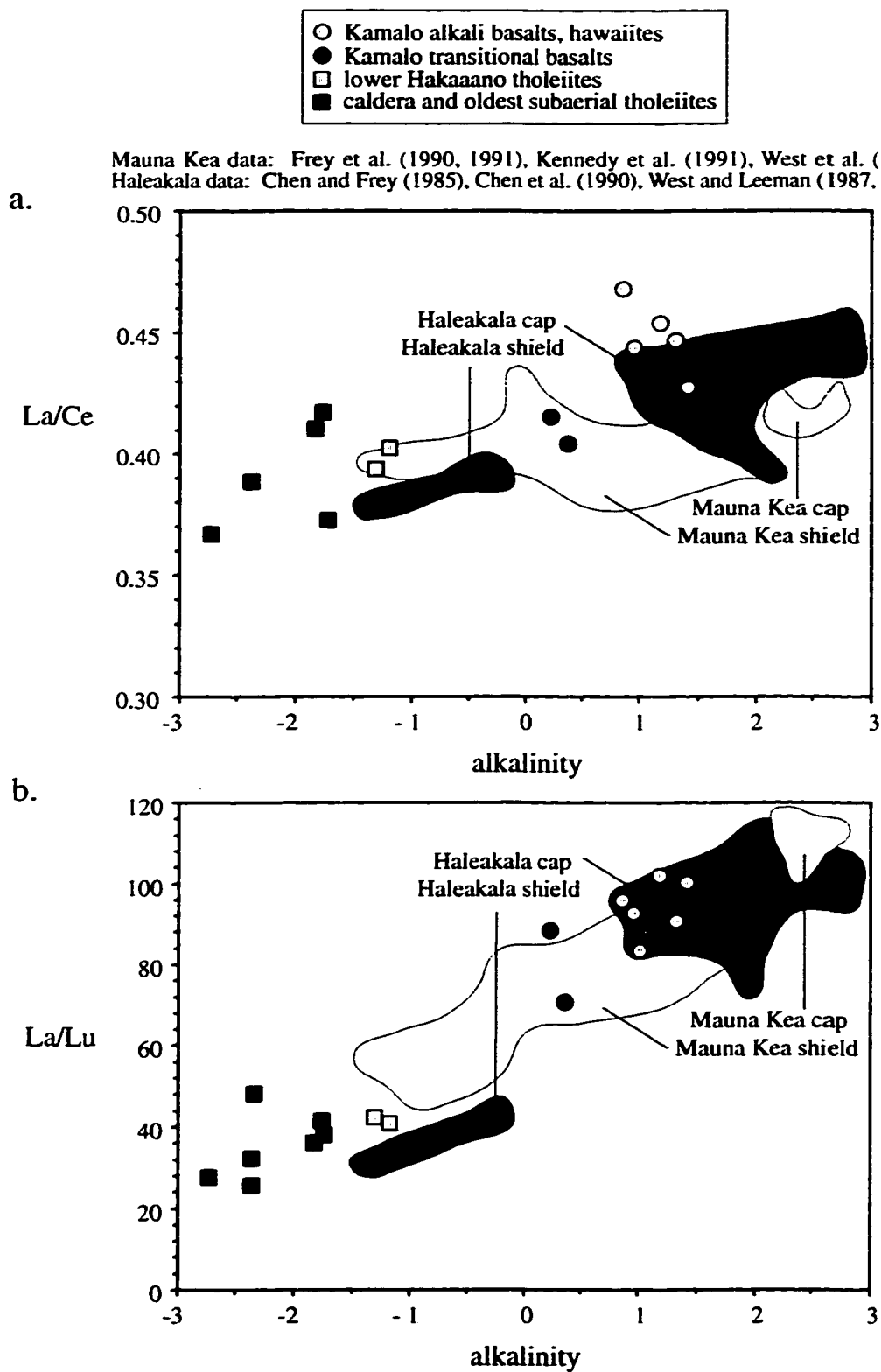


Figure 5.10 Alkalinity vs. a) La/Ce and b) La/Lu for Subaerial Basalts of East Molokai Volcano and Other Haleakala-Types (Haleakala and Mauna Kea Volcanoes)

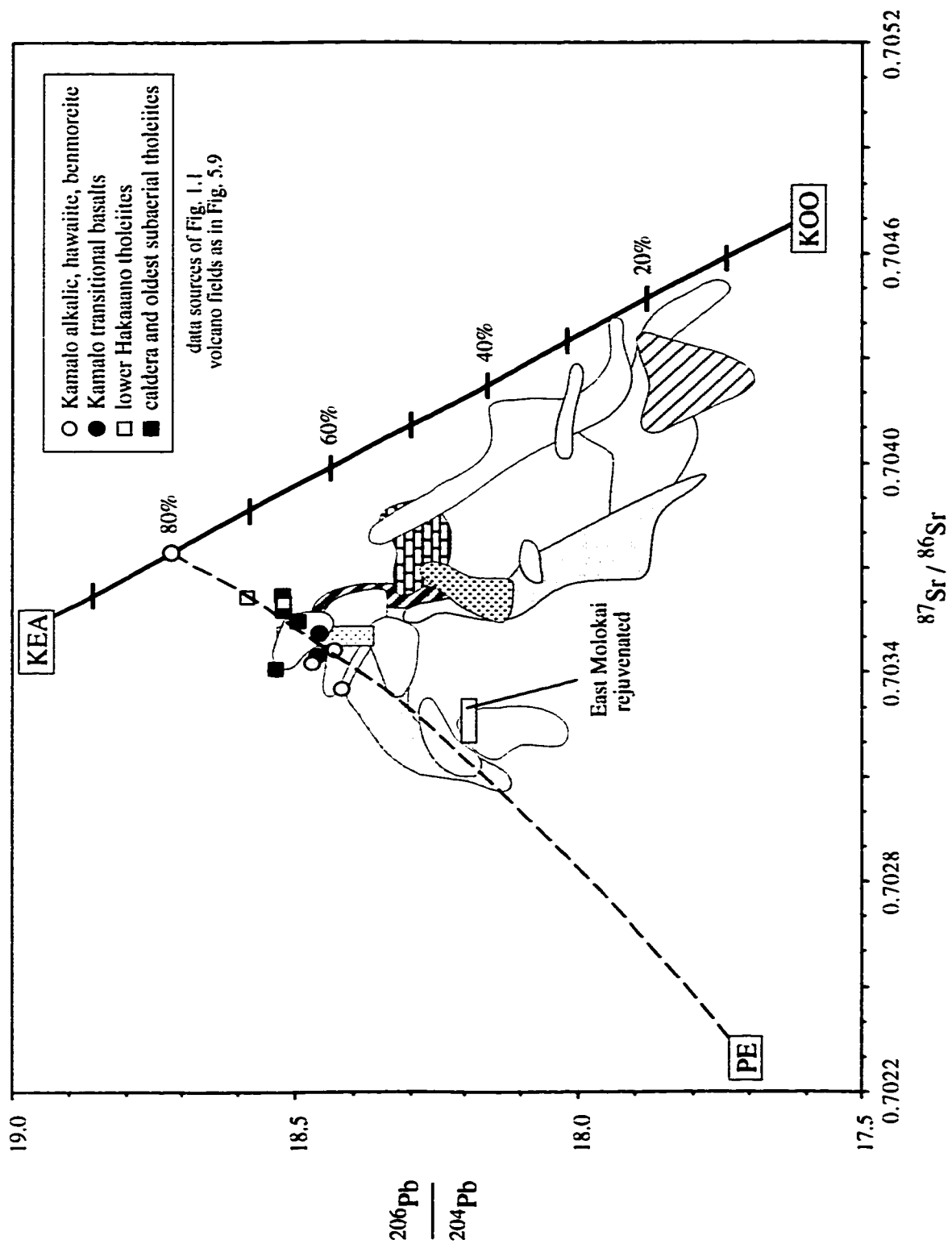


Figure 5.11 $^{87}\text{Sr}/^{86}\text{Sr}$ vs. $^{206}\text{Pb}/^{204}\text{Pb}$ for East Molokai with Model for KOO-KEA Mantle Mixing as Hawaiian Shield Source

% melting (vertical lines) of PE mantle source, and sources produced by an 80%KEA-20%KOO mix metasomatised by 0.1% PE melts in amounts 0.2%, 0.5%, 0.5%, 2%. Non-vertical lines describe KEA-KOO mixing, and % metasomatism of the KEA-KOO mix. Mix and melt lines constructed using parameters listed and described in Table 5.2

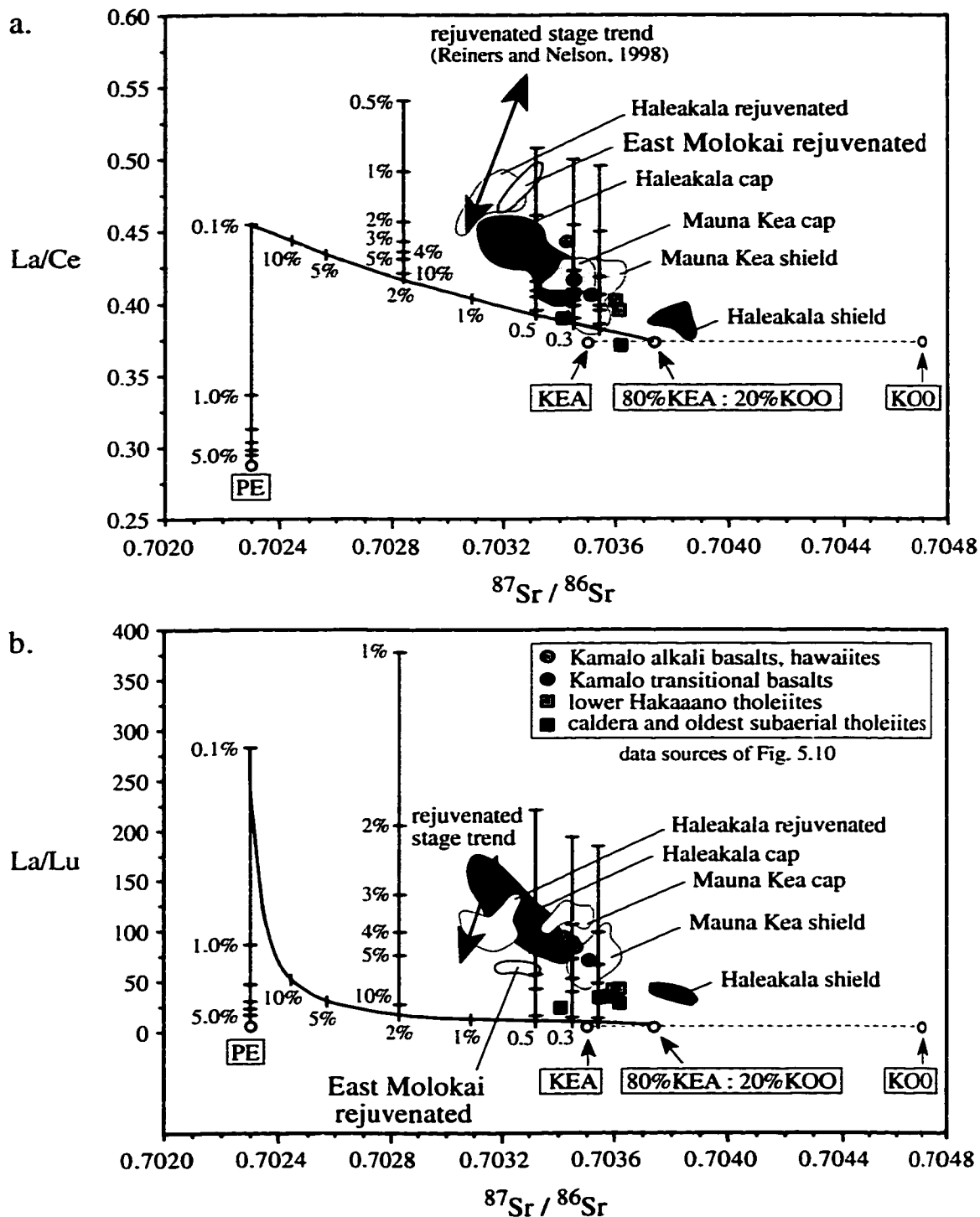


Figure 5.12 $^{87}\text{Sr}/^{86}\text{Sr}$ vs. a) La/Ce and b) La/Lu for Subaerial Basalts of East Molokai Volcano and Other Haleakala-types (Haleakala and Mauna Kea Volcanoes) with Model for Mixing between Shield Source and Small Degree Melts of Depleted Mantle

% melting (vertical lines) of PE mantle source, and sources produced by an 80%KEA-20%KOO mix metasomatised by 0.1% PE melts in amounts 0.2%, 0.5%, 0.5%, 2%. Non-vertical line describes % metasomatism of the KEA-KOO mix. Mix and melt lines constructed using parameters listed and described in Table 5.2

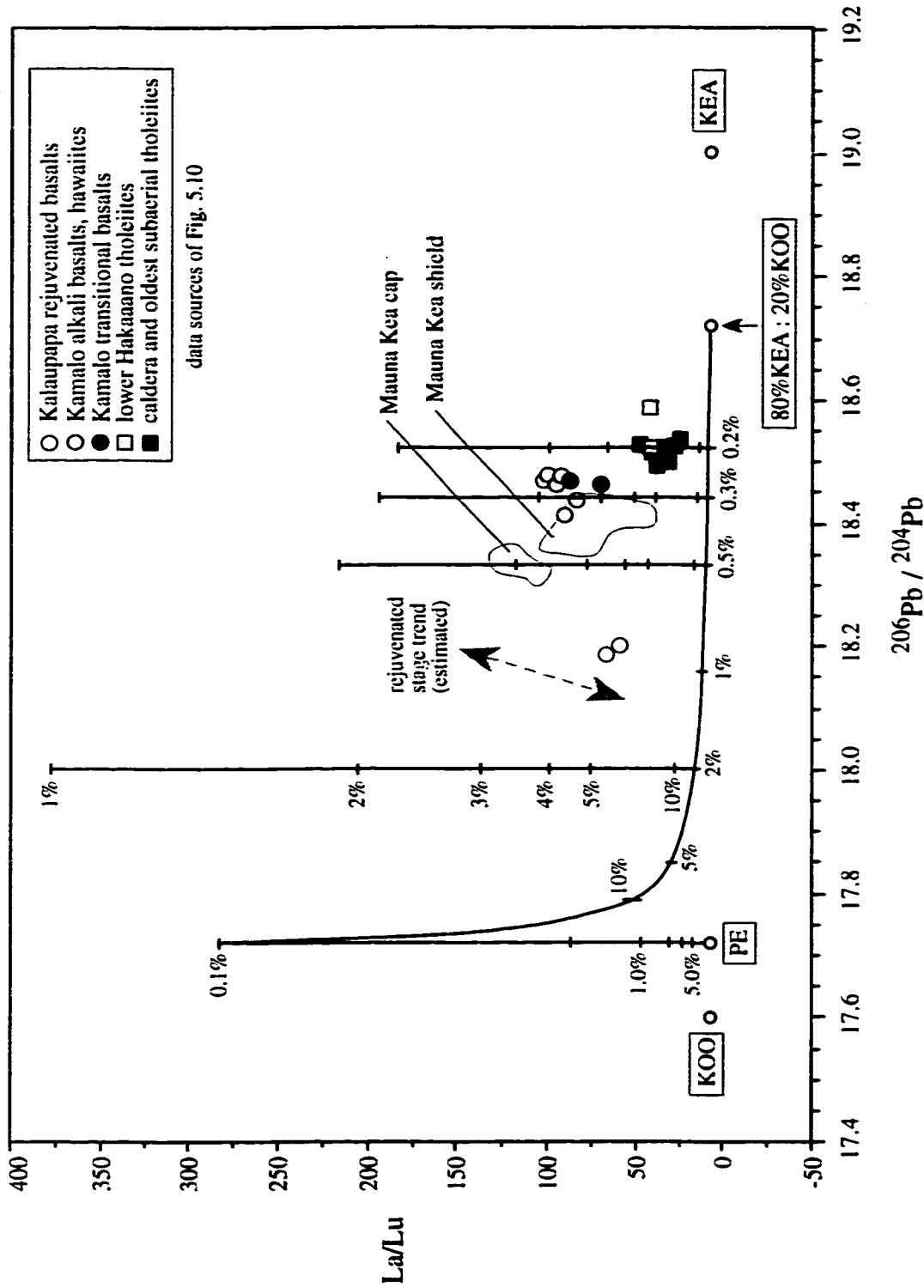


Figure 5.13 $^{206}\text{Pb}/^{204}\text{Pb}$ vs. La/Lu for Subaerial Basalts of East Molokai Volcano and Other Haleakala-types (Haleakala and Mauna Kea Volcanoes) with Model for Mixing between Shield Source and Small Degree Melts of Depleted Mantle

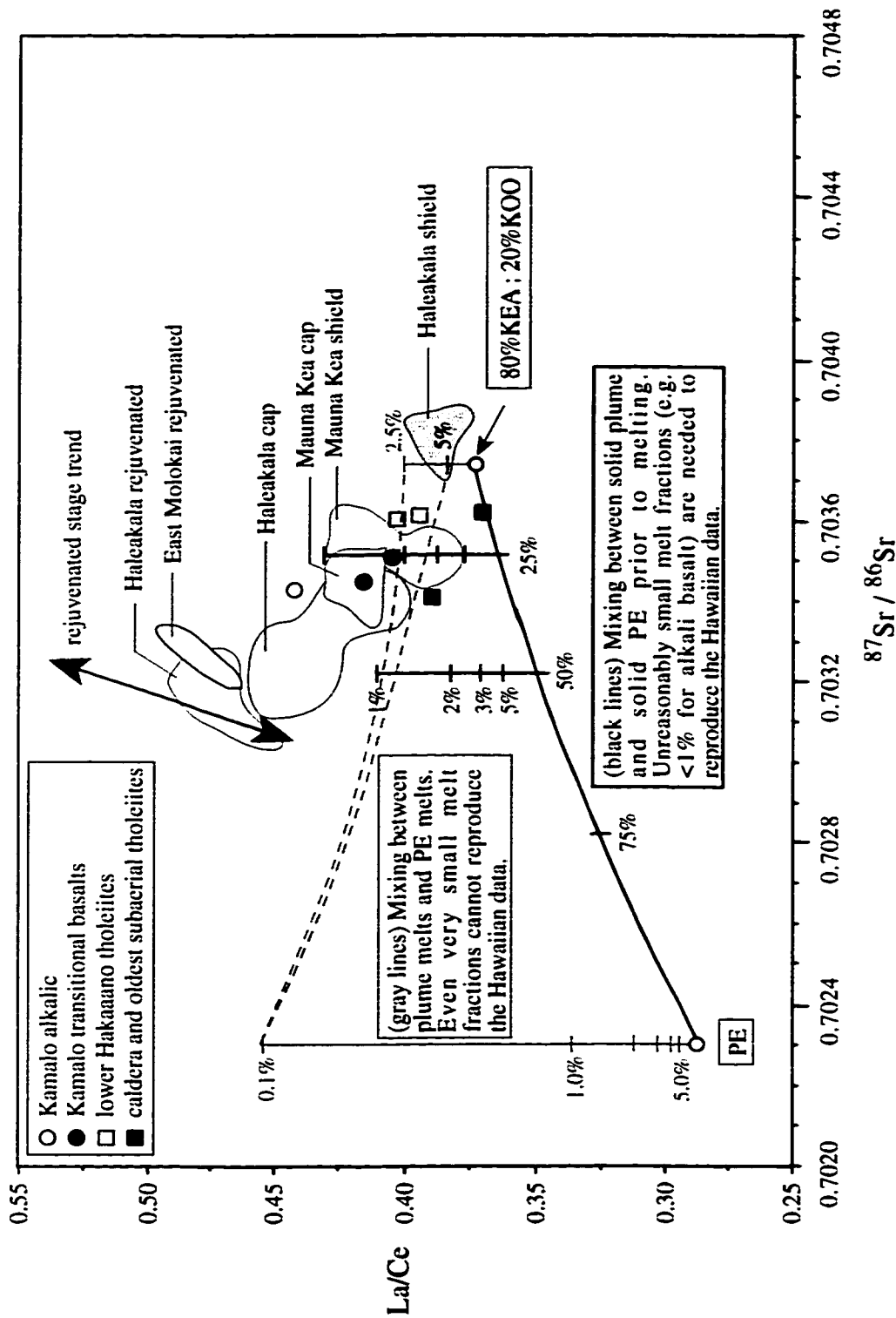


Figure 5.14 $^{87}\text{Sr}/^{86}\text{Sr}$ vs. La/Ce for Subaerial Basalts of East Molokai Volcano and Other Haleakala-types (Haleakala and Mauna Kea Volcanoes) with Alternative Models for Mixing between Shield Source and Depleted Mantle (both as solids, both as melts)

TABLE 5.1 a) Major and Trace Element and Isotopic Compositions - Haupu Section

Haupu Sampled Section								
sample	90PE 3	90PE 5	90KB 3	90KB 4	90HB 1	90HB 850	90HB 960	90HB 1000
rock type elevation (m)	tholeiite	tholeiite	tholeiite 6	tholeiite 6	tholeiite 216	tholeiite 259	tholeiite 293	tholeiite 305
SiO ₂	48.6	49.5	50.6	51.0	49.4	48.5	49.9	47.6
TiO ₂	1.87	2.85	3.09	3.07	2.38	2.25	2.58	2.82
Al ₂ O ₃	10.7	13.1	12.9	13.1	12.9	14.6	15.8	14.9
Fe ₂ O ₃	12.0	12.6	13.7	13.6	12.9	11.9	12.1	13.5
MnO	0.17	0.18	0.17	0.18	0.17	0.17	0.16	0.18
MgO	11.5	6.38	5.54	5.80	8.18	6.51	5.44	6.10
CaO	9.06	10.7	9.77	9.96	10.3	10.4	11.2	10.2
Na ₂ O	1.62	2.00	2.43	2.42	1.87	1.87	2.23	1.86
K ₂ O	0.13	0.13	0.45	0.50	0.14	0.07	0.25	0.12
P ₂ O ₅	0.19	0.24	0.35	0.34	0.24	0.22	0.27	0.26
Pb	0.52	0.72				0.64		0.89
Rb								
Sr	232	298	316	322	267	288	383	300
Ba	61	74	130	124	72	49	102	105
La	7.2	10.0		13.8	14.4	12.0	11.7	13.0
Ce	20	26		37	26	26	28	32
Nd	14	19		25	21	23	20	24
Sm	4.00	5.62		7.02	5.78	6.73	5.83	6.48
Eu	1.43	2.05		2.38	2.08	2.45	2.12	2.26
Tb	0.71	0.99		1.17	1.05	1.27	0.99	1.02
Yb	1.66	2.69		2.68	2.23	2.70	2.25	2.33
Lu	0.26	0.39		0.36	0.30	0.37	0.28	0.36
Y	11	26	30	33	30	30	25	19
Zr	109	143	190	190	135	126	14	174
Hf	3.06	4.25		5.36	3.93	3.69	4.06	4.54
Ta	0.54	0.76		1.09	0.65	0.60	0.77	0.84
Th	0.4	0.5		1.0	0.6	0.5	0.6	1.0
Ni	384	100		133	187	129	115	116
Cr	728	283		180	502	303	242	215
Sc	27.5	33.8		30.0	30.7	30.6	27.1	32.2
²⁰⁶ Pb/ ²⁰⁴ Pb	18.523	18.535	18.474	18.492	18.526	18.498	18.512	18.521
²⁰⁷ Pb/ ²⁰⁴ Pb	15.490	15.483	15.482	15.474	15.474	15.475	15.456	15.476
²⁰⁸ Pb/ ²⁰⁴ Pb	38.026	38.022	38.011	37.979	38.012	37.979	37.974	38.008
⁸⁷ Sr/ ⁸⁶ Sr	0.70362	0.70341				0.70354		0.70358
εNd	7.22	7.26				7.06		7.16

Major element oxides in wt%. Fe₂O₃ = total iron. Trace element abundances in ppm.

TABLE 5.1 b) (cont.) Major and Trace Element and Isotopic Compositions - Hakaano

Upper Hakaano Sampled Section								
sample	45	49A	54	55	58	60	62	66
rock type	tholeiite	trans	tholeiite	tholeiite	tholeiite	tholeiite	tholeiite	tholeiite
elevation (m)	140	177	210	218	241	250	262	323
SiO ₂	47.6	44.9	48.5	48.5	46.7	48.2	47.9	48.9
TiO ₂	2.87	3.61	2.93	3.11	3.63	2.99	3.48	2.87
Al ₂ O ₃	15.5	15.3	15.9	14.0	14.6	15.3	14.1	15.7
Fe ₂ O ₃	13.1	14.6	13.6	15.1	15.4	13.0	14.6	13.4
MnO	0.18	0.18	0.18	0.20	0.20	0.17	0.19	0.17
MgO	6.22	6.16	5.26	5.96	5.61	6.31	5.91	4.92
CaO	11.1	10.2	10.7	10.3	9.83	10.2	10.4	10.5
Na ₂ O	2.26	2.71	2.60	2.51	2.53	2.60	2.66	2.80
K ₂ O	0.16	0.35	0.33	0.45	0.22	0.46	0.48	0.54
P ₂ O ₅	0.36	0.57	0.42	0.40	0.50	0.42	0.48	0.39
²⁰⁶ Pb/ ²⁰⁴ Pb		18.500	18.430	18.422	18.458	18.441	18.445	18.461
²⁰⁷ Pb/ ²⁰⁴ Pb		15.473	15.449	15.463	15.475	15.483	15.466	15.482
²⁰⁸ Pb/ ²⁰⁴ Pb		37.992	37.869	37.909	37.952	37.938	37.924	37.955

TABLE 5.1 c) Major and Trace Element and Isotopic Compositions - Kamalo Section

Kamalo Gulch Sampled Section - Transitional and Alkalic Basalts								
sample	RTH93	93Kamalo	93Kamalo	93Kamalo	93Kamalo	93Kamalo	94EKAM	90KAM
	113	2	3	4	5	10	4	6
rock type	trans	alkalic	alkalic	alkalic	trans	trans	alkalic	alkalic
elevation (m)	198	262	274	293	299	378	427	439
SiO ₂	48.1	47.2	47.7	46.8	47.6	46.5	46.2	46.9
TiO ₂	3.82	4.02	3.70	4.28	3.52	2.99	3.72	3.54
Al ₂ O ₃	13.9	14.2	17.0	14.0	15.9	14.3	16.4	17.3
Fe ₂ O ₃	13.7	15.2	12.5	15.2	12.8	13.5	13.4	12.0
MnO	0.19	0.19	0.15	0.20	0.16	0.17	0.17	0.17
MgO	5.20	4.45	3.39	4.21	4.59	8.24	3.74	3.00
CaO	9.41	8.68	9.21	9.41	10.4	10.1	9.55	8.96
Na ₂ O	3.13	3.33	3.38	3.38	3.25	2.62	3.24	3.27
K ₂ O	0.94	1.03	1.04	1.12	0.89	0.65	1.04	1.11
P ₂ O ₅	0.60	0.80	0.60	0.64	0.52	0.44	0.59	0.57
Pb	1.93	2.30				1.44		
Rb	30	27		28		24	31	
Sr	518	569		556		565	672	760
Ba	240	308		290		214	285	577
La	27.5	44.3		34.4		22.0	32.7	30.7
Ce	68	84		77		53	72	66
Nd	41	58		50		34	46	42
Sm	10.70	15.90		12.90		8.55	10.80	9.77
Eu	3.36	4.74		3.95		2.61	3.35	3.12
Tb	1.46	2.69		1.59		0.89	1.41	1.32
Yb	3.20	4.10		3.05		1.88	2.43	2.21
Lu	0.39	0.53		0.38		0.25	0.32	0.32
Y	35	57		36		23	32	40
Zr	311	394		335		234	304	261
Hf	8.00	9.84		8.66		5.75	7.68	6.88
Ta	1.91	2.43		2.16		1.48	2.21	2.04
Th	1.9	2.5		2.3		1.5	2.4	2.3
Ni	84	91		89		258	83	77
Cr	92	27		60		477	60	92
Sc	26.2	23.3		24.3		25.0	21.7	19.9
²⁰⁶ Pb/ ²⁰⁴ Pb	18.461	18.434	18.456	18.412	18.424	18.466	18.466	18.462
²⁰⁷ Pb/ ²⁰⁴ Pb	15.476	15.477	15.522	15.462	15.472	15.468	15.474	15.469
²⁰⁸ Pb/ ²⁰⁴ Pb	37.951	37.947	38.071	37.900	37.943	37.947	37.980	37.951
⁸⁷ Sr/ ⁸⁶ Sr	0.70351	0.70346				0.70345		
εNd	7.06	6.98				7.15		

TABLE 5.1 c) (continued) Major and Trace Element and Isotopic Compositions - Kamalo

Kamalo Gulch Sampled Section (continued) - Transitional and Alkalic Basalts									
sample	93Kamal 0 6	93Kamal 0 7	93Kamal 0 8	93Kamal 0 9	93Kamal 0 11	93Kamal 0 12	93Kamal 0 13	93Kamal 0 17	93Kamal 0 19
rock type elevation m	alkalic 317	alkalic 329	alkalic 347	trans 360	trans 384	trans 390	alkalic 402	alkalic 445	alkalic 457
SiO ₂	47.2	46.2	46.2	46.3	46.9	45.6	47.0	46.8	46.5
TiO ₂	3.49	3.68	3.71	2.95	3.32	3.29	4.02	3.62	4.13
Al ₂ O ₃	16.9	15.6	15.7	13.1	14.6	14.8	14.7	17.0	15.8
Fe ₂ O ₃	12.2	13.8	13.9	13.3	12.9	13.1	14.2	12.0	13.7
MnO	0.15	0.17	0.18	0.17	0.16	0.16	0.18	0.15	0.18
MgO	3.88	5.26	5.13	9.67	6.64	6.91	4.64	3.85	4.12
CaO	9.92	9.31	9.48	10.3	9.95	10.1	9.52	10.2	9.88
Na ₂ O	3.45	3.53	3.24	2.64	2.93	2.71	3.64	3.58	3.32
K ₂ O	0.95	1.06	0.97	0.69	0.85	0.70	1.12	1.00	1.07
P ₂ O ₅	0.43	0.54	0.53	0.40	0.48	0.43	0.54	0.44	0.53

TABLE 5.1 d) Major and Trace Element and Isotopic Compositions - Kamalo Alkali Cap

Kamalo Gulch Section Hawaiites				Kamalo Gulch Section Mugearites, Benmoreites					
sample	93Kamal o l	93Kamal o 14	90KAM 9	93Kamalo 22	93Kamalo 24	93Kamalo 26	93Kamalo 28	90KAM 3	90KAM 4
rock type	hawaiite	hawaiite	hawaiite	mugearite	mugearite	mugearite	mugearite	benm	benm
elevation (m)	232	414	424	488	533	555	579	585	600
SiO ₂	48.7	49.8	49.1	53.3	52.7	49.8	50.3	58.4	56.7
TiO ₂	3.26	3.68	3.36	1.86	1.93	2.60	2.59	1.20	1.19
Al ₂ O ₃	16.0	14.4	14.6	17.3	17.5	17.9	17.4	17.8	17.7
Fe ₂ O ₃	12.3	13.8	12.8	9.43	9.63	11.1	11.0	7.15	6.98
MnO	0.14	0.20	0.21	0.21	0.20	0.19	0.20	0.24	0.29
MgO	3.24	3.99	3.68	2.53	2.72	2.58	3.21	1.63	1.34
CaO	7.82	8.22	7.94	5.39	5.58	5.81	6.49	3.52	3.33
Na ₂ O	3.97	4.13	3.68	5.59	5.56	4.74	4.68	6.55	6.32
K ₂ O	1.57	1.40	1.50	2.18	1.98	1.77	1.77	2.78	2.72
P ₂ O ₅	0.58	0.84	0.81	1.10	1.06	1.00	0.98	0.58	0.58
Pb			2.40					5.12	
Rb		38	24					56	56
Sr		605	686					1200	1220
Ba		357	474					1540	3230
La		43.2	39.9					108.7	121.8
Ce		101.	90					172	226
Nd		64	51					101	111
Sm		14.60	12.79					19.27	22.01
Eu		4.29	4.08					6.00	6.31
Tb		2.07	1.78					2.40	2.65
Yb		3.44	3.22					4.64	5.40
Lu		0.43	0.43					0.62	0.69
Y		42	36					80	99
Zr		436	389					608	581
Hf		10.2	9.67					13.61	13.53
Ta		2.52	2.73					5.33	5.24
Th		3.1	2.9					6.8	6.9
Ni			67					39	46
Cr		18	100					18	9
Sc		18.9	17.1					2.9	2.9
²⁰⁶ Pb/ ²⁰⁴ Pb	18.549	18.477	18.474	18.448				18.421	18.434
²⁰⁷ Pb/ ²⁰⁴ Pb	15.502	15.473	15.477	15.466				15.460	15.466
²⁰⁸ Pb/ ²⁰⁴ Pb	38.052	37.963	37.985	37.961				37.949	37.952
⁸⁷ Sr/ ⁸⁶ Sr			0.70342					0.70335	
ε Nd			6.71					6.83	

Table 5.2 Melting and Melt Mixing Parameters for Model Mantle Source of East Molokai Lavas

	La	Ce	Lu	Sr	Pb	$\frac{87\text{Sr}}{86\text{Sr}}$	ϵ_{Nd}	$\frac{206\text{Pb}}{204\text{Pb}}$	$\frac{208\text{Pb}}{204\text{Pb}}$
partition coefficients ^a	ol / liquid	0.00045	0.00065	0.00315	0.00019	0.0001			
	opx / liquid	0.00125	0.00195	0.049	0.007	0.0013			
	cpx / liquid	0.037	0.069	0.235	0.0670	0.01			
	gt / liquid	0.007	0.0122	5.60	0.0011	0.0005			
compositions	KOO ^b	0.71	1.9	0.1	23.0	0.071	0.7047	17.6	37.7
	KEA ^c	0.71	1.9	0.1	23.0	0.071	0.7035	19.0	38.3
	PE ^d	0.206	0.722	0.054	12.9	0.018	0.7023	17.72	37.0

Melting of mantle sources is non-modal batch melting. Source minerals olivine (ol), orthopyroxene (opx), clinopyroxene (cpx), and garnet (gt) are in modal proportions 0.65, 0.24, 0.06, 0.05, and melt proportions 0.1, 0.1, 0.4, 0.4 (Reiners and Nelson, 1998).

^aREE K_ds of Reiners and Nelson (1998). Sr and Pb concentrations of McKenzie and O'Nions (1991).

^bREE concentrations from EM of Reiners and Nelson (1998) and Chen and Frey (1983, 1985). Sr, Pb concentrations from primitive mantle data of Rollinson (1993). Sr, Nd isotope compositions of Reiners and Nelson (1998). Pb isotope composition consistent with Stille et al. (1986) and West and Leeman (1987).

^cREE concentrations from EM of Reiners and Nelson (1998) and Chen and Frey (1983, 1985). Sr, Pb concentrations from primitive mantle compilation of Rollinson (1993). Isotope compositions consistent with Stille et al. (1986) and West and Leeman (1987).

^dREE concentrations from MORB of Reiners and Nelson (1998) and Chen and Frey (1983, 1985). Sr, Pb concentrations of Geochemical Earth Reference Model (GERM). Sr, Nd isotope compositions of Reiners and Nelson (1998). Pb isotope composition of West and Leeman (1987) and data trends.

REFERENCE LIST

- Albarède F. (1992) How deep do common basaltic magmas form and differentiate? *J. Geophys. Res.* **97**, 10,997-11,009.
- Basaltic Volcanism Study Project (1981) *Basaltic Volcanism on the Terrestrial Planets*, 1286 pp. Pergamon.
- Beeson M. H. (1976) Petrology, mineralogy, and geochemistry of the East Molokai Volcanic Series, Hawaii. *USGS Prof. Paper* **961**, 1-53.
- Bogue S. W. (1987) Magnetostratigraphy of Kauai, Hawaii. *Geol. Soc. Amer. Abs. Programs* **19**, 359-360 (abstr.).
- Bonhommet N., Beeson M. H., and Dalrymple G. B. (1977) A contribution to the geochronology and petrology of the island of Lanai, Hawaii. *Geol. Soc. Amer. Bull.* **88**, 1282-1286.
- Boynton W. V. (1984) Geochemistry of the rare earth elements: meteorite studies. In *Rare Earth Element Geochemistry* (ed. P. Henderson), pp. 63-114. Elsevier.
- Chen C.-Y. and Frey F. A. (1983) Origin of Hawaiian tholeiite and alkalic basalt. *Nature* **302**, 785-789.
- Chen C.-Y. and Frey F. A. (1985) Trace element and isotopic geochemistry of lavas from Haleakala volcano, east Maui, Hawaii: Implications for the origin of Hawaiian basalts. *J. Geophys. Res.* **90**, 8743-8768.
- Chen C.-Y., Frey F. A., and Garcia M. O. (1990) Evolution of alkalic lavas at Haleakala volcano, east Maui, Hawaii: Major, trace element, and isotopic constraints. *Contrib. Mineral. Petrol.* **105**, 197-218.
- Chen C.-Y., Frey F. A., Garcia M. O., Dalrymple G. B., and Hart S. R. (1991) The tholeiite to alkalic basalt transition at Haleakala Volcano, Maui, Hawaii. *Contrib. Mineral. Petrol.* **106**, 183-200.
- Chen C.-Y., Frey F. A., Rhodes J. M., and Easton R. M. (1996) Temporal geochemical evolution of Kilauea Volcano: Comparison of Hilina and Puna Basalt. In *Earth Processes: Reading the Isotopic Code* (ed. A. Basu and S. Hart), *Geophys. Monogr. Ser.* **95**, pp. 161-182. AGU.
- Clague D. A. and Beeson M. H. (1980) Trace element geochemistry of the East Molokai Volcanic Series, Hawaii. *Amer. J. Sci.* **280-A**, 820-844.
- Clague D. A. and Dalrymple G. B. (1987) The Hawaiian-Emporer volcanic chain, I, Geologic evolution. *USGS Prof. Paper*, **1350**, 5-54.

- Clague D. A., Dao-gong C., Murnane R., Beeson M. H., Lanphere M. A., Dalrymple G. B., Friesen W., and Holcomb R. T. (1982) Age and petrology of the Kalaupapa Basalt, Molokai, Hawaii. *Pac. Sci.* **36**, 411-420.
- Clague D. A., Moore J. G., Dixon J. E., and Friesen W. B. (1995) Petrology of submarine lavas from Kilauea's Puna Ridge, Hawaii. *J. Petrol.* **36**, 299-349.
- Coe R. S., Gromme S., and Mankinen E. A. (1984) Geomagnetic paleointensities from excursion sequences in lavas on Oahu, Hawaii. *J. Geophys. Res.* **89**, 1059-1069.
- Davies G. F. (1992) Temporal variation of the Hawaiian plume flux. *Earth Planet. Sci. Lett.* **113**, 277-286.
- DePaolo D. J. and Stolper E. M. (1996) Models of Hawaiian volcano growth and plume structure: Implications of results from the Hawaii Scientific Drilling Project. *J. Geophys. Res.* **101**, 11,643-11,654.
- Doell R. R. and Dalrymple G. B. (1973) Potassium-argon ages and paleomagnetism of the Waianae and Koolau Volcanic Series, Oahu, Hawaii. *Geol. Soc. Amer. Bull.* **84**, 1217-1242.
- Farley K. A., Natland J. H., and Craig H. (1992) Binary mixing of enriched and undegassed (primitive?) mantle components (He, Sr, Nd, Pb) in Samoan lavas. *Earth Planet. Sci. Lett.* **111**, 183-199.
- Feigenson M. D., Hofmann A. W., and Spera F. J. (1983) Case studies on the origin of basalt: II. The transition from tholeiitic to alkalic volcanism on Kohala volcano, Hawaii. *Contrib. Mineral. Petrol.* **84**, 390-405.
- Fodor R. V., Frey F. A., Bauer G. R., and Clague D. A. (1992) Ages, rare-earth element enrichment, and petrogenesis of tholeiitic and alkalic basalts from Kahoolawe Island, Hawaii. *Contrib. Mineral. Petrol.* **110**, 442-462.
- Frey F. A. and Rhodes J. M. (1993) Intershield geochemical differences among Hawaiian volcanoes: implications for source compositions, melting process and magma ascent paths. *Phil. Trans. Roy. Soc. London. A* **342**, 121-136.
- Frey F. A., Wise W. S., Garcia M. O., West H., Kwon S.-T., and Kennedy A. (1990) Evolution of Mauna Kea Volcano, Hawaii: Petrologic and geochemical constraints on postshield volcanism. *J. Geophys. Res.* **95**, 1271-1300.
- Frey F. A., Garcia M. O., Wise W. S., Kennedy A., Gurriet P., and Albarède F. (1991) The evolution of Mauna Kea Volcano, Hawaii: Petrogenesis of tholeiitic and alkalic basalts. *J. Geophys. Res.* **96**, 14347-14375.
- Frey F. A., Garcia M. O., and Roden M. F. (1994) Geochemical characteristics of Koolau Volcano: Implications of intershield geochemical differences among Hawaiian volcanoes. *Geochim. Cosmochim. Acta* **58**, 1441-1462.

- Garcia M. O. (1979) Introduction to the geology of Oahu. In *Field Trip Guide to the Hawaiian Islands* (ed. M. O. Garcia and J. M. Sinton), pp. 1-14. Hawaii Institute of Geophysics, Honolulu.
- Garcia M. O., Muenow D. W., Aggrey K. E., and O'Neil J. R. (1989) Major element, volatile, and stable isotope geochemistry of Hawaiian submarine tholeiitic glasses. *J. Geophys. Res.* **94**, 10,525-10,538.
- Garcia M. O., Foss D. J. P., West H. B., and Mahoney J. J. (1995) Geochemical and isotopic evolution of Loihi volcano, Hawaii. *J. Petrol.* **36**, 1647-1674.
- Ghiorso M. S. and Sack R. O. (1993) MELTS: Software for the thermodynamic analysis of phase equilibria in magmatic systems. *Geol. Soc. Amer. Abstr. Programs* **25**, A-96 (abstr.).
- Griffiths R. W. and Campbell I. H. (1991) On the dynamics of long-lived plume conduits in the convecting mantle. *Earth Planet. Sci. Lett.* **103**, 214-227.
- Hart S. R. (1988) Heterogeneous mantle domains: Signatures, genesis and mixing chronologies. *Earth Planet. Sci. Lett.* **90**, 273-296.
- Hart S. R., Hauri E. H., Oschmann L. A., and Whitehead J. A. (1992) Mantle plumes and entrainment: Isotopic evidence. *Science* **256**, 517-520.
- Hauri E. H. (1996) Major-element variability in the Hawaiian mantle plume. *Nature* **382**, 415-419.
- Hauri E. H., Whitehead J. A., and Hart S. R. (1994) Fluid dynamic and geochemical aspects of entrainment in mantle plumes. *J. Geophys. Res.* **99**, 24,275-24,300.
- Hauri E. H., Lassiter J. C., and DePaolo D. J. (1996) Osmium isotope systematics of drilled lavas from Mauna Loa, Hawaii. *J. Geophys. Res.* **101**, 11,793-11,806.
- Hegner E., Unruh D., and Tatsumoto M. (1986) Nd-Sr-Pb isotope constraints on the sources of West Maui volcano, Hawaii. *Nature* **319**, 478-480.
- Hofmann A. W. (1999) The Gabbro-Harzburgite Connection in OIB Sources. *Eos* **80**. (abstr.)
- Hofmann A. W. and White W. M. (1982) Mantle plumes form ancient oceanic crust. *Earth Planet. Sci. Lett.* **57**, 421-436.
- Hofmann A. W. and White W. M. (1983) Ba, Rb, and Cs in the Earth's mantle. *Z. Naturforsch.* **38**, 256-266.
- Hofmann A. W. and Jochum K. P. (1996) Source characteristics derived from very incompatible trace elements in Mauna Loa and Mauna Kea basalts, Hawaii Scientific Drilling Project. *J. Geophys. Res.* **101**, 11,831-11,839.

- Hofmann A. W., Feigenson M. D., and Raczek I. (1984) Case studies on the origin of basalt, III, Petrogenesis of the Mauna Ulu eruption, Kilauea, 1969-1971. *Contrib. Mineral. Petrol.* **88**, 24-35.
- Hofmann A. W., Jochum K. P., Seufert M., and White W. M. (1986) Nb and Pb in oceanic basalts: new constraints on mantle evolution. *Earth Planet Sci. Lett.* **79**, 33-45.
- Hofmann A. W., Feigenson M. D., and Raczek I. (1987) Kohala revisited. *Contrib. Mineral. Petrol.* **95**, 114-122.
- Holcomb R. T. (1985) The caldera of East Molokai Volcano, Hawaii. *Natl. Geogr. Soc. Res. Rep.* **21**, 81-87.
- Holcomb R. T. (1990) Wailau (East Molokai), Hawaii. In *Volcanoes of North America* (ed. C. A. Wood and J. Kienle), pp. 328-330. Cambridge University Press.
- Holcomb R. T., Anders N. E., Reiners P. W., and Carrecedos J.-C. (1993) Magnetostratigraphy used to outline the caldera of Waianae Volcano, Oahu. *Eos* **74** (abstr).
- Holcomb R. T., Reiners P. W., Nelson B. K., and Anders N. L. (1995) Isotopic evidence for two shield volcanoes exposed on the island of Kauai, Hawaii. *Eos* **76**, F669 (abstr.).
- Holcomb R. T., Reiners P. W., Nelson B. K., and Sawyer N. E. (1997) Evidence for two shield volcanoes exposed on the island of Kauai, Hawaii. *Geology*, **25**, 769-864.
- Irvine T. N. and Baragar W. R. A. (1971) A guide to the chemical classification of the common volcanic rocks. *Can. J. Earth Sci.* **8**, 523-548.
- Kennedy A. K., Kwon S.-T., Frey F. A., and West H. B. (1991) The isotopic composition of postshield lavas from Mauna Kea volcano, Hawaii. *Earth Planet. Sci. Lett.* **103**, 339-353.
- Kinzler R. J. (1992) Mantle melting processes at the spinel-garnet transition. *Eos* **73**, 615 (abstr.).
- Kurz M. D., Kenna T., Kammer D., Rhodes J. M., and Garcia M. O. (1995) Isotopic evolution of Mauna Loa volcano: A view from the submarine southwest rift zone. In *Mauna Loa Revealed: Structure, Composition, History, and Hazards* (ed. J. M. Rhodes and J. P. Lockwood), *Geophys. Monogr. Ser.* **92**, pp. 289-306. AGU.
- Kurz M. D., Kenna T. C., Lassiter J. C., and DePaolo D. J. (1996) Helium isotopic evolution of Mauna Kea volcano: First results from the 1-km drill core. *J. Geophys. Res.* **101**, 11,781-11,791.
- Kushiro I. (1996) Partial melting of fertile mantle peridotite at high pressures: An experimental study using aggregates of diamond. In *Earth Processes: Reading the*

- Isotopic Code* (ed. A. Basu and S. Hart), *Geophys. Monogr. Ser.* **95**, pp. 109-122. AGU.
- Langenheim V. A. M. and Clague D. A. (1987) The Hawaiian-Emperor Volcanic Chain, II, Stratigraphic framework of volcanic rocks of the Hawaiian Islands. *USGS Prof. Paper*, **1350**, 55-84.
- Langmuir C. H. and Hanson G. N. (1980) An evaluation of major element heterogeneity in the mantle source of basalts. *Phil. Trans. Roy. Soc. London A* **297**, 383-407.
- Lanphere M. A. and Frey F. A. (1987) Geochemical evolution of Kohala Volcano, Hawaii. *Contrib. Mineral. Petrol.* **95**, 100-113.
- Lassiter J. C., DePaolo D. J., and Tatsumoto M. (1996) Isotopic evolution of Mauna Kea volcano: Results from the initial phase of the Hawaii Scientific Drilling Project. *J. Geophys. Res.* **101**, 11,769-11,780.
- Leeman W. P., Gerlach D. C., Garcia M. O., and West H. B. (1994) Geochemical variations in lavas from Kahoolawe volcano, Hawaii: evidence for open system evolution of plume-derived magmas. *Contrib. Mineral. Petrol.* **116**, 62-77.
- Le Bas M. J., Le Maitre R. W., Streckeisen A., and Zanettin B. (1986) A chemical classification of volcanic rocks on the total alkali-silica diagram. *J. Petrol.* **27**, 745-750.
- Lipman P. W., Rhodes J. M., and Dalrymple G. B. (1990) The Ninole Basalt - implications for the structural evolution of Mauna Loa Volcano, Hawaii. *Bull. Volcanol.* **53**, 1-19.
- McKenzie D. and O'Nions R. K. (1991) Partial melt distributions from inversion of rare earth element concentrations. *J. Petrol.* **32**, 1021-1091.
- Macdonald G. A. (1968) Composition and origin of Hawaiian lavas. *Mem. Geol. Soc. Amer.* **116**, 477-522.
- Macdonald G. A. (1940) Petrography of the Waianae Range, Oahu. In *Supplement to geology and ground-water resources of the Island of Oahu, Hawaii, Hawaii Div. Hydrog. Bull.* **5**, pp. 61-91.
- Macdonald G. A. and Katsura T. (1964) Chemical composition of Hawaiian lavas. *J. Petrol.* **5**, 82-133.
- Martin C. E., Chen C.-Y., Frey F. A., Carlson R. W., and Shirey S. B. (1994) Os isotopic variation in basalts from Haleakala Volcano, Maui, Hawaii: Implications for melt interactions with upper mantle and crust. *Earth Planet Sci. Lett.*, **128**, 287-301.
- Moore J. G. (1964) Giant submarine landslides on the Hawaiian Ridge. *USGS Prof. Paper* **501-D**, D95-D98.

- Moore J. G. and Chadwick W. W. Jr. (1995) Offshore geology of Mauna Loa and adjacent areas, Hawaii. In *Mauna Loa Revealed: Structure, Composition, History, and Hazards* (ed. J. M. Rhodes and J. P. Lockwood), *Geophys. Monogr. Ser.* **92**. AGU.
- Moore J. G. and Clague D. A. (1992) Volcano growth and evolution of the island of Hawaii. *Geol. Soc. Amer. Bull.* **104**, 1471-1484.
- Moore J. G., Clague D. A., Holcomb R. T., Lipman P. W., Normark W. R., and Torresan M. E. (1989) Prodigious submarine landslides on the Hawaiian Ridge. *J. Geophys. Res.* **94**, 17,465-17,484.
- Moore J. G., Clague D. A., Ludwig K. R., and Mark R. K. (1990) Subsidence and volcanism of the Haleakala Ridge, Hawaii. *J. Volcanol. Geotherm. Res.* **42**, 273-284.
- Nelson B. K. (1995) Fluid flow in subduction zones: Evidence from neodymium and strontium isotope variations in metabasalts of the Franciscan Complex, California. *Contrib. Mineral. Petrol.* **119**, p. 247-262.
- Presley T. K., Sinton J. M., and Pringle M. (1997) Postshield volcanism and catastrophic mass wasting of the Waianae Volcano, Oahu, Hawaii. *Bull. Volcanol.* **58**, 597-616.
- Reiners P. W. and Nelson B. K. (1998) Temporal-compositional-isotopic trends in rejuvenated-stage magmas of Kauai, Hawaii, and implications for mantle processes. *Geochim. Cosmochim. Acta* **62**, 2347-2368.
- Rhodes J. M. (1995) The 1852 and 1868 Mauna Loa Picrite eruptions: Clues to parental magma compositions and the magmatic plumbing system. In *Mauna Loa Revealed: Structure, Composition, History, and Hazards* (ed. J. M. Rhodes and J. P. Lockwood), *Geophys. Monogr. Ser.* **92**, pp. 241-262. AGU.
- Rhodes J. M. (1996) Geochemical stratigraphy of lava flows sampled by the Hawaii Scientific Drilling Project. *J. Geophys. Res.* **101**, 11,729-11,746.
- Rhodes J. M. and Hart S. R. (1995) Episodic trace element and isotopic variations in historical Mauna Loa lavas: Implications for magma and plume dynamics. In *Mauna Loa Revealed: Structure, Composition, History, and Hazards* (ed. J. M. Rhodes and J. P. Lockwood), *Geophys. Monogr. Ser.* **92**, pp. 263-288. AGU.
- Roden M. F., Frey F. A., and Clague D. A. (1984) Geochemistry of tholeiitic and alkalic lavas from the Koolau Range, Oahu, Hawaii: implications for Hawaiian volcanism. *Earth Planet. Sci. Lett.* **69**, 141-158.
- Roden M. F., Trull T., Hart S. R., and Frey F. A. (1994) New He, Nd, Pb, and Sr isotopic constraints on the constitution of the Hawaiian plume: Results from Koolau Volcano, Oahu, Hawaii, USA. *Geochim. Cosmochim. Acta* **58**, 1431-1440.
- Roeder P. L. and Emslie R. F. (1970) Olivine-liquid equilibrium. *Contrib. Mineral. Petrol.* **29**, 275-289.

- Rollinson H. R. (1993) *Using Geochemical Data: Evaluation, Presentation, Interpretation*. 352 pp. Wiley and Sons.
- Sinton J. M. (1979) Geology and petrography of volcanic rocks of Lualualei Valley, Waianae Range, Oahu. In *Field Trip Guide to the Hawaiian Islands* (ed. M. O. Garcia and J. M. Sinton), pp. 51-66. Hawaii Institute of Geophysics, Honolulu.
- Sinton J. M. (1987) Revision of stratigraphic nomenclature of Waianae Volcano, Oahu, Hawaii. *U.S. Geol. Survey Bull.* **1775-A**, A9-A15.
- Sleep N. H. (1990) Hotspots and mantle plumes: some phenomenology. *J. Geophys. Res.* **95**, 6715-6736.
- Stearns H. T. (1935) Geography and geology. In *Geology and groundwater resources of the Island of Oahu, Hawaii, Hawaii Div. Hydrog. Bull.* **1**, pp. 1-198.
- Stearns H. T. (1939) Geologic map and guide of the Island of Oahu, Hawaii. *Hawaii Div. Hydrog. Bull.* **2**, 75 pp.
- Stearns H. T. (1946) Geology of the Hawaiian Islands. *Hawaii Div. Hydrog. Bull.* **8**, 106 pp.
- Stearns H. T. and Macdonald G. A. (1947) Geology and groundwater resources of the island of Molokai, Hawaii. *Hawaii Div. Hydrog. Bull.* **11**, 113 pp.
- Stearns H. T. and Vaksvik K. N. (1935) Geology and groundwater resources of the island of Oahu, Hawaii. *Hawaii Div. Hydrog. Bull.* **1**, 479 pp.
- Stille P., Unruh D. M., and Tatsumoto M. (1983) Pb, Sr, Nd and Hf isotopic evidence of multiple sources for Oahu, Hawaii basalts. *Nature* **304**, 25-29.
- Stille P., Unruh D. M., and Tatsumoto M. (1986) Pb, Sr, Nd and Hf isotopic constraints on the origin of Hawaiian basalts and evidence for a unique mantle source. *Geochim. Cosmochim. Acta* **50**, 2303-2319.
- Stolper E. M., DePaolo D. J., and Thomas D. M. (1996) Introduction to special section: Hawaii Scientific Drilling Project. *J. Geophys. Res.* **101**, 11,593-11,598.
- Takasaki K. J. (1971) Groundwater in the Waianae District, Oahu, Hawaii, *U. S. Geol. Surv. Hydrol. Invest. Atlas.* **HA-358**.
- Tatsumoto M. (1978) Isotopic composition of lead in oceanic basalt and its implication to mantle evolution. *Earth Planet. Sci. Lett.* **38**, 63-87.
- Walter M. J. and Presnall D. C. (1994) Melting behavior of simplified lherzolite in the system CaO-MgO-Al₂O₃-SiO₂-Na₂O from 7 to 35 kbar. *J. Petrol.* **35**, 329-359.

- West H. B. and Leeman W. P. (1987) Isotopic evolution of lavas from Haleakala Crater, Hawaii. *Earth Planet. Sci. Lett.* **84**, 211-225.
- West H. B. and Leeman W. P. (1994) The open-system geochemical evolution of alkalic cap lavas from Haleakala crater, Hawaii, U.S.A. *Geochim. Cosmochim. Acta* **58**, 773-796.
- West H. B., Gerlach D. C., Leeman W. P., and Garcia M. O. (1987) Isotopic constraints on the origin of Hawaiian lavas from the Maui Volcanic Complex, Hawaii. *Nature* **330**, 216-220.
- West H. B., Garcia M. O., Frey F. A., and Kennedy A. (1988) Nature and cause of compositional variation among the alkalic cap lavas of Mauna Kea volcano, Hawaii. *Contrib. Mineral. Petrol.* **100**, 383-397.
- West H. B., Garcia M. O., Gerlach D. C., and Romano J. (1992) Geochemistry of tholeiites from Lanai, Hawaii. *Contrib. Mineral. Petrol.* **112**, 520-542.
- White W. M. and Duncan R. A. (1996) Geochemistry and geochronology of the Society Islands: New evidence for deep mantle recycling. In *Earth Processes: Reading the Isotopic Code* (ed. A. Basu and S. Hart), *Geophys. Monogr. Ser.* **95**, pp. 183-206. AGU.
- Wright T. L. (1971) Chemistry of Kilauea and Mauna Loa lava in space and time. *USGS Prof. Paper* **735**, 40 pp.
- Wright T. L. and Helz R. T. (1987) Recent advances in Hawaiian petrology and geochemistry. *USGS Prof. Paper* **1350**, 625-640.
- Yang H.-J., Frey F. A., Garcia M. O., and Clague D. A. (1994) Submarine lavas from Mauna Kea volcano, Hawaii: Implications for Hawaiian shield-stage processes. *J. Geophys. Res.* **99**, 15,577-15,594.
- Yang H.-J., Frey F. A., Rhodes J. M., and Garcia M. O. (1996) Evolution of Mauna Kea volcano: Inferences from lava compositions recovered in the Hawaii Scientific Drilling Project. *J. Geophys. Res.* **101**, 11,747-11,767.
- Zbinden E. A. and Sinton J. M. (1988) Dikes and the petrology of Waianae Volcano, Oahu. *J. Geophys. Res.* **93**, 14,856-14,866.

APPENDIX A

ANALYTICAL METHODS

Whole rock major element concentrations were determined by X-ray fluorescence spectrometry at X-Ray Assay Laboratories (Ontario, Canada), the Radiation Center (Oregon State University), Chemex Laboratories (Sparks, Nevada), and the United States Geological Survey (Denver, Colorado). Major element analytical precision is better than 0.5%. Rare earth element analyses were performed by instrumental neutron activation at the Radiation Center. Analytical uncertainties are better than 5%, except for Ce and Nd analyses with uncertainties of 7% and 12%, respectively. Abundance of trace elements Rb, Sr, Ba, Y, and Zr were determined by X-ray fluorescence at X-Ray Assay Laboratories with analytical precision approximated at better than 10%. Trace elements Hf, Ta, Th, Ni, Cr, and Sc were analyzed by neutron activation methods at the Radiation Center and X-Ray Assay Laboratories with uncertainties better than 5%, except for Ni and Cr with uncertainties of 12% and 10%, respectively. Strontium and neodymium isotopic analyses were performed at the University of Washington using procedures described in Nelson (1995). Lead isotopic analyses at the University of Washington followed procedures described here.

LEAD ISOTOPE ANALYTICAL PROCEDURE

Sample powders

Extreme care was taken to avoid contamination. Rock chips were sawed from the interior of the rock sample and saw blade marks were removed by rotating grinder. Each rock chip

was washed with a brush and distilled water, dried, powdered in an alcohol-cleansed alumina mill, and stored in a new air-tight glass container.

Sample digestion

Chemical procedures were performed in a clean environment with reagents purified through multiple distillation. Based on estimates of sample Pb concentrations, aliquots containing 50-100 ng Pb were measured from the sample powders. Aliquots were digested in 0.25 ml 8N HNO₃ and 2 ml concentrated HF for 24 hours in an oven. The digested samples were evaporated to dryness, then taken up in 1 ml 6.2N HCl.

Ion exchange

The samples were evaporated to dryness and taken up in 600 μ l 0.5N HBr. Ion exchange columns containing 50 μ l AGI-X8 (100-200 mesh) resin were washed twice with 600 μ l 6.2N HCl followed by 100 μ l H₂O, and conditioned with 100 μ l 0.5N HBr. The sample solutions were centrifuged and the supernate loaded on the column. The column was washed twice with 100 μ l 0.5N HBr and Pb was eluted from the columns with 600 μ l 6.2N HCl. The ion exchange procedure was repeated for each sample.

Mass Spectrometry

Samples were loaded onto zone-refined outgassed Re filaments with 0.05N H₃PO₄ and silica gel. Pb isotope ratios were measured using a VG Sector mass spectrometer in static multicollector mode, and maintaining the ²⁰⁸Pb ion beam intensity between approximately 0.5 x 10⁻¹² A and 3 x 10⁻¹¹ A on a 10 ohm resistor.

Data

Assuming standard NBS 981 true values of $^{206}\text{Pb}/^{204}\text{Pb} = 16.937$, $^{207}\text{Pb}/^{204}\text{Pb} = 15.491$, $^{208}\text{Pb}/^{204}\text{Pb} = 36.721$, repeated measurements ($n=48$) yielded a mass fractionation correction of 0.12% per amu, and 2σ analytical uncertainties of ± 0.028 for $^{206}\text{Pb}/^{204}\text{Pb}$, ± 0.032 for $^{207}\text{Pb}/^{204}\text{Pb}$, and ± 0.092 for $^{208}\text{Pb}/^{204}\text{Pb}$. A procedural blank of 62 pg ($n=3$) was determined through isotope dilution. Approximately 30% of the samples received duplicate procedural analyses. Approximately 18% of the samples received duplicate procedural analyses following leaching for 60-90 minutes in 6N HCl. Results were averaged for these samples.

APPENDIX B

Section Descriptions
Waianae Volcano

Appendix B.1 Puu Heleakala North Ridge Section Description

Lualualei and Kamaileunu Members lower precaldera Heleakala (R). Nanakuli (N) magnetic polarity units				
MP	Elev (m)	Outcrop Exposure	Outcrop Description	Inter- outcrop
(+)	576	_____ <i>peak</i> _____ patchy	ves, aphyric, microplag groundmass	< 3 cover
		n.d.	nonves, sparse ol (1mm)	< 3 cover
	570	n.d.	nonves, sparse ol (1mm), abund microplag, rare px (2mm)	< 3 cover
	561			< 3 cover
	558	n.d.	two outcrops, ves, aphyric	15 grass
		_____ <i>flat run above to peak</i> _____ blocky	two outcrops, ves, aphyric	< 3 rubble
	536	thin, blocky	ves, aphyric, microplag groundmass	< 3 cover
	533	patchy	two outcrops, ves, aphyric	< 3 cover
		thin, blocky	ves (flattened), rare ol, plag/px clusters	< 3 cover
	524	blocky	four outcrops, ves, rare ol, sparse plag clusters	< 3 cover
(+)	515	thin, blocky	ves, aphyric	< 3 cover
		thin, blocky	two outcrops, ves, sparse plag clusters (3mm)	< 3 cover
	512	blocky	ves, sparse plag clusters (3mm)	< 3 rubble
		blocky	ves, 30% ol (3-6mm)	< 3 rubble
	509	blocky	ves, rare ol	< 3 cover
		blocky	ves, rare ol, microplag groundmass	6 brush
	500	blocky	two outcrops, ves, aphyric	< 3 rubble
		blocky	three outcrops, ves, aphyric	< 3 cover
		blocky	ves, sparse ol, some bladed	< 3 rubble
	(-)	491	blocky	ves, sparse ol (1mm), microplag _____ <i>slope lessens above</i> _____

Appendix B.1 (continued) Puu Heleakala North Ridge Section Description

MP	Elev (m)	Outcrop Exposure	Outcrop Description	Inter-Outcrop
(-)	488	thin, blocky	ves, sparse ol (2mm)	< 3 cover
		thin, blocky	sl ves, sparse ol, some bladed, microplag	< 3 rubble
	485	thin, blocky	two outcrops, ves (flattened), aphyric	< 3 rubble
		thin, blocky	ves, 5% ol (2-3mm), sparse microplag	< 3 cover
	482	thin, blocky	ves, abundant microplag	< 3 cover
		thin, blocky	ves, sparse ol (2-3mm)	< 3 rubble
		blocky	ves, sparse ol (1-6mm), rare px (<1mm)	< 3 cover
	475	blocky	ves, aphyric, microplag groundmass	< 3 cover
		blocky	two outcrops in grass, ves, 5% ol (2-3mm)	< 3 rubble
		blocky	ves, 5% ol (2-3mm), sparse px	< 3 rubble
	472	blocky	ves, 5% ol (2-3mm)	< 3 rubble
		blocky	nonves, aphyric	< 3 rubble
	469	blocky	three outcrops in grass, ves, aphyric	< 3 rubble
		blocky	four outcrops in grass, ves, aphyric	< 3 rubble
	442	blocky	ves, 10% ol (3mm) some bladed	< 3 rubble
		thick, blocky	ves (flattened), sparse ol, some bladed	< 3 rubble
		thick, blocky	sl ves, sparse ol (1mm)	< 3 rubble
	433	thick, blocky	sl ves, sparse ol, microplag	< 3 rubble
		thick, blocky	ves, aphyric	< 3 rubble
		thick, blocky	ves, sparse ol (2-3mm) some bladed, sparse microplag	< 3 cover
	427	n.d.	two outcrops in grass, ves, sparse ol (1mm) some bladed	< 3 cover
		n.d.	two outcrops in grass, ves, aphyric	< 3 cover
		n.d.	sl ves, aphyric	< 3 rubble
		thin, blocky	— <i>slope steepens above, change in ridge trend</i> —	< 3 cover
		blocky	nonves, aphyric	< 3 cover

Appendix B.1 (continued) Puu Heleakala North Ridge Section Description

MP	Elev (m)	Outcrop Exposure	Outcrop Description	Inter-Outcrop
(-)	418	blocky	ves, aphyric, microplag groundmass	< 3 cover
		blocky	ves, sparse ol, microplag, micropx	< 3 rubble
		blocky	six outcrops in grass, ves, aphyric, microplag groundmass	< 3 cover
		blocky	five outcrops in grass, ves, aphyric	< 3 rubble
	396	blocky	sl ves, aphyric	< 3 cover
		blocky	sl ves, sparse ol	< 3 cover
		blocky	ves, 5% ol (2mm)	< 3 cover
		blocky	ves, 15% ol (2-3mm)	< 3 cover
		blocky	ves, 5% ol (2-3mm)	< 3 cover
		blocky	ves, 5-10% ol (2-3mm)	< 3 cover
	384	blocky	<i>slope steepens above</i> ves, sparse ol, plag (1-2mm)	< 3 cover
		blocky	six outcrops in grass, ves, aphyric	< 3 cover
	378	blocky	ves, aphyric	< 3 rubble
		blocky	two outcrops in grass, ves, sparse microplag	< 3 cover
	366	blocky	three outcrops in grass, ves, aphyric	< 3 rubble
		blocky	two outcrops in grass, ves, aphyric	< 3 rubble
	360	blocky	ves, sparse ol, microplag	< 3 rubble
		blocky	ves, sparse microplag	< 3 rubble
	354	blocky	<i>flat spot</i>	< 3 cover
		thin, blocky	sl ves, sparse ol (3mm)	< 3 rubble
	351	thin, blocky	ves, sparse ol, plag (1-2mm)	< 3 rubble
		thin, blocky	ves (flattened), aphyric	< 3 cover
		thin, blocky	four outcrops in brush, sl ves, sparse microplag	< 3 rubble
		thin, blocky	ves, aphyric	< 3 rubble
	341	thin, blocky	ves, sparse plag clusters (2mm)	< 3 cover
		thin, blocky	four outcrops in brush, ves, aphyric	< 3 rubble

Appendix B.1 (continued) Puu Heleakala North Ridge Section Description

MP	Elev (m)	Outcrop Exposure	Outcrop Description	Inter-Outcrop
	332	thick, blocky	sl ves, aphyric	< 3 rubble
		thin, blocky	four outcrops in brush, ves, aphyric	< 3 rubble
		thin, blocky	two outcrops in brush, ves, sparse ol (3mm), abund microplag	< 3 cover
		thin, blocky	ves (flattened), 10% ol (2-4mm)	< 3 cover
		thin, blocky	ves, aphyric	< 3 cover
		blocky	prominent outcrop, ves, sparse ol (2mm)	< 3 cover
	317	blocky	ves, ol, abund (<1mm) sparse (1-2 mm)	< 3 rubble
	314	blocky	ves, sparse ol (3-4mm) some bladed	< 3 cover
	311	cliff	ves, sparse ol (2-3mm), sparse microplag	< 3 rubble
	305	n.d	two outcrops in grass, ves, sparse ol (1-5mm)	< 3 rubble
		n.d	three outcrops in grass, ves, sparse ol (1-2mm)	< 3 rubble
	293	thick, blocky	prominent outcrop, ves, aphyric <i>big centipede</i>	< 3 cover
		blocky	ves, aphyric <i>vertical dike cliff face</i>	< 3 cover
		thick, blocky	ves, sparse ol, plag (1-2mm)	< 3 cover
		blocky	nonves, sparse microplag	< 3 cover
		blocky	ves, sparse microplag	< 3 cover
		blocky	ves, sparse ol, microplag	< 3 cover
		blocky	ves, sparse microplag	< 3 cover
	274	blocky	ves, sparse ol, plag <i>slope steepens above</i>	< 3 rubble
		blocky	ves, sparse plag	< 3 rubble
	271	patchy	ves, aphyric	< 3 rubble
		blocky	sl ves, abund ol (<1-2mm), sparse plag (2-3mm)	< 3 rubble
		blocky	ves (flattened), sparse ol (2-3mm)	< 3 rubble
	265	blocky	ves, rare ol (2-3mm) <i>top of knob, large flat spot</i>	< 3 cover
	259	blocky	ves (flattened), sparse ol (2-3mm)	sharp

Appendix B.1 (continued) Puu Heleakala North Ridge Section Description

MP	Elev (m)	Outcrop Exposure	Outcrop Description	Inter-Outcrop
		blocky	five outcrops in grass, ves (some flattened), 10-20% ol	< 3 cover
	241	patchy	ves, sparse ol (3mm)	< 3 cover
	235	blocky	multiple outcrops in grass, ves, sparse microplag	< 3 cover
		patchy	multiple outcrops in grass, ves, sparse ol (5mm)	3 grass
	226	patchy	multiple outcrops in grass, ves, aphyric	< 3 rubble
		blocky	ves, sparse ol (1-3mm) some bladed, microplag	< 3 rubble
	219	thick, blocky	ves, sparse ol (6mm)	< 3 rubble
	216	n.d.	ves, sparse ol (2mm), abund microplag	< 3 cover
	207	cliff	ves, 3-10% ol (1-5mm)	< 3 cover
	201	blocky	ves, aphyric	< 3 rubble
	195	blocky	ves, 5% ol (2-5mm), abund microplag	< 3 rubble
	189	cliff	three outcrops, ves, 10-15% ol (3-10mm), some bladed	< 3 cover
		blocky	ves, malformed ol	3 rubble
	183	blocky	ves, sparse ol	< 3 cover
		blocky	sparse ol	< 3 rubble
		blocky	5% plag (1-3mm)	< 3 rubble
		blocky	four outcrops, rubble margins, ves, aphyric	< 3 rubble
		blocky	ves, 10-15% ol (5mm)	< 3 rubble
	162	blocky	two outcrops, rubble margin, 5% ol (1-2mm) <i>top of knob, spire</i>	< 3 cover
	152	cliff	ves, aphyric	5 grass
	149	blocky	ves, rare microplag clusters	< 3 rubble
	140	blocky	ves, 25% ol (4-6mm), up to 50% (10mm)	< 3 rubble
	125	thin, blocky	five outcrops, discolored margins, ves, sparse ol	< 3 cover
	122	blocky	ves, aphyric	< 3 cover
	116	blocky	ves, sparse ol (2mm)	< 3 rubble
	113	blocky	ves, sparse ol (2-3mm)	< 3 rubble

Appendix B.1 (continued) Puu Heleakala North Ridge Section Description

MP	Elev (m)	Outcrop Exposure	Outcrop Description	Inter-Outcrop
		thick, blocky	four outcrops in grass, ves, sparse ol (2-3mm)	< 3 cover
	101	n.d.	ves, 5% ol (2-3mm)	< 3 cover
		blocky	sparse ol, plag	< 3 rubble
	98	blocky	sparse ol (2-3mm)	< 3 rubble
		blocky	ves, aphyric	< 3 cover
		thin, blocky	four outcrops in grass, 5% ol (2-3mm)	< 3 cover
	88	blocky	aphyric	< 3 cover
		cliff	30-40% ol (up to 6mm)	< 3 cover
	82	blocky	ves, 3-5% ol (up to 5mm) some bladed <i>upper end of rock fence</i>	< 3 cover
	73	cliff	ves, 3-5% ol (up to 5mm) some bladed	< 3 rubble
		blocky	ves, rare plag, ol (1mm)	< 3 rubble
	67	blocky	ves, aphyric	< 3 rubble
		blocky	ves, aphyric	< 3 rubble
		cliff	ves, sparse microplag, ol	< 3 rubble
	61	n.d.	ves, aphyric	< 3 cover
		n.d.	ves, aphyric	< 3 rubble
(-)	55	cliff	ves, 5% ol (2-5mm)	< 3 cover
		blocky	ves, aphyric	< 3 cover
	49	blocky	5% microplag	< 3 cover
		blocky	ves, sparse ol (1-3mm)	< 3 cover
	43	blocky	sparse tiny ol	< 3 cover
	37	blocky	ves, 5% ol (3mm) some bladed	< 3 cover
		blocky	ves, aphyric	< 3 cover
(-)		blocky	ves, aphyric	< 3 cover

MP = magnetic polarity, Elev = elevation, n.d. = not described, ves = vesicular, abund = abundant
 ol = olivine, px = pyroxene, plag = plagioclase. Inter-outcrop measured in meters

Appendix B.2 Nanakuli Ridge Section Description — lower section

Kamaileunu Member upper precaldera Nanakuli (N) magnetic polarity unit				
MP	Elev (m)	Outcrop Exposure	Outcrop Description	Inter- Outcrop
(+)	546	thin, blocky	————— <i>peak, elevation equivalent to unconformity</i> ————— multiple outcrops, ves, aphyric, microplag groundmass	< 3 cover
		thin, blocky	eight outcrops in grass, ves, aphyric, microplag groundmass	< 3 cover
	515	thin, blocky	————— <i>east into saddle and back up</i> ————— ten outcrops in grass, ves, aphyric, microplag groundmass	< 3 cover
	497	patchy	————— <i>long very low slope above</i> ————— multiple thin outcrops, ves, aphyric, microplag groundmass	< 3 cover
	488	thin, blocky	five outcrops, ves, aphyric, microplag groundmass	< 3 cover
	485	thin, blocky	five outcrops, ves, aphyric, microplag groundmass	< 3 cover
	475	thin, blocky	five outcrops, ves, aphyric, microplag groundmass	< 3 rubble
	469	thick, blocky	ves, aphyric	< 3 cover
	466	cliff	thick rubble top, ves, aphyric	< 3 cover
	457	thin, blocky	two outcrops, ves, aphyric	< 3 rubble
		thin, blocky	ves, sparse plag (2mm)	< 3 cover
	454	blocky	three outcrops in grass, ves, aphyric, microplag groundmass	< 3 cover
		blocky	ves, sparse ol (2-3mm), microplag groundmass	< 3 rubble
		blocky	ves, sparse plag (1-2mm)	< 3 rubble
		blocky	ves, sparse plag, ol, some bladed	< 3 rubble
		thick, blocky	ves, sparse plag (2-3mm)	6 grass
		blocky	four outcrops in grass, ves, aphyric, microplag groundmass	< 3 cover
	430	n.d.	————— <i>slope steepens above</i> ————— ves, sparse malformed plag, microplag groundmass	< 3 cover
		blocky	ves, aphyric	reddened
		blocky	ves, sparse plag clusters (2mm), ol (3mm)	< 3 cover
	424	patchy	ves, aphyric, microplag groundmass	< 3 cover
		thin, blocky	three outcrops, ves, 10% plag/px clusters (2-3mm)	sharp
		blocky	ves, sparse microplag, rare ol	< 3 cover
	418	blocky	nonves, aphyric	< 3 cover

Appendix B.2 (continued) Nanakuli Ridge Section Description — lower section

MP	Elev (m)	Outcrop Exposure	Outcrop Description	Inter-Outcrop
	411	patchy	multiple thin outcrops, ves, rare plag/px clusters	< 3 rubble
		patchy	multiple outcrops, ves, sparse plag/px clusters (2-3mm)	< 3 rubble
	405	thick, blocky	ves, 20% ol (3-5mm)	< 3 cover
		thick, blocky	ves, aphyric	< 3 cover
	396	patchy	lots of thin outcrops, ves, aphyric	< 3 cover
	393	patchy	rubble, ves, aphyric	< 3 cover
	390	blocky	ves, sparse plag, rare ol <i>long lesser slope above</i>	< 3 cover
	384	patchy	ves, aphyric	5 grass
		patchy	multiple outcrops in grass, ves, aphyric	5 grass
	366	blocky	ves, aphyric	5 grass
		blocky	ves, aphyric	6 grass
		patchy	multiple outcrops in grass, ves, rare ol, some bladed	< 3 cover
	351	blocky	two outcrops in grass, ves, aphyric	< 3 rubble
		thick, blocky	ves (flattened), sparse tiny ol, microplag	3 rubble
(+)	341	cliff	prominent outcrop, ves, rare ol	< 3 cover
		blocky	ves, aphyric	6 grass
		blocky	two outcrops, discolored rubble margin, ves, aphyric	< 3 rubble
	329	patchy	rubble, ves, sparse ol (4mm)	< 3 cover
		thick, blocky	prominent outcrop, ves, sparse ol (4mm)	< 3 cover
(+)	323	blocky	ves, 50% ol (3-4mm)	< 3 cover
	320	thick, blocky	prominent outcrop, ves (flattened), sparse ol	< 3 cover
	314	thin, blocky	ves, sparse tiny ol	< 3 cover
		blocky	ves, 5% ol (4-5mm)	< 3 cover
	308	blocky	ves, rare ol	< 3 cover
	302	patchy	rubble in grass, aphyric	3 grass
(+)		cliff	n.d.	< 3 cover

Appendix B.2 (continued) Nanakuli Ridge Section Description — lower section

MP	Elev (m)	Outcrop Exposure	Outcrop Description	Inter-Outcrop
(T)	285	thin, blocky	multiple outcrops, ves, rare ol, px (<1mm)	< 3 cover
	274	patchy	multiple outcrops in grass, ves, aphyric	< 3 cover
(T)		thick, blocky	ves, 15% ol (5mm)	< 3 cover
	265	thick, blocky	ves, 5% ol (5mm)	3 grass
(T)	262	patchy	ves (flattened), aphyric	9 grass
	259	n.d.	sl ves, sparse microplag	9 grass
	253	thick, blocky	sl ves (flattened), aphyric	< 3 rubble
		cliff	ves, sparse microplag clusters (3mm), ol	9 grass
(-)	244	thick, blocky	ves, sparse microplag clusters (3mm), ol	< 3 cover
		thin, blocky	ves, sparse ol, plag	< 3 cover
		thin, blocky	ves, 5% plag clusters (3-5mm), ol (1-2mm)	< 3 rubble
		thin, blocky	two outcrops, sharp discolored margin, sparse microplag, ol	sharp
		thin, blocky	ves, aphyric	< 3 cover
(-)	238	cliff	ves, sparse ol (3mm), plag (1mm)	3 grass
	235	cliff	sl ves, 20-25% ol (3mm), microplag	3 grass
(-)	232	thin, blocky	ves, sparse ol (1mm)	< 3 cover
		thin, blocky	ves, aphyric	< 3 cover
		thin, blocky	ves, aphyric, microplag groundmass	< 3 cover
		thin, blocky	ves, sparse plag (1mm)	sharp
		thin, blocky	ves, sparse ol	sharp
		thin, blocky	ves, aphyric	sharp
	226	thin, blocky	ves, aphyric, microplag groundmass	3 grass
		thin, blocky	four outcrops, sharp discolored margins, ves, rare tiny ol	sharp
		thin, blocky	ves, aphyric	< 3 rubble

Appendix B.2 (continued) Nanakuli Ridge Section Description — lower section

MP	Elev (m)	Outcrop Exposure	Outcrop Description	Inter- Outcrop
		thin, blocky	multiple flows, ves, rare ol (<1mm)	reddened < 3 cover
		thin, blocky	multiple flows, ves, rare ol, some bladed	
(-)	213	cliff	sl ves, sparse ol, some bladed (<1mm)	

Appendix B.3 Ulehawa Ridge Section Description

Kamaileunu Member intracaldera Paheehee (N), Kepauula (R) magnetic polarity units				
MP	Elev (m)	Outcrop Exposure	Outcrop Description	Inter- Outcrop
(-)	686	blocky	————— <i>top of unnamed peak</i> ————— nonves, aphyric, rare microplag	
	683	thick, blocky	multiple outcrops, 5% plag, plag/px clusters, ol, px (3-4mm)	< 3 rubble
	671	thick, blocky	two outcrops, ves, sparse plag/px clusters	< 3 rubble
	661	blocky	nonves, aphyric	< 3 rubble
	658		<i>top of westernmost small peak, move to same elevation on large, unnamed peak to east</i>	
	637	thick, blocky patchy	four outcrops, nonves, aphyric, mostly microplag groundmass nonves, 30% plag (to 10mm), microplag groundmass	< 3 rubble < 3 rubble
	628	patchy	nonves, aphyric	< 3 cover
		thin, blocky	two outcrops, sl ves, sparse ol (3-4mm), plag	< 3 cover
		blocky	three outcrops, ves, aphyric	< 3 cover
	610	blocky	ves, 40-50% ol, microplag groundmass	< 3 rubble
	607	patchy	ves, sparse plag/px clusters (1-3mm)	< 3 cover
		patchy	ves, rare plag (to 3mm), microplag groundmass	< 3 rubble
	588	blocky	ves, 5-10% plag/px clusters, light gray color	< 3 cover
	582	blocky	abund ol, some bladed (2-5mm), small plag	< 3 cover
	567	blocky	————— <i>top of main pitch, dog-leg to east</i> ————— outcrops in grass, ves, sparse plag/px clusters, rare ol	< 3 cover
	552	n.d.	outcrops in grass, sl ves, rare plag, ol, microplag groundmass	< 3 cover
	543	n.d.	ves, 20% plag, plag clusters	< 3 cover
	540	n.d.	multiple outcrops in grass, ves, sparse plag (2mm), ol, px	< 3 rubble
	530	blocky	ves, sparse plag (1-2mm)	5 grass
		blocky	ves, sparse plag (1-2mm), microplag groundmass	5 grass
		blocky	two outcrops in grass, ves, 10% plag (1-3mm), ol (2-4mm)	< 3 rubble
	518	thin, blocky	ves, aphyric, microplag groundmass	< 3 cover

Appendix B.3 (continued) Ulehawa Ridge Section Description

MP	Elev (m)	Outcrop Exposure	Outcrop Description	Inter-Outcrop
	515	blocky	ves. 10% plag (1-3mm), rare ol	< 3 cover
	509	blocky	ves, 10% plag (1-3mm), ol (2-4mm), microplag groundmass	< 3 cover
		blocky	ves, 10% plag (1-3mm), ol (2-4mm), microplag groundmass	5 grass
		blocky	ves, 5% plag, plag/px clusters (2-5mm), microplg groundmass	5 grass
		blocky	ves, 5% plag, plag/px clusters (2-5mm), microplg groundmass	6 grass
	488	patchy	ves, aphyric	< 3 cover
	485	blocky	ves, plag, plag clusters (3-6mm), rare ol <i>top of prominent knob</i>	< 3 cover
	475	thick, blocky	20% plag, (5-10mm)	< 3 cover
	466	thick, blocky	sl ves, nearly aphyric, rare plag	< 3 cover
	460	thick, blocky	20% plag (3-6mm)	< 3 cover
	451	thick, blocky	20% plag (2-4mm), rare px	< 3 cover
	442	thick, blocky	nearly aphyric, rare plag	< 3 cover
	427	thick, blocky	multiple outcrops in grass slope, 5-10% plag (2-5mm)	12 grass
	415	thick, blocky	prominent outcrop in grass, rare plag, nearly aphyric	6 grass
	405	n.d.	outcrop in grass, 5% malformed plag, microplag groundmass <i>top of knob</i>	< 3 cover
	393	cliff	sparse plag (2mm), microplag groundmass	18 grass
	384	n.d.	ves, sparse plag/px clusters (2mm) <i>top of knob</i>	< 3 cover
	366	blocky	outcrop in grass slope, 40% ol	< 3 cover
	351	n.d.	outcrop in grass slope, 40% ol <i>top of large knob</i>	9 grass
	344	cliff	40% ol (2-6mm), sparse px	< 3 rubble
	335	blocky	ves, sparse ol, rare large plag	< 3 cover
	320	thick, blocky	sl ves, rare plag (10mm)	< 3 cover
	317	thick, blocky	sl ves, rare plag (10mm) <i>top of knob</i>	< 3 cover
	290	thick, blocky	sl ves, rare plag (10mm) <i>top of knob</i>	< 3 cover
(-)	277	cliff	ves, nearly aphyric	< 3 cover
(-)	253	n.d.	multiple outcrops, ves, nearly aphyric, rare plag (to 10mm)	< 3 rubble
(-)	250	blocky	ves, 10% plag, ol, px	3 rubble

Appendix B.3 (continued) Ulehawa Ridge Section Description

MP	Elev (m)	Outcrop Exposure	Outcrop Description	Inter-Outcrop
(+)	247	blocky	sl ves, rare plag, plag/px clusters (to 8mm), ol <i>top of knob</i>	< 3 cover
		n.d.	ves, rare ol, px, plag, nearly aphyric	
	244			< 3 rubble
	241	n.d.	ves, 30% ol, px, plag (2-3mm)	
		n.d.	ves, 5% plag (1-3mm), sparse ol <i>top of knob</i>	< 3 cover
(+)	232	cliff	ves, 30% ol, px, plag (2-3mm) <i>single thin, ves, px flow</i>	< 3 cover
	226	patchy	mostly grass, ves, 10% plag (3-10mm), sparse px (2-3mm)	< 3 cover
	201	n.d.	sl ves, 10% plag (3-10mm), sparse px (2-3mm) <i>top of knob</i>	< 3 cover
	189	cliff	sl ves, 25% plag (3-5mm)	< 3 cover
	162	thick, blocky	prominent outcrop, ves, 30% ol, px (3mm, up to 10mm)	< 3 rubble
	155	n.d.	ves (flattened), 5% oriented plag (5-10mm), sparse ol	< 3 cover
	149	n.d.	ves, 5-10% plag (1-10mm), sparse ol, px	< 3 cover
	140	patchy	mostly cover, rubble, ves, 40-50% plag (5-10mm)	< 3 cover
		patchy	mostly cover, rubble, ves, 40% plag (5-25mm)	< 3 cover
		thin, blocky	nonves, tiny plag	< 3 cover
	131	patchy	mostly cover, rubble, ves, 40% plag (5-25mm)	< 3 cover
	113			12 grass
	101	thick, blocky	30% tiny plag, rare ol (2mm)	
	95	thick, blocky	sl ves (flattened), 5% ol (<1mm)	< 3 cover
	82			< 3 cover
	70	n.d.	ves, 20% ol (2mm), cut by thick vertical dike	
	61	cliff-upper	<i>pumphouse</i>	9 grass
				< 3 rubble
(+)	43	cliff-lower	ves, rare ol <i>at roadcut</i>	

Appendix B.4 Puu Paheehee North Ridge Section Description

Kamaileunu Member intracaldera Paheehee (N), Kepauula (R) magnetic polarity units				
MP	Elev (m)	Outcrop Exposure	Outcrop Description	Inter- Outcrop
	219		<i>peak</i>	
(-)	216	n.d.	ves, 10% plag (3mm)	< 3 cover
	213	n.d.	ves, 20% plag (3mm)	< 3 cover
		n.d.	ves, 10% plag (3mm)	< 3 cover
	195	n.d.	ves, 5-10% plag (3mm)	< 3 cover
		n.d.	ves, aphyric	< 3 cover
		n.d.	nonves, 5-10% plag (3mm)	< 3 cover
	189	patchy	<i>flat spot, graffiti "Kaeo"</i>	< 3 cover
	186	patchy	rubble, aphyric	< 3 cover
	177	patchy	rubble, aphyric	< 3 cover
	171	blocky	ves, aphyric	< 3 cover
(-)	155	blocky	<i>big cactus</i>	< 3 cover
		blocky	multiple outcrops, large plag/px clusters	< 3 cover
(-)		cliff	ves, 20% plag/px clusters (up to 50mm)	< 3 rubble
(-)	131	n.d.	aphyric, microplag groundmass	< 3 cover
		n.d.	40% large plag	< 3 cover
(-)	128	blocky	ves, aphyric, microplag groundmass	< 3 cover
		blocky	ves, sparse large plag, microplag groundmass	< 3 cover
	125	blocky	ves, aphyric, microplag groundmass	< 3 cover
	119	patchy	ves, 40% plag/px clusters (up to 25mm)	< 3 rubble
	116	blocky	three outcrops, rubble margins, ves, rare plag, ol	< 3 rubble
	113	n.d.	ves, 20% ol (1 - rare 6mm), plag clusters (2 - rare 10mm)	< 3 cover
	110	patchy	ves, 15% small plag, rare ol	< 3 cover
		n.d.	ves, sparse small ol, plag	< 3 cover
		n.d.	sparse ol, rare plag/px clusters	< 3 cover
		n.d.	ves, aphyric	< 3 cover

Appendix B.4 (continued) Puu Paheehē North Ridge Section Description

MP	Elev (m)	Outcrop Exposure	Outcrop Description	Inter-Outcrop
(-)	101	blocky	ves, 15% ol (3-10mm), sparse plag, plag/px clusters	< 3 rubble
(+)	95	cliff	patchy at top, ves, sparse plag, some clusters, ol	< 3 rubble
(+)	79	blocky	multiple outcrops, sparse plag/px clusters (3-5mm), ol (2mm)	< 3 cover
	73	cliff	ves, rare large plag, ol (5mm)	< 3 rubble
(+)	64	cliff	ves, 20% ol (1-2mm, some 6-15mm), px	< 3 rubble
	58	cliff	ves, 10% ol, sparse px, rare plag (2-4mm)	< 3 cover
(+)	52	patchy	multiple outcrops in grass, ves, abund ol (1-3mm)	< 3 cover
	49	blocky	nonves, 5-10% ol (1-3mm), rare plag (to 6mm)	sharp
		cliff-upper	ves, aphyric	< 3 cover
		cliff-main	ves, 5% ol, plag, px (2mm)	< 3 cover
	37	cliff-lower	ves, 20% ol, plag, plag clusters, px (3-6mm)	sharp
	34	patchy	multiple outcrops, ves, 5% plag/px clusters (2-3mm)	sharp
		patchy	two outcrops in grass, ves, 10-15% plag	sharp
	24	blocky	ves, rare ol, plag, px (3mm)	< 3 rubble
	18	blocky	ves, rare ol, plag, px (3mm)	< 3 rubble
	12	blocky	ves, 10% plag (3-4mm), ol (2mm), sparse px (3mm)	< 3 rubble

Appendix B.5 Kamaileunu Ridge Section Description

Kamaileunu Member intracaldera, Palehua Member alkalic cap Paheehee (N), Kamaile transitional, Kepauula (R), Kaala (N) magnetic polarity units				
MP	Elev (m)	Outcrop Exposure	Outcrop Description	Inter-Outcrop
	927	_____	_____ <i>small unnamed peak</i> _____	
(+)	899	thick, blocky	nonves, sparse plag (10-20mm), microplag groundmass	
	893	_____	_____	< 3 cover
(+)	887	thick, blocky	n.d.	
	875	_____	_____	< 3 cover
(+)	875	thick, blocky	nonves, aphyric	
	869	_____	_____	< 3 cover
(-)	869	thick, blocky	nonves, aphyric	
	856	_____	_____ <i>long shallow slope</i> _____ <i>east into saddle and back up (40' thick reddened weathered horizon in saddle)</i>	< 3 cover
	820	_____	_____ <i>small unnamed peak east of Puu Kepauula</i> _____	
	802	n.d.	sl ves, aphyric, light-gray color	
	802	blocky	saddle rock, ves, 15% plag (up to 25mm)	< 3 cover
	799	_____	_____ <i>contour northeast to saddle, dog-leg east</i> _____	< 3 cover
(-)	799	blocky	multiple outcrops, sl ves, aphyric, microplag groundmass	
	783	_____	_____ <i>slope steepens above to Puu Kepauula</i> _____	< 3 cover
	783	n.d.	multiple outcrops in grass, ves, 10% plag, ol, px (3-6mm)	
(-)	783	n.d.	multiple outcrops in grass, sparse small plag, ol, px	< 3 cover
	765	_____	_____	< 3 cover
	765	thin, blocky	six outcrops, rubble margins, ves, 10% plag, ol, px (3-6mm)	
	750	_____	_____ <i>top of knob, trees</i> _____	< 3 cover
	750	blocky	multiple outcrops, ves, 15% plag (micro to 3mm)	
	735	_____	_____	thin rubble
	735	blocky	ves, 10% plag, plag/px clusters (3-6mm), sparse ol, px	
	722	_____	_____	< 3 rubble
(-)	722	patchy	sparse plag (1-3mm), microplag groundmass	
	722	_____	_____ <i>top of knob</i> _____	< 3 cover
	722	blocky	three outcrops, thin rubble margins, rare plag, px	
	722	_____	_____	3 rubble
	722	thin, blocky	sparse plag (1-2mm)	
	722	_____	_____	< 3 rubble
	722	blocky	four outcrops in grass, sl ves, aphyric, microplag groundmass	
	722	_____	_____	< 3 rubble
	722	blocky	six outcrops in grass, sl ves, aphyric, microplag groundmass	
	722	_____	_____	< 3 rubble
	722	n.d.	multiple outcrops in grass, ves, aphyric	
	652	_____	_____ <i>slope steepens above</i> _____	< 3 cover
	652	patchy	ves, sparse plag/px clusters (2-6mm), microplag groundmass	
	652	_____	_____	< 3 cover
	652	patchy	ves, sparse ol (2-3mm)	
	640	_____	_____ <i>top of prominent knob, large flat spot</i> _____	< 3 cover
(-)	640	blocky	sparse plag, plag clusters, ol (3mm), microplag groundmass	
	637	_____	_____	reddened
	637	patchy	rubble, ves, 10% ol (3-5mm), rare plag	
	628	_____	_____	< 3 cover

Appendix B.5 (continued) Kamaileunu Ridge Section Description

MP	Elev (m)	Outcrop Exposure	Outcrop Description	Inter-Outcrop
(-)	610	blocky	five outcrops, thin rubble margins, sparse plag/px clusters, ol <i>slope steepens above</i>	reddened
	600	patchy	sl ves, sparse plag, plag/px clusters (3mm), rare ol (2mm)	reddened
		blocky	two outcrops, ves, sparse plag, plag/px clusters, rare ol	thin rubble
	585	patchy	sl ves, sparse plag, plag/px clusters (3mm), rare ol (2mm)	thin rubble
		blocky	nonves, 40% ol, px (3-4mm, up to 15mm) <i>top of knob</i>	< 3 cover
		blocky	ves, aphyric	reddened
		blocky	ves, sparse plag, plag clusters (1mm), microplag groundmass	thin rubble
		blocky	three outcrops in brush, thin rubble margins, ves, aphyric	thin rubble
		thick, blocky	three outcrops in brush, thin rubble margins, ves, aphyric	reddened
		thick, blocky	ves, 10% plag/px clusters (2-3mm)	reddened
		blocky	ves, 10% plag/px clusters (2-3mm), microplag groundmass	< 3 rubble
	549	blocky	ves, sparse plag, plag/px clusters (1-3mm), ol (5-8mm)	< 3 rubble
		blocky	two outcrops in brush, ves, sparse ol	< 3 cover
		patchy	ves, sparse plag, plag clusters (1-3mm) <i>top of prominent knob, large flat spot</i>	< 3 cover
thick, blocky		ves, 10% ol (1-5mm), rare plag (3mm)	< 3 cover	
540		n.d.	ves, sparse plag/px clusters (10mm), rare ol	< 3 cover
530		n.d.	ves, sparse ol (1-2mm), plag/px clusters (2mm), microplag	< 3 cover
		n.d.	ves, aphyric, microplag groundmass	< 3 cover
		n.d.	ves, 10% ol (2mm), plag (3-5mm), rare px	reddened
		509	thin, blocky	multiple outcrops, long grass slope, ves, abund microplag
thick, blocky			ves, 15% ol	< 3 rubble
503	blocky	ves, aphyric, microplag groundmass <i>small flat spot</i>	< 3 cover	
	blocky	multiple outcrops, 30% ol (2mm), sparse px, plag (3-5mm)	< 3 cover	
	thick, blocky	30% ol (2mm), sparse px, plag (3-5mm)	< 3 cover	
494	thin, blocky	40% ol, px (3mm)	< 3 cover	
491	blocky	<i>top of small knob</i> 30-50% plag, plag clusters (3-4mm)	< 3 cover	
(-)				< 3 cover

Appendix B.5 (continued) Kamaileunu Ridge Section Description

MP	Elev (m)	Outcrop Exposure	Outcrop Description	Inter-Outcrop
(-)	451	thick, blocky	30-50% plag, plag clusters (3-4mm)	< 3 cover
		thick, blocky	10% plag, plag clusters (3-4mm), sparse ol (2mm)	< 3 rubble
	448	thick, blocky	ves, aphyric	reddened
		blocky	multiple outcrops, 25% plag/px clusters (10-20mm)	< 3 cover
	439	thin, blocky	ves, rare ol	< 3 cover
		patchy	ves, nearly aphyric	< 3 cover
	430	blocky	nonves, sparse ol, plag	< 3 cover
		patchy	_____ <i>slope steepens above</i> _____	< 3 cover
		patchy	rubble, ves, sparse ol	< 3 cover
	421	patchy	ves, sparse ol (3mm)	reddened
		n.d.	ves, sparse plag clusters (2mm), microplag groundmass	reddened
		patchy	multiple outcrops in brush, ves, aphyric	< 3 cover
	402	blocky	_____ <i>small knob, slope steepens above</i> _____	< 3 cover
		blocky	nonves, rare plag (4mm)	< 3 rubble
	399	patchy	ves, aphyric, microplag groundmass	< 3 cover
		thin, blocky	three outcrops, ves, 25% plag/px clusters (10mm)	reddened
		thin, patchy	ves, aphyric, microplag groundmass	< 3 cover
		blocky	ves, 25% plag/px clusters (10mm)	< 3 cover
		patchy	ves, aphyric, microplag groundmass	< 3 cover
		blocky	ves, variable: plag clusters and nearly aphyric	< 3 cover
	387	patchy	ves, 10% plag/px clusters (10mm)	< 3 cover
		thin, blocky	_____ <i>top of small knob</i> _____	< 3 cover
		thin, blocky	multiple outcrops, ves, aphyric, sparse plag clusters	< 3 cover
		thin, blocky	ves, aphyric	< 3 cover
		blocky	ves, sparse plag clusters (2-3mm)	< 3 cover
		blocky	three outcrops, ves, aphyric, microplag groundmass	cavernous
357	blocky	multiple outcrops, ves, aphyric, rare px	< 3 cover	
344	thick, blocky	_____ <i>small knob, dike face starts steeper slope above</i> _____	< 3 rubble	
	blocky	ves (flattened), rare plag (20mm), rare px (1mm)	< 3 rubble	
332	blocky	five outcrops, ves, aphyric	< 3 cover	
		_____ <i>small flat spot</i> _____	< 3 cover	

Appendix B.5 (continued) Kamaileunu Ridge Section Description

MP	Elev (m)	Outcrop Exposure	Outcrop Description	Inter-Outcrop
(-)		blocky	two outcrops, ves, sparse plag, plag/px clusters (10-15mm)	< 3 cover
		patchy	ves, plag/px clusters (20mm)	< 3 cover
(T)	326	patchy	nonves, microplag groundmass (may be sill)	< 3 cover
		blocky	ves, large plag, microplag groundmass	< 3 cover
	320	patchy	ves, sparse plag (4-5mm), microplag groundmass	< 3 cover
		blocky	ves, 10% plag (10-15mm), microplag groundmass	< 3 rubble
(T)	314	thin, blocky	multiple outcrops in grass, ves, 20% plag clusters (20mm)	< 3 cover
		blocky	thin outcrops, ves, aphyric, microplag groundmass	< 3 cover
	311	thin, blocky	multiple outcrops in grass, ves, 20% plag clusters (20mm)	reddened
		patchy	ves, rare small ol, px, microplag groundmass	< 3 rubble
	305	thick, blocky	ves, rare small ol, px, microplag groundmass <i>top of prominent knob, little spire</i>	< 3 cover
		cliff	30% plag/px clusters (20mm), microplag groundmass	< 3 cover
	290	blocky	aphyric	< 3 cover
		patchy	ves, 30% plag (20mm), microplag groundmass	< 3 cover
		cliff top	ves, aphyric	< 3 cover
		cliff-mid	rubbly, cavernous	< 3 cover
(T)	277	cliff-base	sl ves, sparse plag, ol, px (1-2mm), microplag groundmass	reddened
		n.d	thin outcrops in grass, 5% plag, ol, px (2-3mm)	6 grass
	265	thin, blocky	multiple outcrops in grass, aphyric, microplag groundmass	3 grass
		thick, blocky	nonves, aphyric (may be dike face)	
	256	cliff	<i>top of prominent knob</i> ves, sparse plag, microplag groundmass	< 3 cover
		n.d	six thin outcrops in grass, ves, sparse plag (6mm)	< 3 cover
(T)	228	thick, blocky	multiple outcrop, ves, sparse plag, ol, microplag groundmass	< 3 rubble
		n.d.	15% plag laths, clusters (3mm), microplag groundmass	< 3 rubble
(+)	226	thick, blocky	20% plag/px clusters (6-10mm)	< 3 cover

Appendix B.5 (continued) Kamaileunu Ridge Section Description

MP	Elev (m)	Outcrop Exposure	Outcrop Description	Inter-Outcrop
(+) 204		blocky	multiple outcrops, ves, 20% plag/px cluster (6-10mm), laths <i>top of prominent knob</i>	< 3 cover
		cliff-top	ves, 5-10% ol, px, plag (2-3mm)	< 3 rubble
		cliff-base	ves, 10% plag (2-3mm)	< 3 cover
(+) 189		blocky	multiple outcrops in grass, 10% malformed plag (3-4mm) <i>slope steepens above</i>	< 3 cover
		186	patchy	multiple outcrops in grass, ves, some plag/px clusters (4mm)
171		thick, blocky	ves, 10-15% plag (6mm), plag/px clusters (to 15mm)	< 3 cover
		168	patchy	ves, 10% plag (1-2mm), microplag groundmass
137		blocky	three outcrops in grass, 30% ol <i>top of lowermost prominent knob</i>	< 3 cover
		cliff-top	multiple outcrop, ves, 5% ol (5 mm), plag/px cluster (5mm)	< 3 cover
		cliff-main	multiple outcrops, ves, nearly aphyric	< 3 cover
		cliff-base	multiple outcrops, ves, 10% plag (10mm), some clusters <i>slope steepens above</i>	< 3 cover
113		patchy	multiple outcrops in grass, 20% plag/px clusters (5-10mm)	< 3 cover
		cliff	sl ves, 5% plag (3mm), plag/px clusters (5mm), ol (3-5mm)	thin rubble
95		blocky	ves, sparse plag, px (2-4mm), microplag groundmass	sharp
		patchy	5% plag/px clusters (4-5mm), sparse ol (1-2mm)	sharp
		n.d.	ves, sparse plag, ol (4mm), microplag groundmass	3 grass
		blocky	ves, sparse malformed plag, microplag groundmass	< 3 rubble
95		blocky	ves, 5% malformed plag (1-3mm), microplag groundmass	< 3 rubble

Appendix B.6 Nanakuli Ridge Section Description - upper section

Palehua Member alkalic cap Kaala (N) magnetic polarity unit				
MP	Elev (m)	Outcrop Exposure	Outcrop Description	Inter-Outcrop
	780	_____	_____ <i>peak of large weathered knob, ghosts of plag</i> _____	
	777	_____	_____ <i>peak of large weathered knob, ghosts of ol? px?</i> _____	
	765	blocky	sl ves, sparse weathered small ol? px?	brush
		blocky	sl ves, sparse weathered ol? px? (2-4mm)	< 3 cover
	750	blocky	two outcrops, ves, abund microplag	< 3 cover
		blocky	ves, aphyric	< 3 cover
		blocky	sl ves, rare small plag, px	< 3 cover
	741	blocky	sl ves, aphyric	< 3 cover
		blocky	nonves, aphyric	< 3 cover
	732	thick, blocky	nonves, aphyric	< 3 cover
	725	blocky	nonves, aphyric	< 3 cover
	722	_____	_____ <i>top of knob</i> _____	< 3 cover
		cliff	nonves, aphyric	< 3 cover
	719	blocky	three outcrops in grass, nonves, aphyric	< 3 cover
		blocky	nonves, rare tiny ol? px?	< 3 cover
	704	blocky	three outcrops in grass, nonves, aphyric	< 3 cover
		n.d.	_____ <i>flat area, brush and grass</i> _____	< 3 cover
	686	thick, blocky	nonves, aphyric	< 3 cover
(+)	674	thick, blocky	nonves, 30-40% plag/px clusters (to 20mm)	< 3 cover
	658	thick, blocky	two outcrops, rubble margin, nonves, aphyric	< 3 cover
		cliff-upper	_____ <i>top of knob</i> _____	< 3 cover
		cliff-lower	ves, aphyric	< 3 cover
		cliff-lower	nonves, aphyric	< 3 cover
	646	thick, blocky	sl ves, sparse plag (1mm)	9 rubble
	637	thick, blocky	multiple outcrops in brush, nonves, aphyric	reddened
		blocky	_____ <i>pitch steepens above in brush and tall grass</i> _____	
	625	blocky	nonves, aphyric	< 3 rubble
		patchy	three outcrops, nonves, plag/px clusters, microplg groundmass	< 3 cover
	610	thin, blocky	_____ <i>large patch of brush, shallow-sloped area</i> _____	< 3 cover
(+)		thin, blocky	three outcrops, ves, 40% plag/px clusters (to 20mm), rare ol	< 3 cover
		n.d.	ves, sparse ol (3mm), rare plag, px	< 3 cover

Appendix B.6 (continued) Nanakuli Ridge Section Description - upper section

MP	Elev (m)	Outcrop Exposure	Outcrop Description	Inter-Outcrop
(+)	600	blocky	two outcrops in brush, ves, sparse plag/px clusters, ol (2mm)	< 3 cover
	594	thin, blocky	multiple outcrops in grass, ves, 5-10% plag clusters	< 3 rubble
		thin, blocky	ves, sparse large plag/px clusters, ol, microplag groundmass	< 3 rubble
		blocky	ves, sparse large plag/px clusters, ol, microplag groundmass	< 3 rubble
		thin, blocky	three outcrops, thin rubble margins, ves, aphyric	< 3 rubble
		blocky	ves, aphyric	< 3 cover
	579	thin, blocky	sl ves, sparse plag, plag/px clusters (1-3mm)	< 3 rubble
		thin, blocky	ves, aphyric	< 3 cover
		blocky	two outcrops, rubble margin. ves, aphyric	< 3 rubble
	570	blocky	ves, sparse plag, plag/px clusters (3-4mm)	sharp
		blocky	three outcrops, rubble margins, ves, aphyric	
		543		<i>unconformity - 3 ft thick, strongly weathered, orange-yellow stained, platy dark material, abund microplag</i>

APPENDIX C

**Sample Descriptions
East Molokai Volcano**

Appendix C.1 Haupu Section Sample Description

Sample	Data Table 5.1	Elev (M)	Description
90HB-1000	yes	305	highly ves. 10-20% 2mm plag, px clusters in very fine groundmass
90HB-960	yes	293	nonves. 30% 5mm plag, px, ol cluster in coarse feldspathic groundmass
90HB-850	yes	259	slightly ves, coarse feldspathic groundmass
90HB-1	yes	216	ves, scattered small plag, px clusters in coarse feldspathic groundmass
90KB-3, 4	yes	6	slightly ves, fine feldspathic groundmass

Elev = elevation. ves = vesicular. ol = olivine. px = pyroxene. plag = plagioclase

Appendix C.2 Hakaano Section Sample Description

Sample	Data Table 5.1	Elev (m)	Description
Upper Hakaano Section			
#66	yes	323	n.d.
#62	yes	262	n.d.
#60	yes	250	n.d.
#58	yes	241	n.d.
#55	yes	218	n.d.
#54	yes	210	n.d.
#49A	yes	177	n.d.
#45	yes	140	n.d.
Lower Hakaano Section			
93HAK-30	yes	122	slightly ves, aphyric
93HAK-31		119	no t/s. ves, aphyric
93HAK-32	yes	113	no t/s. slightly ves, aphyric
93HAK-1		107	no t/s. slightly ves, scattered ol, plag, px
93HAK-2	yes	98	no t/s. slightly ves, scattered ol, plag, px
93HAK-3		94	no t/s. ves, 30% 1-3mm, some up to 8mm ol
93HAK-4		93	no t/s. ves, scattered plag
93HAK-5	yes	88	no t/s. ves, 5% 3-5 mm plag clusters with small ol, px
93HAK-6		75	no t/s. ves, scattered 1-5mm malformed plag
93HAK-7		68	no t/s. ves, 10% 2mm plag clusters with small ol, px
93HAK-8	yes	67	no t/s. slightly ves, aphyric
93HAK-9		55	no t/s. ves, aphyric
93HAK-12		53	no t/s. ves, 25% 3-5mm plag clusters with small ol, px
93HAK-13		52	no t/s. 5-10% 3-5mm plag clusters, some with small ol, px
93HAK-14		47	no t/s. ves, 40% 1-2mm malformed plag
93HAK-10		52	no t/s. ves, scattered 1-3mm plag clusters, some with small ol, px
93HAK-11		47	no t/s. slightly ves, 10% 3-5mm plag clusters with small ol, px
93HAK-15	yes	46	no t/s. ves, 40% 2mm malformed plag
93HAK-16	yes	35	no t/s. slightly ves, scattered 1mm ol, plag
93HAK-17		32	no t/s. slightly ves, scattered 1mm ol
93HAK-18	yes	31	no t/s. ves, scattered malformed plag
93HAK-19		30	no t/s. ves, aphyric
93HAK-20		27	no t/s. ves, aphyric
93HAK-21	yes	26	no t/s. ves, scattered small malformed plag
93HAK-22		23	no t/s. ves, 25% 5-10mm plag clusters with small ol, px
93HAK-23		20	no t/s. ves, aphyric
93HAK-24		17	no t/s. dike. nonves, aphyric
93HAK-25		14	no t/s. ves, aphyric
93HAK-26		9	no t/s. slightly ves, 5% 5-10mm plag clusters with small ol, px
93HAK-27		7	no t/s. ves, 10% 5-10mm plag clusters with small ol, px
93HAK-28	yes	6	ves, 20-25% 1-5mm plag, px clusters in very fine groundmass
93HAK-29		3	no t/s. slightly ves, 10% 5-10mm plag clusters with small ol, px
n.d = not described, t/s = thin section			

Appendix C.3 Kamalo Gulch Section Sample Description

Sample	Data Table 5.1	Elev (M)	Description
90KAM-4	yes	600	nonves, 10% 1-2mm oriented plag in very fine groundmass
90KAM-3	yes	585	nonves, 10% 1-2mm oriented plag in very fine groundmass
90KAM-6	yes	439	nonves, 20-30% 2-5mm plag in fine feldspathic groundmass
90KAM-9	yes	424	nonves, aphyric
94EKAM-4	yes	427	ves, 30% 2-8mm plag in very fine groundmass.
93Kamalo-30		591	nonves, 10-20% 1-2mm oriented plag in very fine groundmass
93Kamalo-29		585	no t/s. ves, 50% 1-2mm plag
93Kamalo-28	yes	579	no t/s. nonves, aphyric
93Kamalo-27		567	no t/s. slightly ves, aphyric
93Kamalo-26	yes	555	no t/s. ves, aphyric
93Kamalo-25		548	no t/s. nonves, aphyri
93Kamalo-24	yes	533	nonves, aphyric
93Kamalo-23		512	no t/s. nonves, aphyric
93Kamalo-22	yes	488	slightly ves, aphyric
93Kamalo-21		481	no t/s. slightly ves, 30-40% 15mm plag, 5mm px, scattered small ol
93Kamalo-20		463	no t/s. 15% 6-7mm plag, 2-3mm px, scattered small ol
93Kamalo-19	yes	457	no t/s. ves, 40% 10mm plag, 5mm px. small ol
93Kamalo-18		451	no t/s. ves, scattered 15mm plag, some with px
93Kamalo-17	yes	445	no t/s. ves, 30-40% up to 10mm plag
93Kamalo-16		439	no t/s. slightly ves, 30% up to 15mm plag, scattered px. ol
93Kamalo-15		420	no t/s. slightly ves, 30-40% 6mm plag, some with 2mm px
93Kamalo-14	yes	414	nonves, aphyric
93Kamalo-13	yes	402	no t/s. nonves, 5% malformed plag
93Kamalo-12	yes	390	no t/s. ves, 10% 2-3mm plag, 5mm px, 2mm ol
93Kamalo-11	yes	384	no t/s. ves, 10% 2-3mm plag, up to 10mm px, 3mm ol
93Kamalo-10	yes	378	slightly ves, 15% 3-5mm px, plag, ol in fine feldspathic groundmass
93Kamalo-9	yes	360	no t/s. slightly ves, 25% 3-4mm px, 1-2mm ol
93Kamalo-8	yes	347	no t/s. slightly ves, scattered 3mm plag
93Kamalo-7	yes	329	no t/s. slightly ves, scattered 2mm ol, px, plag
93Kamalo-6	yes	317	no t/s. slightly ves, 20% 2-3mm malformed plag
93Kamalo-5	yes	299	nonves, 25% 3-5mm plag, scattered ol, px fine feldspathic groundmass
93Kamalo-4	yes	293	ves, 10-20% 3-4mm plag in fine feldspathic groundmass
93Kamalo-3	yes	274	slightly ves, 25% 2-5mm plag in fine feldspathic groundmass
93Kamalo-2	yes	262	ves, aphyric
93Kamalo-1	yes	232	nonves, 20% 1-3mm plag, scattered small ol, px very fine groundmass
RTH93-113	yes	198	slightly ves, scattered 1-3mm ol, plag in fine feldspathic groundmass

Appendix C.4 Caldera Section Sample Description

Sample	Data Table 5.1	Elev (m)	Description
90PE-5	yes	0	slightly ves, feldspathic groundmass with variable coarseness
90PE-3	yes	220	slightly ves, 20-30% 2-3mm ol, px in coarse feldspathic groundmass

Appendix C.5 Kalapaupa Peninsula Section Sample Description

Sample	Data Table 5.1	Elev (m)	Description
90KAL-4	yes	n.d.	highly ves, scattered small ol in very fine groundmass
90KAL-2	yes	n.d.	slightly ves, 25% 2-5mm ol, px, plag in very fine to coarse groundmass
90KAL-1	yes	n.d.	ves, 25% 2-5mm ol, px, 1-2mm plag in very fine groundmass

VITA

Nuni-Lyn E. Sawyer

MiraCosta College, Oceanside, Ca.

A.S. 1984 Physics

University of California at San Diego, La Jolla, Ca.

B.A. 1986 Chemistry, with specialization in Earth Sciences

California State University at Long Beach, Long Beach, Ca.

M.S. 1988 Geological Sciences

Thesis: Effect of clay fraction extraction procedure on clay mineral chemistry and mineralogy

University of Washington, Seattle, Wa.

Ph.D. 1999 Geological Sciences

Dissertation: Systematic geochemical and eruptive relations in the late stage evolution of volcanoes from the Hawaiian plume - with case studies of Waianae and East Molokai volcanoes